University of Strathclyde
Department of Naval Architecture and Marine Engineering

Strength and Reliability of Thin Walled Structures for Marine Applications

Pretheesh Paul C

A thesis presented in fulfilment of the requirements for the
Degree of Doctor of Philosophy

Glasgow, United Kingdom
September 2011

Completeness and ultimate truth is with the almighty god, the creator of universe. The more we explore the more we understand how far the truth is

Dedicated to my parents C Paul Varghese and Eliyamma Paul they sacrificed their entire life for the children

Dedicated to my dearest wife Binu and my daughters Liya and Shreya for the endless support, love and patience

Contents

Contents

Contents

List of Tables

List of Figures

Nomenclature

a	Length of the plate
A_s	Area of the stiffener
b	Stiffener spacing
B	Total width of the stiffened plate
b'_e	Reduced effective width
b_e	Effective width of the plate
b_{eu}	Effective width of the plate at failure
E	Young's modulus
E_t	Tangent modulus
f	flange width
h	stiffener web height
h_{fr}	Flange width of the ring stiffener
h_{fs}	Flange width of the stringer stiffener
h_r	height of the web with compressive residual stress
h_{wr}	Web height of the ring stiffener
h_{ws}	Web height of the stringer stiffener
I'_e	Tangent effective moment of inertia
K	Buckling coefficient
L	Length of the cylinder
L_e, l_e	Effective length
m, n	number of longitudinal half waves (aspect ratio) and transverse half waves
NB	Number of bays
N_s	Number of stringer stiffeners
p_r	Structural proportional limit
R	Mean radius of the cylinder
r	Radius of gyration
r_e	Effective radius of gyration

R_r	Reduction factor due to residual stress
s	Stringer stiffener spacing
t, t_p	Thickness of the plate/shell
t_{fr}	Flange thickness of the ring stiffener
t_{fs}	Flange thickness of the stringer stiffener
t_s	Thickness of the stiffener
t_{wr}	Web thickness of the ring stiffener
t_{ws}	Web thickness of the stringer stiffener
v_s, v_{s1}	Stiffener warping
w_b, w_{bl}	Longitudinal stiffener bowing
w_{bt}	Transverse stiffener bowing
w_p	Plate distortion
x_m	Model uncertainty factor
y_c	Distance from elastic neutral axis to the outer fiber
Z, Z_l, Z_s	Batdrof length/width parameter
α	Bowing slenderness
β	Plate slenderness, Reliability index
β_e	Effective plate slenderness
γ	Warping slenderness
δ_0	Column initial imperfection
$\delta_p, \delta_b, \delta_w$	Non-dimensional plate, bowing and warping distortions
δ_u	Displacement at failure
ε	Strain
ε_y	Yield strain
η	Residual stress tension block width factor
λ	Column slenderness
λ_e	Effective column slenderness
ρ_n	Shell knockdown factor
σ	Stress
σ_{av}	Average end stress across the full plate
σ_c	Column collapse stress

σ_{cr}	Elastic critical buckling stress
σ_e	Plate edge stress acting over the effective width
σ_{ps}	Structural proportional stress
σ_r	Compressive residual stress
σ_u	Ultimate stress
σ_y	Yield stress of the material
υ	Poisson ratio

Acknowledgements

Abstract

The evolution of thin walled structures has made it possible to minimise the gross weight of the marine and aerospace structures to a substantial extent and substantially enhanced the operating capability. Since then, the design optimisation of thin walled structures has become a necessity and major focus to maximise the capacity with adequate level of safety with minimum cost and material. In general, marine and aerospace structures need higher factor of safety and reliability compared to land based structures. The modern structural engineering capabilities have grown to such an extent that it can handle majority of the real life problems at extreme level of accuracy. Adequate theories and techniques are developed to predict the behaviour and performance of the structural systems. Standard rule based design codes are also available for a better design of similar structures of any size and capacity. The efficiency of any method or procedure for the structural strength assessment or design optimisation is significantly dependent on the performance of the strength model. A subtle enhancement of the strength model may contribute a lot for a better overall design and cost of the structure. In this thesis, two typical thin walled structural components used extensively in marine structures are studied in two different perspectives to propose better strength models to illustrate the scope and possibilities in this area.

Stiffened plates are the fundamental building blocks of steel ships and other marine structures. The fabrication processes including sizing and welding will develop geometrical imperfections and residual stresses in the stiffened plates. Available design codes and analytical formulations for the strength prediction of these structural components are incorporating the imperfection effects with a suitable correction factor and it may not always predict the real strength. The imperfection sensitivity is closely related to the topological structural instability in certain bifurcation forms defined in Thompson and Hunt (1984). For thin stiffened panels the distortion is not always reducing the structural strength

according to Pretheesh *et al.* (2009). This obscurity or uncertainty indirectly introduces an added or reduced safety margin in the design of structures. Rigorous numerical studies are carried out to understand the contribution of parametrically defined imperfections and its interaction effects on the buckling strength of the structure. Design curves are proposed to predict the strength at various levels of imperfections with respect to appropriate structural slenderness to produce more realistic and accurate predictions of the overall structural performance.

Cylindrical shells are one of the major structural components in offshore engineering world. They are particularly important in buoyant semi-submersible and Tension leg type offshore platforms. The legs of these structures are generally and most likely made of stiffened cylinders because of its inherent capability to resist high axial loads and bending moments with lateral pressure loads. The strength of stiffened cylinders is predicted by many practicing codes satisfactorily. The design process becomes more and more accurate and beneficial as the robustness and accuracy of prediction increases. A large number of experimental test data are collected and based on the analysis of these data, an existing formulation is modified to propose a better strength model compared to the most widely used codes of practice.

The modern design approaches consider reliability as one of the essential criteria to be satisfied for structural integrity. The proposed strength models of the two structural components are used to conduct the reliability analysis of these structural elements. The reliability analyses of these structural components are carried out with RSM also and the results are compared.

Chapter 1. Introduction

1.1 Background

The design of offshore structures and ships has developed and became a matured field of engineering science over the last centuries with the contributions of scientists and researchers from around the world. One of the major characteristic of technological development is that it will never be satisfied and never stops to grow, it always strive for excellence. Today's technology is capable of installing offshore facilities or building ships of any scale and size one would ever imagine. The change from wood as the major material for construction to steel was one of the foremost turning point in the revolution of offshore industry. Initial steel ships were very heavily built metal chunks floating over the sea with limited operating features compared to today's ships. Then came the era of light weight structures to meet the new challenge, they were high energy efficient, having better manoeuvrability, reduced overall cost of construction, reduced operating cost, high load carrying capacity etc.

The exploration of subsea oil fields during the end of 19th century and early 20th century increased the demand for static offshore platforms for the recovery, production, storage and transfer of petroleum products. The platforms went through a development cycle from conventional fixed platforms to present day semi-submersible via, compliant tower type, vertically moored tension leg and mini-tension leg platform, Spar and finally Semi-submersibles. The modern tension leg platform (TLP) decks are made of flat plates and the legs are of stiffened cylindrical shells using steel material. The aspects of cost, installation, maintenance and handling of these facilities ended up with light weight (thin) plates and shells for the construction.

Over the years, the offshore structural engineering started to focus on the development of efficient thin walled structural concepts for the use of offshore

platforms and ships. There were many hurdles to be crossed for ensuring the safe and guaranteed operation of light weight or thin walled marine structures under various sea conditions. The strength requirements were the major challenge as the plates become thinner. With proper stiffening methods and load distribution techniques with appropriate geometrical arrangements of components, designers could overcome the issues successfully. The knowledge continues to grow up with lessons from various accidents and accidental observations.

Due to the risk of leaking, the welding remains the major method for joining the steel components in offshore industry unlike aerospace industry where the major fastening method is riveting. Since the welding zone is being identified as the major points prone to initiate fatigue failure of the structure, more sophisticated techniques are imposed to ensure flawless welding and effective investigation of the welded zones. The welding process introduces geometrical distortions and weld induced residual stresses in the structure. These factors affect the structure on its overall strength, aesthetics and when joining welded blocks together, it becomes a serious issue. There are effective mitigation techniques available to control and reduce the distortion to an allowable tolerance level. These techniques are not that easy to implement and in general, strictly followed over the areas where the blocks are to be joined together. This result in substantial amount of distortion left knowingly or unknowingly in the structure. The classification societies consider this problem with utmost care and put stringent tolerances to ensure the levels of distortion minimum. This often results in great amount of rework and cost huge amount of money, material wastage and man hours. An optimised design based on the estimate of strength allowing nominal distortion and residual stress can be proposed if the consequences due to these factors are well understood and accounted. Although there are many convincing approaches available to predict the strength capacity of stiffened plated structures, the treatment of fabrication related imperfections, the geometrical distortions and weld induced residual stresses are not

addressed explicitly. The effect of weld induced geometrical distortions and residual stresses and their interaction effects on the strength and behaviour of plated structures seems to be not fully understood and often included in the practicing codes and regulations as correction factors. But in reality, the estimate often tends to be rather pessimistic or optimistic because of the interaction effects and influences of other structural parameters. The issue should be viewed in a broad canvas to portrait the effect of these factors considering the structural parameters. An improved strength model for the stiffened plate considering the effect of distortion and residual stress with the interaction between these factors will help the designers to produce a rational estimate of the strength of similar structures under the influence of these factors.

The strength of stiffened cylinders is predicted by many practicing codes satisfactorily. The design process becomes more and more accurate and beneficial as the robustness and accuracy of prediction increases. Advanced design methods and procedures are getting published from all corners of the world. But the practicing codes could not always append all the refined or essential recommendations timely. Most of the offshore platforms legs are made of stiffened cylinders and any improvement in the predictive capacity of a strength model will increase the efficiency of the structural design optimisation.

The modern design approaches consider reliability as one of the essential criteria to be satisfied for structural integrity. The partial safety factor approach has been proved superior to conventional factor of safety approach as it provides a rational estimate of the parameter level structural requirements. The reliability based design optimisation need a tool to predict the structural capacity as accurately as possible. Hence the strength analysis of structures with a higher degree of accuracy is quite important and crucial in the reliability assessment. A robust analytical model for the structural response is the most essential requirement for this purpose. In the absence of such models, say with

the influence of distortion parameters and complicated loading conditions, a validated numerical analysis tool is the immediate option.

1.2 Scope and Objectives
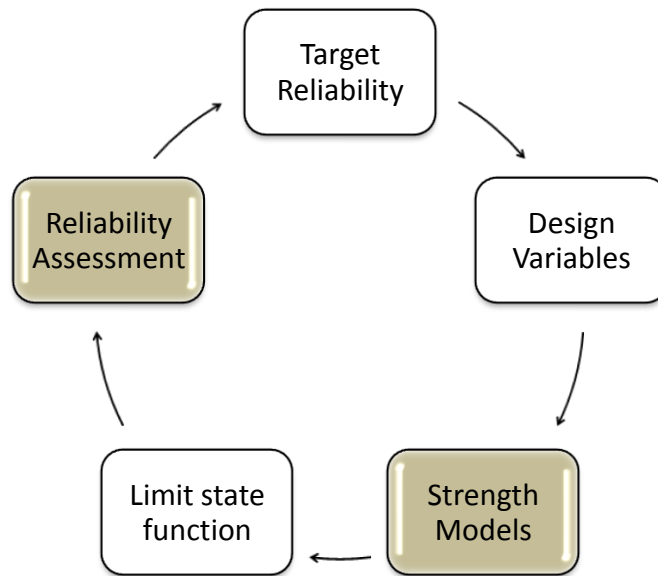
Figure 1-1 Reliability based design cycle

The reliability based design is an iterative procedure where the design variables are modified as shown in Figure 1-1 till the achievement of the target reliability or safety level. The effectiveness of the procedure is majorly dependent on the efficiency of the strength models to predict the structural response and the way the reliability assessment is performed.

The overall objective of this thesis is to rationalise the above procedure for the determination of the structural strength and reliability of thin walled components used in the construction of marine structures by enhancing the accuracy of structural strength models and suitably incorporating for the reliability analysis. Being the major thin walled structural elements in the ship and offshore industry, Stiffened/unstiffened plates and stiffened cylindrical shells are chosen for the study in this thesis.

The welding process induces geometrical imperfections and residual stresses in the structure. These imperfections are assumed to have a deteriorating effect on the strength based on many analytical and numerical investigations. There are some concerns in a research point of view,

1.   In reality, do these imperfections influence structural performance?
2.   To what extent the structural performances are affected?

This thesis presents an experimental study with varying geometrical distortions and residual stresses to answer the above questions.

The influence of the imperfections for a general structural dimension with some random imperfection cannot be directly interpolated from a limited number of experimental test results. The most effective tool at present for engineers to predict structural behaviour is the finite element method (FEM). When trusting the numerical analysis tools, there are worries like,

1.   How sensible are the failure modes predicted by FE models?
2.   How accurate the FE models predict structural response?
3.   What are the type and range of imperfections in panel structures?
4.   How big is the impact of imperfections for common ship scantlings?

This thesis illustrates the procedure to apply finite element methods for unstiffened and stiffened plate panels incorporating fabrication induced imperfection effects. The FE models will be validated with the experimental tests. A comprehensive parametric definition of imperfection will be defined because the existing parametric plate imperfection is not sufficient for the application of stiffened panels. Design curves will be proposed based on the imperfection parameters using the validated FE model for common structural scantlings used in the ship building industry.

Considering the computational costs and efforts involved in the numerical techniques, an analytical approach is always preferred by designers. There are

many analytical methods available which can predict the response of the plate panels quite sensibly. But none of the methods effectively incorporate both the fabrication induced geometrical distortions and weld induced residual stresses. So there are some issues prevailing as,

1.   How to deal with complex distortion patters in stiffened panels?
2.   How to deal residual stresses and geometrical distortions together?
3.   How the interaction between these two effects is accounted?

An empirical formulation will be developed which can incorporate the complex geometrical imperfections and residual stresses in the stiffened panels and also the interaction effects between these two factors.

There are number of design codes available to predict the strength of stiffened cylinders under various loading conditions. The accuracy of the strength model needs to be as high as possible to propose a sensible design catering all the safety and reliability requirements. While following the design codes, there are some apprehensions to be resolved like,

1.   How accurately can the major design codes predict the capacity?
2.   How an analytical strength model can be improved?
3.   How accurate is the proposed (improved) strength model?

A large number of experimental results will be collected and the major design codes will be compared based on the prediction and the actual experimental results. Based on the results a modified strength model will be developed so that it can predict the results more accurately compared to the existing codes.

The reliability analysis needs a robust strength model to predict the structural response for accurate estimation of safety and reliability. When carrying out the reliability analysis with the new strength models, the following queries are coming up.

1. How to incorporate realistic imperfections of stiffened panels in the reliability calculations?
2. How the parametric FE models can be used for reliability calculations?
3. What is the influence of imperfection effects on the reliability?
4. How accurate is the proposed strength model for stiffened cylinder predicts reliability compared to an FE model?

Even though the empirical or analytical methods can be used for the reliability calculation incorporating the imperfection effects, it may be difficult to use these models in complicated loading and boundary conditions with very specific imperfection combinations. In such situations, we have to use FE models to predict the structural strength. It is not a straight forward method to calculate reliability with FE models. Response surface method will be used for the reliability assessment of stiffened panels and the results will be compared with the prediction from analytical reliability estimates. Similarly the analytical estimate of reliability for stiffened cylinders using the proposed strength models will be compared with the estimates from Response surface methodology.

Chapter 2. Literature Review

2.1 Strength of Unstiffened and Stiffened Plates

Steel structures such as ships and offshore platforms, bin/bunkers, box girder bridges and land-based structures, are mainly fabricated by welding as assemblies of individual steel plate elements. If a ship structure is divided into elements like stiffened and unstiffened plates, then around 80% of the ship structure constitutes stiffened and unstiffened plates, and therefore they should be designed for a set of failure modes that govern their states.

Historically, the earliest attempts to incorporate the plate buckling and its effects of ship strength were made by Claldwell (1965) using simplified formula where the ultimate moment of a mid-ship cross-section in the sagging condition was calculated introducing the concept of a structural instability strength reduction factor for the compressed panels. This factor would account for the reduced strength of the cross-section due to early failure and uploading of some plate elements. Smith (1977) developed a simplified approach to incorporate the load shortening curves of the plate elements in the calculation of the hull girder collapse. The ultimate strength of ship plates is very important from the design and safety point of view because the collapse loads of plates can often act as an indicator of the ultimate strength of the whole stiffened panel in ship structures (Guedes Soares, 1992). The problem has been addressed for centuries for the general plated structures and for several decades even with regard to ship structures (Mansour, 1971). The methods which have been proposed can be divided into,

1. Experimental method
2. Analytical or semi-analytical approaches
3. Finite element method
4. Empirical formulae based on either numerical or experimental results

Most of the researchers studied longitudinal compression only. Steem (1995) and Fujikubo *et al.* (1997) considered the combined load cases but they used empirical approaches based on FE or experimental results.

Faulkner (1975) presented a comprehensive review of effective plating for the use in the analysis of stiffened plating in bending and compression. He presented the ultimate plate strength concepts, and how this is affected by individual distortion, normal pressure and boundary condition. He presented the reduced effective width concept for defining plate element stiffness, as required for the use in the stiffened-plate collapse theories and proposed the effective width concept with a new effective width formula, which become widely popular. Faulkner presented the concept of initial distortion and welding induced residual stress, but he assumed average value of these initial imperfections in the effective breadth formulae. But attention should be paid to take into account of different levels of imperfection according to Smith (1977) while predicting the compressive strength of plate and stiffened plate.

Many of the beam column approaches used in the ISSC Technical Committee III.I investigation as per Jensen *et al.* (1994), were developed from Smith's method. The main differences are in the derivation of the stress-strain (σ-ε) relationship of the individual components. For this reason, Jensen et al. investigated the theoretical stress strain relationship of ten stiffened plates using different methods. Significant variances were noticed between the predictions of a series of stiffened plates. This was found to be a result of the use of different effective width formulations and the integration of initial large deflection of the plate. As an example of the care necessary in applying the effective width method, consider the ultimate strength of a thin walled box structure. The effective width of the complete box cross-section is obtained by adding the effective widths of each of the component plates. However, the method assumes that when any one plate reaches its ultimate load it is able to carry on shortening at constant stress while the other (narrow) sides build up to their (higher) maximum stress.
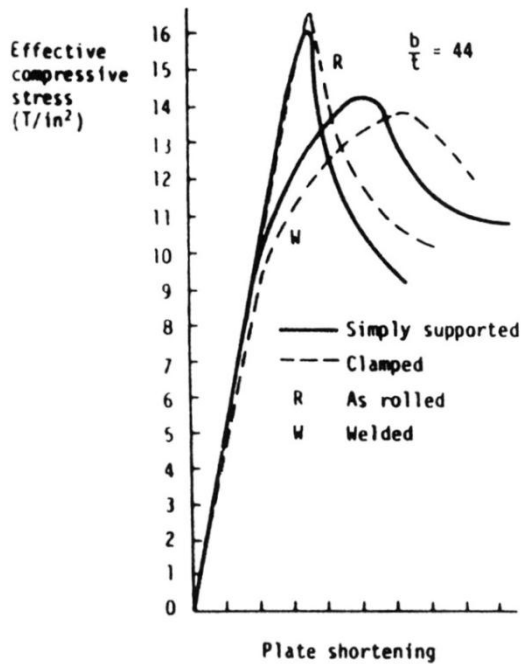
Figure 2-1 Load/Shortening Curves for Steel Specimens (Dwight and Ratcliffe, 1969)

Figure 2-1 taken from Dwight and Ratcliffe (1969) suggests that the component plates in a non-welded member do not in fact hold their load after reaching σ_u but tend to shed it catastrophically, before the narrow sides reach their full carrying capacity. This throws some doubt on the logic of the effective width method of design when applied to non-welded members. The curves for welded members do not fall off so sharply and hence the assumption of redistribution of load as explained by the effective width method is applicable for welded members.

Precise modelling of stiffened panels can be achieved by means of analysis tools and computing power. Initial imperfections such as welding induced residual stressed and initial deflections of the cross section can be explicitly incorporated into numerical models. In a series of studies, Grondin *et al.* (1998, 1999) have considered the behaviour of structural elements under axial compression, both experimentally and numerically. The goal of that study was to investigate the tripping failure mode and validate with experiments, a sophisticated non-linear finite element model that would allow a more extensive study of the behaviour to be conducted numerically.

Many simplified design methods to predict the ultimate strength of stiffened plates have been improved, considering on or more of the failure modes. Some of those methods have been addressed by the ISSC technical committee III.I on the ultimate hull girder strength as explained in ISSC (2000).

Hoglund (1997) presented a comprehensive study of the shear buckling resistance of steel and aluminium plate girders. Based on the ideal tension field theory, Hoglund described rotated stress field theory, which is applicable to unstiffened, transversely and longitudinally stiffened and trapezoidal corrugated web girders.

Mahendran (1997) predicted an analytical study of two idealised collapse mechanisms in plate elements under compression and presented the roof and flip-disc mechanisms. It was postulated that initial knuckling and first yield determine the post buckling collapse pattern. Based on solutions of Marguerre's equations for varying imperfections it was shown that plates with large slenderness (b/t) ratios or large imperfections are more prone to collapse in the flip-disc mode (sudden flipping to a sinusoidal wave form as a disk) whereas the roof mechanism (develop plastic hinges as a triangle to mimic a roof like shape) governs the collapse of thicker plates. The ultimate strength is determined as the intersection between elastic solution of Marguerre's equations and rigid plastic solutions based on the two considered mechanism. Experiments verified the predicted dependence of the mechanism on the slenderness ratio and imperfections. By increasing the imperfections, it was possible to change the collapse mode from the roof-type to flip-disc as predicted theoretically. However, the experiments showed that the difference in ultimate capacity was less than predicted.

Hughes & MA (1996a, 1996c) and Ma & Hughes (1996) presented and energy method for the lateral buckling behaviour (tripping) of beams subjected to axial load, end moment, distributed lateral load and a lateral point load. The classical analysis based on a rigid web (i.e angles between members in the cross section

are retained during the buckling) is extended to take into account of the distortion of the web. A strain distribution along the stiffener is assumed and the total potential energy function is derived. The study explored the effect of plate rotational restraint and the previously unresolved question regarding plate mode shape was solved. The accuracy of the method was verified using ABAQUS. The analysis showed that for short beams the classical method may seriously overestimate the critical load. In Hughes & Ma (1996b) the elastic model was extended into the inelastic range, using deformation theory and iterative and incremental formulation showing good agreement with the experimental results.

Paik & Pedersen (1996) presented a method for prediction of the ultimate strength of plate panels, which have welding induced residual stresses and initial imperfections. The first part of the load deflection curve is determined by elastic large deflection theory and post ultimate part by idealised rigid plastic mechanisms. A comparison with 33 elasto-plastic FEA solutions shows good agreement. Cui & Mansour (1990, 1999) adopted the same basic solution methodology to investigate the effect of various parameters in the ultimate strength. It was confirmed that in addition to the amplitude, initial deflection shape has a significant effect on the ultimate strength values. Based on the parameter study, empirical formulae were proposed for the strength reduction due to geometric imperfections and the welding induced residual stress.

Gaudes Soares & Gordo (1996) emphasised the need for taking into account the biaxial loading of plate panels. They presented a compressive literature review for the ultimate strength of bi-axially loaded plates. Based on a total of 385 data points they proposed new interaction curves for the ultimate strength of plates subjected to a combination of longitudinal and transverse compression, given by

$$\frac{\sigma_x^2}{\sigma_{x,u}} + \frac{\sigma_y^2}{\sigma_{y,u}} = R_{r\delta}^2$$

Where σ_x and σ_y are the longitudinal and transverse loads on the plate, $\sigma_{x,u}$ and $\sigma_{y,u}$ are the ultimate strengths under uniform loading and $R^2_{r\delta}$ is a correction term that depends on the initial distortions and residual stresses. The proposed formulae are unbiased with less model uncertainty than other known interaction formulae.

Pu *et al.* (1997) presented an extension to Faulkner's original stiffened panel model to include an effective width formulation by Guedes Soares (1988), which explicitly considers initial imperfections. Comparisons with experimental data reveal a bias of 1.09 and COV of 0.143 for the original model and a bias of 0.992 and COV 0.099 for the new model. Gaudes Soares & Gordo (1997) compared three strength prediction models to experimental and numerical analysis results for longitudinally stiffened panels under uniaxial compression and lateral pressure. The methods attributed to Faulkner, Carlsen and the American Bureau of Shipping (ABS) was compared to experimental results.

Paik *et al.* (1998b) investigated numerically the characteristics of tripping failure of flat bar stiffened panels subjected to uniaxial compressive loads and studied the accuracy of two available design formulations.

Paik *et al.* (1998c) studied analytically the characteristics of local buckling of the stiffener web in the stiffened panels under uniaxial compressive loads. A plate stiffener combination model is used as representative of the stiffened panel. The elastic buckling condition for the stiffener web is analytically derived by solving the characteristic value problem involving the governing differential equation under the corresponding loading and boundary conditions. The closed form approximate expressions for predicting the buckling strength of the stiffener web are derived taking into account the influence of rotational restraints at the plate stiffener connection and stiffener web-flange intersections. Finally design considerations for preventing buckling of the stiffener were discussed, especially for the flat bar stiffener case.

Wang & Moan (1997) performed a study on the ultimate strength of stiffened plate subjected biaxial and lateral loading. The objective was to assess the beam-column approach used in design rules for ships and offshore structures. Non-linear finite element analysis of two representative midship bottom and deck panels from an offshore oil production ship were performed, for which the corresponding ultimate longitudinal compressive strengths were calculated taking initial imperfections into account. The calculated results were compared with the prediction using a beam column approach. For the interaction of axial compression and significant lateral pressure, it was found that the considered beam-column model is non-conservative in plate induced failure mode, while it is generally very conservative in stiffener induced failure mode. The bias associated with the model was found to be a function of the transverse stress and lateral pressure.

Hurst & Campbell (1997) presented a comparison of FEA modelling practice for stiffened panel structures applying to SESAM package. The main focus of this study was to determine how to model stiffened plate behaviour in global models of floating structures. Results from 10 different FEA models representing the same geometry were compared and recommendations for proper FEA modelling were given. Also, Yao *et al.* (1998c) have studied the FEA modelling principles for stiffened plates concluding that a triple span model is somewhat better than a 2 span model for studying the collapse behaviour under combined thrust and lateral loads.

Grillages are one of the major structural components of various onshore and offshore structures. Generally, plates of ship structures are stiffened longitudinally by stiffeners of a relatively small size and transversely by girders of a large size. There are many kinds of strength formulations proposed for predicting the ultimate strength of stiffened plates, but few are applicable to grillages. Cho et al. (1998a, 1998b) have developed a robust ultimate strength formulation applicable to grillages subjected to combined axial compression, end bending moment and lateral pressure loadings. The generalised Merchant-

Rankin formula is adopted as its basis. The prediction using the proposed formulation provided improved accuracy compared with other existing approaches, and optimisation can be performed on all the design variables for grillage structures. Test results of stiffened panels which undergo loading far beyond their ultimate state show the interaction of the tripping failure of the stiffener. A simple equation is also derived to represent the average stress-strain relationship of stiffened plates for post ultimate strength behaviour.

Cui *et al.* (2002) presented a simplified analytical formula to determine the ultimate strength of plate considering the geometric deflection and residual stress subjected to combined loading.

Sheikh *et al.* (2003) have studied the stability of steel stiffened plates of T-shape section under uniaxial compression and combined uniaxial compression and bending using FEM analysis. A comparison of numerical analysis results with API and DNV design guidelines indicates that the guidelines lack the potential interaction buckling phenomenon between various failure-modes i.e. plate, stiffener, or overall buckling, which can cause a sudden loss of capacity.

Dunbar *et al.* (2004) have addressed the influence of local corrosion on stability of a plat and then on a combination of plates forming a stiffened panel. Local corrosion was applied to a stiffened panel with typical residual stress and initial deflection values. A finite element model was verified through comparison to an experimental model, followed by the creation of several models with local corrosion.

Hughes *et al.* (2004) derived modified expressions for elastic local plate-buckling and overall panel-buckling expressions from 55 ABAQUS eigen value buckling analysis. Inelastic RIKS analysis for the ultimate collapse stress and post collapse behaviour using ABAQUS FEM was conducted on their models. Ultimate stress was also calculated using orthotropic methods. It was found that for panels having crossover proportions, Orthotropic based methods are unsatisfactory.

Steen *et al.* (2004) have performed a direct calculation model (PULS) for the calculation of ultimate capacity of stiffened panels, which was developed using energy principles and non-linear plate theory according to Marguerre and Von Karman. Extensive verifications were conducted by means of more advanced numerical programs. This code is also recognised by ABS and Lloyds Register and is available as the advanced analysis method in the Joint Tanker Project (JTP) launched by ABS/DNV/Lloyd's Register since January 2004, which led to the development of IACS Common structural rules for tankers.

2.2 Initial Imperfections and Residual Stresses

A plate must be welded because it is a component of structure. This action results in the distortion, which are called weld induced initial imperfections. To evaluate the strength of a stiffened or gross panel element, it is necessary to review various models taking into consideration of the initial imperfections and damages.

It is a well-recognised fact that the magnitude of initial imperfection plays an important role to affect (mainly to reduce) the ultimate strength of the welded steel un-stiffened plate structures. A number of studies related to the influence of initial imperfection on the collapse behaviour of the steel plate elements have been carried out previously Dwight and Moxham (1969), Faulkner *et al.* (1973), Carlsen & Czujko (1978), Koichi Masubuchi (1980), Ueda & Yao (1985) and Paik *et al.* (2004). While shape of initial imperfection in unstiffened plate is normally very complex, it has been realised that the shape of initial imperfection can significantly affect the behaviour of the plate elements until and after the ultimate strength is reached. Considerable research efforts have been devoted to investigate the effect of welding induced initial deflection shape on plate collapse behaviour (Ueda & Yao (1958), Paik & Pedersen (1996), among others). The ideas developed by these studies are quite useful to accommodate initial imperfection shapes into the ultimate limit state design of unstiffened plate elements as a parameter of influence.

The initial imperfection shape strongly depends on the aspect ratio of the plating as well as on the other factors, such as material properties, welding condition etc. according to the available sources, although the geometric configuration of such initial imperfection is quite complex a simple approach has been adopted to design the initial imperfection on the stiffened plate. Based on the experimental measurements, Smith (1977) classified the initial imperfection as slight, average and severe.

In the practical range of plate slenderness, the reduction of plate strength due to the presence of distortions or of residual stress can be as much as 20% to 23% of the perfect plate strength. If both types of imperfections coexist simultaneously, it reduces the ultimate strength to a much larger extent. It is worth mentioning that the effect of both imperfections is not equal to the sum of the effect of each imperfection considered separately.

The residual stress problem should come out as a reduction in the stress resistance of the steel. In the American code (AISC), they deal with this by subtracting an amount from the specified yield stress of the steel and then using that number for design. But the behaviour of the structure under this internal stress state upon loading will not be reflected due to many reasons like the complex residual stress directions, its non linear effects etc. So it is worth to model the residual stress to the maximum possible accuracy for the judgement of the effects produced.

There are different methods and approaches for the FE simulation of residual stress. Different methods are adopted according to the level of the study. The welding process involves the effects of combined thermal and mechanical stresses and strains and hence the phenomenon of residual stress development is extremely complex. A complete thermo-elastic–plastic welding simulation may be required to evaluate the distortion of the structure and the residual stress accurately. But when the focus of the study is to find out some of the strength related parameter of the structure, the inclusion of the residual stress

effects can be achieved through some simple methods. The variation in results due to the approximation/exclusion on the actual thermo-mechanic phenomenon can be made negligible by appropriately controlling the parameters. If the detailed internal mechanics of the process is not targeted, the simple methods provide good control, clarity and easiness while carry out strength analysis.

According to Deaconu, (2007), there are three main coupled fields to be considered for the welding process simulation, the microstructure variation, the heat transfer effects and the associated mechanical actions. When we need to analyse the mechanical effects of the welding, i.e. residual stress and distortion, the metallurgy part can be neglected or suitably incorporated by material description through the microstructure dependency on the temperature and deformation. Since the heat generation trough the mechanical deformation is negligible, the mechanics to heat flow coupling is weak, a sequentially coupled thermal and mechanical analysis is the most widely used approach.

There are lot many people who made trial based on this technique and got good results as well. Michaleris & DeBiccari (1996) has presented a good methodology to predict the welding distortion using the thermo-elastic-plastic method. Tsai *et al.* (1999) made some studies on the welding distortions using the same method and they presented an optimum welding sequence to reduce the distortion effects. They have considered the effect of residual stresses as well. The studies conducted by Biswas *et al.* (2007), Mahapatra *et al.* (2006), Murugan & Narayanan (2008) and many more deal with different aspects and perspectives of welding process using the same thermo-elastic-plastic approach.

Chang Doo Jang et al. (2007) present the equivalent load method through inherent strain. SSC-435 latter published this work as an accepted practice and some bench marks are introduced for this procedure. The welding deformation simulation is carried out in three steps. First step analyses the heat transfer to calculate temperature distribution of each welding section with the given

information on welding parameters. The FE model uses heat conduction elements and considers convection in the surface and cooling rate is calculated to determine phase transformation. The second step computes the degree of restraint by the FE analysis. The third step calculates the inherent strain components and their equivalent loads, and the welding deformation of a structure is obtained by FE analysis.

Hu *et al.* (1997), Hu & Jiang (1998), and Hu (1993), introduce an effective simplified method for incorporating residual stress using temperature strain. They have conducted some physical tests to verify this approach. Derek Graham (2007) used the temperature strain technique to effectively simulate the effect of residual stress for some works in the strength of stiffened cylinders.

The above method produces additional deformation in the structure and will be different from the initial geometric imperfections. To overcome this difficulty, Hu & Jiang (1998) introduce a method to produce the real geometrical distortions by suitably adjusting temperature within the structure.

The above method can also be adopted with no correction in the initial imperfection when the deformation caused due to the temperature variation is very less as shown by Imtiaz *et al.* (2001). The procedure can be simplified by setting the initial temperature to the maximum value and then bring down to the ambient value in one step.

A most simple and efficient method to incorporate the effects of residual stress is by providing initial compressive and tensile stresses. This procedure does not involve an analysis step and hence it is required to apply the forces in equilibrium. This method provides facility to apply the stresses in all the three directions. An efficient combination of the initial stress can well generate the idealised pattern of residual stresses. The method is suggested in ISSC 2003. The same pattern is followed if there is transverse welding.

2.3   Strength of Stiffened Cylinders

Relatively stocky unstiffened tubes have been used for many years for land based civil engineering and more recently for offshore platforms in shallow water depths. However, the behaviour of stiffened curved think shells and cylinders has only been studied seriously since the 1920s and 30s for the emerging aircraft industries in Europe and the USA.

In the 1960s and early 1970s the offshore industry started drilling for oil and designing fixed platforms in the deeper more hostile waters of the North Sea and elsewhere. About the same time, some of the traditional ship classification societies became certifying authorities for the design of offshore drilling and production platforms. There had been several structural failures, and the loss in January 1974 of the twin hull drilling barge *Transocean III* caused a stir because one of its two cylindrical legs buckled. This, take with the low redundancy implicit in such designs, highlighted the need for greater knowledge for semi-buoyant cylindrical structures.

In 1974, Marine Technology Directorate (MTD) of UK's Science Research Council (now the Science and Engineering Research Council) was created. In 1975 they commissioned a study in the UK to examine the state of structural knowledge and to recommend future research in UK universities aimed to help the offshore industry to understand such weaknesses and to provide a sound basis for new design rules. In 1975, Faulkner undertook the study and started with a questionnaire to the industry. Whilst the response from industry was generally very supportive for R&D, the attitude of the Certifying Authorities (CAs) was rather different. Bureau Veritas (BV) felt nothing more was needed since Euler's work 200 years ago, and the reaction of Lloyd's Register was somewhat similar. DNV had created their first offshore structures code by 1974 and were undertaking their own research. This was loosely based on ultimate limit state methods, coupled to partial safety factors that were in embryo form a step towards reliability based methods. Recognising that this document as a

good starting point for his own study, the author reviewed existing data as seen against the DNV formulations, which was inevitably based on aircraft technology. The general conclusions were that the rather free transfer of technology from aerospace had left various shortcomings for predicting collapse in welded steel structures. There was a tendency also to neglect the proper curvature effects in collapse loads of axially stiffened cylinders.

As a result of the study, a jointly funded programme by the SERC and UK Department of Energy was started for axial compression loads tests. Small scale tests were undertaken at University College of London (UCL) and large scale tests at Imperial College of London (ICL) and Glasgow University. Unstiffened tubes were tested at AMTE (now DERA) Rosyth by Smith *et al.* (1977). White & Dwight (1977, 1978) at Cambridge University reviewed the nature and distribution of fabrication imperfections, as these were recognised as being a very major difference from aerospace. They provided details of all these tests in a state-of-the-art review of the buckling of offshore structures.

Faulkner became the Chairman of the Conoco-ABS RCC code drafting committee and The Rule Case Committee (RCC) code was adopted but adapted by the American Petroleum Institute (API) in 1987. Up to that time API had no rules for stiffened cylinders. Unfortunately, the adaption suffered badly in the process (API Bulletin 2U). In some respects DNV's rules of 1977 have likewise suffered in modelling simplifications incorporated in the Classification Notes 30.1 of 1982.

Meanwhile, Faulkner's original approximation is used in the 1983 RCC code formulations. These included elasto-plastic collapse effects and the total model did correlate acceptably well with the limited test data that was available where tripping was the primary mode of failure. Unfortunately, these formulations were not transferred to the 1987 API Bulletin 2U. In 1991 Faulkner attempted to remedy this situation by producing an approximate theory for ring and stringer cylinders.

Das, Faulkner & Zimmer (1992) established a set of criteria to select robust strength models for the strength and reliability analysis of structural components for offshore marine applications. The work proposes how to rate the statistical quantities and also compare different codified rules for the strength of stiffened cylinders.

Das, Thavalingam & Bai (2003) presented a study of the strength models of stiffened cylinders proposed by Faulkner with large number of test data. The modelling uncertainty is calculated and compared with API and DNV codes. The proposed strength model found to produce good correlation with the test data.

2.4 Application of Reliability Analysis for Offshore Structures

The determination of Probability of failure is the most researched part in the theory of reliability. Before the sixties a variety of studies on second moment were carried out, a milestone in this direction was laid by Freudenthal (1956) who used complete probability models. However, it is the work by Cornell (1967) which gave second moment concept a wide acceptance. To date, second moment concept have become so popular that it has a significant place in any text books concerning structural safety. Typical of them are those by Ang and Tang (1984), Madsen, Krenk & Lind (1986), Ditlevsen & Madsen (1996), and Melchers (1998). The first order and second order moment theories (FOSM and SOSM) are now increasingly used in a variety of engineering fields. In these theories the tedious part of integrating of the joint probability density functions (JPDF) of the design variables are circumvented by transforming the actual problem into a least distance problem in a standard normalised space. Orthogonal transform is used to uncouple the correlated design variables which essentially show that the problem is in its core an optimization procedure.

Monte Carlo Simulation (MCS) plays a very important role in reliability analysis. MCS is not affected by the number and distribution type of the basic variables. The method solves highly non-linear problems and problems where the limit

state function is not known explicitly. A number of variation reduction techniques have been proposed such as the Importance Sampling Method but as always the computation cost in large complex structural systems is still significantly high as shown by Bucher (1988).

The latest development in the field of structural reliability analysis is the Response Surface Method (RSM). It is very suitable in cases where the limit state function is known only point-wisely by such numerical methods as the FEM rather that in closed form. In short, RSM is a system identification procedure, in which a transfer function relates the input parameters (loading and system conditions) to the output (response in terms of displacements or stresses). The observations required for the identification of the most suitable way to relate those two are usually taken from systematic numerical experiments with the dull mechanical model and the transfer function obtained approximately defined as the response surface (RS). It was in the early 1950s that the basis concept of RSM first developed in experimental fields, but only recently, it has been introduced into the field of reliability analysis. It combines the deterministic structural analysis software and the basic reliability ideas aforementioned. In addition to this, even for those problems that other approximate methods seem to be susceptible to, the RSM is shown to be superior in both accuracy and efficiency with its only drawback being the experiment design and the identification of unknown parameters in the RS which influence the whole algorithm. Work by Bucher (1990) and Rajashekahar *et al.* (1993) have led the ways of future research. Advanced algorithm based on that work can be found in work published by Kim *et al.* (1997), Zheng & Das (2000, 2001) and Yu, Das & Zheng (2001).

The first work on ship structural reliability was reported by Nordenstron (1971). He calculated the failure probability by integrating the failure domain assuming a normal distribution for both ultimate strength and still water bending moment and Weibull distribution for wave bending moment. Mansour (1972) and Mansour & Faulkner (1973) presented the level three formulations

to provide the first complete reliability analysis of a ship structure. They adopted Nordenstrom's model for wave induced loads and developed a probabilistic model for the ship strength for various modes of failure.

Mansour adopted the distribution of the wave-induced vertical bending moment at a random point in time to calculate the reliability index of 19 merchant ships using the second order reliability method. Faulker & Sadden (1979) considered the most probable maximum load given by Poisson distribution whose mean value is the most probable maximum calculated at the 10^{-8} probability level. Using this approach, they obtained a reliability index of 2 for warships, while the one calculated by Mansour for merchant ships were in the range of 7.

Das, Frieze & Faulkner (1984) conducted reliability analysis of stiffened cylinders using a simplified strength model according to DNV technical report 80-0590, 1980. Six different model geometries are used for the study and variation of safety index with load is considered in detail.

Mansour (1990) presented an introduction to structural reliability theory in the form of ship structural committee report (SSC-351). The author presented a state-of-the-art report in structural reliability theory directly specifically for marine industry.

Mansour & Wirsching (1994) studied the sensitivity factor and their application to marine structures. They considered four different ships for their study and presented the potential of using sensitivity factors in decision making and trade-off studies.

Zheng & Das (2000) proposed an improved response surface method for reliability analysis of stiffened plate structures. The response surface function is formed in a cumulative manner in order to account properly for the second order effects in the response surface with acceptable computational effort involved in the evaluation of the state function.

Guedes Soares & Teixeira (2000) performed structural reliability analysis of two bulk carriers. They considered the time dependent degrading effect of corrosion on the capacity of structure. First-order reliability method was used for calculating the probability of failure. It was shown that the loss in ultimate strength in sagging is equivalent to the reduction in total area of the section, but the ultimate moment in hogging exhibits a larger reduction. Comparison of reliability indices for single and double skin tankers were performed and it was observed that the single skin tankers exhibits lower reliability index.

Das *et al.* (2003) presented modelling uncertainty evaluations of strength predictions of ring stiffened shells and ring and stringer stiffened shells for various modes of buckling and various radius to thickness ratio values (range used in offshore structures). Comparisons are made for API BUL 2U and DNV buckling strength of shell models.

Fang & Das (2005) used Monte Carlo simulation to predict hull-girder collapse reliability for intact and damaged ships. The strength predictions were based on Smith's method which was presented in Fang and Das (2004). Paik *et al.* (2003) carried out time-dependent reliability model on a bulk carrier, a double hull tanker and a FPSO. The reliability model accounts for the effects of fatigue-induced cracking and corrosion. Timelines are presented for each vessel relating the probability of hull-girder failure to ship age. Each timeline is heavily dependent upon the modelling assumptions such as severity and location of corrosion or cracking.

Khan & Das (2008) carried out a sensitivity analysis to determine the most important random variable responsible for the failure of ship structures. This he study shows the importance of the contribution of the design variables towards the uncertainty of the limit state function and the advantages for using the sensitivity factors for safety assessment of ship structures.

Zhi Shu & Moan (2010) used an interaction equation based on ultimate hull girder strength assessment obtained by nonlinear finite element analysis as the

basis for the failure function. The annual probability of failure was obtained by FORM analysis considering two typical load cases, namely, pure longitudinal hogging bending moment and local lateral pressure loads. The results show that the local lateral pressure has a significant influence on the annual probability of failure of bulk carrier in the hogging and alternative hold loading.

2.5 Critical Review

From the above state of the art review of the works in the field of strength and reliability of thin walled structures, it is understood that there are many works carried out to understand and predict the structural response under various loading conditions. The imperfection sensitivity of stiffened panel structures is addressed by many researches and there are approximate solutions also proposed. From different approaches, it is observed that none of these methods appear to handle both the weld induced geometrical distortions and residual stresses together. Conceptually, the formulation proposed by Faulkner (1975) is not able to incorporate the contribution of geometrical effects due to imperfections on the structural capacity. On the other hand, the well known Perry-Robertson eccentric column approach cannot incorporate the contribution of residual stresses in the formulation. Pu. *et al.* (1997) modified the Faulkner's approach so that it can incorporate the geometrical imperfection but it is not a straight forward approach. There are some empirical formulae available but none of these relations explicitly taking the imperfection effects into consideration. There are many experimental works carried out for the strength of the stiffened panels but none of these tests explicitly focusing the effects of imperfections on the strength of structures. So the present beliefs with respect to the influence of imperfections on the structural strength are theoretical perceptions.

There are design codes to predict the structural capacity of stiffened cylinders but the basic formulations and various design factors are included directly from the aerospace industry. So the predictions using these factors may not

completely applicable for marine environments and loading conditions. The accuracy of the strength models are highly dependent on various empirical constants and factors which are developed with the observations of the researchers and the specific area of application. A proper validation of the design codes is necessary with experimental and numerical results before these codes can be used for the design and reliability analysis.

Chapter 3. Experimental Analysis of Stiffened Plates

3.1 Introduction

There are many analytical approaches which can incorporate the imperfection effects in the plated structures. However the theoretical predictions have many limitations in incorporating the imperfections with all its parametric aspects. Furthermore, the insights on the effect of imperfection parameters are theoretical to a great extent. Different approaches predict the influence in different perspectives and there are often contradictions. Paik *et al.* (2004) and Pretheesh *et al.* (2009) suggest that the distortion is not always reducing the strength of the structure but at certain levels it enhances the structural capacity. This thesis is particularly looking into the structural response of thin walled stiffened components with more precisely defined structural imperfections on plates which are quite difficult to incorporate in the presently available formulae. So the estimates of imperfection influence based on theoretical assumptions or analytical approaches may not always reflect the reality. The time, effort and cost for the reworks and increased safety factor to compensate for the imperfections could not be justified if the assessment of the strength with imperfections is not correct. Considering these factors, it is required to investigate the effects on practical structures. The experimental test conducted by Horne *et al.* (1976, 1977) and Faulkner (1977) recorded the initial geometrical imperfections and residual stresses in each stiffened panels. But these tests do not reveal the contribution of the imperfection parameters on the strength of the structure. None of the experimental test programs are found to address the influence of imperfection factors explicitly but only as matter of consideration.

An experimental test program was planned in collaboration with BAE Systems, Glasgow to understand this problem in depth. Ten stiffened panels made of the

typical material used for the 'Type 45 destroyer' warship were planned to fabricate with varying imperfection parameters and to be tested for the ultimate compressive strength. This study was carried out to identify the effect and influence pattern of geometrical imperfections and residual stresses.

The designing of the test specimen, the frame design (for the boundary condition simulations), supervising and monitoring the fabrication process, measuring the imperfections, recording and processing the test data etc. were carried out by the author in collaboration with Mr. Tony Crow (Principal structural engineer, BAE Systems).

3.2 Experimental Facility

The tests at Corus (Tata Steel) Laboratories, Rotherham were undertaken on a hydraulic press testing machine predominantly used for the tensile strength testing. The hydraulic testing machine is shown in Figure 3-1 & Figure 3-2.

The size and capacity limitations of the machine were as follows:

1. Central chuck size 200mm
2. Depth of panel 1200mm
3. Height of panel 1500mm
4. Load capacity 2000kN

The machine is applying load on the specimen through the bottom hydraulic ram shown in Figure 3-2. The machine is capable of real time monitoring and recording of the applied load and the axial displacement at the hydraulic ram during the test. This data can be used to generate the load-extension or stress-strain plot of the mounted specimen. The facility also includes heavy lifting tools to move and handle the specimen safely.

Figure 3-1 Corus (Tata Steel) Test Rig
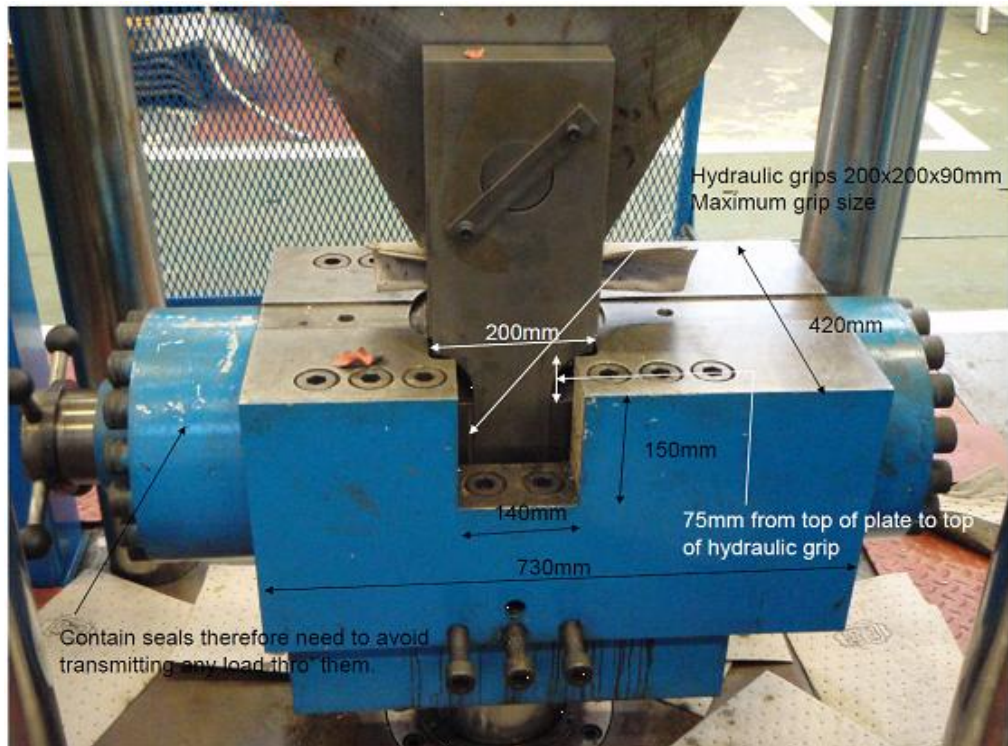
Figure 3-2 Corus (Tata Steel) Test Rig Grips

3.3 Material Properties of the Specimen

The material used for the stiffened plates was DH36 grade Steel. The normal yield stress being 355 MPa, Young's Modulus was taken as 203.5 GPa and Poisson's ratio as 0.3. A laboratory test was also carried out to verify the Yield and Ultimate Stress values. The certificated values are as shown in Table 3-1. The material type is designated as M1, M2, M3 and M4. The material testing results are presented in Appendix A.

Table 3-1 Material Properties

Type	Part	Youngs Modulus (Gpa)	Poissons ratio	Yield stress (Mpa)	Ultimate stress (Mpa)
M1	4mm Plate - LR Grade DH 36	203500	0.3	400	504
M2	80x5 OBP – LR Grade DH 36	203500	0.3	367	478
M3	5mm Plate – LR Grade DH 36	203500	0.3	405	574
M4	60x4 OBP - LR Grade DH 36	203500	0.3	339	459

3.4 Fabrication of Specimen Panels

The above explained machine constraints in Section 3.2 limited the panel size to 4mm plate with three 80x5mm OBP longitudinal stiffeners spaced at 340mm (*b*) apart so that the area multiplied with the material yield stress reaches nearly 2000kN. The panels used for the tests were 1020mm long (length, a) by 1400mm wide (Total width, B). A variation in the scantling is achieved with a 5mm plate of the same dimensions with three 60x4mm OBP stiffeners. The typical specimen geometry is shown in Figure 3-3.
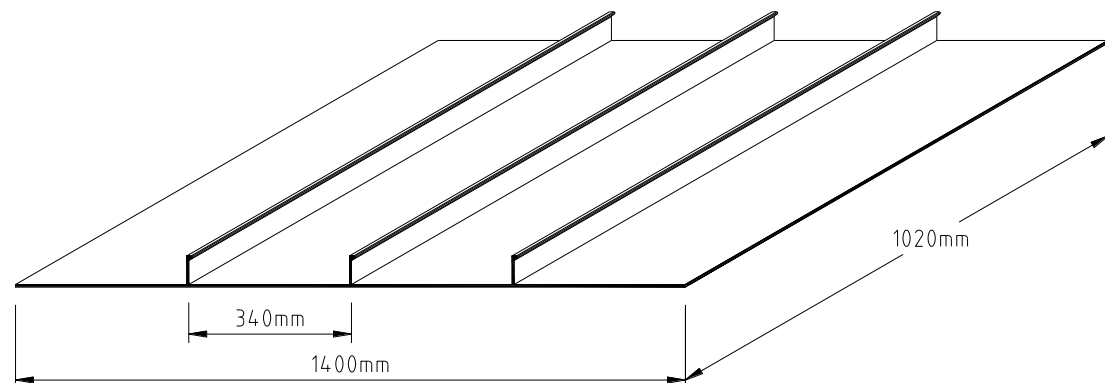
Figure 3-3 Geometry and dimensions of the panel specimen

These panel sizes represented approximately 2/3 scaled panels with respect to the panel dimensions and scantlings that are to be considered for the parametric study on the strength and reliability of stiffened and unstiffened plate scantlings to represent frigate/destroyer type ships.

The scantlings and dimensions of two types of stiffened plate configurations and corresponding material properties (Table 3-1) are shown in Table 3-2. The cross sectional centre of gravity of the two panels should be aligned with the line of action of the force.

Table 3-2 Stiffened plate scantlings and dimensions

Type	Plate thickness t_p (mm)	Stiffener height h (mm)	Stiffener thickness t_s (mm)	Centre of gravity from plate bottom (mm)	Plate material	Stiffener material
SP1	4	80	5	11.7	M1	M2
SP2	5	60	4	6.5	M3	M4

Eight panels of the first scantling size (SP1) and two panels of the second scantling size (SP2) were fabricated in the weld training centre at BAE Govan, Glasgow with differing levels of weld distortion and size of weld to investigate the effects from these.

Figure 3-4 Restraints on the panels and welding process

The plates were continues without any joints (1020x1400mm). The stiffeners were fillet welded (single pass) at both sides. The variation in residual stresses

is achieved by changing the heat in put by changing between Metal Arc welding (high heat) and TIG welding (low heat). The variation in the initial distortion is achieved by welding the structure with and without restraints on the plates and changing the heat input as well. Figure 3-4 shows the restraints and welding used for the fabrication of the plates. The method of fabrication and welding details for each panels are tabulated in Table 3-3.

A stress relieving process has been carried out to remove the trapped residual stresses for two plates to understand the change in structural behaviour. Heating pads were attached to each weld line and heated to 450℃ and maintained at that temperature for two hours and then allowed to cool slowly. The stress relieving process is carried out for panels 7 and 8 which are high heat welded without restrains.

3.5 Measurements of Panel Distortion

The geometrical distortions in each specimen plates are measured as the plate distortion (w_p), longitudinal and transverse stiffener bowing (w_{bl} & w_{bt}) and stiffener warping (v_s) for the three stiffeners as shown in Figure 3-5.
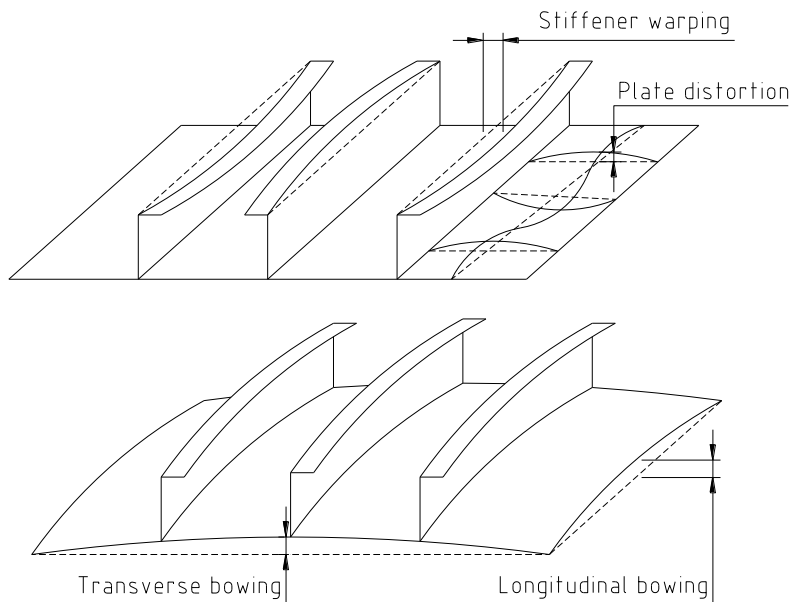
Figure 3-5 Distortions in a stiffened panel

Figure 3-6 Measuring distortion (Pretheesh Paul & Tony Crow at BAE Systems, Glasgow)

The distortion levels of the 10 panels were measured using a frame attached with wires and measuring the distance from the reference wire to the plate at 108 points in each panel using a steel rule (Figure 3-6). Figure 3-7 shows the measured distortion patterns (amplified for illustration) of Panel 3 and Panel 5 with the initial distortion on plates.
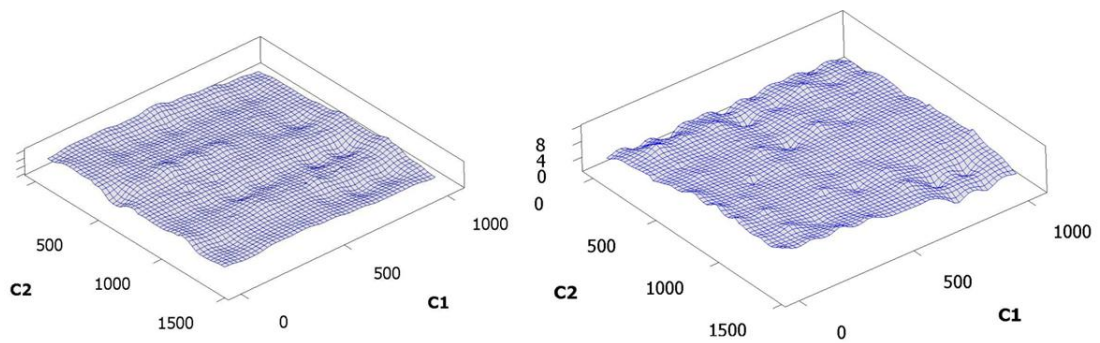
Figure 3-7 Record of Panel 3, and Panel 5 Initial Distortion (Amplified)

The maximum levels of plate distortion (w_p), longitudinal and transverse stiffener bowing (w_{bl} and w_{bt}) and stiffener warping (v_s) for the three stiffeners (refer Section 6.3) are provided in Table 3-3. From the table, it is observed that the high heat welding produced more distortion. It also indicates the presence of high residual stresses. Plate numbers 7 and 8 were stress relieved models. The values for 7a, 8a and 7b, 8b indicate the distortion levels before and after stress relieving. The stress relieving process appears to reduce the distortion and it indirectly confirms the fact that the weld induced residual stress was also reduced by this reheating process.

Table 3-3 Record of panel fabrication and Initial distortions

Plate No.	Type	Fix	Weld	Current (Amp)	Voltage (Volt)	Heat Input (kJ/mm)	Torch Speed (mm/min)	w_p	w_{bl}	w_{bt}	v_{s1}	v_{s2}	v_{s3}
1	SP1	Restrained	Low heat	195	22.5	8.3	520	8	4	0	0	0	0
2	SP1	Unrestrained	High heat	300	24	13.3	410	15	5	8	0	0	-1
3	SP1	Restrained	Low heat	195	22.5	8.3	520	7	2	5	0	0	0
4	SP1	Restrained	Low heat	195	22.5	8.3	520	8	1	4	0	0	0
5	SP1	Unrestrained	High heat	300	24	13.3	410	10	5	8	0	0	0
6	SP1	Unrestrained	High heat	300	24	13.3	410	10	3	6	0	0	0
7a	SP1	Unrestrained	High heat	300	24	13.3	410	8	3	5	0	0	0
7b	SP1	Unrestrained	Stress relieved	300	24	13.3	410	7	0	3	2	0	0
8a	SP1	Unrestrained	High heat	300	24	13.3	410	11	2	3	1	0	2
8b	SP1	Unrestrained	Stress relieved	300	24	13.3	410	9	3	0	0	0	2
9	SP2	Restrained	Low heat	195	22.5	8.3	520	9	2	3	0	2	2
10	SP2	Restrained	Low heat	195	22.5	8.3	520	9	0	0	0	0	0

w_p - Plate distortion, w_{bl} - Longitudinal bowing, w_{bt} - Transverse bowing, V_s - Warping of stiffeners 1, 2 and 3

3.6 Design of Test Rig Frame

The boundary conditions chosen to represent ship structure were simply supported edges but with the side edges being free to slide, with the stiffeners being constrained against warping, but free to rotate about a vertical axis, at their ends.
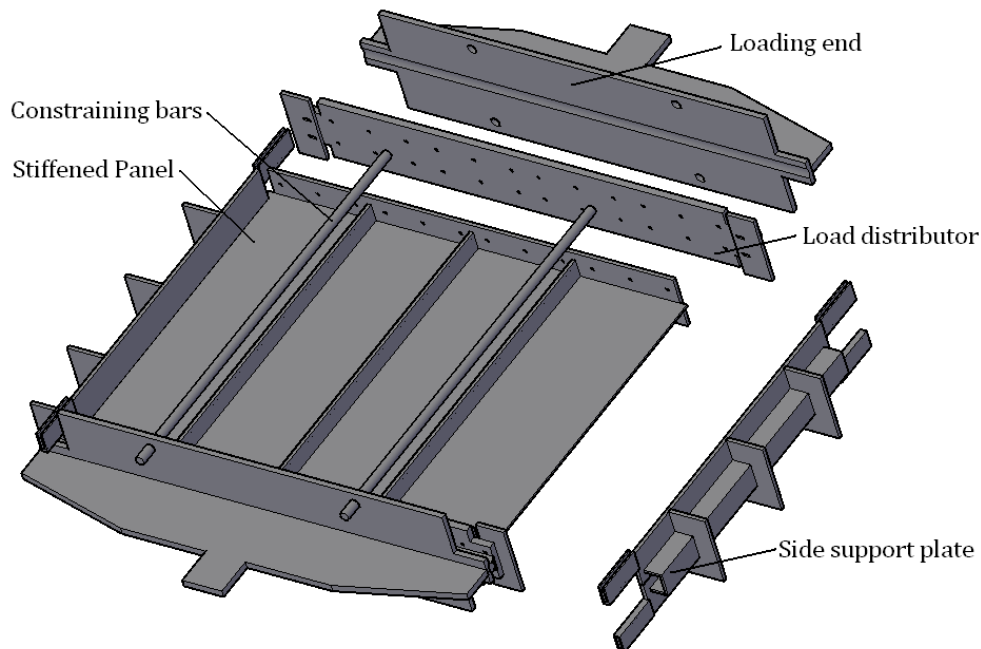
Figure 3-8 Initial Test Frame Set-Up

A test frame was designed on this basis to achieve the boundary conditions for a typical structural panel. This was to be accomplished by means of a circular bar between the loading end and load distributor placed in a grove. The line of action of the force should be at the cross sectional centre of gravity and this was achieved by suitably adjusting the holes to bolt the panel to the distribution plates. The sides were assumed to be able to slide freely in a gap provided in the side support plates. The side support plates would be kept in position through lugs which is locked to the load distributor through a gap as shown in Figure 3-8.
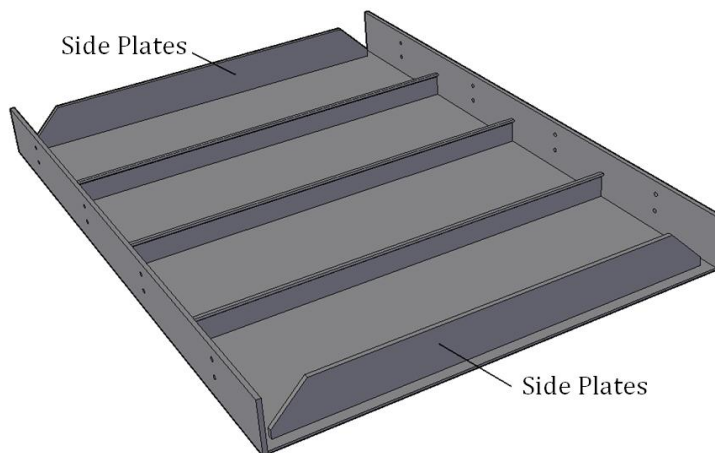
Figure 3-9 Final Panel Configuration with side plates to replace the side support frame

The initial design of the testing frame set-up, as shown in Figure 3-8, with a channel at the sides was seemed too complicated to manufacture and eventually a simpler design was designed with tapered flat bar edge stiffeners cut short of the ends by 25mm to avoid them contributing to the buckling performance of the panel (see Figure 3-9). This model was shown a reasonable agreement with the desired boundary conditions according to FEA results.

A 10mm thick load end plate was welded to the ends of each panel to keep the stiffener end fixed against translational and rotational degrees of freedom. The end loading was achieved by means of 20mm thick load distribution plates bolted to the panel end plates. A tapered loading plate was added at each end, in order to spread the load over the full width of the panel, from the 200mm wide throat that fitted into the chuck of the test machine.
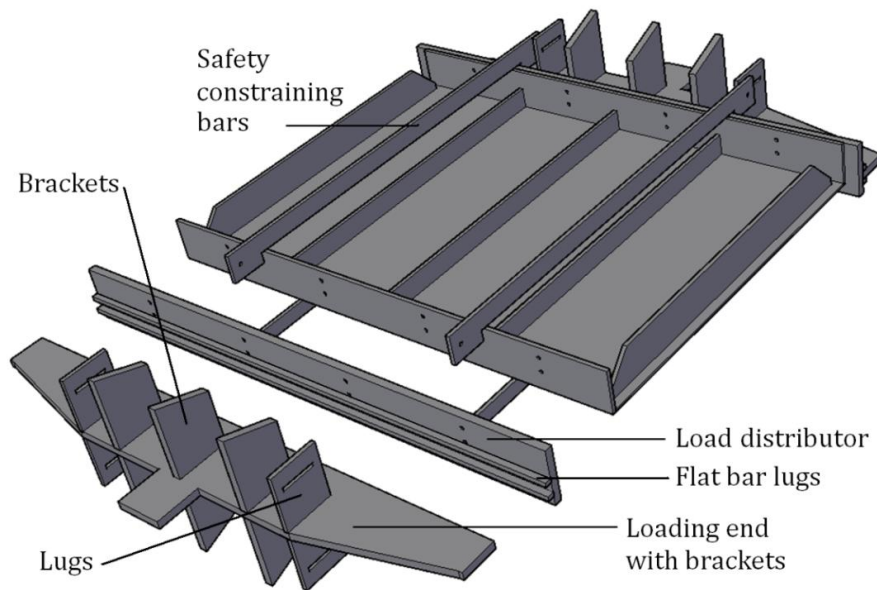
Figure 3-10 Final Loading Plate Arrangement

It was found necessary to add six 20mm thick brackets to each loading plate bearing on the face of the test machine to avoid a tripping of the loading plate. The edge of the loading plate bore on the face of the 20mm thick distributor plate that was bolted to the end plates of each panel, and was held in place by flat bar lugs fitted to the face of the distributor plate. Safety constraining bars were fitted into lugs with slotted holes to ensure that the panels did not become free at the point when buckling occurred (See Figure 3-10).

3.7 Axial Compression Testing

The tests at Corus (Tata Steel) Laboratories, Rotherham were undertaken on a hydraulic testing machine with maximum capacity up to 2000 kN. The machine is normally used for the tensile testing.

Two strain gauges were fitted to each panel as shown in Figure 3-11 for the strain in plate and stiffener under the action of axial loading. During the tests two additional strain gauges were fitted on Panel No. 7 to the web of outer stiffeners to monitor the relative loading of the centre stiffener and the outer stiffeners during the test.
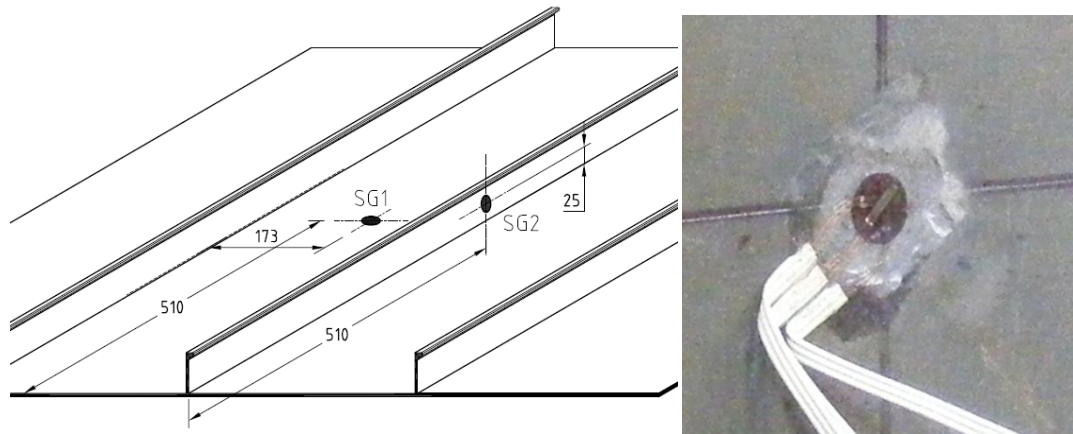
Figure 3-11 Strain Gauge Positioning

The typical test arrangement with the frame and panel mounted on the testing machine is shown in Figure 3-12.

Figure 3-12 Panel Mounted on the Test Rig

The tests were carried out so that the displacement of the loading end and the total load applied were directly recorded in a computer from the probes attached to the machine. The loading (displacement) was applied till the maximum load capacity of the panel was reached and then continued with the load dropping down substantially with the increased displacement. By that time, the panel had lost stability to withstand any more loads which could be visually identified as well. A typical test monitoring and structural collapse is shown in

Figure 3-13. The computer record and store the load and displacement in a spread sheet data file. Apart from the load displacement data, the computer also record the strain gauge readings (micro strain) against each increment of the load.

Figure 3-13 Monitoring of the compression test and the collapse of the structure

A limitation of the test rig was that the lower chuck connected to a hydraulic ram (circular piston) was free to rotate about the axis. This gave an extra rotational degree of freedom for the panel end. So a full pinned edge condition was not established at the panel end where the hydraulic ram axis became free to rotate relatively about this pivot point. This caused the test panels fail in a torsional mode before the full axial buckling failure load for the preferred condition was reached. The Figure 3-14 shows that the structure is rotated about its longitudinal centrodial axis at failure. The rotation of the hydraulic chuck is clearly detectable from the picture.

Figure 3-14 Unconstrained rotational degree of freedom

3.8 Test Results

The first panel was set up in January 2011 and tested by Corus. During this trial, the loading plates were getting distorted at the neck before the full load was achieved. New loading plates were manufactured with additional brackets to avoid this distortion as discussed in the previous sections and the first panel was again tested successfully in February 2011. Following this, the tests of the remaining 9 panels were performed in a single programme of tests lasting two days in early March. These were undertaken on 1st and 2nd March 2011.

Figure 3-15 Panel 1 Failure

The buckled Panel 1 is shown in Figure 3-15 and the load – deflection and stress-strain curves are shown in Figure 3-16. The stress is the load per cross sectional area and the strain is the displacement divided by the length of the plate. The stress is non dimensionalised using the yield stress of the stiffener material and the strain is non dimensionalised using the strain corresponding to the yield stress. The curve indicates that the ultimate load was achieved at about 11.11mm of axial displacement. The ultimate load for this panel was 1229.2kN.
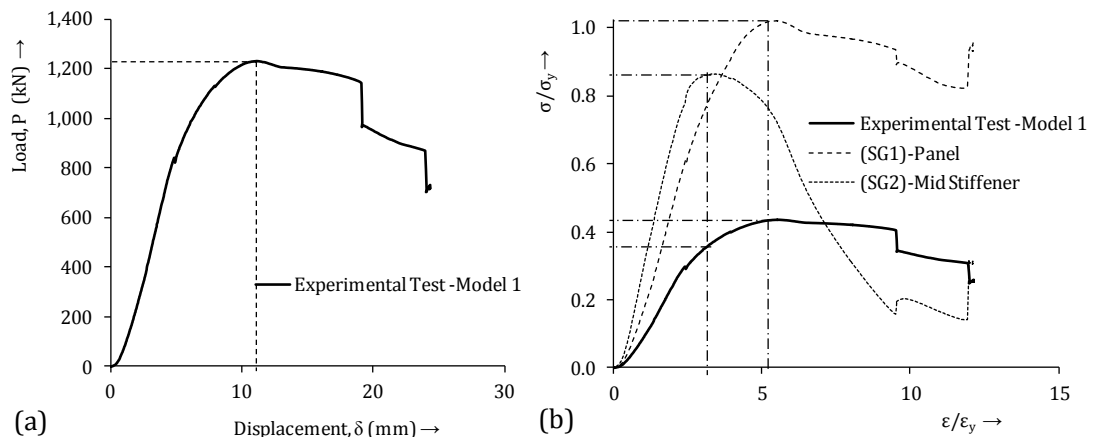
Figure 3-16 (a) Load shortening curve of Panel-1 (b) Non-dimensional stress strain curve for Panel-1

Figure 3-16(b) shows the strain gauge readings including the structural response in a non-dimensional stress strain space. It is found that the panel and stiffener show yield stress values of corresponding material nearly at the failure point. It further illustrates the fact that the stiffener is taking major portion of the load right from the beginning (increased slope) and it reaches its yield stress and then started to yield. Further, the plate started to take some additional load and goes to its yield value extending the capacity of the whole structure and finally the ultimate load is reached at around the non-dimensional strain value reached 5.2. The structure kept carrying nearly the same load till the strain reaches 10 and then suddenly dropped. This indicates the sudden torsional instability happened to the structure due to the unconstrained axial rotational degree of freedom.

A comparison of the strain gauge readings gives an indication of the critical axial stress for the stiffener plate combination. The structure loses its integrity when the stiffener reaches its yield stress and the extra strength from that point is the plate strength along with plastic deformation of the stiffener. So the actual limit state of the structure in terms of the structural integrity is at a lower point than the observed structural limit load as indicated in Figure 3-16(b). In Figure 3-16(b), the non-dimensional stress value appears to shoot above 1 because the yield stress used to non-dimensionalise the stress is of the stiffener which is lower than the plate (Table 3-1).

Panels 1-8 all failed by initial convex bowing of the stiffeners. Then most of these showed a critical failure point when torsional buckling occurred. This was particularly pronounced for the heavily welded/high heat input panels (Panels 2, 5, 6, 7 & 8), even if stress relieving was applied. It was observed that the upper loading plate edge was not straight and as a result a gap was evident when the centre of the loading plate was in contact with the panel. Thus for panels 4 and 5 shims were added at the outer stiffener positions to ensure a more even loading of the outer stiffeners along with the centre stiffener. This did not significantly alter the results, and was not applied to the later panel tests.

Figure 3-17 shows the behaviour of the Panel-7 in which additional strain gauges were mounted on both the outer stiffeners. It is observed that unlike the Panel-1, the plate started to experience more strain and hence more stress from the beginning. The yielding of both the plate and centre stiffener occurs nearly around the non-dimensional strain value of 2.5. The structure shows inelastic or elasto-plastic behaviour from that point and continues to take additional load till the centre stiffener collapses. From the strain gauge readings, it is clear that the outer stiffeners are not effectively bearing the load. This is because of the rotational freedom at the end so that it cannot resist axial thrust as the axes of the outer stiffeners slip away when the load increases. Finally it offers some resistance from within the structural boundary when the centre stiffener

collapses. This clearly explains why the structural strength is less than the proposed strength with the additional rotational degree of freedom.
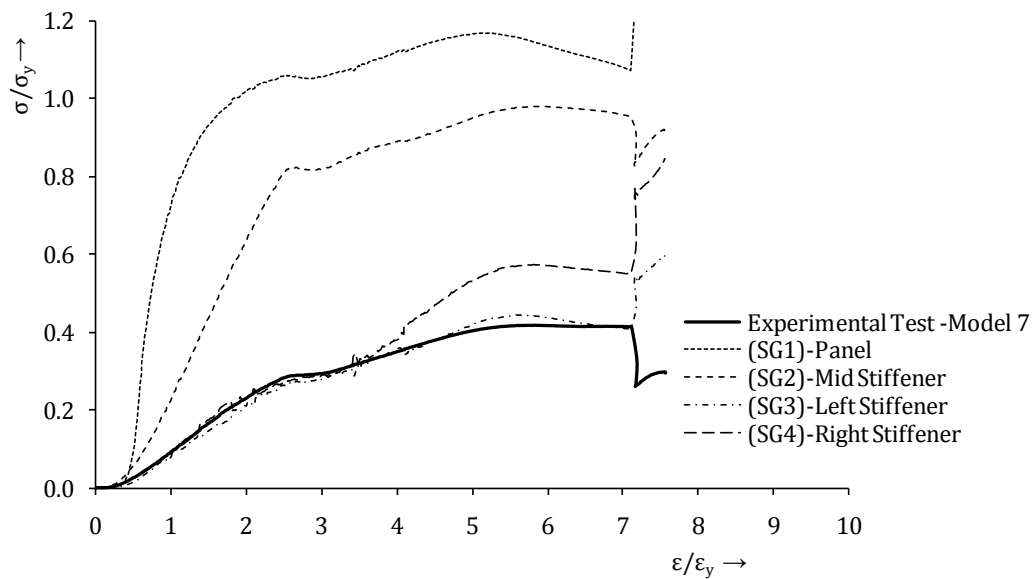
Figure 3-17 Test results of Panel-7 with 4 strain gauges
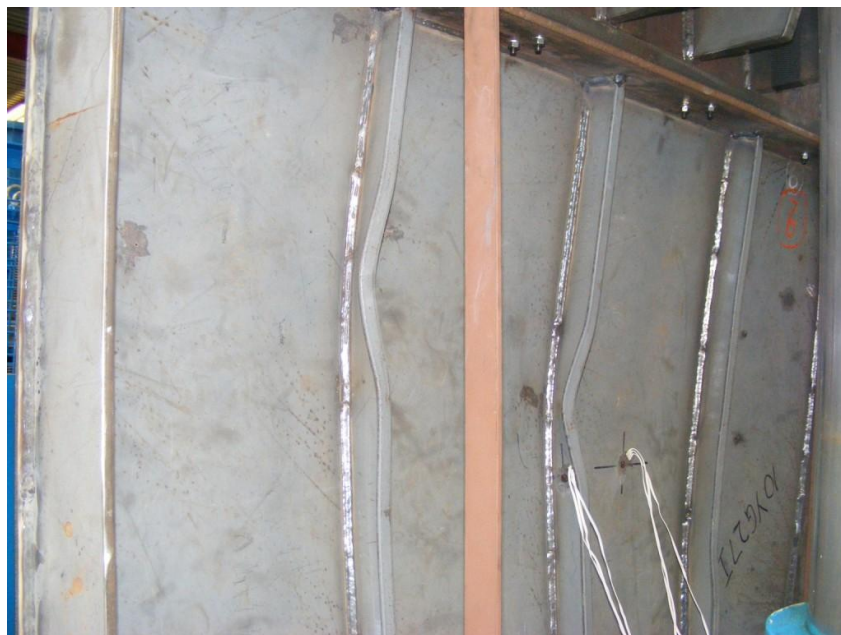
Figure 3-18 Stiffener induced failure of Panel-9

Panel-9 and 10 were of different scantlings but the structural behaviour observed was similar to that predicted by the strength analysis. In these cases the stiffeners were comparatively weak and the plate thickness was relatively greater (Table 3-2). The Panel-9 failed in a classical stiffener induced mode as

shown in Figure 3-18. This was believed to be because of the high stiffener bowing distortions in the model as can be noticed in Table 3-3.

The actual test recording for each panel includes the incremental load-displacement effect points and the strains recorded for each strain gauge. The full test recording for all 10 panels is given in Appendix B. A summary of the ultimate load achieved and corresponding displacement for the panels are given in Table 3-4.

Table 3-4 Summary of Test Results

Plate No.	Experimental Results			
	σ_u/σ_y	δ_u (mm)	σ_u (kN/mm^2)	P_u (kN)
1	0.44	11.11	174.03	1229.20
2	0.40	14.73	161.25	1138.93
3	0.44	12.52	176.18	1244.35
4	0.45	13.07	181.11	1279.15
5	0.37	8.35	146.26	1033.02
6	0.41	12.29	164.30	1160.48
7b	0.42	11.66	167.28	1181.48
8b	0.40	8.95	161.31	1139.30
9	0.29	4.13	116.02	913.56
10	0.38	6.90	151.26	1191.00

P_u - Ultimate load in kN, δ_u- Displacement at failure

 One of the primary objectives of this study was to understand the influence of weld induced distortion and residual stresses on the buckling strength of the stiffened plates. So, in the following sections, a comparison is made based on the test results and initial measurements.

3.8.1 Effect of Distortion on Buckling Strength

From Table 3-3, the unrestrained-high heat welding produced more distortion so Panels 2, 5, 6 and 8 are considered to have increased initial distortion. The restrained-low heat welded Panels 1, 3 and 4 are considered to have lower initial distortion. Panel 7 is actually an unrestrained-high heat case, but the distortion is comparatively lower owing to the stress relieving, and hence is added to the low distortion category. Figure 3-19 shows the comparison of the

two categories of structures. It is observed that the increased distortion of panels 2, 5, 6 and 8 caused a lower torsional failure of the panel than for Panels 1, 3, 4 and 7, and this is matched with lower strength values for the specific FEA predictions performed for these cases. However, no significant comparison of the shape of the ultimate strength curve, for the more heavily distorted panels, can be made owing to the premature failure of the panels in torsion.
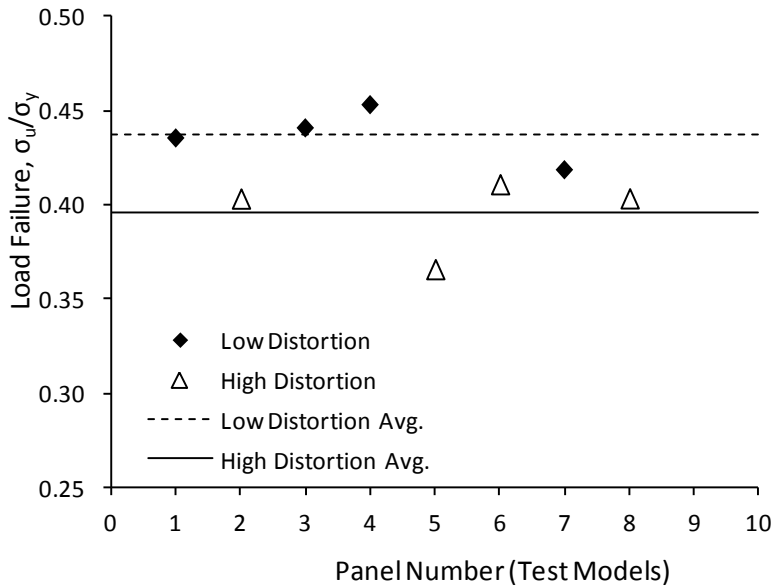
Figure 3-19 Effect of Initial Distortion

The average strength of low distortion panels in terms of (σ_u/σ_y) is 0.437 and for high distortion is 0.396. So the reduction in strength is 9.38%. So experimentally, a reduction of nearly 10% or more can be expected in a structure with moderate distortion from heavy welding. The average of the two categories shows good distinction from each other indicating clearly the deteriorating effect of initial distortion on the strength of structures with identical scantlings. The performance of the more highly distorted panels evidently also includes effects from higher residual stresses.

3.8.2 Effect of Residual Stress on Buckling Strength

The residual stresses are induced on the structure primarily because of the welding. Conventionally and with proved experiments, the heat affected zone

(HAZ) is directly related to the extent of residual stresses trapped in the structure. So the total heat input on to the structure during the welding operation will determine the extent of heat affected zone. The measurement of HAZ is practically not very easy to determine. But the Panels can be categorised same as before based on the welding techniques adopted. Three category are considered here as, Low heat welding (Low HAZ and low residual stress), High heat welding (High HAZ and high residual stress) and stress relieved (heat treated after welding so intermediate residual stress).

The average strength of low heat welded panels in terms of (σ_u/σ_y) is 0.443 and for high heat welded is 0.393. So the reduction in strength is 11.29%. When the high heat welded panels are stress relieved, the average strength becomes 0.411 and which is 7.22% less than the low heat welded panels. So experimentally, a reduction of nearly 10-12% or more can be expected in a structure with moderate weld induced residual stress from heavy welding and the stress relieving improves the strength by approximately 4%. This distinction between results for the panels provides evidence for the separate effects of distortion and residual stress.
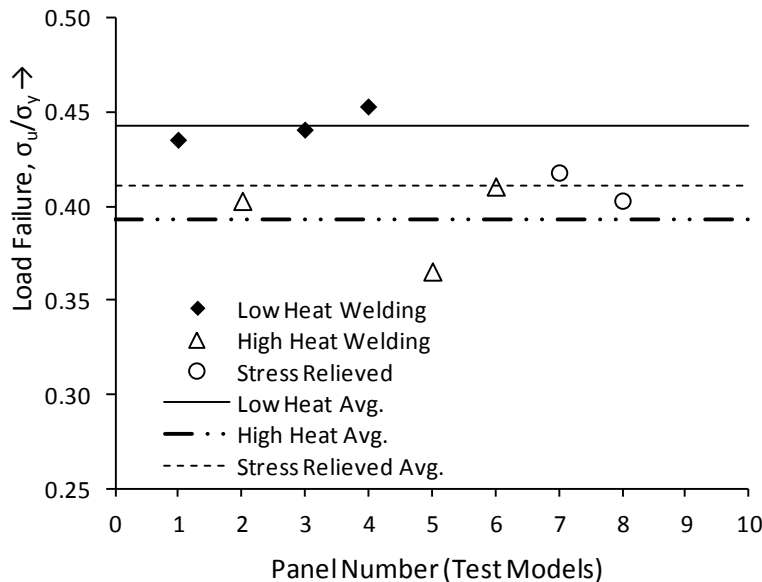
Figure 3-20 Effect of Residual Stress/Heat Input

Figure 3-20 shows the comparison of the results. The averages of the three categories explicitly illustrate the fact that residual stress deteriorates the strength of the structure and the stress relieving process improves the strength capacity of the structure.

3.9 Summary

The test program focusing on the fabrication imperfections were conducted successfully providing unique set of experiment data. The hydraulic loading ram which was free to rotate about the axis was a limitation in this program as it prevented the structure to reach the full capacity under axial loading situation.

The data collected and presented in Appendix A for the 10 panels and the material properties provided in Appendix B can be used for further study as there is lot of information available about the structural response which can be utilised by researchers focusing areas beyond the scope of this study.

The effect of initial distortion is experimentally verified and a 10% reduction is observed from the models used for the study. This is further considered while expanding the numerical study with more realistic stiffened plate models and the reliability calculations.

The effect of weld induced residual stress is also experimentally studied. It is observed that there is nearly a 12% reduction in strength with the high heat welding compared with the low heat welding which also contains less residual stress due to the low heat input. The stress relieving processes appear to produce a 4% saving in the strength. They also appear to change the initial distortion.

Chapter 4. Finite Element Analysis of Plates and Shells

4.1 Introduction - Nonlinear Finite Element Analysis

Finite Element Analysis carried out under the assumptions of linear elastic, small deflection behaviour, known as linear analysis, is well known for its simplicity, limited number of inputs required, computational cost effectiveness, provision for the superposition of loads and lot more. There are cases where a linear approach fails completely to predict the response. A realistic ultimate strength analysis of a structure can only be carried out through a sophisticated nonlinear approach as it involves many nonlinear structural aspects. Nonlinear analysis has been used throughout this study since major structural analyses carried out are ultimate strength analysis.

In linear analysis, the displacements are assumed to be linearly dependent on the applied loads, and the behaviour of the structure is assumed to be completely reversible. This means that solutions for various load cases can be superimposed. In many engineering applications, however, the behaviour of the structure may depend on the load history or may result in large deformations beyond the elastic limit. For such non-linear problems, the user must carefully consider how to approach the analysis, model the problem using FE, and use the results of the analysis.

The main feature of linear analysis is that all loads can be applied instantaneously and the loading history is irrelevant. In other words, the displacements are linearly dependent on the loads and, if required, the solution can be scaled. In non-linear problems, however, the loading history is usually important and the actually un-scaled material properties and loads must be specified. Non-linear FE analysis usually involves the solution of a large system

of non-linear equations. The main differences between linear and non-linear analyses are summarised in Table 4-1.

Table 4-1 Comparison of linear and nonlinear analysis

Feature	Linear problems	Non-linear problems
Load-displacement relationship	Displacements are linearly dependent on the applied loads	The load-displacement relationships are usually non-linear
Stress-strain relationship	A linear relationship is assumed between stress and strain.	In problems involving material non-linearly, the stress-strain relationship is often a non-linear function of stress, strain and/or time.
Magnitude of displacement	Changes in geometry due to displacement are assumed to be small and hence ignored, and the original (un-deformed) state is always used as the reference state.	Displacements may not be small, hence an updated reference state may be needed.
Material properties	Linear elastic material properties are usually easy to obtain.	Non-linear material properties may be difficult to obtain and may require additional experimental testing.
Reversibility	The behaviour of the structure is completely reversible upon removal of the external loads.	Upon removal of the external loads, the final state may be different from the initial state.
Boundary conditions	Boundary conditions remain unchanged throughout the analysis	Boundary conditions may change, e.g. a change in the contact area.
Loading sequence	Loading sequence is not important, and the final state is unaffected by the load history.	The behaviour of the structure may depend on the load history.
Iterations and increments	The load is applied in one load step with no iterations	The load is often divided into small increments with iterations performed to ensure that equilibrium is satisfied at every load increment.
Computation time	Computation time is relatively small in comparison to non-linear problems.	Due to the many solution steps requires for load increments and iterations, computation time is high, particularly if a high degree of accuracy is sought.
Robustness of solutions	A solution can easily be obtained with no interaction from the user.	In difficult non-linear problems, the FE code may fail to converge without some interaction from the user.
Use of results	Superposition and scaling allow results to be factored and combined as required.	Factoring and combining of results is not possible.
Initial state of stress/strain	The initial state of stress and/or strain is unimportant.	The initial state of stress and/or strain is usually required for material non-linearity problems.

4.1.1 Numerical Methods for Plate Analysis

The finite difference method (FDM) and the finite element method (FEM) are the two of the most important numerical methods. FDM is simple, versatile, suitable for computer use, and accurate, provided that a relative fine mesh is used. In FDM, the derivative of a function with respect to a coordinate direction at a point is approximated by a weighted sum of the function values at a set of nearby points on the line in that direction. In this way, the plate differential equations and the expressions defining the boundary conditions are replaced by equivalent difference equations. The solution of the plate problem thus reduces to the simultaneous solution of a set of algebraic equations, written for every nodal point within the plate domain.

On the other hand, FEM has been proven to be a very powerful and versatile tool for solving a plethora of plate problems. This method was developed in the 1960s when the increasing emphasis on numerical methods was generated due to the advent of computers. In FEM, the plate is discretized into a finite number of elements (usually triangular or rectangular in shapes), connected at their nodes and along hypothetic inter-element boundaries. Instead of solving the governing differential equations, the weak form equations are solved for solution. The application of FEM has already been extended to practical problems in most engineering fields and coded into many well known commercial programs such as ABAQUS, ANSYS, NASTRAN, COSMOS etc.

4.2 FE Analysis of Stiffened and Unstiffened Panels

A nonlinear finite element method (FEM) has been used to predict the ultimate compressive strength for simply supported stiffened and unstiffened panels. The commercial finite element software ABAQUS version 6.6-1 has been used for this study.

4.2.1 Model Geometry

The geometry and basic dimensions of a typical stiffened plate panel is as shown in Figure 4-1. For unstiffened plates, there will not be any stiffeners considered and the plate portion between two stiffeners will only be considered. The value of stiffener spacing and the length of the panel are taken so as to match with the typical dimensions used in the shipyards.
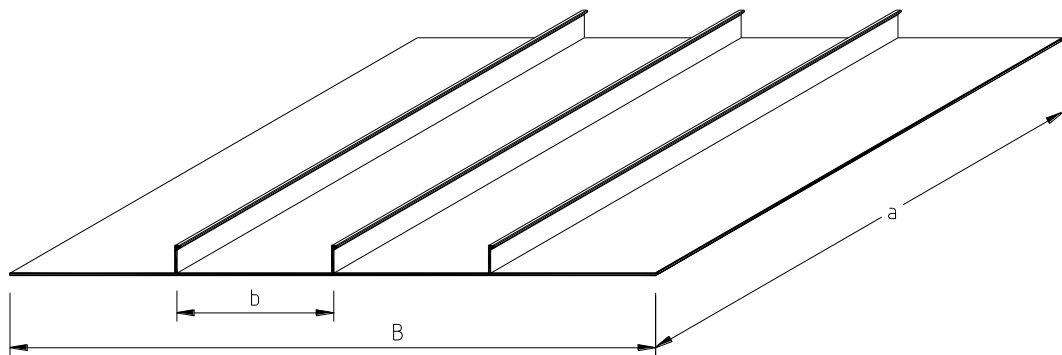
Figure 4-1 Stiffened panel dimensions

The stiffeners used in the structure were OBP (Offset bulb plate) stiffeners. To simplify the FE modelling using shell elements, the stiffener is approximated with the equivalent dimensions as shown in Figure 4-2.
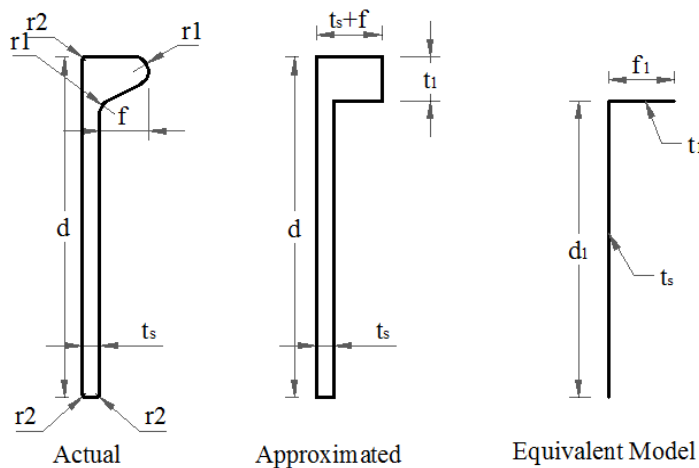
Figure 4-2 Equivalent stiffener model

The actual OBP is approximated as an angle bar by redistributing the area and then the flange is assigned with appropriate thickness to represent the OBP. In

the equivalent model, $f_1=t_s+f$, $t_1=(A_s-d*t_s)/f$ and $d_1=d-t_1/2$ where A_s is the total area of the stiffener

The FE models used in this whole study are broadly classified into four categories as follows:

- *Distortion model (M1):* This model is used to predict the effect of initial plate, bowing and warping distortions in stiffened plate panels. The values of distortions are defined parametrically with some reference observations made onsite.

- *Residual stress model (M2)*: This model is used to predict the effect of weld induced residual stresses in the panel structure due to welds along the plate stiffener joints. The variation in residual stress is assumed parametrically from a range generally followed in the ship/offshore industry. This parametric model is used to conduct a detailed parametric study on the effect of initial distortion, residual stresses and the combined effect of distortion and residual stress in a wide range of unstiffened and stiffened plate scantlings used in ship building. The results are generated to indicate the imperfection effects on the plate and column slenderness.

- *FE model for the test panels with proposed Boundary conditions (M3):* A scaled version of the above models is used for experimental tests fabricated in BAE Systems Surface Ships, Glasgow. The initial distortion was applied according to the measurements from the actual physical panels and the residual stresses are assumed based on the heat input and types of welding. The model is prepared with side frames so as to reduce the complexities in achieving simply supported boundary conditions at sides.

- *FE model for the test panels with actual boundary conditions (M4):* Since the test facility was not capable of achieving the simply supported boundary conditions used in the above models, another parametric FE model is used to predict the axial compressive behaviour of experimental tests.

M1, M2 and M3 and M4 is shown in Figure 4-3.
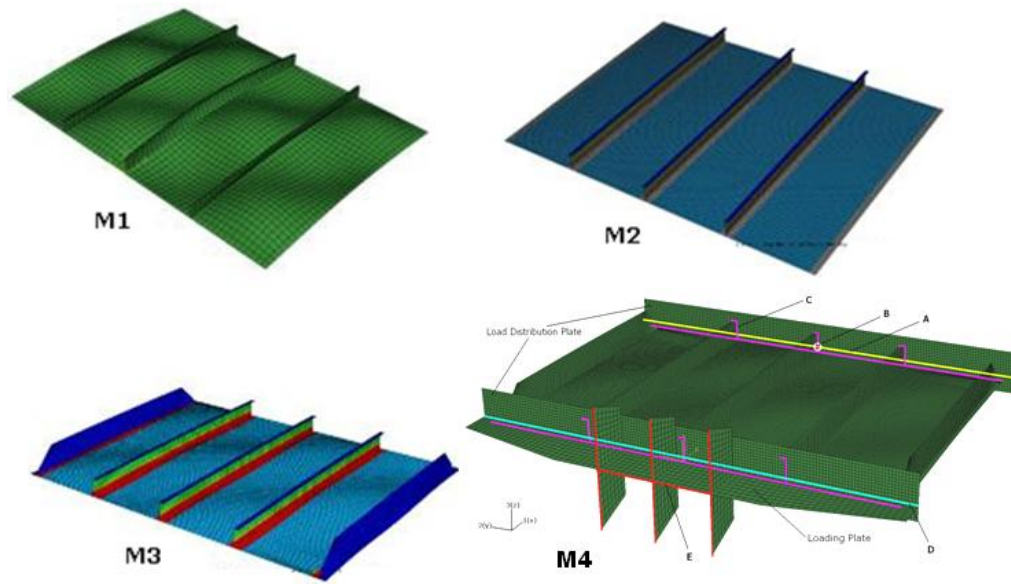
Figure 4-3 FE models M1, M2, M3 and M4

4.2.2 Material Properties

The material used in the study is mainly steel material used for marine applications which is ASTM A131 Steel, DH36 grade. A bilinear perfectly elastic perfectly plastic material model is used for the FE Analysis as shown in Figure 4-4. The yield stress of the DH36 grade steel is 315MPa, the Young's modulus of the material is 203.5GPa and the Poisson's ratio is 0.3.
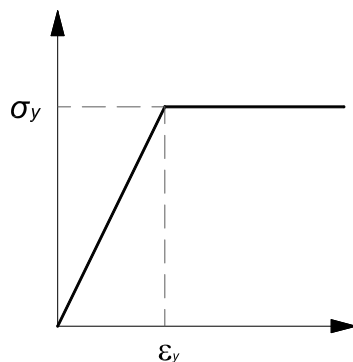
Figure 4-4 Bilinear perfectly elastic plastic behaviour of a steel material

4.2.3 Meshing and Element Types

Shell elements are used to model structures in which one dimension (the thickness) is significantly smaller than the other dimensions and the stresses in

the thickness direction are negligible. Two types of shell elements are available in ABAQUS, conventional shell elements and continuum shell elements. Conventional shell elements discretise a reference surface by defining the element's planar dimensions, its surface normal, and its initial curvature. The nodes of a conventional shell element, however, do not define the shell thickness; the thickness is defined through section properties. Continuum shell elements, on the other hand, resemble three-dimensional solid elements in that they discretise an entire three-dimensional body yet are formulated so that their kinematic and constitutive behaviour is similar to conventional shell elements. Continuum shell elements are more accurate in contact modelling than conventional shell elements, since they employ two-sided contact taking into account changes in thickness as shown in Figure 4-5.
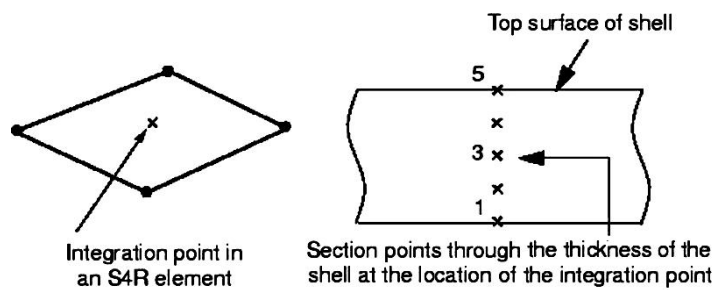
Figure 4-5 Section points in numerically integrated shells

Four-noded, iso-parametric shell elements with reduced integration (S4R) have been used for all FE models used in this study. A homogeneous shell section is assumed for the entire structure with uniform meshing.

A mesh sensitivity analysis was carried out for the plated structures under study. Both the mesh size and element aspect ratio have been changed to study the response. Figure 4-6 shows the mesh density and aspect ratios of elements used for the sensitivity study. The plots in Figure 4-7 show the results of a mesh sensitivity study carried out for two sample scantlings of stiffened plates used in this study. The mesh has been altered in its size and aspect ratio.
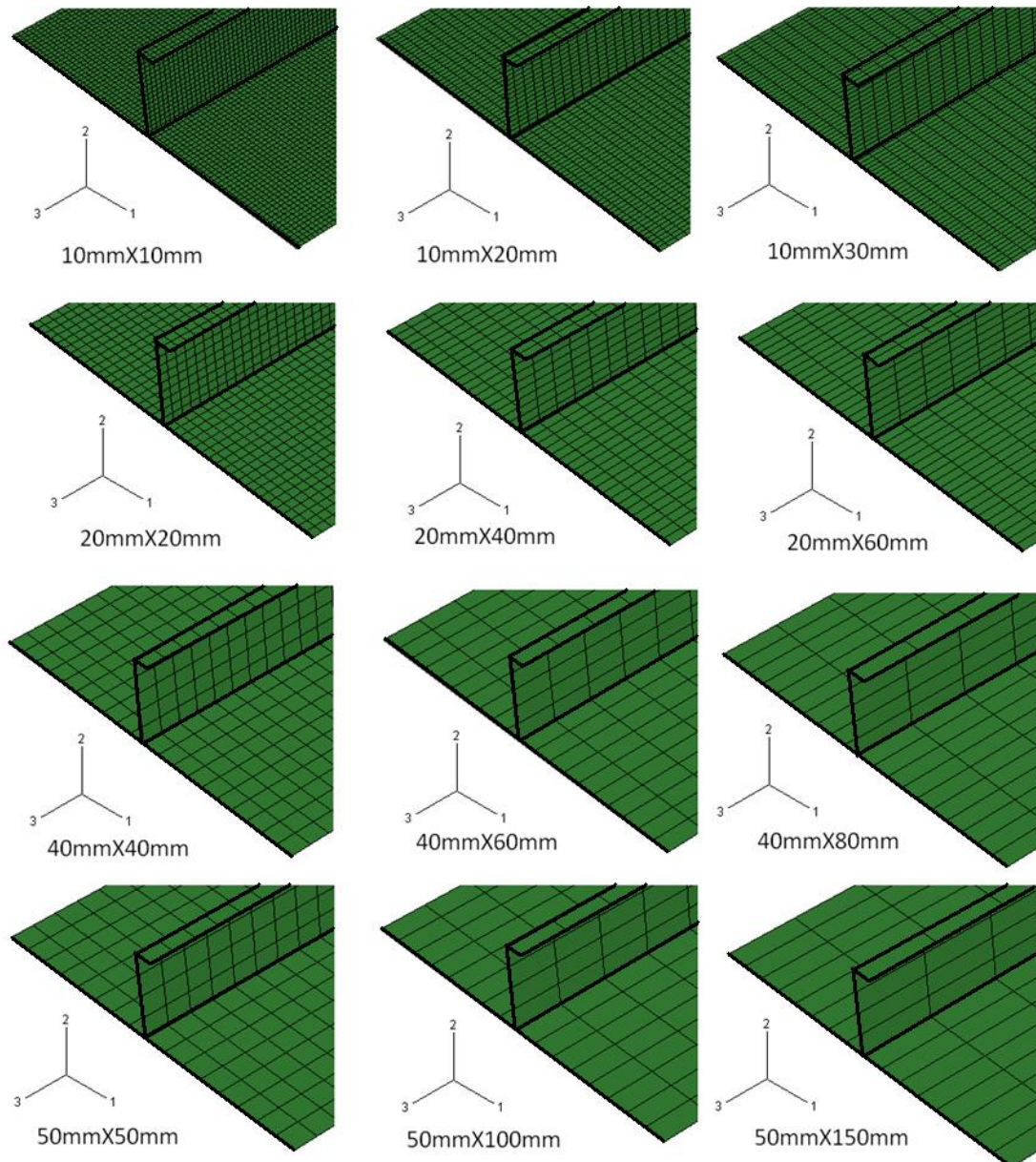
Figure 4-6 Element size used for the mesh sensitivity study (a x b x t x OBP – 2400 x 800 x 12 x OBP200 x 12, all dimensions in mm)

The analysis results suggest that the elements with aspect ratio (a'/b') 3 and width (b') in the range of 20mm appears to be a mesh which is computationally effective with minimum cost and reasonably accurate for the type of structure studied. For the models used in the study, the mesh size varied from 10mm to 20mm depends on the case and mesh density needed for a sensible input of the residual stresses.

(a) 12mm Plate- 200X12 OBP   (b) 8mm Plate- 200X12 OBP
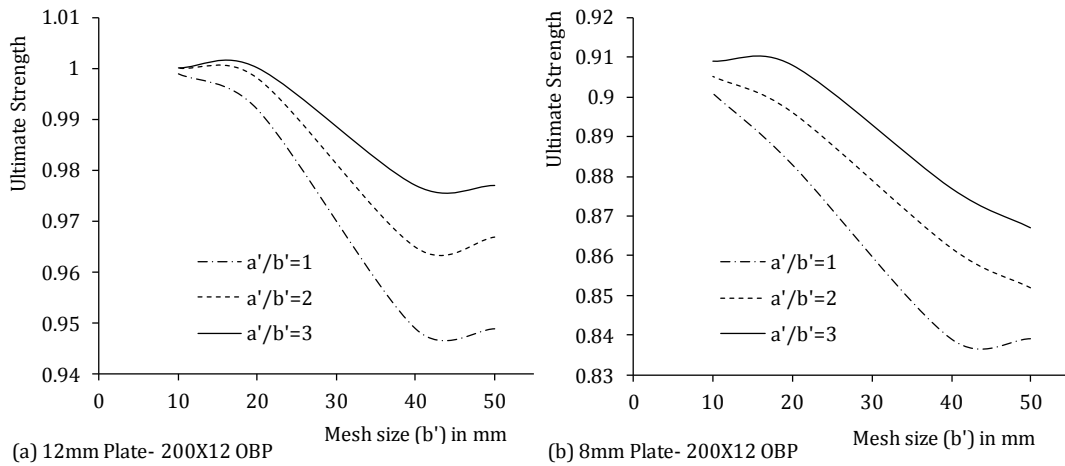
Figure 4-7 Mesh sensitivity study for two plate scantlings (a) and (b)

4.2.4 Boundary Conditions and Loading

One of the most important aspects of a finite element analysis for sensible results is the definition of realistic boundary conditions. The boundary conditions have great effect on the results of FE analysis. Particularly for plated structures, most of the theoretical equations and design codes are formulated based on the assumption of simply supported edges and pinned ends boundary conditions. Some of the codes provide correction factors for clamped and other types of boundary conditions in order to represent the influence of boundary conditions on the response of structures.
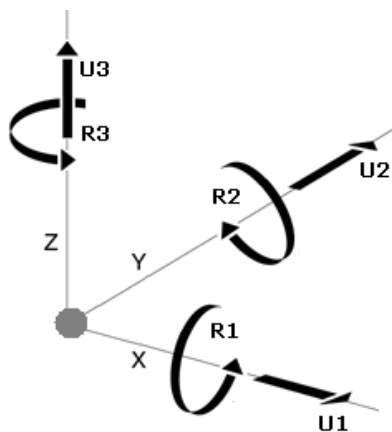
Figure 4-8 Six Degrees of Freedom at a node

Figure 4-8 shows U1, U2, U3 and R1, R2, R3 as the displacement and rotational degrees of freedom at a node in x, y, z directions respectively. The coordinate

56

directions for stiffened plates are x along the line of the stiffeners or along the length of the plate, y along the width of the plate and z along the height of the stiffeners.

Pinned condition at the loaded ends and simply supported conditions at the sides were used for models M1, M2 and M3 explained in the previous section. Figure 4-9 shows the pictorial representation of boundary conditions used for the three models M1, M2 and M3. A detailed explanation of the model M4 and the boundary conditions are discussed in Section 4.7.
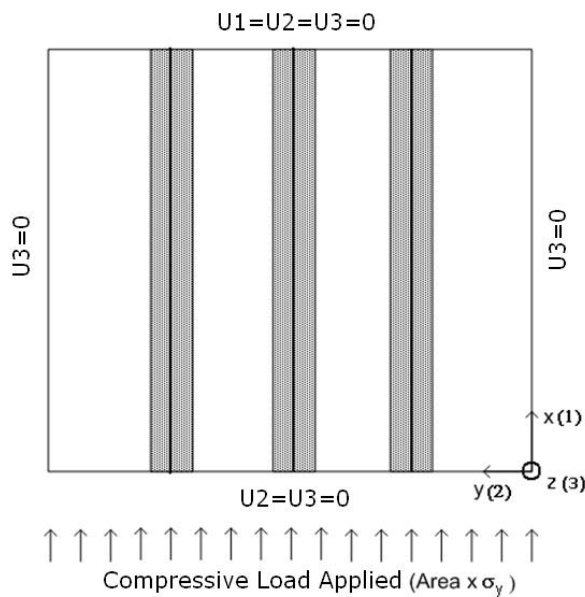
Figure 4-9 Load and Boundary Conditions for Models M1, M2 and M3

4.2.5 Loading of Panels

A reference compressive load equal to the product of yield stress and cross sectional area of the panel structure is applied axially (along x-axis) at one end keeping the other end constrained. Static Riks method which can provide solutions even in cases of complex and unstable response is used for the non-linear FE analysis. The ultimate strength of the structure from the analysis is then characterised as a fraction of yield strength of the material. For the first three models M1, M2 and M3, the load was applied uniformly through all nodes at the loading end. For M4, The compressive load was applied through a part of

the 'Loading Plate' (fixed to the test machine) and to the panel through 'Load Distribution Plate' similar to the actual test situation which is explained in Section 4.7.

4.3 Initial Distortion

Imperfections should be incorporated on a model to perform post buckling analysis or limit state analysis on any structure. The structure has to deform predominantly in the buckling mode under the action of load or displacements. There are three methods for the incorporation of buckling mode imperfection in a numerical model.

1. Geometric imperfections: Perturbations in the models initial geometry cause the structure to buckle in the appropriate manner.
2. Loading imperfections: Small fictitious 'trigger loads' are used to deform the model so that it buckles correctly.
3. Custom imperfections.

4.3.1 Geometric Imperfections

The geometrical imperfections are typically based on a previous eigenvalue buckling analyses. A few of the buckling modes are used typically to perturb the geometry. However, the lowest buckling modes are assumed to provide the most critical imperfections, so usually the lower modes are scaled and added to the perfect geometry to create the perturbed mesh. The magnitude of the imperfection should be chosen realistically from the manufacture tolerances or from the practical observations. In ABAQUS, to introduce the buckling modes of the structure for imperfections, two analysis runs must be carried out with the same model definition.

a) The ABAQUS/Standard BUCKLE perturbation procedure to establish the probable collapse modes.
b) General analysis procedure to perform the post buckling analysis.

While doing the buckling analysis, the buckling Eigen modes in the default global system are written to the results file (*.fil) using 'Nodefile' option. This option is not currently supported by Abaqus/CAE so it should be included using the keyword editor. This command is added at the end of keywords. The syntax of the keyword is,

*NODEFILE, GLOBAL=YES(default), LAST MODE=(eigen modes required)
U

The mode shapes from a buckling analysis can be introduced for post buckling analysis through to the 'Imperfection' option. This option also is not supported by the Abaqus/CAD and hence to be included through the keyword editor. This keyword is added after the boundary condition definitions or before the analysis steps. The nodal displacements written to the results (*.fil) file is used in the command without extension. The step parameter in the syntax must be used to identify the step from the previous buckling analysis containing the results that will define the geometric imperfection. The initial step should count as step 0. So normally the parameter will be 1. The imperfection can be restricted to a subset of nodes using the NSET parameter.

*IMPERFECTION, FILE=(File name), STEP=(n), [NSET=name]

Mode number, scale factor

……
n, (scale factor)

Imperfections can be formed by the superposition of weighted eigenmodes form 1 to n number of modes by specifying the appropriate number of mode shape and its scale factor as given in the syntax. The eigenmodes are stored such that the largest component of displacement has a magnitude of 1.0 (the minimum unit used to create the model) so the scale factor must be chosen carefully to give sensible values of imperfection.

4.3.2 Loading Imperfections

For loading imperfections, the trigger load should perturb the structure in the expected buckling modes. Typically, these loads are applied as 'dead' loads prior to the Riks step so that they have a fixed magnitude. The magnitude must be sufficiently small so that the trigger loads do not affect the overall post buckling solution.

4.3.3 Custom Imperfections

In this study, the initial distortion of the unstiffened and stiffened plates are incorporated directly to the input (*.inp) file by suitably modifying the coordinate values according to the type and amplitude of distortion for the parametric range considered in practical structures.

4.4 Residual Stress Modelling in FEA

According to various theoretical, practical and numerical studies and predictions done by Faulkner 1975, Tsai et al 1999 etc., the residual stress pattern in stiffened plates and the stiffeners can be idealised as blocks of tension and compression they are self-equilibrating. The simulation of residual stress using the initial stress method depends on the meshing of the structure. The initial stress is being applied over elements according to the intended stress pattern and it must exist in equilibrium. So the product of tensile stress (which is the yield stress) and the area of the tension block should be equal to the product of compressive residual stress and the area of compressive zone. The variation of residual stress is achieved either by changing the value of σ_r or ηt. Variation with σ_r is used in this study for the generation of design curves based on effects of residual stresses.
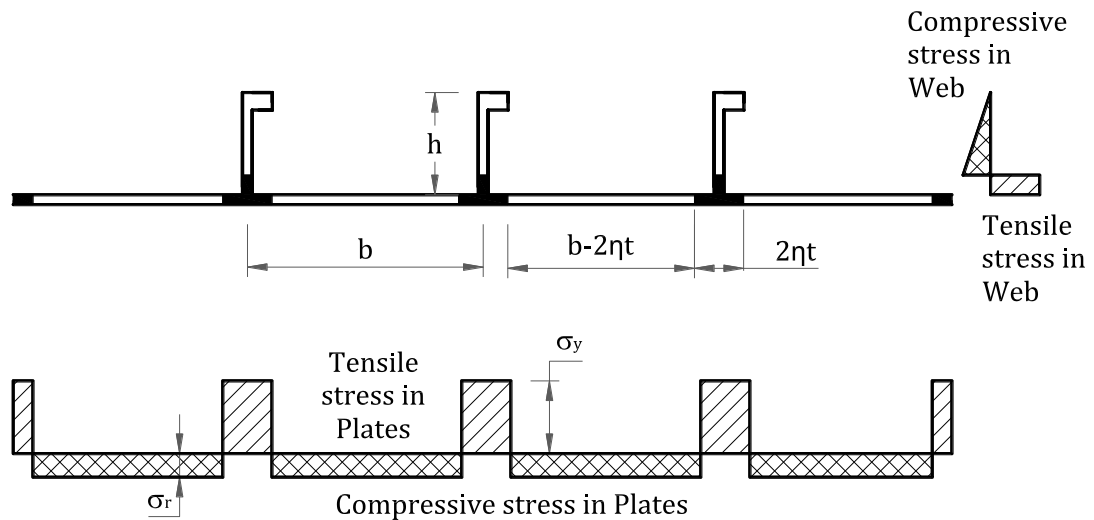
Figure 4-10 Idealised residual stress pattern in stiffened plate

The residual stress is incorporated in the FE model as a self-equilibrating system of tensile and compressive forces as shown in Figure 4-10. The force system is defined in the form of pre stress. The syntax of 'initial conditions' option in ABAQUS for this purpose is,

*INITIAL CONDITIONS, TYPE=STRESS
(Element set name), (x-direction stress), (y-direction stress), (z-direction stress)

The stress values given using this keyword is applied uniformly over the elements. In the case of shells, initial conditions can be specified only for the membrane forces, the bending moments, and the twisting moment. In both shells and beams, initial conditions cannot be prescribed for the transverse shear forces. When initial stresses are given in ABAQUS/Standard, the initial stress state may not be an exact equilibrium state for the finite element model. Therefore, an initial step should be included to allow ABAQUS/Standard to check for equilibrium and iterate, if necessary, to achieve equilibrium. To achieve equilibrium for all other analyses, a first step using the static procedure should be used. It is recommended that you specify the initial time increment to be equal to the total time specified in this step so that ABAQUS/Standard will attempt to find equilibrium in one increment. By default, ABAQUS/Standard ramps down the unbalanced stress over the first step. This allows

61

ABAQUS/Standard to use automatic incrementation if equilibrium cannot be found in one increment.

The compressive stress in web is distributed in a triangular form to match with the observed results of studies by Faulkner (1975) and Tsai et al (1999). The author proposes the following method to incorporate triangular distribution in stiffener web. As the distribution of the compressive stress becomes triangular, one end of the stress distribution should be double the compressive stress in linear form and the other end becomes zero as illustrated in Figure 4-11.
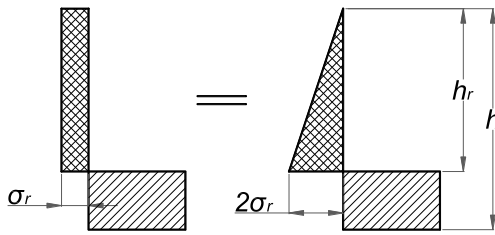
Figure 4-11 Ideal triangular RS distribution in stiffener web

When incorporating the compressive stress on the web elements, the magnitude on each element should be according to the triangular form of stress distribution. Let the web height is h and the height in compression zone be h_r, the length of the stiffener (perpendicular to the plane of the paper) is a. The height h_r is divided into n elements as shown in Figure 4-12. According to the self equilibrating condition of residual stress, the compressive stress $\sigma_r.h_r.a$ should be equal to the tensile stress $\sigma_y.(h-h_r).a$

Applying 'sine rule' at the ith and $(i-1)$th segment,

$$\frac{2\sigma_r}{h_r} = \frac{\sigma_{r(i)}}{\left(\dfrac{h_r}{n}\right)(n-i)} = \frac{\sigma_{r(i-1)}}{\left(\dfrac{h_r}{n}\right)(n-i+1)} \tag{4-1}$$

Re-arranging Equation (4-1),

$$\sigma_{r(i)} = \frac{2\sigma_r(n-i)}{n} \text{ and } \sigma_{r(i-1)} = \frac{2\sigma_r(n-i+1)}{n} \tag{4-2}$$

So compressive residual force at ith element acting along the length a,

$$S_i = a(A_1 + A_2) = a\left(\frac{h_r}{n}\sigma_{r(i)} + \frac{1}{2}\frac{h_r}{n}\left(\sigma_{r(i-1)} - \sigma_{r(i)}\right)\right) \tag{4-3}$$

Using Equation (4-2) in Equation (4-3), we get,

$$S_i = \frac{ah_r}{n^2}\sigma_r(2n - 2i + 1) \tag{4-4}$$

Now the compressive residual stress at each element can be applied with rectangular approximation of the force in each element as shown in Figure 4-12. Hence $\sigma_{r(i)}$ can be redefined as,

$$\sigma_{r(i)} = \frac{S_i}{a\left(\dfrac{h_r}{n}\right)} = \frac{\sigma_r}{n}(2n - 2i + 1) \tag{4-5}$$
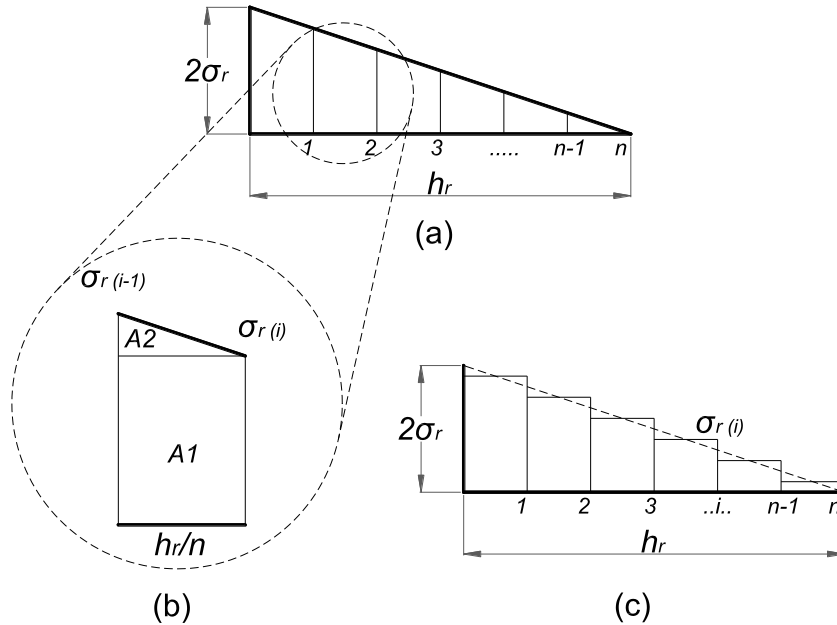
Figure 4-12 Triangular Stress distribution

From the definition of residual stress as discussed in Chapter 3, when the thickness (t) and stiffener spacing (b) is constant for a structure, the compressive residual stress is a function of η and the material yield stress. So we get,

$$\sigma_r = \sigma_y\left(\frac{2\eta t}{b - 2\eta t}\right) \tag{4-6}$$

It is obvious from the above equation that the variation of residual stress can be achieved either by changing η or σ_y.
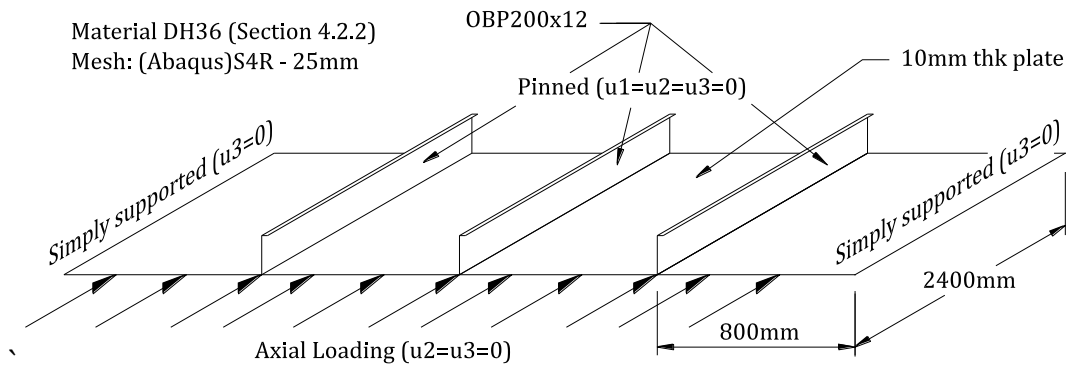
Figure 4-13 Details of FE Model used for the comparison

The structural geometry dimensions, boundary conditions, material and meshing is shown in Figure 4-13.

Table 4-2 shows the strength results of a stiffened plate with OBP200 and plate thickness 10mm with varying residual stresses by both approaches discussed before. The residual stress is varied from 5% to 25% either by changing η from 2 to 8 by keeping σ_y constant and then by changing σ_y from 15% to 75% by keeping η constant.

Table 4-2 Varying Residual stresses with η and Tensile residual stress

	Comp. Residual Stress	Ten. Residual Stress	η	σ_u/σ_y
	0	0	0	0.99
Changing width of yield tension block, ηt	5%	100%	2	0.955
	11%	100%	4	0.916
	18%	100%	6	0.872
	25%	100%	8	0.851
Changing Tensile residual stress	5%	15%	10	0.975
	11%	33%	10	0.94
	18%	55%	10	0.905
	25%	75%	10	0.873

Figure 4-14 illustrates the difference between the two approaches. Both the methods show approximately equal rate of strength degradation. But the method of increasing tension block appears to be more sensitive. The variation in residual stress is actually occurs when the extent of heat affected zone

changes. So technically speaking, the method of varying tension block size is more justified.
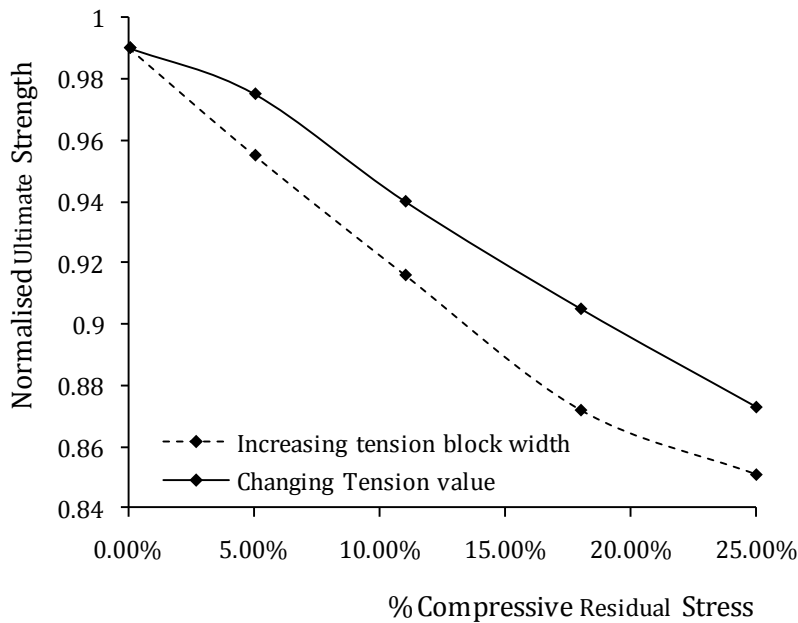
Figure 4-14 Comparison of Change in residual stress by width of tension block and tensile stresses

4.5 Effect of Varying Material Properties

A study was carried out with change in yield stress and variation in residual stresses for a typical stiffened plated structure. The stiffened plate with OBP160 and 8mm thick plate is used for the study as illustrated in Figure 6-6. Figure 4-15 shows the variation in structural strength for yield stresses, 255 MPa, 285MPa and 315MPa for no residual stress and with η=5. The results reveal some interesting facts about the structural strength. Figure 4-15(a) shows the load shortening curves for the analysis trials described above. It demonstrates that when the value of yield stress increases, the non-dimensional ultimate stress in terms of yield stress decreases and the effect is similar when residual stress is included. Figure 4-15(b) shows the reduction in ultimate strength against yield stresses. On the other hand if we calculate the ultimate stress as shown in Figure 4-15(c), we find that the stress value increases with increase in yield stress. So the load bearing capacity increases for structures of materials

with higher yield stress value. But the reduction in the non-dimensional strength confirm the fact that buckling induced limit strength is a combination of elastic buckling strength which is dependent on the structural slenderness and the yield stress is only affecting the additional inelastic part of strength. So the effect of yield stress is significantly in the latter part of failure process.
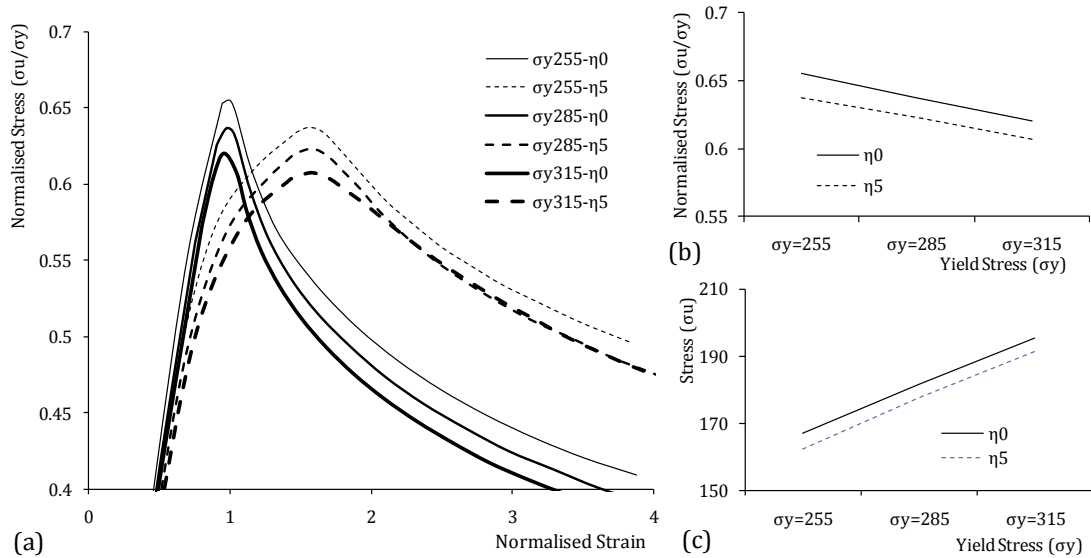
Figure 4-15 Effect of changing material yield stress

4.6 Economic Structural Configuration

The number of plate spans and bays of stiffened plates are selected for the development of design curves (Chapter 6) based on the effect of fabrication imperfections based on a sensitivity study conducted by the author. For the sensitivity analysis, a typical configuration of OBP200 stiffener and 12mm plate with a medium level (refer Section 6.2) of overall imperfection is used. The geometry, boundary conditions, material properties and meshing were as shown in Figure 4-13.

Figure 4-16represent different plate stiffener combinations considered for the sensitivity analysis. Figure 4-17 shows the sensitivity analysis results for the optimum number of plates and stiffeners to be used for the strength analysis. Figure 4-17(a) shows the load shortening curves for various combinations of plates and stiffeners. Number of plates is varied from two to seven (P1 to P7)

and correspondingly number of stiffeners from one to six (S1 to S6) as one stiffener should be placed at the middle of two plate spans. It is clear from the figure that the strength of the structure keeps on increasing as the number of plates and stiffeners increase. The strength appears to vary from approximately, 0.6 to 0.67. There is a huge variation from one stiffener to two stiffeners and from three stiffeners to more, the variation in strength is comparatively less and the computation cost increases drastically.
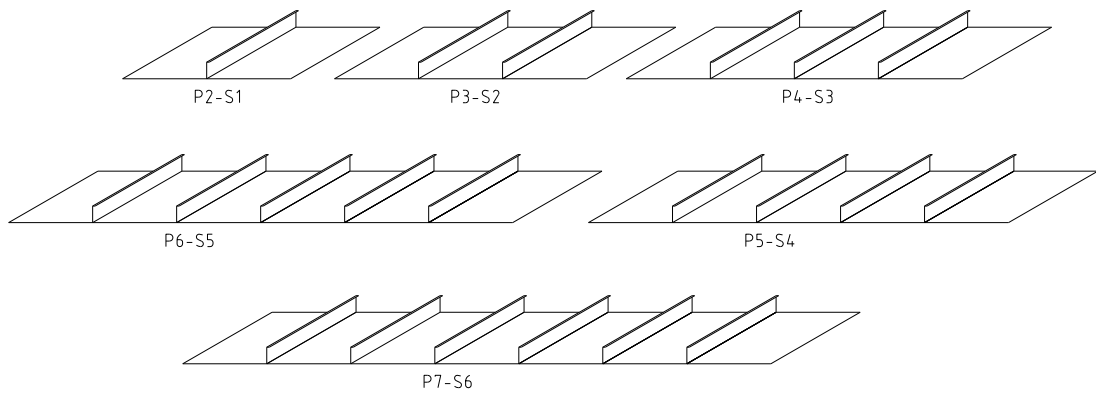
Figure 4-16 Structural configuration with varying number of plates and stiffeners
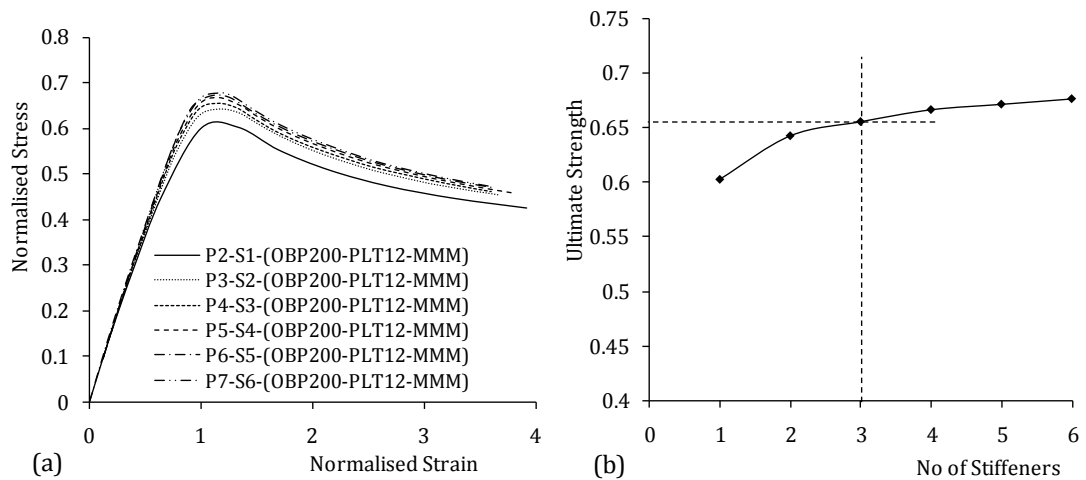
Figure 4-17 Sensitivity study for the number of plates and stiffeners (a) the load shortening curves (b) the strength comparisons

Figure 4-17(b) shows that for sensible results with reasonable cost of computation, the optimum size is a three stiffener configuration, P4-S3, i.e., four plates and three stiffeners. This is the most recommended configuration for similar studies explained in various technical documents like ISSC

(International ship and offshore structures congress) dealing FE analysis for ultimate strength of stiffened plates for marine applications.
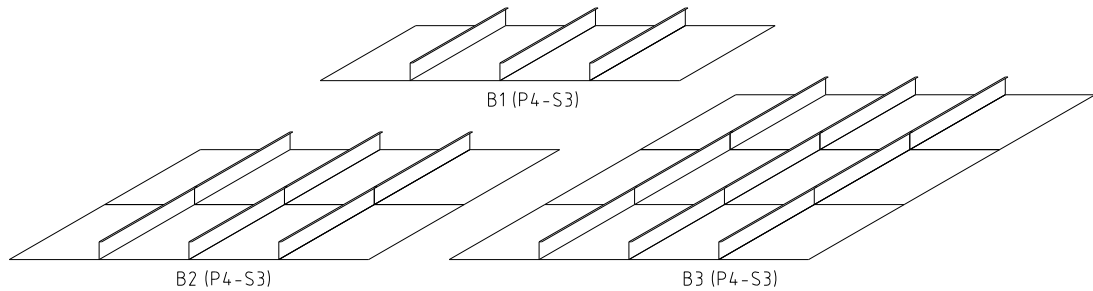
Figure 4-18 Structural configuration with varying number of bays

One bay is the length of plate between two transverse frames. The transverse frames are simulated in FE analysis by restraining the transverse out of plane movements of nodes at the corresponding locations. Figure 4-18 illustrates three strucutral configurations with varying number of bays with same scantlings used for the previous number of plate-stiffener sensitive study.
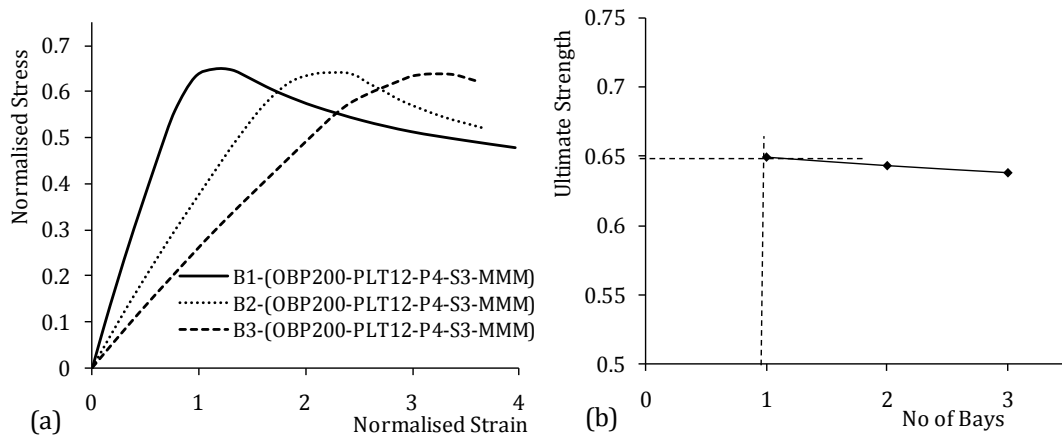
Figure 4-19 Sensitivity study for the number of bays (a) the load shortening curves (b) the strength comparisons

Figure 4-19(a) shows the strength results for one, two and three bays structures respectively. It is very interesting to see that all the models show nearly identical strength values with increased strains as the number of bays increases. It is very clear from the results that all the bays are equally strained before the entire structure reaches its ultimate strength. For a strength point of view, the analysis confirms that the use of a single bay gives good estimate with reduced cost of computation for the types of structure in this study. A stiffened panel

structure with 4 spans of plates of aspect ratio 1:3 (stiffener spacing/length) with 3 stiffeners is used throughout the study.

4.7 FE Analysis of Experimental Test Panels
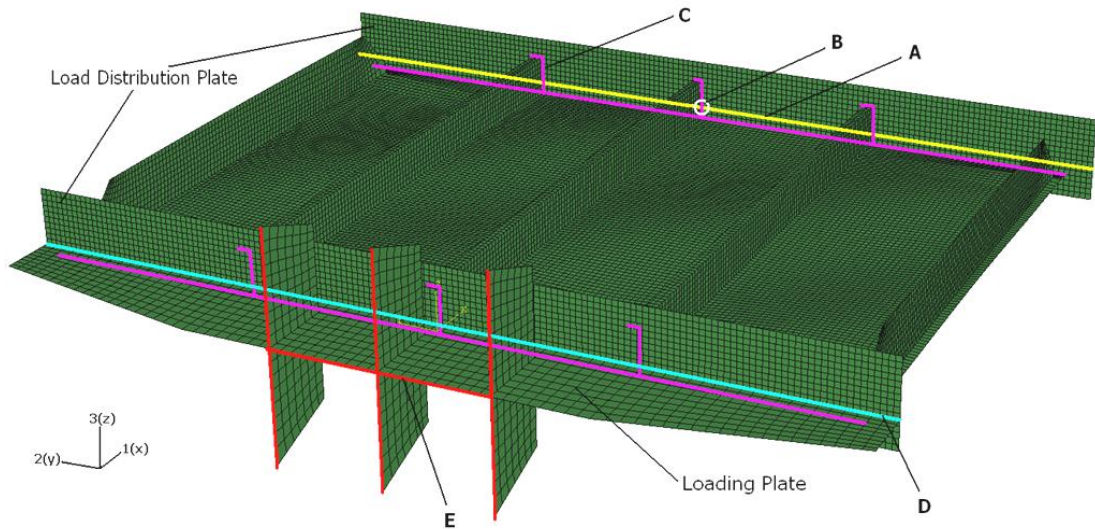
Figure 4-20 Load, Boundary conditions, contacts and Constraints for Model M4

The initial FE analysis predictions were carried out with a model type, M3 which is explained in Section 4.2.4. These predictions were not reflecting the reality because the loading end attached to the hydraulic ram was free to rotate about longitudinal axis. The ultimate load from the experiment for the first panel was 1229.2kN and which is substantially below the FEA prediction using M3 model which was 1675.34kN. So another FE model M4 was created for this purpose. This condition is simulated by constraining U1 along the support line and constraining U1, U2 and U3 at the central node, acting at the pivot point for rotation. The uniform loading was achieved through the arrangement of a 'Loading Plate' and 'Load distribution Plate'. The interaction between these two parts is defined with contact elements so that load is conveyed with rotation about transverse axis (R2) allowed along the intersection line. U3 is fixed along the line to simulate the grove in the physical model which maintained the relative positions of the two parts. The Stiffened Panel is joined to the 'Load Distribution Plates' at both ends through a Tie constraint in order to simulate

the rigid fastening in the physical model. The above explained conditions are illustrated in Figure 4-20 as A, B, C, D and E explained below.

1. A (Yellow line): U1=0 along the transverse support line
2. B (White circle): U1=U2=U3 =0, on a single node at the centre crossing the transverse support line shown inside the white circle.
3. C (Magenta line): The Magenta lines show the tie constraints between the Stiffened Panel and the Load Distribution Plate to indicate the bolted fastening.
4. D (Cyan line): U3=0, to model the position grove. Node to surface contact elements are modelled at this intersection.
5. E (Red line): U2=U3=R1=R2=R3=0 and Compressive load applied through the red line.

However, when the rotational freedom was included in the analysis the prediction becomes 1206.36kN and with an allowance being made in strain for take-up of load in the physical set-up, a reasonable fit of result is achieved.

(a)   (b)
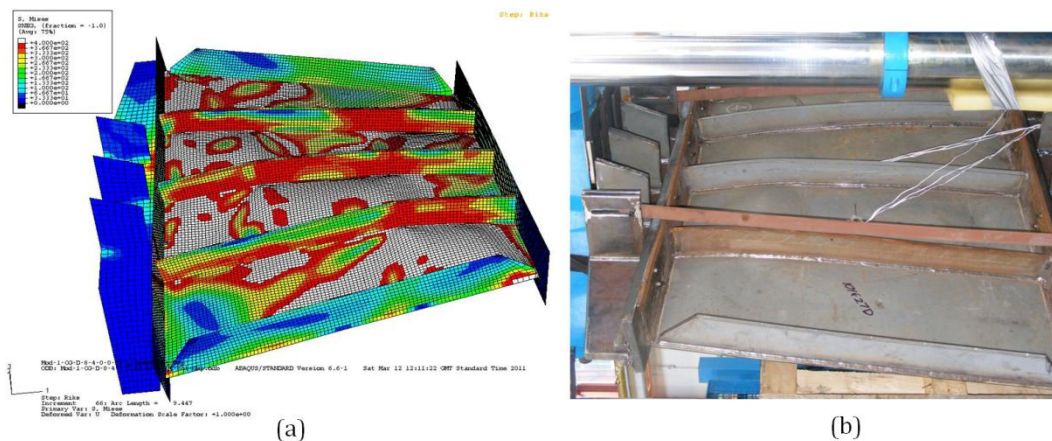
Figure 4-21 Comparison of Experimental and numerical predictions (a) FE analysis (b) Experimental test

Apart from the above end conditions, an initial gap, observed during the tests, between the loading plate and the load distributor plates attached to the panels was assessed by a specific FE run. The line of loading plate touching the distribution plate was modelled with an arc shape of very large diameter with a 5mm gap at each end. This increased the concentration of the loading on the

central stiffener and helped to explain the discrepancy between the strain for the FE results and the experimental results.

Figure 4-21 shows the comparison of FE analysis and the Experimental collapse mode of Panel-1. The image of FE analysis is bit amplified and shows the deformations more prominent. Both the images exhibit close geometrical shapes at the time of failure. The Figure 3-15 also shows the same panel closely and the similarity of distortion with FE analysis can be recognised. It confirms that, in addition to the agreement between the predicted and measured failure loads, the behaviour of the panel is also predicted well by FE analysis.

4.7.1 Comparison of Experimental and FE Results

Figure 4-22 shows the comparison of FE results with the ideal (proposed) boundary conditions (M3 in Section 4.2.4) and the Test boundary conditions during the experiment against the experimental results of Panel-1.
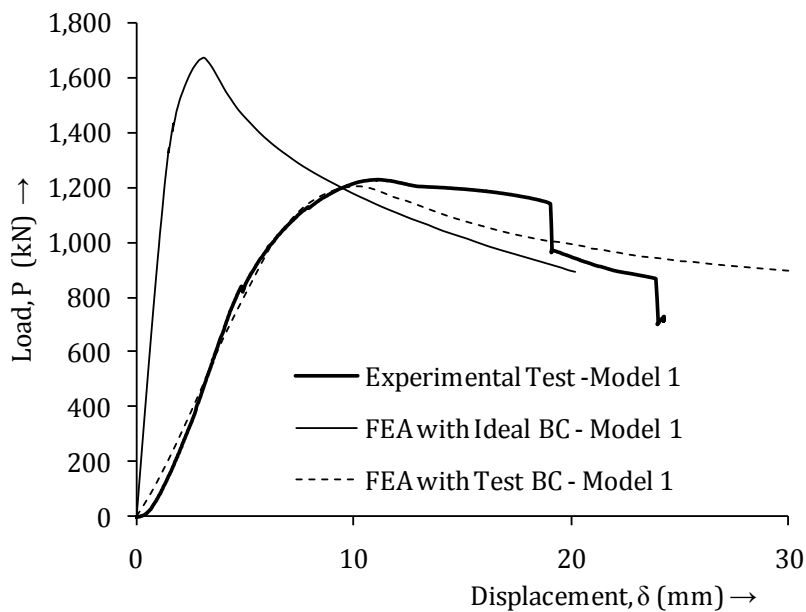
Figure 4-22 Experimental and FE predictions of Panel-1

The additional rotational degree of freedom affects the strength quite substantially when compared with the Ideal boundary conditions (M3). Considering the inherent uncertainties which are likely to be present in the

experiments, the FE analysis predicts the strength quite accurately for the majority of the cases. The test results are plotted in Appendix B and are summarised in Figure 4-23.

This indicates that when the boundary conditions are modelled correctly, there exists a better correlation between the test and FE results. In most of the tests it is observed that the initial buckling of the centre stiffener is marked by a noticeable inflection of the load-deflection curve, and in the strain gauge reading for the centre stiffener.
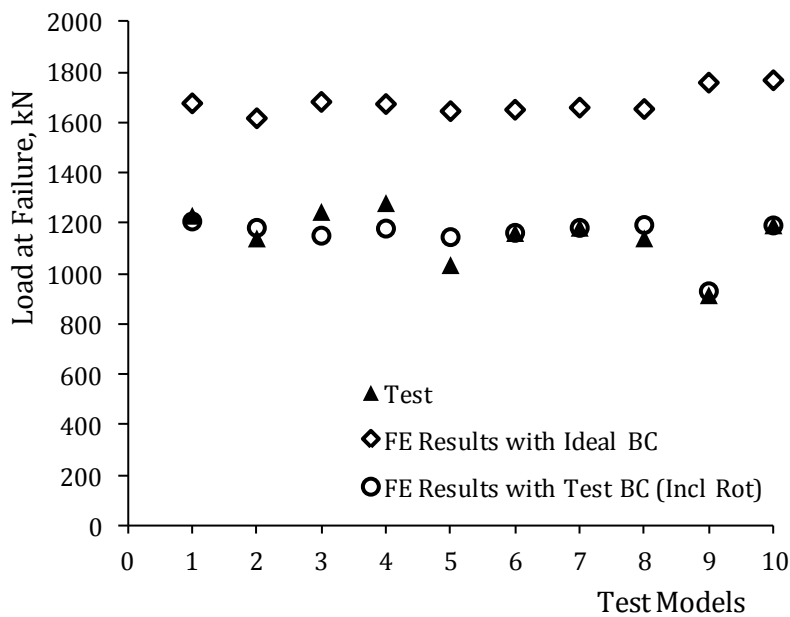
Figure 4-23 Comparison of Experimental and FE results

Although many FE models with corrections and adjustments to reflect the reality had been attempted, most importantly, FE results with proposed BC and Test BC (with rotation and a gap in the loading end) along with the experimental results are presented in Table 4-3.

The variations in the FE results are statistically represented with the mean and coefficient of variation (COV) of the model uncertainty factor, X_m which is the ratio of experimental result and the Predicted result.

Table 4-3 Comparison of Experimental and FE Results

Plate No.	FE Results with proposed BC		FE Results with Test BC		Experimental Results		% Error (Experiment with FE Test BC)	X_m
	σ_u/σ_y	P_u (kN)	σ_u/σ_y	P_u (kN)	σ_u/σ_y	P_u (kN)		
1	0.59	1675.34	0.43	1206.36	0.44	1229.20	1.86%	1.02
2	0.57	1616.01	0.42	1180.93	0.40	1138.93	-3.69%	0.96
3	0.60	1680.99	0.41	1149.86	0.44	1244.35	7.59%	1.08
4	0.59	1672.52	0.42	1178.11	0.45	1279.15	7.90%	1.09
5	0.58	1644.27	0.41	1144.21	0.37	1033.02	-10.76%	0.90
6	0.58	1649.92	0.41	1161.16	0.41	1160.48	-0.06%	1.00
7b	0.59	1658.39	0.42	1180.93	0.42	1181.48	0.05%	1.00
8b	0.59	1652.74	0.42	1192.23	0.40	1139.30	-4.65%	0.96
9	0.56	1757.48	0.30	929.13	0.29	913.56	-1.70%	0.98
10	0.56	1766.93	0.38	1190.55	0.38	1191.00	0.04%	1.00

P_u - Ultimate load in kN, X_m - Model uncertainty factor

Mean: 0.9993

COV: 5.52%
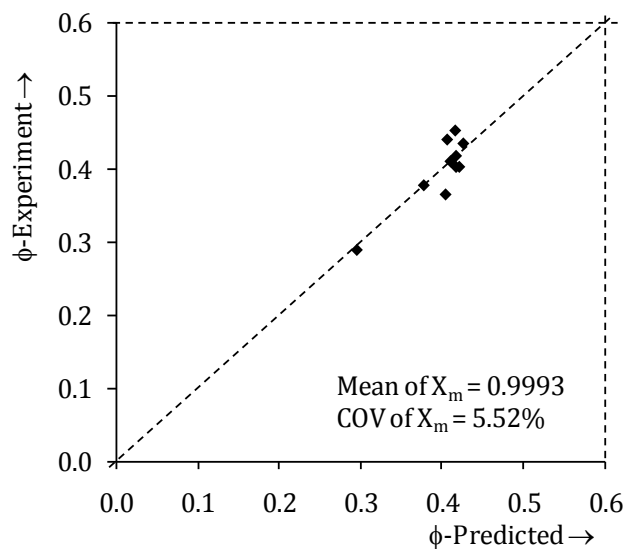
Figure 4-24 Statistical representation of Test results

The statistical modelling parameters exhibit very low bias (mean) and spread (COV) which are the most desirable characteristics for a better structural response model. The statistical behaviour of the experimental results is shown in Figure 4-24. ϕ-Experimental and ϕ-Predicted are the corresponding ultimate loads normalised with the equivalent yield load for the material. This modelling uncertainty factor and COV can be used for reliability analysis of similar structures which is discussed further in Chapter 8.

4.8 FE Modelling and Analysis of Stiffened Cylinders
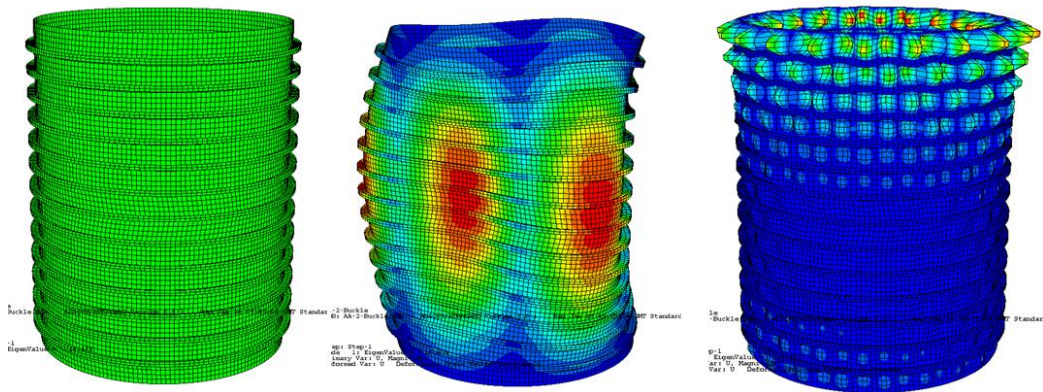
(a) Ring stiffened cylinder and Buckling modes
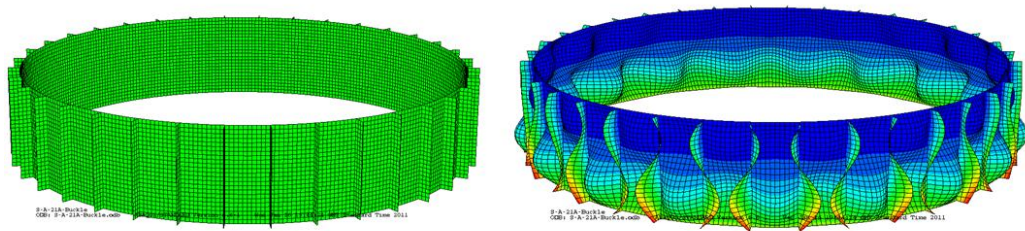
(b) Stringer stiffened cylinder and Buckling modes

Figure 4-25 FE Model and buckling modes of stiffened cylinders

The same modelling aspects described above are used to model the stiffened cylinders. The buckling mode imperfection for the stiffened cylinder analysis has incorporated based on the *IMPERFECTION keyword rather than modifying the coordinates. The analyses have basically carried out to do the reliability assessment of ring stiffened and Stringer stiffened cylinders using Response Surface Method (RSM) under axial and combined loading cases, which is explained in Chapter 8. Also, the verification of models by comparing the collapse load with the experimental collapse load is given in Table 8-5 of Chapter 8. The FE model and included buckling modes are illustrated in Figure 4-25.

4.9 Summary

The nonlinear FE analysis has been evolved over the years and proved to be a potential tool to evaluate the structural responses for varying problems. The structural response analysis of plates is one of the most important areas of

application for the numerical tools as these are one of the most interesting topics for researchers all over the world with new era of composite materials and other intricacies of advanced fabrication processes. Even though the stiffened plates of steel material used for marine applications are very simple in its geometry and construction, its strength and collapse mechanism are really complex and still not understood fully. These structures exhibit biased column or plate behaviour according to the geometrical parameters as it includes plates and column elements. The fabrication introduce weld induced non linear residual stresses and geometrical imperfections and when linked with material non linearity makes the problem extremely complicated. So the analytical framing of this highly nonlinear problem with all the influencing factors is quite difficult and face lot of limitations. A carefully constructed numerical model to an extent is the best method to reflect the response of these structures close to reality.

The analyses carried out for an optimum geometry of the stiffened plates reveal the fact that the approach in analytical formulations is totally different form numerical techniques. Established analytical methods for the ultimate strength evaluation are based on the shear lag and effective width concept. Numerical models show convergence in the result with more number of plates and stiffeners. It is observed that, for the ultimate strength analysis, a numerical model with four spans of plate with three stiffeners produces a reasonable result. The increase in the number of bays appears to generate the same strength result with an increased failure strain. This indicates the fact that the spans are absorbing strains or deflecting equally before one of them actually collapses.

The mesh sensitivity analysis actually revel the requirement of element size and aspect ratio for a better result. The size of elements has great influence in the accuracy of the result. At the same time it increases the cost of computation dramatically if the mesh is too fine. So the optimisation process confirms that

the analysis is carried out at an optimum level of accuracy and computational cost.

The analytical formulations can never incorporate the imperfections with all its parametric aspects for strength calculations. The complex interactions and sensitivity considerations behind the development of a formula with capability of handling all the distortion aspects is almost impossible. A parametric numerical model can handle the real distortion or imperfection very effectively. The analyses of various geometrical imperfection mode shapes with identical distortion parameters indicate the fact that the response of the structure is very much dependent on the mode shape and amplitude of the imperfection. The Type-1 imperfection profile or mode shape is chosen for the study based on the high level of sensitivity on the strength of the structure.

The residual stresses in a structure if incorporated through the initial stress method, the variation can be achieved either by increasing the width of tension block or by varying the value of tensile residual stress. The analyses indicate the fact that the variation in residual stress through the width of tension block seems to be more sensitive and conceptually correct.

When varying the yield stress of the material, the reduction in the non-dimensional strength and increase in the actual load bearing capacity can be understood with the elasto-plastic failure concept. It further confirm the fact that buckling induced limit strength is a combination of elastic buckling strength which depends on the structural slenderness and the yield stress is only affecting the additional inelastic part of strength and its contribution is less compared to the elastic part.

The proper modelling of test set-up for experimental trials for the compressive strength of stiffened panels with specific boundary conditions and loading pattern to provide convincing and valid results is extremely challenging. The theoretical or numerical predictions are very sensitive to the assumptions used for the theoretical formulation and hence the discrepancy is obvious and

subjected to the extent of effective analytical/numerical modelling, various nonlinearities and other uncertainties involved. The tests have provided a validation of the predicted strength of stiffened panels where the rotational degree of freedom is not constrained. The comparison confirms the load bearing predictions of the stiffeners and plates in a compressive axial loading condition leading to the failure of the structure. The tests have displayed more displacement compared to the numerical predictions. These were adjusted with some correction factors to enable comparison of strength. This additional displacement is believed to be either because of the uneven loading or the machines frame displacement. But the variation is a few millimetres. The failure loads show close agreement.

The study shows close matching of experimental results for strength with the numerical simulations. The model uncertainty factor is almost unity with very low spread of 5.5%. The better statistical correlation validates the numerical model for further studies including strength analysis and reliability calculations.

Chapter 5.   Strength of Plated Structures

5.1 Introduction

The flat plate elements are used in the engineering world extensively, from airplanes to ships, from space stations to offshore platforms, buildings and so on. A structural element is classified as flat plates when one of the three dimensions is much smaller than the other two. In general, the thickness will be much smaller than other length dimensions. As far as the behaviour and flexural properties are being considered, the thickness of the plate is the most significant parameter. The basic theories used for plate analysis can be classified into 'thin plate with small deflection', 'thin plate with large deflections' and 'thick plate' (shear deformable) theories. The distinction between thin and thick plate are characterised based on the ratio of the thickness to the smallest length dimension. A plate is considered thin if the aforesaid ratio is less than 1/20 according to Reddy (1999).

The strength analysis is carried out based on the assumption that stable equilibrium exists between internal and external forces and a slight load increment does not disturb the equilibrium of the system. There is a limit for the above equilibrium state and beyond which the system will move to an unstable state of equilibrium. This sudden change in structural configuration is known as Buckling. For slender structures (one or two of the three dimensions are considerably less than the other), there can be excessive elastic deformation before the structure actually reaches its material elastic limit. This is known as elastic buckling. When the applied stress reaches the material yield stress, the deflection will increase plastically and is known as the inelastic buckling. For stocky structures on the other hand, as the elastic deflection is too small, the buckling or a change in structural configuration will occur when the applied stress reaches the material yield stress. So the stocky structures will experience inelastic buckling only. However, the buckling type and buckling stress is hence a function of structural slenderness and material properties. Most of the plate

elements used in offshore industry fall under slender category and the buckling failure is the most important mode of failure under various loading conditions. Hence the strength of the plate is generally represented with the term buckling strength.

The elastic small deflection buckling deals with the case of plates loaded up to the critical elastic buckling stress σ_{cr}. However, although this provides a good design datum it does not represent true failure in a load-carrying sense. Further loads can be carried as the lateral deflections grow sufficiently large for membrane stresses to be taken into account. This increase of load with deflection is finally limited by breakdown of the plate material due to plasticity when the ultimate load σ_u is reached. In general, the ultimate strength of a plate is greater than the elastic critical buckling stress, but it is possible with sturdy sections for the plate to yield before buckling occurs, i.e., $\sigma_u < \sigma_{cr}$. This constitutes inelastic or plastic buckling.

Contrary to the idealised small deflection analysis, there is no catastrophic deformation at σ_{cr} in actual structures. A plate loses effectiveness immediately upon application of load because of initial imperfections. Even the large deflection theory which is valid for stresses up to about $5\sigma_{cr}$, predicts a step by step change in the plate stiffness. Hence the buckling of a real plate is a progressive increase of deformation, starting from some initial distortion, as the load is progressively increased.

If post-buckling deflections can be allowed before the onset of plasticity, a design can be based on σ_u, with some safety margin, rather than σ_{cr} and thereby generally make considerable savings in weight and cost. There is virtually no reserve of strength for plating in compression when $\sigma_{cr} > 0.6\sigma_y$ or aspect ratio, $\alpha < 0.25$ (long edge loaded) or any one edge is free.

This post-buckling reserve of strength is most easily determined by means of an '*effective width*' approach. In the post-buckling range the stress on the loaded edges is no longer uniform across the plate width, but varies such that the edges

carry an ever increasing proportion of the load, with the stress near the centre of the plate almost constant. The effective width is that width of plate which, when loaded uniformly to the plate edge stress, would produce the same overall plate end load. Failure can be said to occur when the edge stresses reach yield. This approach has led to a series of empirical expressions relating the strength of a plate at this failure point known as the ultimate strength to the plate slenderness. When a plated grillage is loaded the plating is required to enhance the stability of the stiffeners, and so plate stiffness just prior to collapse is an important factor. This can be expressed in terms of a *'reduced effective width'*.

5.2 Impact of Weld Induced Imperfection in Steel Ships

Figure 5-1 shows the typical distortions in ship structures observed in the hull, deck plate and transverse bulk heads.

Figure 5-1 Distortions in hull, deck and bulkhead of Type 45 destroyer

The most significant ship building problems commonly encountered as a result of weld induced geometrical distortion are,

1. The difficulty in joining blocks during hull erection due to inaccuracies in the overall block dimensions and the misalignment of structural members due to weld distortion, resulting in much rework at the erection stage.

2. Aesthetic beauties of the ships are greatly affected with the plate deformations giving a wavy body appearance.

3. The ultimate strength or the structural capacity degradation of the structure with weld induced geometrical imperfections and residual stresses.

The misalignment during block joining is one of the major issues encountered by the ship building industry around the globe. Extended research by individual organisations and professional institutions across the world established lot of effective distortion mitigation techniques and procedures which effectively brought this issue under control.

The aesthetic beauty of the ship is particularly important in ship construction as it creates a first sight impression about the construction and performance quality in the eyes of potential buyers and common layman. Hence it is very important in the commercial point of view and this also controlled with effective techniques for distortion mitigation, and surface finishing techniques.

Designers and institutions have made a lot of research to produce effective methods for strength calculations considering the imperfection effects. There are number of potential techniques evolved over the years to predict the distortion and residual stresses in welding processes. The numerical simulation of welding can be performed with many existing commercial FE packages and proved to be very close to the actual experimental results. This study is focused on the effect of these factors in the buckling strength and post buckling behaviour of the unstiffened and stiffened panels used in steel ships.

5.3   Welding Deformations in Plated Structures

The high heat input to the material during welding process results in a complex state of strain within the body. This will generate complex internal forces and cause complex metal movement during welding. Finally, the resultant forces and strains will produce the net distortion.
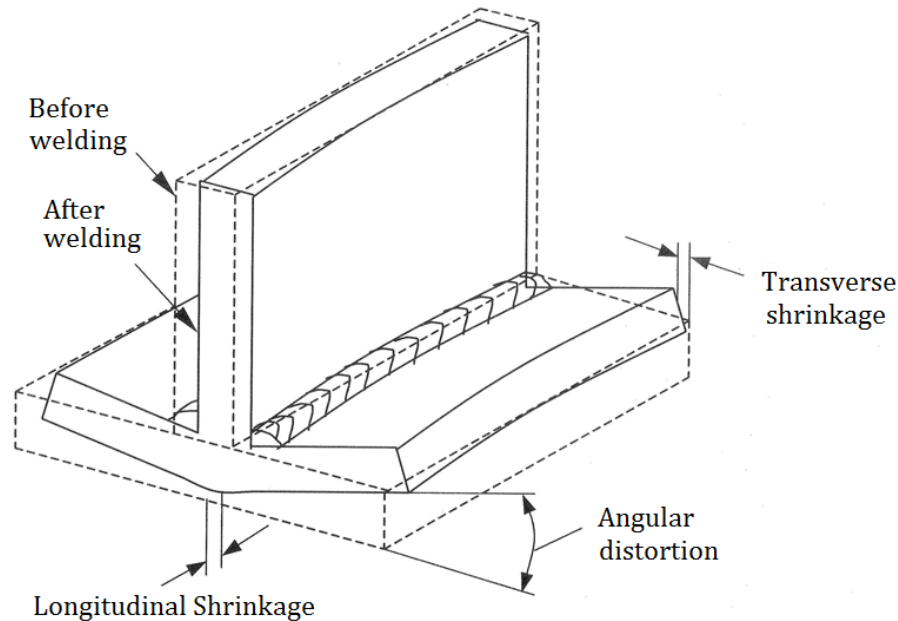
Figure 5-2 Types of welding distortion in a fillet weld

Three fundamental distortion types are,

1.   Transverse shrinkage
2.   Longitudinal shrinkage
3.   Angular/rotational distortion

Figure 5-2 shows the graphical representation of the above distortions in a fillet welded plate.

The distortions can be generally classified as in-plane distortion and out of plane distortion. The in-plane distortions are those two dimensional geometrical changes observed with respect to a plane parallel to the line of welding and the out of plane distortions are in a three dimensional space.
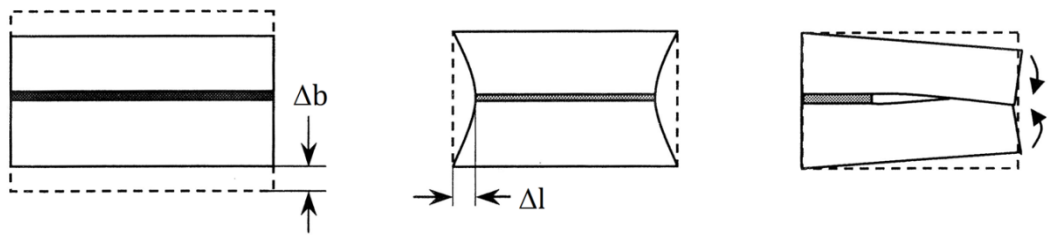
(a) Transverse shrinkage   (b) Longitudinal shrinkage   (c) Rotational distortion

Figure 5-3 In plane distortions

The in-plane distortions shown in Figure 5-3 are,

1. Transverse shrinkage – Shrinkage perpendicular to the weld centreline.
2. Longitudinal shrinkage – Shrinkage in the direction of the weld line.
3. Rotational distortion – Angular distortion in the plane of the plate due to thermal expansion or contraction.

The out of plane distortions shown in Figure 5-4 are,

1. Angular distortion – Distortion caused by non-uniform temperature distribution in the through-thickness direction.
2. Bending distortion – Distortion in a plane through the weld line and perpendicular to the plate. This occurs as a result of bending moments induced by the longitudinal shrinkage of the weld metal when the weld line does not coincide with the neutral axis of the weldment.
3. Buckling distortion – Distortion caused by compressive stresses inducing instability when the plates are thin. When thermal or residual compressive stresses are greater than the critical stress of the elements of the structure it induces instability in the plate elements. This will appear in the form of complicated geometry at large magnitude. The amount of buckling distortion in thin plated structures is much greater than other types of distortion as the magnitude is dependent on the slenderness of the plate.
4. Torsional distortion – The uneven heating and cooling along the weld line will generate an effect of a torque causing a twist or torsion in a member.

5. Global distortion – A shrinkage and bend in transverse and longitudinal direction of the whole metal structure as a single entity.

Fillet weld

Butt weld

(a) Angular distortion

(b) Longitudinal bending distortion

(c) Buckling distortion

(c) Torsional distortion
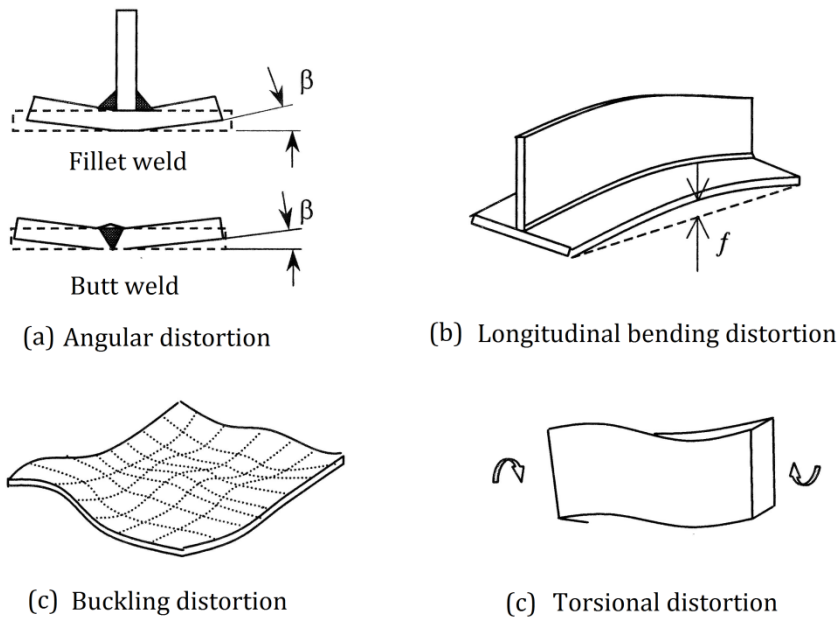
Figure 5-4 Out of plane distortions

All the above discussed distortions are present in every single joint of a structure. So the actual distortion configuration of any welded structure is a result of superposition and interaction of all such individual distortion components making the final geometry extremely complex. Hence for the study purpose, some idealisation of the distortion patterns are used depends on the material, structural scantlings, geometry, welding process etc.

5.4 Weld induced Residual Stresses

Residual stresses can be sufficient to cause a metal part to split into pieces without applying any external load. Though this is very uncommon, people in the metal industry have witnessed this phenomenon. Residual stresses are stresses locked inside a component or assembly of parts. The internal state of residual stress is caused by thermal and/or mechanical effects on the parts during construction operations. Common examples of these are bending, rolling or forging and the thermal stresses induced during welding operations.

The internal stresses are always balanced in a component. Tensile residual stresses are counter balanced by compressive residual stresses. In reality, the residual stresses are three-dimensional and hence it does have so many unimagined effects on the performance of the structure under complex loading conditions. The residual stresses can result in visible distortion of a component and this can be useful in estimating the magnitude or direction of the residual stresses. Thermal residual stresses are primarily due to differential expansion when a metal is heated or cooled. The two factors that control this are thermal treatment (heating or cooling) and restraint. Both the thermal treatment and restraint of the component must be present to generate residual stresses.

5.4.1 Causes of Welding Deformations and Residual Stresses

The parts joined through welding are subjected to a high degree of non-uniform heating. The weld line is often heated to several thousand of degree Celsius and then cooled down. The amount of heat supplied during this process is conducted to the inner body. This sudden heating and cooling invoke microscopic level dislocation producing volumetric variations and finally results in residual stresses and deformations.

Consider a body created out of tiny cubic elements. If the all the elements are heated uniformly, it will cause uniform expansion in all three-dimensional directions and will attain same size. The elements can join to form a solid continuous body at this temperature without any internal stresses. On the other hand, if the heating is non-uniform, each cube will expand according to the heat received and results in elements with non-uniform sizes. The assembly of such cubes becomes difficult to form a solid body. There will be some distortions due to the change in size and residual stresses due to the forced fitting of cubes. In a continuous body, the neighbouring elements will resist a body from free expansion and will cause the same effect as explained above. If the internal stresses and expansion due to heating are in the elastic range, the body will return to its initial size and shape without any internal stresses after cooling. If

there is any plastic deformation, the body can return to its initial temperature with some change in the size and internal stresses and hence the body after cooling will have some distortions and residual stresses.

5.4.2 Residual Stress Distribution

In an actual welding process, material shrinkage or expansion happen in all spatial directions. It ultimately results in a very complicated state of residual stress fields in the body as explained above. Since the longitudinal and transverse directional stresses are the major stress components, these are considered as the residual stress fields while analysing the structural performances of a welded plate.

(a)

(b)
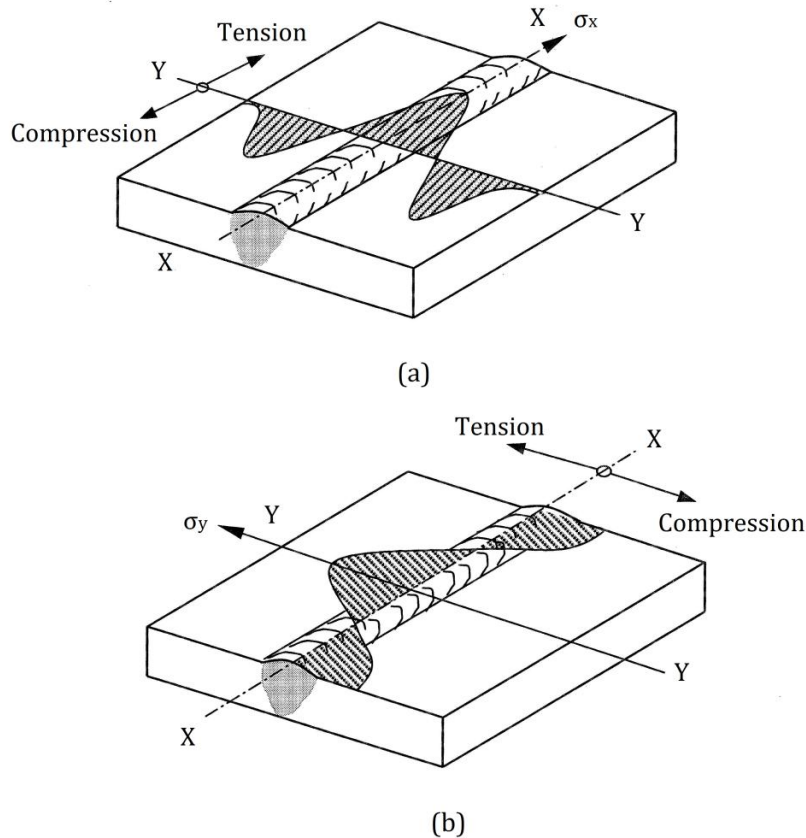
Figure 5-5 Residual stress distribution in butt weld (a) along longitudinal direction of the weld; (b) along transverse direction of the weld

5.4.2.1 Residual Longitudinal Stress

It is experimentally observed that maximum longitudinal residual stresses σ_x in welds are usually close to the yield stress of the material σ_Y and in the tension state. It reduces gradually in the direction perpendicular to the weld line and becomes compressive at about 4 to 6 times the thickness of the plate material away from the weld line. A typical residual stress distribution in a butt weld joining two plates is shown in Figure 5-5 (a). The stress distribution may vary depending on alloying level of the weld- and base metal, cooling rate during welding process and the initial state of the steel.

5.4.2.2 Residual Transverse Stress

After the welding operation, the shrinkage/expansion in the spatial direction induces residual stresses. The longitudinal residual stress is the major component in magnitude. It appears in welds irrespective of restraints. The transverse residual stresses are on the other hand depends on the restraints during welding operation. If there are no restraints in the transverse direction, keeping the edges free, the transverse residual stresses generated will be very minute. The typical transverse residual stress distribution will be as shown in Figure 5-5 (b). The distribution shows maximum compressive stresses at the ends and tensile stress at the middle of the weld length.

5.5 Strength of Unstiffened Plate

The buckling stresses are obtained from the concept of bifurcation of an initially perfect structure. In theory, the buckling of a perfect structure happens suddenly when the applied stress reaches a critical value. But in reality, the response of the structure seems to be continuous due to the unavoidable presence of initial imperfections.

For a long rectangular plate under uniform axial in-plane compression as shown in shown in Figure 5-6(a), the elastic critical stress can be expressed in terms of the geometrical and material parameters as,

$$\sigma_{cr} = K \frac{\pi^2 E}{12(1 - v^2)} \left(\frac{t}{b}\right)^2 \tag{5-1}$$

Where t is the plate thickness, b is the plate width, E is the Young's modulus, v is the poisons ratio and K is the buckling coefficient which is a function of plate geometry and the support conditions.
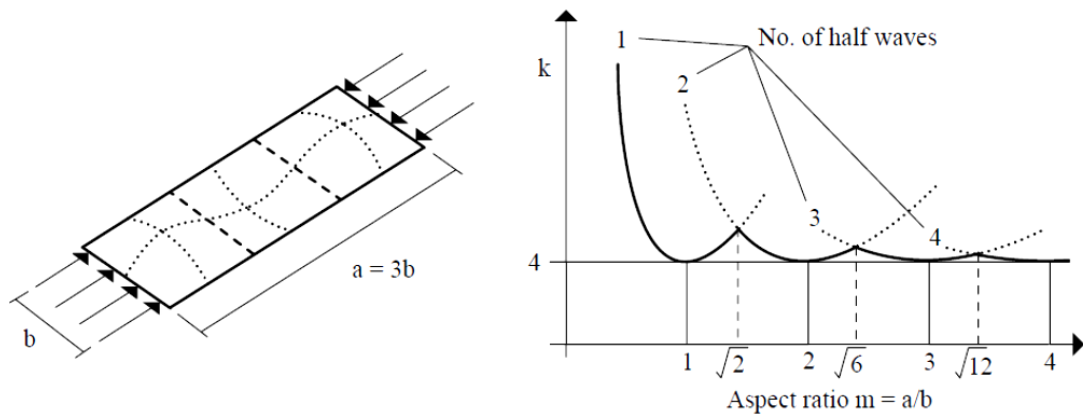
Figure 5-6 (a) Buckling of a plate with m=3, (b) variation of K with respect to *m*

The plate slenderness can be represented as,

$$\beta = \frac{b}{t} \sqrt{\frac{\sigma_y}{E}} \tag{5-2}$$

The plate slenderness below yield stress known as effective plate slenderness can be represented as,

$$\beta_e = \frac{b}{t} \sqrt{\frac{\sigma_e}{E}} = \beta \sqrt{\frac{\sigma_e}{\sigma_y}} \tag{5-3}$$

Tests by Faulkner (1975a) suggest that, for the range of steels currently used in ships, reasonable predictions of pinned plate ultimate strength are given by:

$$\frac{\sigma_u}{\sigma_y} = \frac{b_{eu}}{b} = \begin{cases} \dfrac{2}{\beta} - \dfrac{1}{\beta^2} & \text{when} \quad \beta \geq 1 \\ \\ 1 & \text{when} \ 0 \leq \beta < 1 \end{cases} \tag{5-4}$$

and for edge stresses below yield,

$$\frac{\sigma_{av}}{\sigma_e} = \frac{b_e}{b} = \begin{cases} \dfrac{2}{\beta_e} - \dfrac{1}{\beta_e^2} & \text{when} \quad \beta_e \geq 1 \\ \\ 1 & \text{when} \ 0 \leq \beta_e < 1 \end{cases} \tag{5-5}$$

within the range $\left(0.75\,\sigma_Y \leq \sigma_e < \sigma_Y\right)$

where σ_u is the failure stress across the plate width, b_{eu} is the effective width at failure, σ_{av} is the average stress across the plate, σ_e is the stress at the edge of the plate and b_e is the effective width of the plate.

Equation (5-4) and (5-5) represent a lower bound for plates having reasonable initial distortion $\left(\approx 0.04\,\beta^2 t\right)$ in the buckling mode. Other modes tend to strengthen the plate and stiffen the plate in the post-buckling regime, in the absence of the buckling mode component.

5.5.1 The Effect of Welding Residual Stresses

During welding the local temperatures within a plate can reach twelve times that which would cause yield in resisted thermal expansion of structural steels. It is therefore inevitable that contraction forces of many tonnes will arise on cooling, despite small weld cross-sections. These contraction forces are balanced over the remainder of the plate width by compressive stresses. The resulting residual stress distribution, as shown in Figure 5-7, has a region of tensile yield near to each weld, extending distance ηt across the plate. The residual stress system distorts the plate cross-section, typically towards the stiffener if one is present at the boundary (if the plate edge terminated at a perpendicular plate, ideally there would be no distortion, out-of-plane, of the former plate) and may also distort the plate longitudinally. The compressive

residual stresses and the distortion reduce the compressive strength of the plate and increase the tendency to buckle. In general, longitudinal plate weld seams have little effect on the plate stability and strength.
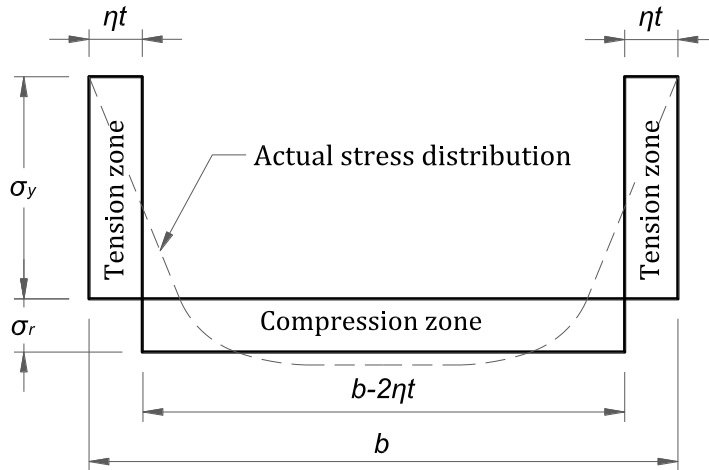
Figure 5-7 Idealised residual stress distribution due to welding in a plate

The width ηt of the yield tension block on each side of the welded joint is governed by the welding process and thickness of the members joined. Many papers have been written on this subject, (Somerville, Swan and Clarke 1977, Cullington and Beales 1977, Faulkner 1977, Kamtekar, White and Dwight 1977, Thompson 1977, Smith and Kirkwood 1976, Faulkner 1975) but for the range of steels and conditions found in ship structures it is normally adequate to assume,

$4.5 < \eta < 6.0$ *as built*

$3.0 < \eta < 4.5$ *after 'shakedown'*

Shakedown is the progressive reduction in residual stresses arising from applied stresses in service. The compressive residual stresses σ_r in the plating are balanced by the tension block on each side of the plate (Figure 5-7), then:

$$\frac{\sigma_r}{\sigma_y} = \frac{2\eta t}{b - 2\eta t} \tag{5-6}$$

It is now possible to define a plate strength reduction factor R_r due to residual stress as,

$$\frac{\sigma_u}{\sigma_y} = \frac{b_{eu}}{b} = \begin{cases} \left[\dfrac{2}{\beta} - \dfrac{1}{\beta^2}\right] R_r & for \quad \beta \geq 1 \\ R_r & for \quad 0 \leq \beta < 1 \end{cases} \tag{5-7}$$

where,

$$R_r = \begin{cases} 1 - \dfrac{\sigma_r}{\sigma_y}\left(\dfrac{E_t}{E}\right)\dfrac{\beta^2}{2\beta - 1} & for \quad \beta \geq 1 \\ 1 - \dfrac{\sigma_r}{\sigma_y}\left(\dfrac{E_t}{E}\right) & for \quad 0 \leq \beta < 1 \end{cases} \tag{5-8}$$

and,

$$\frac{E_t}{E} = \begin{cases} \left[\dfrac{3.62\,\beta^2}{13.1 + p_r(1 - p_r)\beta^4}\right]^2 & for \quad 0 \leq \beta \leq \dfrac{1.9}{\sqrt{p_r}} \\ 1.0 & for \quad \beta \geq \dfrac{1.9}{\sqrt{p_r}} \end{cases} \tag{5-9}$$

The concept of a residual stress reduction factor R_r is here defined for plate ultimate strength. At intermediate loads the effects of residual stresses are complex. A simple approach is to assume that R_r can be directly applied at stresses less than those to cause failure, by modifying Equation (5-5) as given below.

$$\frac{b_e}{b} = \begin{cases} \left[\dfrac{2}{\beta_e} - \dfrac{1}{\beta_e^2}\right] R_r & for \quad \beta_e \geq 1 \\ R_r & for \quad 0 \leq \beta_e < 1 \end{cases} \tag{5-10}$$

The reduced effective width prior to the collapse is,

$$\frac{b_e'}{b} = \begin{cases} \dfrac{1}{\beta_e} R_r & for \quad \beta_e \geq 1 \\ R_r & for \quad 0 \leq \beta_e < 1 \end{cases} \tag{5-11}$$

The above expressions are valid within the range $0.75\sigma_y \leq \sigma_e \leq \sigma_y$

It is important that the limitations of the effective width concept be appreciated. The method makes gross assumptions about stress redistribution and it can

only be justified fully by the fact that it gives results in good agreement with those observed in practice.

5.6 Strength of Stiffened Plates

In the stiffened plate panels, the longitudinal stiffeners have the main function of providing the necessary support to the plates ensuring that they retain the required strength. To fulfil this function, stiffeners must have adequate rigidity and the spacing between them must be chosen according to the main characteristics of the plate namely, its thickness and yield stress. The slenderness of the plate has to be designed in such a way that the ultimate average stress is kept closer to the yield stress as much as possible. Examples of stiffened plates are shown in Figure 5-8.
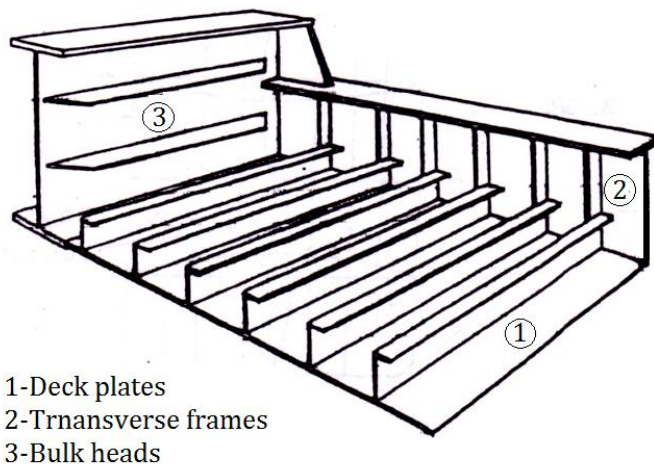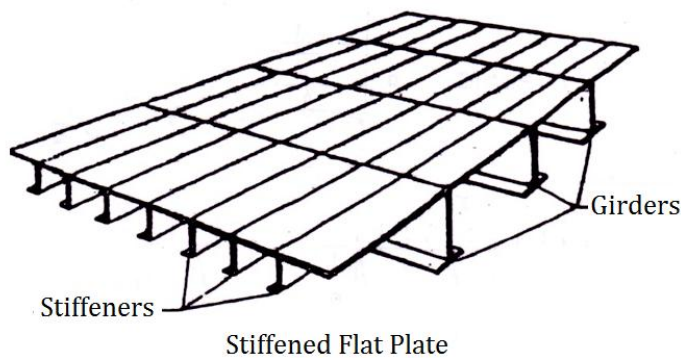
Figure 5-8 Examples of a stiffened plate

The analysis of stiffened plates has been performed by several researchers and many solutions to the problem were presented over the years. The prediction of the panel behaviour has led to the development of several techniques such as nonlinear finite element methods or more simplified formulations applying the beam column concept. Common to all is the need for the application of an incremental end shortening if a realistic description of the post buckling behaviour is required. Also, common to later formulation is the use of load end shortening curves for simply supported plates carried out on separate studies, which have able to describe the loss of plate stiffness after buckling.

Failure of panel is usually classified as,

1. Plate induced failure
2. Stiffener induced failure
3. Tripping induced failure
4. Overall grillage failure

The last mode of failure is normally ignored by ensuring that transverse frames are of adequate size and thereby avoiding any chance of overall grillage failure. The first one occurs when the stiffener is sufficiently stocky and the plate has a lower critical elastic stress. The second failure mode is mainly due to the excessive slenderness of the column (stiffener and effective associated plate acting together) and the failure may be towards the plate or towards the stiffener, depending on the column's initial shape and the type of loading considered, i.e., eccentricity applied or not, following the shift of the neutral axis or not. In a continuous panel, it is usual that the failure is towards the plate in one span and towards the stiffener in the adjacent span. The third mode of failure is the consequence of a lack of torsional rigidity of the stiffener. Interaction with the plate-buckling mode may also occur including premature tripping. Sometimes the first and the second modes are incorporated in the same group because the buckled shape of the panel is similar and is normally towards the stiffener.

(Column buckling mode)

(Tripping mode)

| (a) Plate | (b) Panel | (c) Grillage |
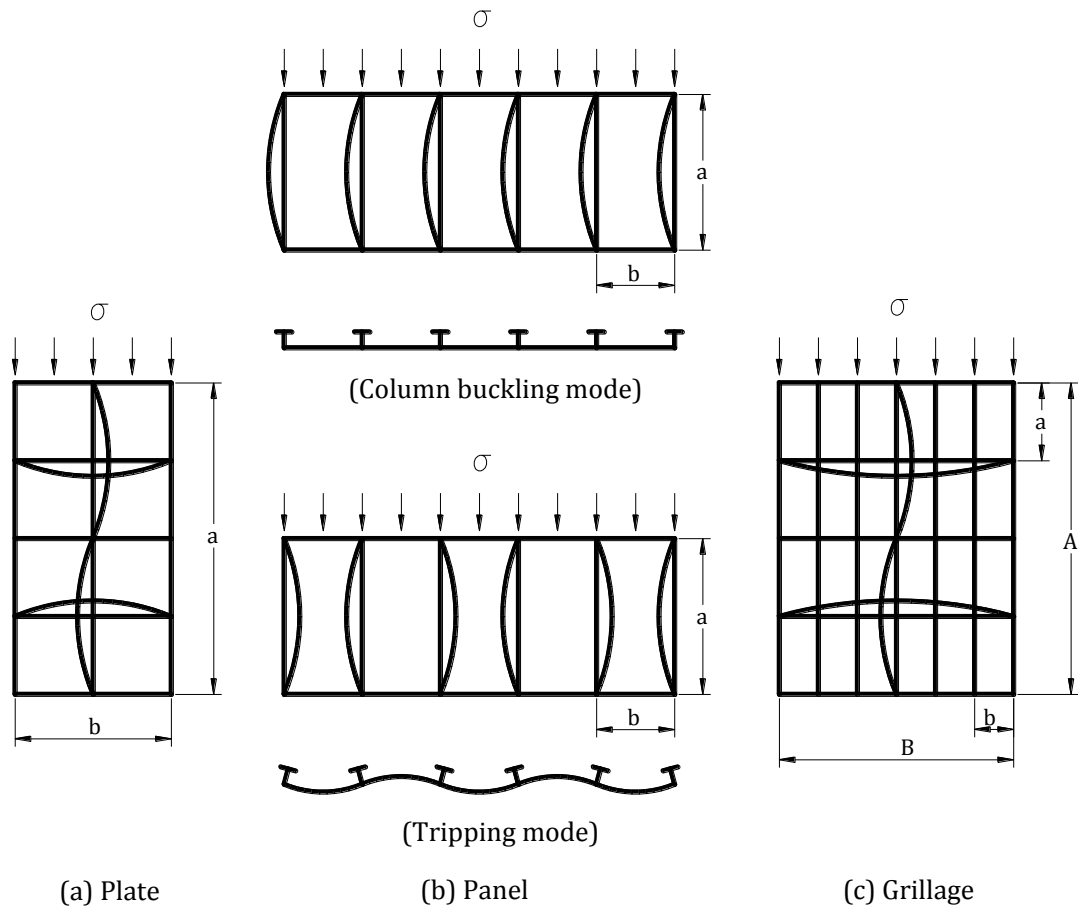
Figure 5-9 Modes of Failure

Design methods to determine the ultimate load of the panels were presented among others by Faulkner based on Johnson-Ostenfield approach, by Carlsen, and Dwight and Little based on Perry-Robertson formulation. One of the major theoretical methods used for predicting the ultimate strength of stiffened panels is the plate stiffener combination approach (also called beam-column approach). This approach uses a representative plate-stiffener combination to represent the behaviour of a stiffened panel since the spacing of stiffeners is normally the same in each direction. Various column strength formulations have been used as the basis of such approaches. Three formulations are discussed here in which the distortion and residual stresses are considered.

1. Faulkner's Method based on Johnson – Ostenfeld formulation
2. Perry – Robertson formulation
3. An empirical formulation obtained by curve fitting experimental data.

5.6.1 Faulkner's Method (Longitudinally Stiffened Panels)

The 'stiffener induced' inter-frame column collapse occurs if the stiffeners are considerably weak (not a common scenario) and generally this mode of failure is ignored. Plate induced column failure between frames can be treated using the tangent modulus buckling methods for stiffeners and also the plate element stiffness and strength expression. Because of structural continuity the longitudinals and associated effective plating may be considered to buckle as a wide stiffened-plate column simply supported between frames. For the limiting value of the edge stress, the Johnson Parabola column collapse equation is used. The tangent modulus approach can now be used to calculate the strength of fabricated steel columns.

The Euler's critical buckling stress for a pinned column with effective length l_e and radius of gyration r in the elastic region is,

$$\sigma_E = \frac{\pi^2 E r^2}{l_e^2} \tag{5-12}$$

The inelastic compressive limiting stress, σ_c for the column can be obtained by substituting the tangent modulus, E_t according to Ostenfeld-Bleich quadratic parabola in the above equation. Assuming the applied stress as the column collapse stress σ_c and substituting E_t in Equation (5-12) and dividing with σ_y gives,

$$\frac{\sigma_c}{\sigma_y} = \frac{\pi^2 r^2}{\sigma_y l_e^2} E\left[\frac{\sigma_c\left(\sigma_y - \sigma_c\right)}{\sigma_{ps}\left(\sigma_y - \sigma_{ps}\right)} \right] = \frac{1}{\lambda^2}\left[\frac{\sigma_c\left(\sigma_y - \sigma_c\right)}{\sigma_{ps}\left(\sigma_y - \sigma_{ps}\right)} \right] \tag{5-13}$$

where column slenderness parameter, $\lambda = \dfrac{l_e}{\pi r}\sqrt{\dfrac{\sigma_y}{E}}$ \hfill (5-14)

Dividing with both numerator and denominator of RHS with σ_y gives,

$$\frac{\sigma_c}{\sigma_y} = \frac{1}{\lambda^2}\left[\frac{\sigma_c / \sigma_y\left(1 - \sigma_c / \sigma_y\right)}{\sigma_{ps} / \sigma_y\left(1 - \sigma_{ps} / \sigma_y\right)} \right] = \frac{1}{\lambda^2 p_r(1 - p_r)}\left[\frac{\sigma_c}{\sigma_y}\left(1 - \frac{\sigma_c}{\sigma_y}\right) \right] \tag{5-15}$$

Substituting structural proportional limit, p_r =0.5 in Equation (5-15) and rearranging,

$$\frac{\sigma_c}{\sigma_y} = 1 - \frac{\lambda^2}{4} \qquad\qquad (5\text{-}16)$$

Based on the above relation, the well-known Johnson Parabola for inelastic column strength has been evolved as,

$$\frac{\sigma_c}{\sigma_y} = \begin{cases} 1 - \dfrac{\lambda^2}{4} & for \quad \lambda \leq \sqrt{2} \\[2mm] \dfrac{1}{\lambda^2} & for \quad \lambda > \sqrt{2} \end{cases} \qquad\qquad (5\text{-}17)$$

The above equation, which define the Johnson parabola for the column strength takes into account the effect of residual stress through structural proportional limit p_r.

The failure of stiffened plate will occur when the compressive stress at stiffener and associated effective plate width reaches the column collapse stress σ_c, which is obtained based on Johnson parabola. These ignore the effect of stiffener shape distortions; but this is nevertheless preferred to the Perry-Robertson approach, which is often used in civil engineering. This preference is based on two facts:

1. The role of residual stresses is considered to be more important than the effects of stiffener shape distortions, and the Perry-Robertson approach cannot include residual stress effects.
2. Comparison with test data shows the tangent modulus approach with p_r=0.5 to give better modelling uncertainties.

The effect of practical plate element shape imperfections is small but is implicitly allowed for in the effective width equations. Effects arising from the welds of the longitudinal stiffeners to the plating are much more important. The

reduction factor, R_r is applied to the plate element effective width and reduced effective width equations.

According to Faulkner, The ultimate strength of the stiffened plate,

$$\frac{\sigma_u}{\sigma_y} = \frac{\sigma_e}{\sigma_y}\left[\frac{A_s + b_e t}{A_s + bt}\right] \qquad (5\text{-}18)$$

An iterative approach is necessary to evaluate the column collapse stress because the effective width and reduced effective width used in the calculation process are also a function of the end stress. So the ultimate strength of the stiffened panel for a simply supported case can be evaluated using an iterative step by step procedure as given below.

Step 1: The compressive end stress σ_e at the plate edges is assumed to have a value in terms of the yield stress of the material (say, $\sigma_e/\sigma_y = 0.8$) as a first approximation to begin with the iterative process.

Step 2: Calculate β and β_e as per Equation (5-2) and (5-3)

Step3: Calculate the tangent modulus as per Equation (5-9)

Step 4: The reduction in stiffness due to the residual stress is evaluated using Equation (5-8)

Step 5: Calculate b_e according to Equation (5-10)

Step 6: Calculate b'_e according to Equation (5-11)

Step 7: The tangent effective moment of inertia I'_e is calculated for the stiffener and tangent effective width of the plate.

Step 8:   The tangent effective radius of gyration is calculated with the tangent effective moment of inertia and effective area (Figure 5-10) as given below,

$$r_e = \sqrt{\frac{I_e^{'}}{A_s + b_e t}} \qquad (5\text{-}19)$$
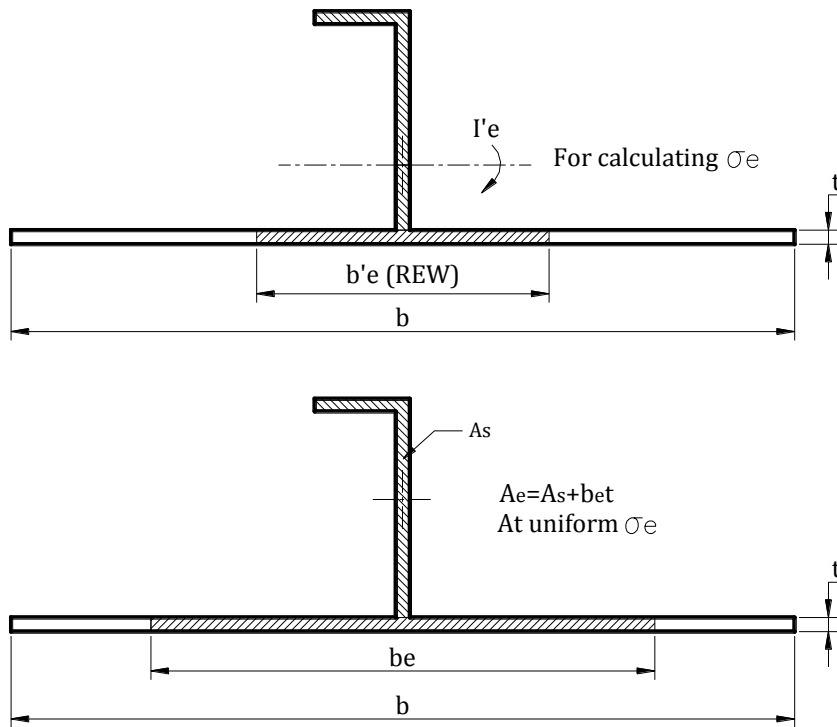
Figure 5-10 Effective and Reduced effective width of the stiffened plate

Step 9:   Calculate the reduced column slenderness λ_e using reduced radius of gyration r_e in Equation (5-14)

Step 10: Calculate the column collapse stress using Equation (5-17). The value obtained from step 10 is compared with the assumed plate edge stress in step 1. Iteration is carried out by updating the edge stress value with the column collapse stress until we get satisfactory level of convergence for σ_e.

Step 11: Calculate the ultimate strength of the stiffened panel using the Faulkner's formula, Equation (5-18) with the converged edge stress value.

5.6.1.1 Residual Stress and Initial Deflection in Faulkner's Method (Pu, Das and Faulkner, 1997)

Although the above explained method predicts the ultimate strength of a stiffened plate quite reasonably, it does not explicitly take care of the effect of initial imperfection. As a result of this, the formulae fail to predict the strength reasonably when the initial distortion is different than that of average level proposed by Smith (1977). Guedes Soares (1988) proposed reduction factors for the residual stresses (R_η), initial distortion (R_δ), and combined initial distortion and residual stress ($R_{\eta\delta}$) as shown below.

$$R_\eta = \left(1 - \frac{\Delta\phi_b}{1.08\phi_b}\right)(1 + 0.0078\eta) \tag{5-20}$$

$$R_\delta = 1 - (0.626 - 0.121\beta_e)\frac{\delta_0}{t} \tag{5-21}$$

$$R_{\eta\delta} = 0.665 + 0.006\eta + 0.36\frac{\delta_0}{t} + 0.14\beta_e \tag{5-22}$$

where η is the residual stress parameter which defines the width of the yield tension residual block as per Equation (5-6), δ_0 is the initial central deflection of the plate, $\Delta\phi_b$ is the compression strength reduction due to residual stress given by,

$$\Delta\phi_b = \frac{\sigma_r}{\sigma_y}\frac{E_t}{E} \tag{5-23}$$

(σ_r/σ_y) is calculated according to Equation (5-6) and (E_t/E) is calculated based on Equation (5-9) for simply supported boundary conditions.

The effective width of a perfect plate is taken as $1.08\,\phi_b$, where,

$$\phi_b = \frac{2}{\beta_e} - \frac{1}{\beta_e^2} \tag{5-24}$$

Pu *et al.* (1997) redefined the tangent (reduced) effective width and effective width of the plate as follows.

$$\frac{b_e'}{b} = \begin{cases} \dfrac{1}{\beta_e} R_\eta R_\delta R_{\eta\delta} & for & \beta_e \geq 1 \\ R_\eta R_\delta R_{\eta\delta} & for & 0 \leq \beta_e < 1 \end{cases} \tag{5-25}$$

$$\frac{b_e}{b} = \begin{cases} 1.08\phi_b R_\eta R_\delta R_{\eta\delta} & for & \beta_e \geq 1 \\ 1.08 R_\eta R_\delta R_{\eta\delta} & for & 0 \leq \beta_e < 1 \end{cases} \tag{5-26}$$

The above equations for effective width and tangent effective width can be used in Step 5 and Step 6 of the Faulkner's method for ultimate strength and hence the effect of initial distortion and residual stress can be incorporated explicitly. This formulation shows better agreement with the test results when compared with the initial formulation.

5.6.2 Perry-Robertson Formula for Stiffener Induced Failure

The Perry – Robertson formulation assumes that the stiffener with associated plating will collapse as a 'beam-column' when the maximum compressive stress in the extreme fiber reaches the yield strength of the material. The two possible collapse modes for the Perry – Robertson formulation are usually considered depending on the failure of the most highly stressed fiber, i.e., 'plate induced failure' and 'stiffener induced failure'. The plate induced failure mode is related to yielding of associated plating due to compression. The stiffener induced failure mode may result from either yielding of the extreme stiffener fiber (without rotation of stiffener) or tripping of stiffener (with rotation of stiffener).

The expression for collapse strength of the column with initial imperfection under axial loading is,

$$\left(\frac{\sigma_c}{\sigma_y}\right) = \left[\frac{1}{2}\left(1 + \frac{1}{\lambda^2} + \frac{y_c\delta_0}{\lambda^2 r^2}\right)\right] - \frac{1}{2}\sqrt{\left[1 + \frac{1}{\lambda^2} + \frac{y_c\delta_0}{\lambda^2 r^2}\right]^2 - \frac{4}{\lambda^2}}$$ (5-27)

Where δ_0 is the initial column distortion, λ is the column slenderness, yc is the distance from elastic neutral axis to the outer fiber of the compressed side and r is the radius of gyration of the section.

The above value for the column collapse strength can be substituted for (σ_e/σ_y) in the Faulkner's formula, Equation (5-18) to obtain the load shortening curve and ultimate strength of the stiffened panel with equivalent column imperfection.

The Perry formula can be modified further to incorporate the residual stress effects by replacing Faulkner's effective slenderness ratio λ_e into the Equation (5-27). But the form of Perry's formula appears to produce increase in strength with reduced slenderness. This is against the observed results and trends and further investigation is needed in this direction to device a proper formulation.

5.6.3 Empirical Formulae

In empirical approaches, the ultimate strength formulations are developed by curve fitting based on mechanical collapse test results or numerical solutions. These types of empirical formulae can often be simple closed-form expressions, which have certain advantages including getting quick first-cut estimates, while their use may be restricted to a specified range of dimensions of be subject to other limitations. A vast number of empirical formulations for ultimate strength of simple beams in steel framed structures have been developed. As an example, Lin (1985), Paik & Thayambilli (1997, 2003) developed empirical formulae for predicting the ultimate strength of a plate-stiffener combination under axial compression in terms of both column and plate slenderness ratios, based on existing mechanical collapse test data for the ultimate strength of stiffened

panels under axial compression and with initial imperfections at an 'average level'.

Formula proposed by Lin (1985)

$$\left(\frac{\sigma_u}{\sigma_y}\right) = \frac{1}{\sqrt{0.960 + 0.765\lambda^2 + 0.176\beta^2 + 0.131\lambda^2\beta^2 + 1.046\lambda^4}} \tag{5-28}$$

Formula proposed by Paik *et al.* (2003)

$$\left(\frac{\sigma_u}{\sigma_y}\right) = \frac{1}{\sqrt{0.995 + 0.936\lambda^2 + 0.170\beta^2 + 0.188\lambda^2\beta^2 + 0.067\lambda^4}} \tag{5-29}$$

Both of the above expressions do not consider the initial imperfection and residual stress explicitly.

5.6.4 Design of Strength of Stiffened Panels

The DNV-RP-C201 code consider the imperfection effects are not necessary to include in the formulations as the contributions of these factors will be accounted with reasonable reduction factors. Even though the code can handle the imperfection effects, it fails to predict the sensitivity of imperfection factors on the strength of the structure. The response is also affected by various other factors which can interact with the imperfection effects to generate quite unpredictable situations. This eventually leads to an uncertain range of reduction factor to be considered and may finally end up with a rather pessimistic estimate.

The API-BULL-2V code is more or less based on the philosophy of Faulkner equation and its modifications. The beam-column approach does not explicitly deals with the initial distortions and hence the sensitivity of this factor is not effectively covered.

5.7 Proposed New Empirical Formula for Stiffened Plates

From the above discussion illustrating the major strength formulations of the unstiffened and stiffened panels, it is clear that,

1. Faulkner model is not taking the initial distortion of the plate into consideration for axial strength evaluation

2. Perry Robertson formula is not considering the residual stress for axial strength evaluation

3. The empirical formulae are not considering imperfection parameters at all for the axial strength evaluation.

4. The modified Faulkner method (Pu-Das-Faulkner) method considers the distortion and residual stresses together but the incorporation of the distortion to modify the slenderness is not conceptually justified.

5. The design codes do not consider the imperfection parameters explicitly but rather as a reduction factor.

As far as a practical stiffened plate is being concerned, the ultimate compressive stress can be considered as a function of plate slenderness (β), column slenderness (λ), initial plate distortion (w_p), initial stiffener distortion (w_s) and weld induced residual stress (σ_r). The geometric distortion and residual stresses are mutually dependent phenomenon. So the author proposes a formulation with terms for initial distortions, residual stresses and an interaction term to account for the combined effects of geometrical distortion and residual stresses. The strength of the stiffened panel takes the general expression in terms of design parameters as follows.

$$\Phi = \left(\frac{\sigma_u}{\sigma_y}\right) = f(\lambda, \beta, w_p, w_s, \sigma_r) \tag{5-30}$$

To fit a function to the numerical data, least square approach has been followed (Gerald and Wheatley, 1998) and the new equation with the interaction term may follow the form,

$$\phi = \frac{1}{\sqrt{n_0 + n_1\lambda^2 + n_2\beta^2 + n_3\lambda^2\beta^2 + n_4\lambda^4 + n_5p^2 + n_6q^2 + n_7r^2 + n_8pqr^2}} \tag{5-31}$$

where $(p=w_p/t)$, $(q=w_s/a)$ and $(r= \sigma_r / \sigma_y)$.

The above formulation can be used with experimental data for ultimate compressive strength of stiffened panels by Faulkner (1977b) and Horne et al. (1976, 1977) to evaluate the constants in the empirical formula.

Let Φ_i be the actual experimental value, and ϕ_i is the corresponding empirical solution. i.e.,

$$\phi_i = \frac{1}{\sqrt{n_0 + n_1\lambda_i^2 + n_2\beta_i^2 + n_3\lambda_i^2\beta_i^2 + n_4\lambda_i^4 + n_5p_i^2 + n_6q_i^2 + n_7r_i^2 + n_8p_iq_ir_i^2}} \tag{5-32}$$

where β_i, λ_i, p_i, q_i, r_i are the corresponding structural parameters of each experimental cases. The coefficients used in the above equation, $n_0, n_1, ..., n_8$ can be evaluated using the least square method as described below.

The above formula can be transformed to a polynomial form by taking inverse and squaring it.

$$x_i = \frac{1}{\phi_i^2} = n_0 + n_1\lambda_i^2 + n_2\beta_i^2 + n_3\lambda_i^2\beta_i^2 + n_4\lambda_i^4 + n_5p_i^2 + n_6q_i^2 + n_7r_i^2 + n_8p_iq_ir_i^2 \tag{5-33}$$

The corresponding term for the experiment is, $X_i = \dfrac{1}{\Phi_i^2}$

The error in the prediction is,

$$Y_i = X_i - x_i \tag{5-34}$$

$$Y_i = X_i - n_0 - n_1\lambda_i^2 - n_2\beta_i^2 - n_3\lambda_i^2\beta_i^2 - n_4\lambda_i^4 - n_5p_i^2 - n_6q_i^2 - n_7r_i^2 - n_8p_iq_ir_i^2 \tag{5-35}$$

According to the least square approach, the sum of the squares of $Y_i = X_i - x_i$ should be a minimum. If there are N data points, the least square function is,

$$Z = \sum_{i=1}^{N}(X_i - x_i)^2 = \sum_{i=1}^{N}(Y_i)^2 \tag{5-36}$$

At the minimum Z, the partial derivatives of the least square function with respect to the each constant should be zero. Thus:

$$\frac{\partial Z}{\partial n_0} = \sum_{i=1}^{N} 2Y_i(-1) = 0$$

$$\frac{\partial Z}{\partial n_1} = \sum_{i=1}^{N} 2Y_i(-\lambda_i^2) = 0$$

$$\frac{\partial Z}{\partial n_2} = \sum_{i=1}^{N} 2Y_i(-\beta_i^2) = 0$$

$$\frac{\partial Z}{\partial n_3} = \sum_{i=1}^{N} 2Y_i(-\lambda_i^2 \beta_i^2) = 0$$

$$\frac{\partial Z}{\partial n_4} = \sum_{i=1}^{N} 2Y_i(-\lambda_i^4) = 0 \tag{5-37}$$

$$\frac{\partial Z}{\partial n_5} = \sum_{i=1}^{N} 2Y_i(-p_i^2) = 0$$

$$\frac{\partial Z}{\partial n_6} = \sum_{i=1}^{N} 2Y_i(-q_i^2) = 0$$

$$\frac{\partial Z}{\partial n_7} = \sum_{i=1}^{N} 2Y_i(-r_i^2) = 0$$

$$\frac{\partial Z}{\partial n_8} = \sum_{i=1}^{N} 2Y_i(-p_i q_i r_i^2) = 0$$

Dividing each of the above equations by -2 and rearranging leads to nine linear simultaneous equations as follows.

$$\sum_{i=1}^{N} X_i = n_0 N + n_1 \sum_{i=1}^{N} \lambda_i^2 + n_2 \sum_{i=1}^{N} \beta_i^2 + n_3 \sum_{i=1}^{N} \lambda_i^2 \beta_i^2 + n_4 \sum_{i=1}^{N} \lambda_i^4 + n_5 \sum_{i=1}^{N} p_i^2$$
$$+ n_6 \sum_{i=1}^{N} q_i^2 + n_7 \sum_{i=1}^{N} r_i^2 + n_8 \sum_{i=1}^{N} p_i q_i r_i^2$$

$$\sum_{i=1}^{N} X_i \lambda_i^2 = n_0 \sum_{i=1}^{N} \lambda_i^2 + n_1 \sum_{i=1}^{N} \lambda_i^4 + n_2 \sum_{i=1}^{N} \lambda_i^2 \beta_i^2 + n_3 \sum_{i=1}^{N} \lambda_i^4 \beta_i^2 + n_4 \sum_{i=1}^{N} \lambda_i^6$$
$$+ n_5 \sum_{i=1}^{N} \lambda_i^2 p_i^2 + n_6 \sum_{i=1}^{N} \lambda_i^2 q_i^2 + n_7 \sum_{i=1}^{N} \lambda_i^2 r_i^2 + n_8 \sum_{i=1}^{N} \lambda_i^2 p_i q_i r_i^2$$

$$\sum_{i=1}^{N} X_i \beta_i^2 = n_0 \sum_{i=1}^{N} \beta_i^2 + n_1 \sum_{i=1}^{N} \beta_i^2 \lambda_i^2 + n_2 \sum_{i=1}^{N} \beta_i^4 + n_3 \sum_{i=1}^{N} \lambda_i^2 \beta_i^4 + n_4 \sum_{i=1}^{N} \lambda_i^4 \beta_i^2$$
$$+ n_5 \sum_{i=1}^{N} \beta_i^2 p_i^2 + n_6 \sum_{i=1}^{N} \beta_i^2 q_i^2 + n_7 \sum_{i=1}^{N} \beta_i^2 r_i^2 + n_8 \sum_{i=1}^{N} \beta_i^2 p_i q_i r_i^2$$

$$\sum_{i=1}^{N} X_i \lambda_i^2 \beta_i^2 = n_0 \sum_{i=1}^{N} \lambda_i^2 \beta_i^2 + n_1 \sum_{i=1}^{N} \beta_i^2 \lambda_i^4 + n_2 \sum_{i=1}^{N} \lambda_i^2 \beta_i^4 + n_3 \sum_{i=1}^{N} \lambda_i^4 \beta_i^4 + n_4 \sum_{i=1}^{N} \lambda_i^6 \beta_i^2$$
$$+ n_5 \sum_{i=1}^{N} \lambda_i^2 \beta_i^2 p_i^2 + n_6 \sum_{i=1}^{N} \lambda_i^2 \beta_i^2 q_i^2 + n_7 \sum_{i=1}^{N} \lambda_i^2 \beta_i^2 r_i^2 + n_8 \sum_{i=1}^{N} \lambda_i^2 \beta_i^2 p_i q_i r_i^2$$

$$\sum_{i=1}^{N} X_i \lambda_i^4 = n_0 \sum_{i=1}^{N} \lambda_i^4 + n_1 \sum_{i=1}^{N} \lambda_i^6 + n_2 \sum_{i=1}^{N} \lambda_i^4 \beta_i^2 + n_3 \sum_{i=1}^{N} \lambda_i^6 \beta_i^2 + n_4 \sum_{i=1}^{N} \lambda_i^8$$
$$+ n_5 \sum_{i=1}^{N} \lambda_i^4 p_i^2 + n_6 \sum_{i=1}^{N} \lambda_i^4 q_i^2 + n_7 \sum_{i=1}^{N} \lambda_i^4 r_i^2 + n_8 \sum_{i=1}^{N} \lambda_i^4 p_i q_i r_i^2$$

$$\sum_{i=1}^{N} X_i p_i^2 = n_0 \sum_{i=1}^{N} p_i^2 + n_1 \sum_{i=1}^{N} \lambda_i^2 p_i^2 + n_2 \sum_{i=1}^{N} \beta_i^2 p_i^2 + n_3 \sum_{i=1}^{N} \lambda_i^2 \beta_i^2 p_i^2 + n_4 \sum_{i=1}^{N} \lambda_i^4 p_i^2$$
$$+ n_5 \sum_{i=1}^{N} p_i^4 + n_6 \sum_{i=1}^{N} q_i^2 p_i^2 + n_7 \sum_{i=1}^{N} r_i^2 p_i^2 + n_8 \sum_{i=1}^{N} p_i^3 q_i r_i^2$$

$$\sum_{i=1}^{N} X_i q_i^2 = n_0 \sum_{i=1}^{N} q_i^2 + n_1 \sum_{i=1}^{N} \lambda_i^2 q_i^2 + n_2 \sum_{i=1}^{N} \beta_i^2 q_i^2 + n_3 \sum_{i=1}^{N} \lambda_i^2 \beta_i^2 q_i^2 + n_4 \sum_{i=1}^{N} \lambda_i^4 q_i^2$$
$$+ n_5 \sum_{i=1}^{N} p_i^2 q_i^2 + n_6 \sum_{i=1}^{N} q_i^4 + n_7 \sum_{i=1}^{N} r_i^2 q_i^2 + n_8 \sum_{i=1}^{N} p_i q_i^3 r_i^2$$

$$\sum_{i=1}^{N} X_i r_i^2 = n_0 \sum_{i=1}^{N} r_i^2 + n_1 \sum_{i=1}^{N} \lambda_i^2 r_i^2 + n_2 \sum_{i=1}^{N} \beta_i^2 r_i^2 + n_3 \sum_{i=1}^{N} \lambda_i^2 \beta_i^2 r_i^2 + n_4 \sum_{i=1}^{N} \lambda_i^4 r_i^2$$
$$+ n_5 \sum_{i=1}^{N} p_i^2 r_i^2 + n_6 \sum_{i=1}^{N} q_i^2 r_i^2 + n_7 \sum_{i=1}^{N} r_i^4 + n_8 \sum_{i=1}^{N} p_i q_i r_i^4$$

$$\sum_{i=1}^{N} X_i p_i q_i r_i^2 = n_0 \sum_{i=1}^{N} p_i q_i r_i^2 + n_1 \sum_{i=1}^{N} \lambda_i^2 p_i q_i r_i^2 + n_2 \sum_{i=1}^{N} \beta_i^2 p_i q_i r_i^2$$
$$+ n_3 \sum_{i=1}^{N} \lambda_i^2 \beta_i^2 p_i q_i r_i^2 + n_4 \sum_{i=1}^{N} \lambda_i^4 p_i q_i r_i^2 + n_5 \sum_{i=1}^{N} p_i^3 q_i r_i^2$$
$$+ n_6 \sum_{i=1}^{N} p_i q_i^3 r_i^2 + n_7 \sum_{i=1}^{N} p_i q_i r_i^4 + n_8 \sum_{i=1}^{N} p_i^2 q_i^2 r_i^4$$

(5-38)

The above simultaneous equations are solved using the experimental data (β_i, λ_i, p_i, q_i, r_i) to evaluate the coefficients n_0, n_1, ..., n_8.

The Equation (5-38) can be expressed in a matrix form as, $[A]x[n]=[B]$ and the coefficient matrix, $[n]$ can be solved as, $[n]=[A]^{-1}[B]$. The new empirical formula for the compressive ultimate strength of a stiffened panel with effects of combined effects of initial distortion and residual stress is,

$$\frac{\sigma_u}{\sigma_y} = \frac{1}{\sqrt{1.29 + 0.44\lambda^2 + 0.09\beta^2 + 0.09\lambda^2\beta^2 + 0.36\lambda^4 + 0.14p^2 - 0.05q^2 + 1.33r^2 + 0.12pqr^2}}$$

(5-39)

The test results are compared with the above formula and the previously proposed formulations by Lin and Paik. Table 5-1 and Table 5-2 show the statistical comparison. The test data used to generate the empirical constants are used to compare the results. There is some concern about the formula as how the fitted equation can be validated based on the data used to generate the equation. The formulation is generated using the entire data and the validation is presented making the data into two sets as conducted by the individual researchers. Further, there is limited test data available with the specific boundary conditions and the imperfection parameters as discussed earlier. The results indicate that the new formulation shows better correlation with the test results. The mean of model uncertainty factor is more close to unity with lower COV.

Table 5-1 Comparison of experimental results by Horne *et al.* (1976, 1977)

Sl. No.	λ	β	$p=w_p/t$	$q=w_s/a$	$r=\sigma_r/\sigma_y$	$\varphi=\sigma_u/\sigma_y$	Lin, (1985)	Paik et al. (2003)	Proposed Formula
1	0.314	1.004	0.13	0.20	0.178	0.976	0.899	0.885	0.822
2	0.330	1.956	0.47	0.10	0.178	0.733	0.749	0.740	0.746
3	0.346	3.069	1.11	0.33	0.178	0.713	0.590	0.585	0.631
4	0.597	0.952	0.03	2.46	0.178	0.824	0.799	0.807	0.863
5	0.648	1.912	0.29	1.01	0.178	0.750	0.658	0.661	0.705
6	0.703	3.152	0.58	2.85	0.178	0.621	0.501	0.497	0.618
7	0.675	4.068	1.36	0.47	0.178	0.515	0.429	0.421	0.498
8	0.918	0.953	0.12	2.43	0.178	0.716	0.619	0.701	0.742
9	0.972	1.912	0.45	1.33	0.178	0.660	0.519	0.569	0.614
10	1.020	2.965	1.08	1.76	0.178	0.494	0.421	0.442	0.512
11	1.020	4.084	2.05	0.72	0.178	0.448	0.351	0.354	0.415
12	0.405	1.000	0.12	0.15	0.178	0.988	0.873	0.861	0.811
13	0.356	2.990	0.49	0.29	0.178	0.764	0.598	0.593	0.655
14	0.376	2.867	1.03	0.36	0.178	0.569	0.610	0.604	0.647
15	0.386	3.952	1.93	0.18	0.178	0.506	0.491	0.486	0.531
16	0.770	0.951	0.03	0.71	0.178	0.882	0.705	0.749	0.740
17	0.690	1.936	0.20	0.39	0.178	0.656	0.638	0.646	0.687
18	0.781	3.027	0.65	0.42	0.178	0.563	0.490	0.491	0.567
19	0.782	4.088	0.83	0.31	0.178	0.455	0.405	0.398	0.485
20	1.223	1.010	0.12	1.12	0.178	0.696	0.455	0.608	0.581
21	1.065	0.990	0.48	0.55	0.178	0.515	0.535	0.653	0.632
22	1.154	2.972	1.08	0.64	0.178	0.491	0.380	0.414	0.469
23	1.145	3.912	1.89	0.45	0.178	0.384	0.332	0.343	0.401
24	0.307	2.961	1.08	0.00	0.178	0.566	0.609	0.605	0.645
25	0.434	1.089	0.07	0.43	0.178	0.779	0.852	0.841	0.804
26	0.434	1.089	0.14	0.00	0.178	0.752	0.852	0.841	0.801
27	0.376	0.956	0.11	0.35	0.178	0.787	0.888	0.875	0.819
28	0.376	0.956	0.11	0.00	0.178	0.723	0.888	0.875	0.817
29	0.714	2.062	0.01	0.95	0.178	0.619	0.614	0.622	0.677
30	0.626	2.905	1.01	0.00	0.178	0.610	0.547	0.542	0.602
31	0.532	1.308	0.21	0.00	0.178	0.744	0.785	0.782	0.769
32	0.446	1.999	0.05	0.75	0.178	0.634	0.714	0.706	0.738
33	0.391	1.397	0.23	0.00	0.178	0.879	0.821	0.810	0.786
34	0.411	0.701	0.06	0.00	0.178	0.820	0.907	0.894	0.825
						Mean(X_m)	1.09	1.06	1.01
						COV(X_m)	14.48%	12.41%	10.38%

Table 5-2 Comparison of experimental results by Faulkner (1977b)

Sl. No.	λ	β	$p=w_p/t$	$q=w_s/a$	$r=\sigma_r/\sigma_y$	$\varphi=\sigma_u/\sigma_y$	Lin, (1985)	Paik et al. (2003)	Proposed Formula
1	0.251	1.708	0.13	1.85	0.129	0.854	0.803	0.795	0.830
2	0.251	1.708	0.13	1.85	0.129	0.854	0.803	0.795	0.830
3	0.440	1.692	0.18	0.30	0.412	0.794	0.762	0.753	0.721
4	0.442	1.717	0.09	0.38	0.125	0.851	0.757	0.749	0.762
5	0.504	1.717	0.08	0.30	0.122	0.782	0.737	0.731	0.751
6	0.449	1.760	0.19	0.66	0.120	0.791	0.749	0.740	0.760
7	0.440	1.692	0.27	0.52	0.418	0.794	0.762	0.753	0.720
8	0.449	1.760	0.61	0.27	0.120	0.750	0.749	0.740	0.746
9	0.440	1.692	0.63	0.46	0.418	0.832	0.762	0.753	0.711
10	0.538	0.971	0.89	0.44	0.120	0.544	0.825	0.824	0.772
11	0.534	2.897	0.23	0.66	0.066	0.569	0.572	0.565	0.645
12	0.527	2.879	0.88	1.39	0.418	0.642	0.576	0.569	0.613
13	0.518	2.832	0.22	0.66	0.418	0.564	0.584	0.576	0.624
14	0.528	2.909	0.23	0.90	0.424	0.608	0.572	0.565	0.617
15	1.096	1.694	0.54	0.68	0.120	0.632	0.480	0.563	0.583
16	1.001	1.540	0.31	0.60	0.132	0.648	0.534	0.607	0.628
17	1.018	1.570	0.57	0.38	0.418	0.574	0.524	0.598	0.591
18	1.032	1.575	0.12	0.44	0.315	0.600	0.517	0.594	0.603
19	1.148	2.840	0.97	0.44	0.120	0.471	0.389	0.427	0.481
20	1.148	2.835	0.26	0.49	0.088	0.476	0.390	0.428	0.489
21	1.139	2.829	0.86	0.98	0.418	0.443	0.393	0.430	0.475
22	1.139	2.815	0.38	0.93	0.330	0.448	0.394	0.431	0.486
23	0.606	0.805	0.08	0.20	0.418	0.892	0.809	0.821	0.743
24	0.593	0.779	0.11	0.40	0.594	0.739	0.818	0.828	0.702
25	0.659	0.816	0.10	0.43	0.418	0.812	0.780	0.802	0.733
26	0.601	0.821	0.09	0.40	0.458	0.660	0.810	0.821	0.735
27	0.737	0.790	0.11	0.47	0.418	0.613	0.738	0.778	0.717
28	0.759	0.796	0.08	0.30	0.545	0.546	0.724	0.770	0.683
29	0.850	0.838	0.05	0.27	0.120	0.681	0.667	0.735	0.722
30	0.867	0.842	0.10	0.40	0.191	0.595	0.656	0.729	0.711
31	0.840	0.828	0.09	0.57	0.418	0.754	0.673	0.739	0.690
32	0.844	0.832	0.09	0.80	0.568	0.709	0.671	0.738	0.660
33	0.728	0.858	0.07	0.41	0.556	0.787	0.737	0.774	0.685
34	0.790	1.344	0.14	0.26	0.329	0.791	0.658	0.695	0.688
35	0.784	1.532	0.16	0.39	0.219	0.750	0.642	0.672	0.690
36	0.839	2.132	0.19	0.41	0.102	0.717	0.556	0.578	0.634
37	0.838	2.138	0.28	0.44	0.177	0.714	0.556	0.577	0.630
38	0.851	2.204	0.20	0.30	0.269	0.636	0.544	0.566	0.614
39	0.866	2.229	0.14	0.30	0.067	0.693	0.536	0.559	0.619
						Mean(X_m)	1.07	1.03	1.02
						COV(X_m)	13.54%	12.83%	10.82%

5.8 Comparison of Strength Models for Plated Structures

In the present situation, with all the analytical and empirical formulae discussed above, a comparison is necessary to evaluate the effectiveness of each approach for the sensitivity study of plated structures against the initial distortions and residual stresses. Apart from the above models, the FE model previously validated against experiment data in Chapter 4 also is used for the comparison. The Analytical models are fundamentally based on a beam-column approach and it eventually limits the scope of considering plate distortion and other interaction aspects of plate and stiffener distortions explicitly.

In this section, a typical stiffened plated scantling is compared with all the strength prediction approaches discussed above. The Experimental model scantlings and results discussed in Chapter 3 cannot be used here as the boundary conditions were different. So the validated FEA result is used as a reference for the comparison.
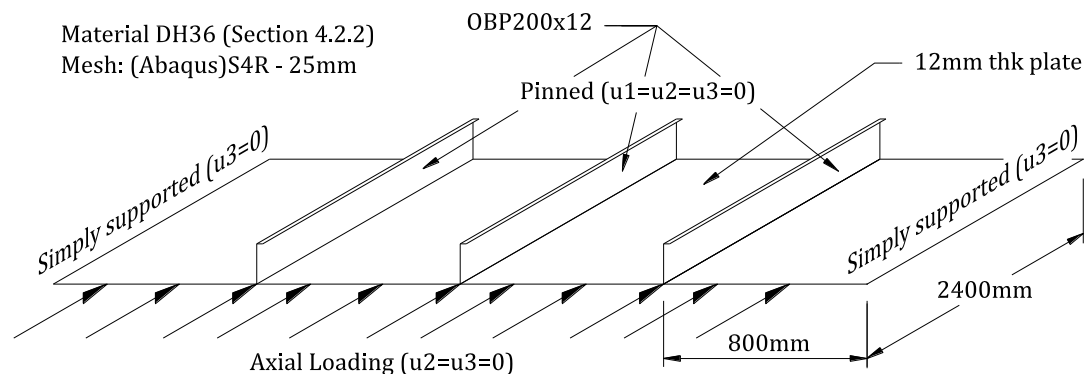
Figure 5-11 Details of FE Model used for the comparison

A stiffened panel of plate thickness 12mm with OBP200 is compared. The details of the geometry, Boundary conditions, material and mesh details of the sample are illustrated in Figure 5-11. The comparison results are shown in Table 5-3. The geometrical distortion and residual stresses were chosen as Low (L), Medium (M), High (H) and Severe (S) for the structure which is parametrically explained in Section 6.2.

Table 5-3 Comparison of Strength models based on imperfections

Sl No.	$\delta 0$ (mm)	$\sigma r/\sigma y$	Analysis methods				
			Faulkner	Pu-Das-Faulkner	Perry Robertson	Proposed Empirical	FEM
1	2.33 (L)	0 (0)	0.65	0.71	0.62	0.67	0.70
2	2.33 (L)	0.05 (L)	0.62	0.68	0.62	0.67	0.68
3	2.33 (L)	0.11 (M)	0.58	0.65	0.62	0.66	0.68
4	2.33 (L)	0.18 (H)	0.52	0.60	0.62	0.66	0.68
5	2.33 (L)	0.25 (S)	0.47	0.55	0.62	0.65	0.67
6	9.30 (M)	0 (0)	0.65	0.69	0.50	0.65	0.66
7	9.30 (M)	0.11 (M)	0.58	0.63	0.50	0.65	0.66
8	27.91 (H)	0 (0)	0.65	0.49	0.33	0.58	0.60
9	27.91 (H)	0.18 (H)	0.52	0.43	0.33	0.57	0.63
10	37.22 (S)	0 (0)	0.65	0.30	0.29	0.53	0.57
11	37.22 (S)	0.25 (S)	0.47	0.27	0.29	0.52	0.61
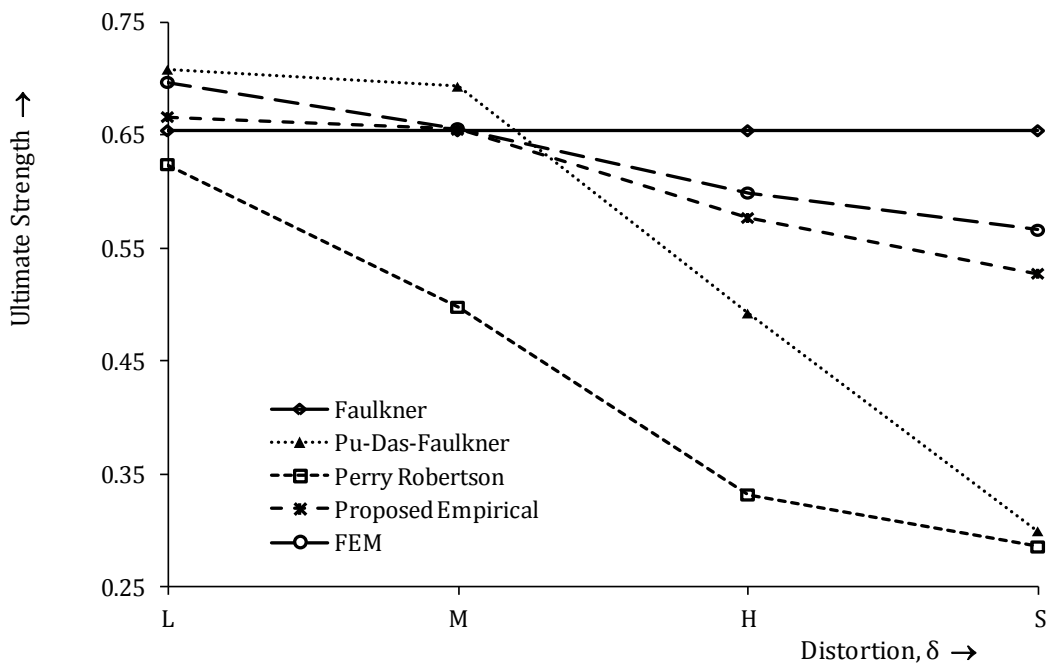
Figure 5-12 Effect of Initial distortion on the strength

Figure 5-12 shows the effect of distortion on the strength of the stiffened plate with the above scantlings. The Faulkner's formula shows little response with respect to distortion on the strength as the formula does not take into account the distortion effects implicitly or explicitly. Pu-Das-Faulkner equation, the modified Faulkner's equation, is responsive to the distortion but the prediction appears to be very pessimistic for this typical structure with high initial distortions and it appears to be incapable of handling high distortions as well.

The Perry formula is very pessimistic in prediction, but it shows identical trend of variation when comparing with the FEA results. The proposed Empirical relation shows good correlation with the FEA results and it shows identical trends with varying levels of distortion. Since the slenderness parameters of the typical structure is within the range considered in Table 5-1 and Table 5-2, the results appears to fit quite close to the reality and hence the FE results again justified.
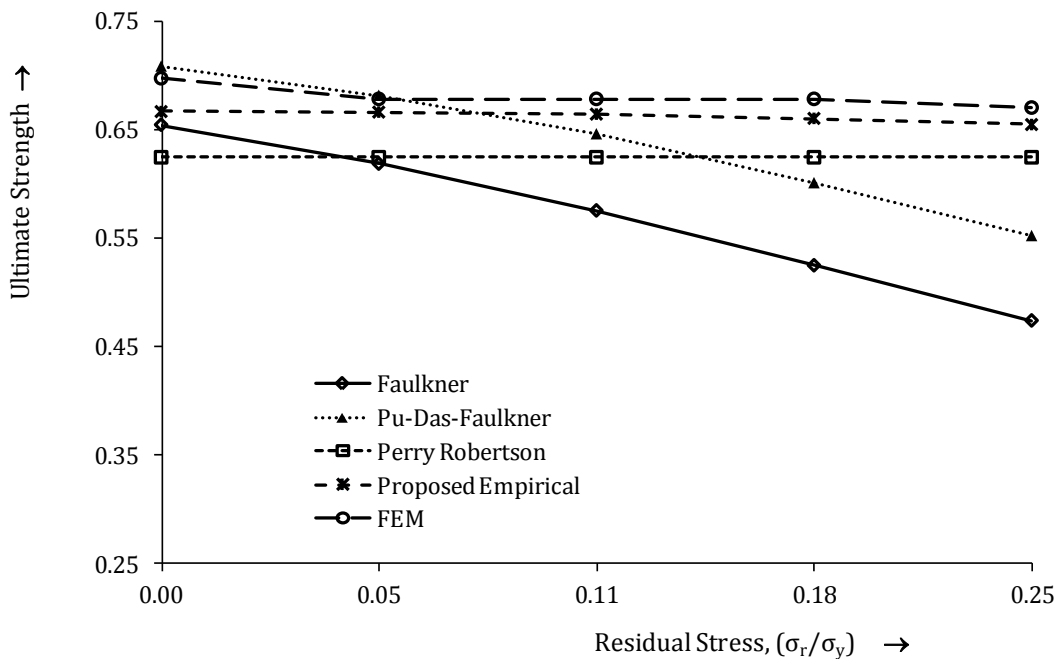
Figure 5-13 Effect of residual stress on the strength

Figure 5-13 shows the results for the same structure with increasing residual stresses. Both the Faulkner and Pu-Das equation shows identical response to the residual stresses but at a steady offset. Perry formula is not affected as it inherently does not capable of handling residual stresses. It can be observed that the Empirical and FE results are quite close and follow similar trend.

Figure 5-14 shows the combined effect of initial distortion and residual stresses on the strength of the typical structure. Faulkner equation shows the effect of residual stress alone and Perry equation responds to initial distortion only. Pu-Das equation shows good agreement with the FE and Empirical predictions for comparatively lower range of distortion and as the distortion increases the

prediction falls too far from the numerical results. Empirical relation shows good agreement with lower values of distortion and it deviates far as the imperfection increases. This is because of the fact that the evaluation of constants for empirical relations have been made with lower ranges of imperfection parameters.
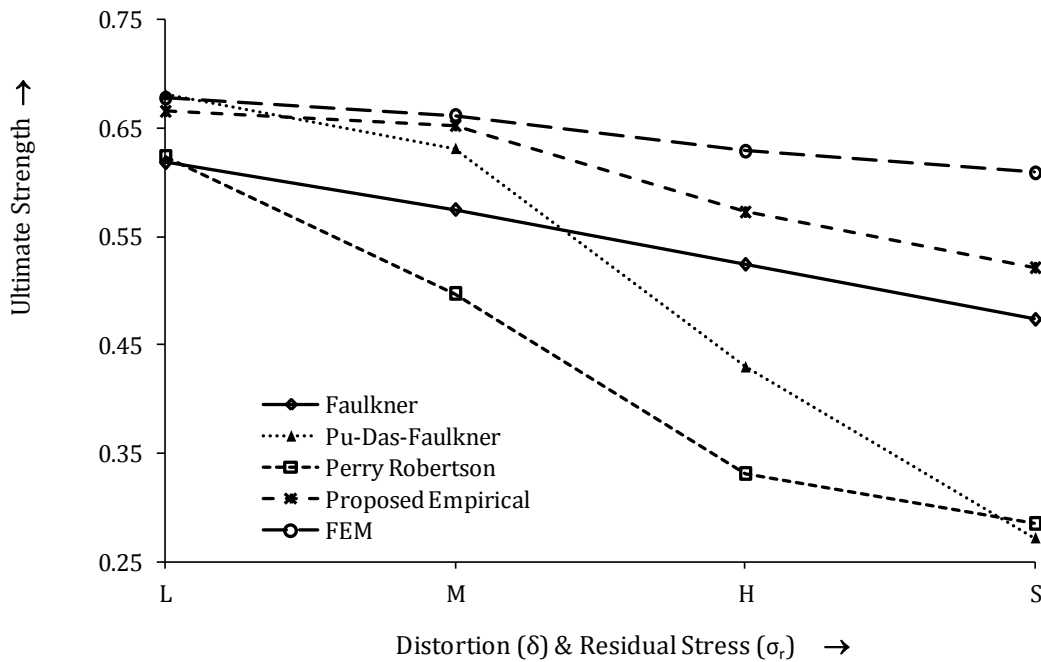
Figure 5-14 Effect of distortion and residual stress on the strength

5.9 Summary

This chapter describes the behaviour of plated structures under the axial compressive loading condition which is the primary concern in the limit state design of marine, particularly for ship structures. The major formulations and codes are based on the beam column approach and hence the types and components of imperfections should also be confined within the frame of this concept. The Faulkner's analytical approach considers the effect of residual stress as a linear and proportional effect. In a similar way the Perry approach takes into effect the distortion but the response is too much when compared to the numerical model. The extension of Faulkner model can take both the distortion and residual stresses, but again the response is found to be valid

within a range. This is probably because of the empirical constants might have chosen based on results for a particular set of experimental results.

A strength model combining the Faulkner approach and the Perry approach can represent the effect of residual stress and distortion simultaneously and conceptually truthful. In the Perry approach, the ultimate strength of the column is defined in terms of the column slenderness along with the distortion and section parameters. The column slenderness can be replaced with the reduced effective column slenderness with the appropriate reduction factors corresponding to the residual stresses. This strength modelling will be conceptually more accurate compared to all other approaches.

In reality, the imperfection of a true stiffened panel is extremely complex to represent and many a times it does not fit into the outline of a beam column model. The effect of initial distortion on the plate part of the structure during compression is totally ignored in the theoretical approaches. The analytical approaches those consider the effect of imperfections are found to be very pessimistic with increasing imperfections when compared with numerical results. The FEA results and the Empirical model based on experimental results show that the effect of distortion on strength is not necessarily linear. From the results of comparison, it is observed that, even though the formulations and codes are proved and established, these are not fully capable of considering the nonlinear influence of distortion parameters on the strength of structures. So the use of a validated FE model is found necessary to evaluate the sensitivity of distortion parameters on the strength of the structure.

Chapter 6. Imperfection Sensitivity of Plated Structures

6.1 Introduction

The behaviour of plated structures based on the operating and various physical factors is a subject of great interest for the researchers from the structural engineering domain, particularly from the offshore engineering field as being the major beneficiary. Since the response of the structure is highly complex and dependent on numerous factors, it is impossible to propose a comprehensive approach to cater for all the requirements. As the behaviour of structure in particular situations is being considered, the study needs to be extended according to the intended usages and particular objectives. This study focuses on the buckling and post buckling strength response and behaviour of unstiffened and stiffened plated structures under the influence of weld induced geometrical imperfections and residual stresses. Some of the analytical approaches already discussed in Chapter 3 are capable enough to predict the behaviour under the aforementioned factors. The analytical models incorporate the effects either by assigning a specific reduction factor or through empirical relations with appropriate constants. In a close observation, the results are not comparable with the verified numerical models. It is because of the fact that the analytical models do not consider or incapable of considering the real mechanism with the influence of imperfection parameters in the failure phenomenon of similar structures with associated nonlinearity and interaction effects.

This study investigates the sensitivity of the distortion parameters for various range of scantlings used in the shipbuilding industry. The classification societies and rule based design codes put stringent constraints on the tolerances for panel fabrication. It often ends up with large reworks and huge financial losses and man hours. Many researchers (Koji M. and Alaa M. 2008, Paik *et al.* 2004,

etc.) carried out works to investigate the effect of imperfections in the plated structures using analytical and numerical techniques. All the researches reveal the fact that the influence of imperfection is highly unpredictable and it affects the strength of the structure in different ways in particular situations. Paik *et al.* (2004) state that sometimes the distortion found to increases the strength of the structure slightly. It further confirms the fact that the treatment of imperfections in the analytical environment does not portray the reality to the full extent. Moreover, the design of stiffened plates in particular is dependent on many parameters which are beyond the scope of any codified rules. The behaviour of offset bulb plate and an angle bar with similar material and geometrical parameter need not behave alike in all design conditions.

The studies carried out by various researchers in this area analyse the problem with some typical scantlings of plated structures alone. Even though some of the studies are covered a wide range of imperfection, the study is restricted to certain limited range of structural slenderness and predominantly based on plate slenderness (β). The parametric definition of a stiffened plate with plate slenderness (β) alone is meaningless as the difference in the stiffener dimensions will keep β value same but the performance will be entirely different. Hence the performance of a stiffened plate should be monitored against its plate slenderness (β) and column slenderness (λ) so as to make the results sensible. This study attempt to explicitly quantify the individual and combined contribution of imperfection parameters on the strength of the structure based on important structural slenderness parameters.

6.2 Proposed Parametric Imperfections

The commonly accepted range of plate distortion and residual stress for the stiffened and unstiffened panels are chosen based on the parametric estimates proposed by Smith et al. (1998) as given in Table 6-1. This range is used by many researchers to investigate the structural response under various circumstances.

Table 6-1 Initial imperfection levels (Smith et al., 1988)

Level	Initial Distortion (w_p/t_p)	Residual Stress (σ'_r)
Slight	$0.025\beta^2$	0.05
Average	$0.1\,\beta^2$	0.15
Severe	$0.3\,\beta^2$	0.3

The initial distortion in an unstiffened panel is assumed as sinusoidal waves along its length. In a stiffened panel, the initial distortion can be considered as a combination of distortions observed separately in plates and stiffeners. So the above parametric definition is not sufficient to address the complicated distortion in a stiffened panel structure.

The distortion in stiffened panels can be broadly categorised into Plate distortion w_p, Stiffener Bowing (or dishing of the stiffened plate) w_s and Stiffener warping (out of plane bending) v_s. The positive directions of the above mentioned distortions used in this study are as shown in Figure 6-1. In reality, the three elements of geometrical distortions in a stiffened panel can exist in many ways. A detailed explanation of three forms of the distortion is given in Chapter 4. The proposed levels of parametric distortion hold good agreement and correlation with measurements of panels fabricated at BAE systems shipyard in Govan, Glasgow for the Experimental analyses as described in Chapter 3.
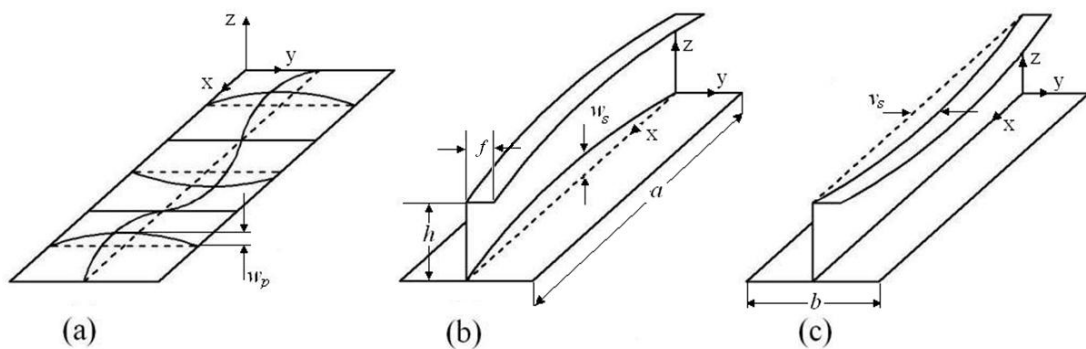
Figure 6-1 (a) Plate distortion (b) Stiffener bowing (c) Stiffener warping

The range of all the distortion parameters is defined in a parametric form based on the slenderness of the structure. The plate distortion is parametrically defined based on the plate slenderness (β), the bowing distortion is based on

the bowing slenderness (α) as defined in Equation (6-4) and the warping distortion is based on the warping slenderness (γ) as per Equation (6-5). The residual stress can also represented parametrically in terms of η, but it is of no physical significance and cannot use for any direct comparison. So the residual stress as a fraction of the material yield stress is a better way of representation with more understanding. The analyses have conducted for a wide range of unstiffened and stiffened plate scantlings based on a sensible range of plate and column slenderness commonly used by the ship building industry. The sensitivity of the imperfection factors in this range will serve the industrial purpose of estimating the loss of strength for the most common structural scantlings. The maximum distortion amplitudes for each type can be represented parametrically as,

Plate distortion, $w_p = \delta_p t_p \beta^2$ (6-1)

Stiffener bowing, $w_s = \delta_b t_p \alpha^2$ (6-2)

Stiffener warping, $v_s = \delta_w t_p \gamma^2$ (6-3)

Where δ_p, δ_b and δ_w are the coefficients to define the range of distortion values

Bowing slenderness, $\alpha = \dfrac{a}{h}\sqrt{\dfrac{\sigma_y}{E}}$ (6-4)

Warping slenderness, $\gamma = \dfrac{a}{f}\sqrt{\dfrac{\sigma_y}{E}}$ (6-5)

The distortions can be represented in a non-dimensional parametric fashion by rearranging the above equations as,

Non-dimensional plate distortion, $\delta_p = w_p / t_p \beta^2$ (6-6)

Non-dimensional Stiffener bowing, $\delta_b = w_s / t_p \alpha^2$ (6-7)

Non-dimensional Stiffener warping, $\delta_w = v_s / t_p \gamma^2$ (6-8)

Table 6-2 Levels of Initial Distortion and Residual stresses

Imperfection Level	Plate Distortion $\delta_p = w_p/t_p\beta^2$	Stiffener Bowing $\delta_b = w_s/t_p\alpha^2$	Stiffener Warping $\delta_w = v_s/t_p\gamma^2$	Residual Stress σ_r/σ_y
L (Light)	0.025	0.020	0.003	0.05
M (Medium)	0.100	0.080	0.010	0.11
H (High)	0.300	0.160	0.020	0.18
S (Severe)	0.500	0.250	0.030	0.25

Considering the shakedown factors (η between 3.0 to 4.5) for marine structures, sample distortion measurements from the shop floor and the present welding technologies, the ranges of the parametric distortion values and residual stresses chosen for this study is shown in Table 6-2. The imperfections are classified into Low (L), Medium (M), High (H) and Severe (S).

6.2.1 Types of Distortions in Stiffened Panels

Using the above distortion elements, there can be endless combinations for the representation of real distortion patterns in a stiffened panel. Three forms of distortion observed during this study are shown in Figure 6-2.
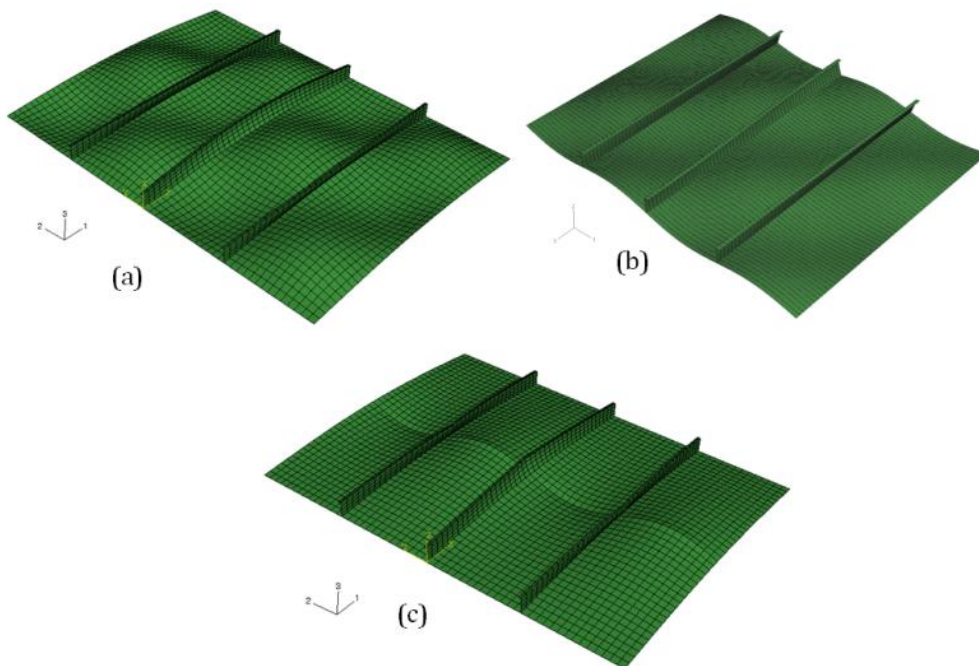
Figure 6-2 (a) Distortion Type – 1; (b) Distortion Type – 2; (c) Distortion Type – 3

These imperfection forms can be incorporated into an FE model by modifying the x,y,z coordinates of a perfect geometry. These imperfections can also be added together to generate a more complicated imperfection configuration.

6.2.1.1 Sinusoidal Distortion–Type 1
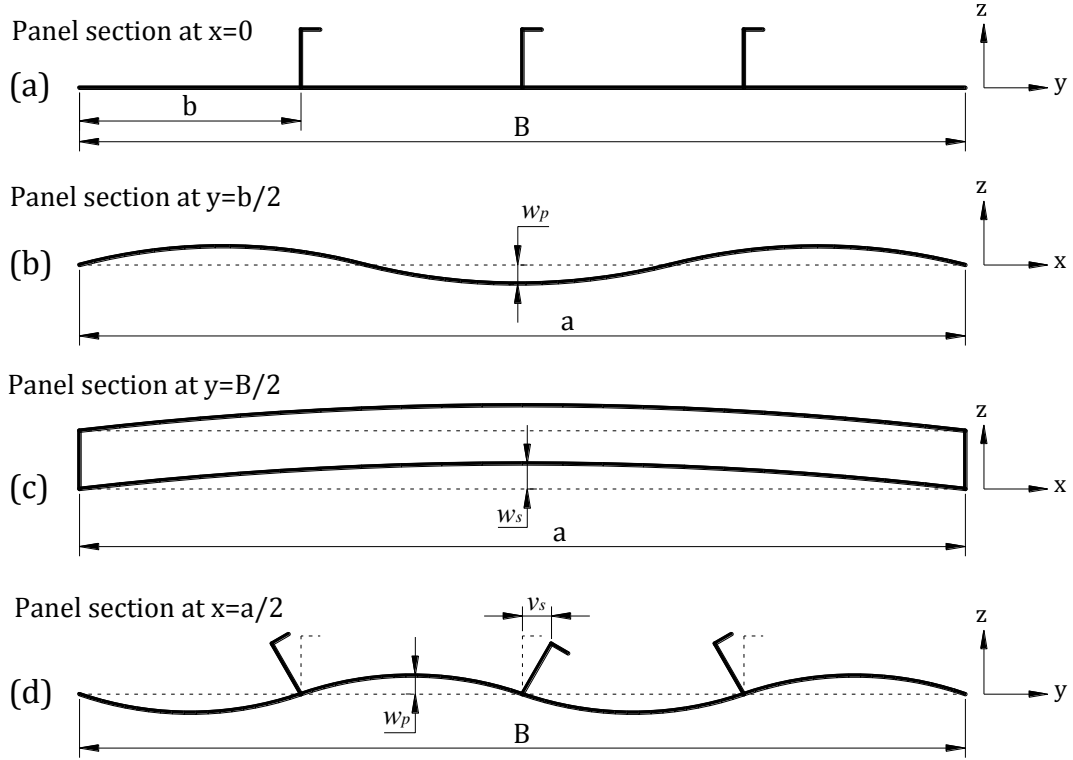
Figure 6-3 Sinusoidal Distortion Type - 1.

The geometry of Type-1distortion shown in Figure 6-3 is defined as (a)Mode of distortion in the plate and web for the panel section at x=0 along the longitudinal direction; (b) Mode of distortion in the plate for the panel section at y=b/2 along the longitudinal direction; (c) Mode of distortion in the plate and web for the panel section at y=B/2 along the longitudinal direction; (d) Mode of distortion in the plate and web for the panel section at x=a/2 along the transverse direction. This geometry is mathematically expressed in Equation (5-1), (6-10) and (6-11).

$$w_{z1} = w_p \sin\left(\frac{m\pi x}{a}\right)\sin\left(\frac{\pi y}{b}\right) \; ; \; m = \text{aspect ratio} = a/b \tag{6-9}$$

$$w_{z2} = w_b \sin\left(\frac{\pi x}{a}\right) \tag{6-10}$$

$$v_{y1} = v_s \sin\left(\frac{\pi x}{a}\right)\sin\left(\frac{0.5\pi z}{h}\right) \tag{6-11}$$

In this form, all the distortion values reach its peak towards the centre of the structure. The total z displacement at each node point will be the $w_{z1}+w_{z2}$ and the total y displacement is v_{y1}. Figure 6-2 (a) shows Type–1 distortion in a sample structure.

6.2.1.2 Sinusoidal Distortion – Type 2
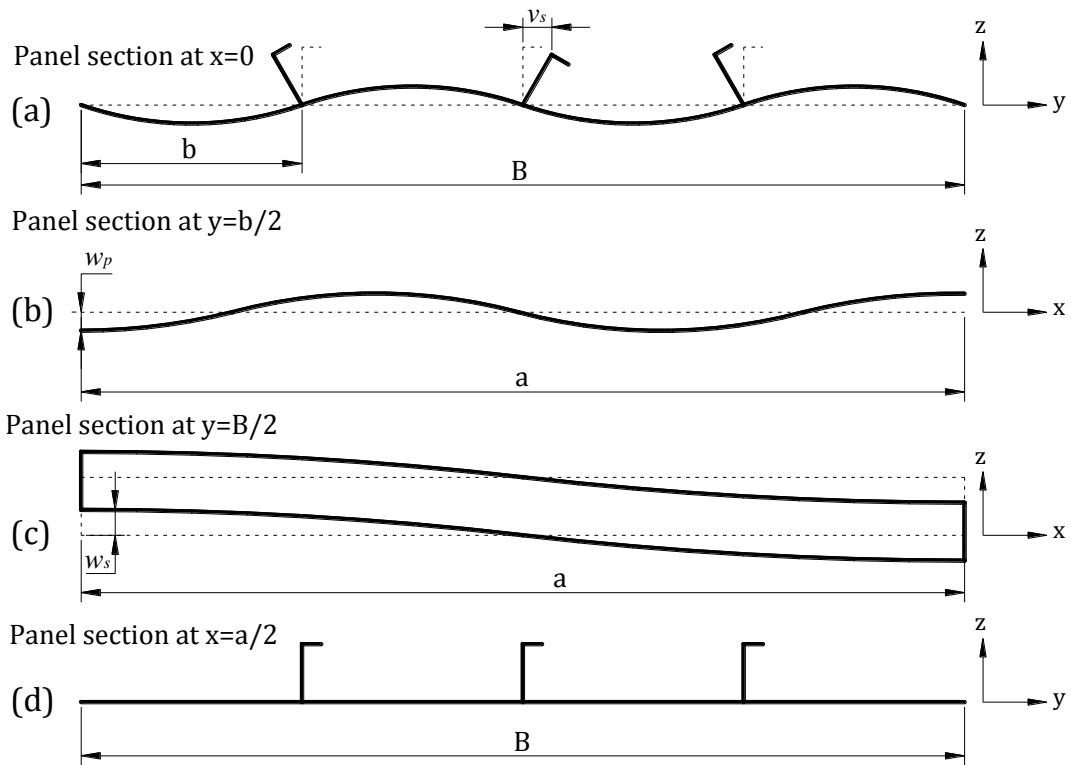
Figure 6-4 Sinusoidal Distortion Type - 2.

The geometry of Type-2 distortion is shown in Figure 6-4 is defined as (a)Mode of distortion in the plate and web for the panel section at x=0 along the longitudinal direction; (b) Mode of distortion in the plate for the panel section at y=b/2 along the longitudinal direction; (c) Mode of distortion in the plate and web for the panel section at y=B/2 along the longitudinal direction; (d) Mode of distortion in the plate and web for the panel section at x=a/2 along the

transverse direction. The geometry is expressed using Equation (6-12), (6-13) and (6-14).

$$w_{z1} = w_p \cos\left(\frac{m\pi x}{a}\right) \sin\left(\frac{\pi y}{b}\right) \quad ; \ m = \text{aspect ratio} = a/b \tag{6-12}$$

$$w_{z2} = w_b \cos\left(\frac{\pi x}{a}\right) \tag{6-13}$$

$$v_{y1} = v_s \cos\left(\frac{\pi x}{a}\right) \sin\left(\frac{0.5\pi z}{h}\right) \tag{6-14}$$

In this form, unlike the previous type, the distortions reach its minimum value at the centre of the structure. The total z displacement at each node point will be the $w_{z1}+w_{z2}$ and the total y displacement is v_{y1}. Figure 6-2 (a) shows Type–1 distortion in a sample structure.

6.2.1.3 Cusp Distortion – Type 3

Apart from the conventional first mode sinusoidal imperfection mode, author presents another form of distortion in the 'cusp' shape which is noticeable in the butt welded plates.

The geometry of cusp distortions shown in Figure 6-5 is defined as (a)Mode of distortion in the plate and web for the panel section at x=0 along the longitudinal direction; (b) Mode of distortion in the plate for the panel section at y=b/2 along the longitudinal direction; (c) Mode of distortion in the plate and web for the panel section at y=B/2 along the longitudinal direction; (d) Mode of distortion in the plate and web for the panel section at x=a/2 along the transverse direction. The geometry is represented using Equation (6-15), (6-16) and (6-17).

$$w_{z1} = 1.58741 w_p \left[0.5^{2/3} - \left(\frac{x}{a} - 0.5\right)^{2/3}\right] \sin\left(\frac{\pi y}{b}\right) \tag{6-15}$$

$$w_{z2} = w_b \sin\left(\frac{\pi x}{a}\right) \tag{6-16}$$

$$v_{y1} = 1.58741 v_s \left[0.5^{2/3} - \left(\frac{x}{a} - 0.5\right)^{2/3} \right] \sin\left(\frac{0.5\pi z}{h}\right) \tag{6-17}$$
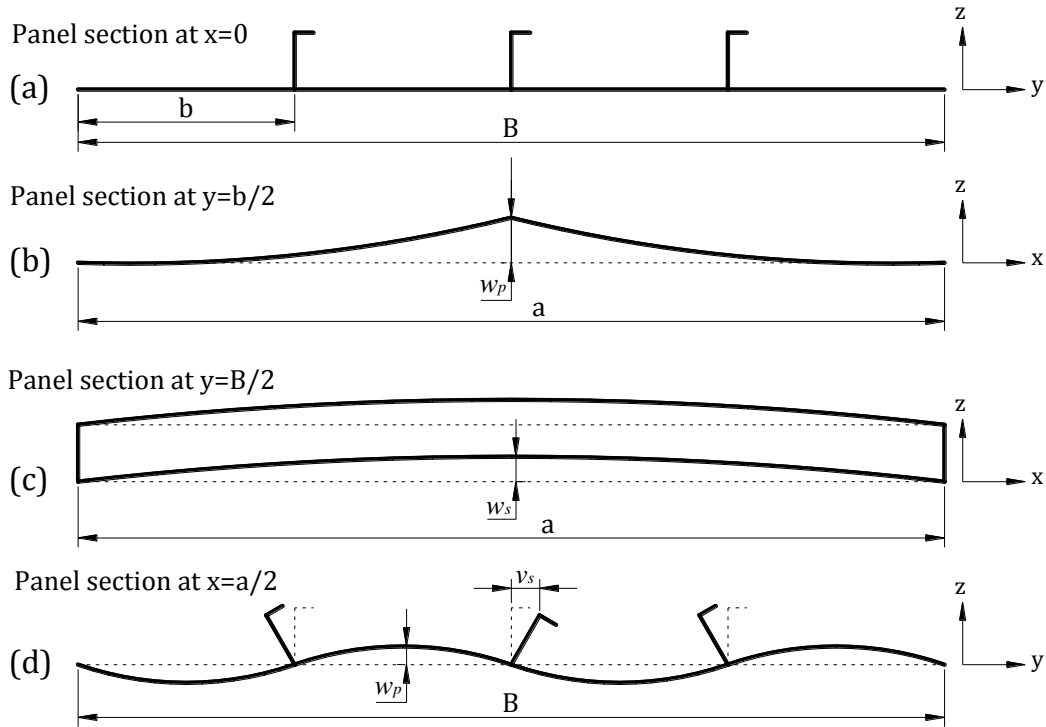
Figure 6-5 Cusp Distortion Type - 3.
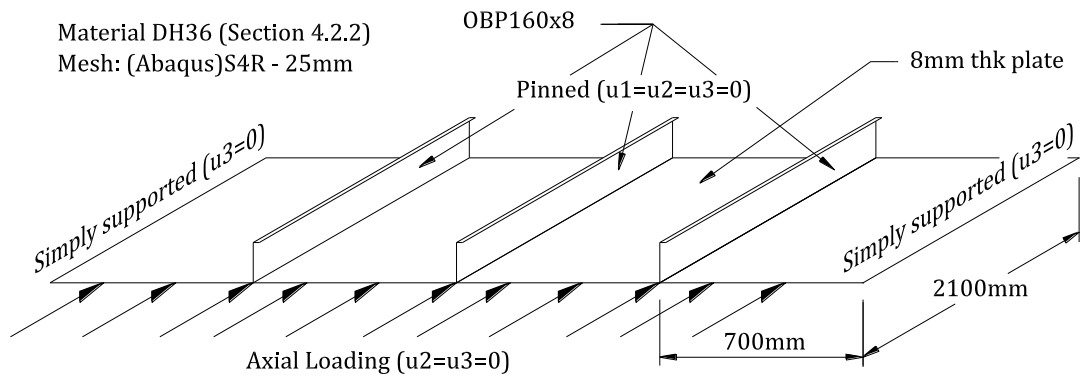
Figure 6-6 Details of FE Model used for the comparison

The constants are chosen to match the geometry of a specimen in shop floor. In this form, the distortion reaches its peak value at the centre of the structure as in Type-1.

A sensitivity study has been done using different distortion types. The structural configuration with geometrical dimensions, material properties and mesh details are shown in Figure 6-6.
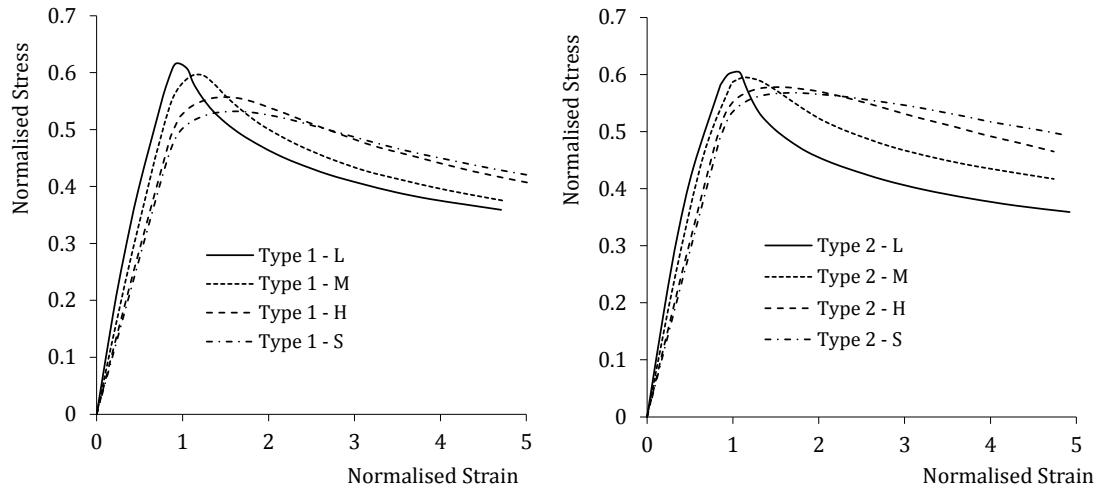
Figure 6-7 Comparison of strength results of Type-1 and Type-2 distortions with varying distortion amplitudes

Sensitivity study with Type-1 and Type-2 distortions show very little difference in the overall structural strength results. A sensitive study comparing Type-1 and Type-2 for increasing distortion amplitudes (L, M, H and S) are illustrated in Figure 6-7. In a close look, the Type-1 distortion appears more sensitive to the distortion effects compared to Type-2. The Type-3 distortion shows some strengthening effect with increased distortion compared to the other two types. Since the Type-1 distortion is the most commonly accepted and gives the lower bound of strength results, the following imperfection sensitivity study for unstiffened and stiffened plates are carried out with the Type-1 distortion.

6.3 Design Curves for Plated Structures

The scheme of numerical experiments is illustrated in Figure 6-8. The initial distortion and residual stresses, individually and in combination are varied parametrically based on the plate, column and combined plate-column slenderness. The design philosophy is to use the lowest value of strength from the appropriate sensitivity curves based on the respective slenderness

parameters corresponding to the parametric range of distortions. It is also possible to make a direct estimate of the reduction in strength for unstiffened and stiffened plates within the range based on the imperfection parameters.
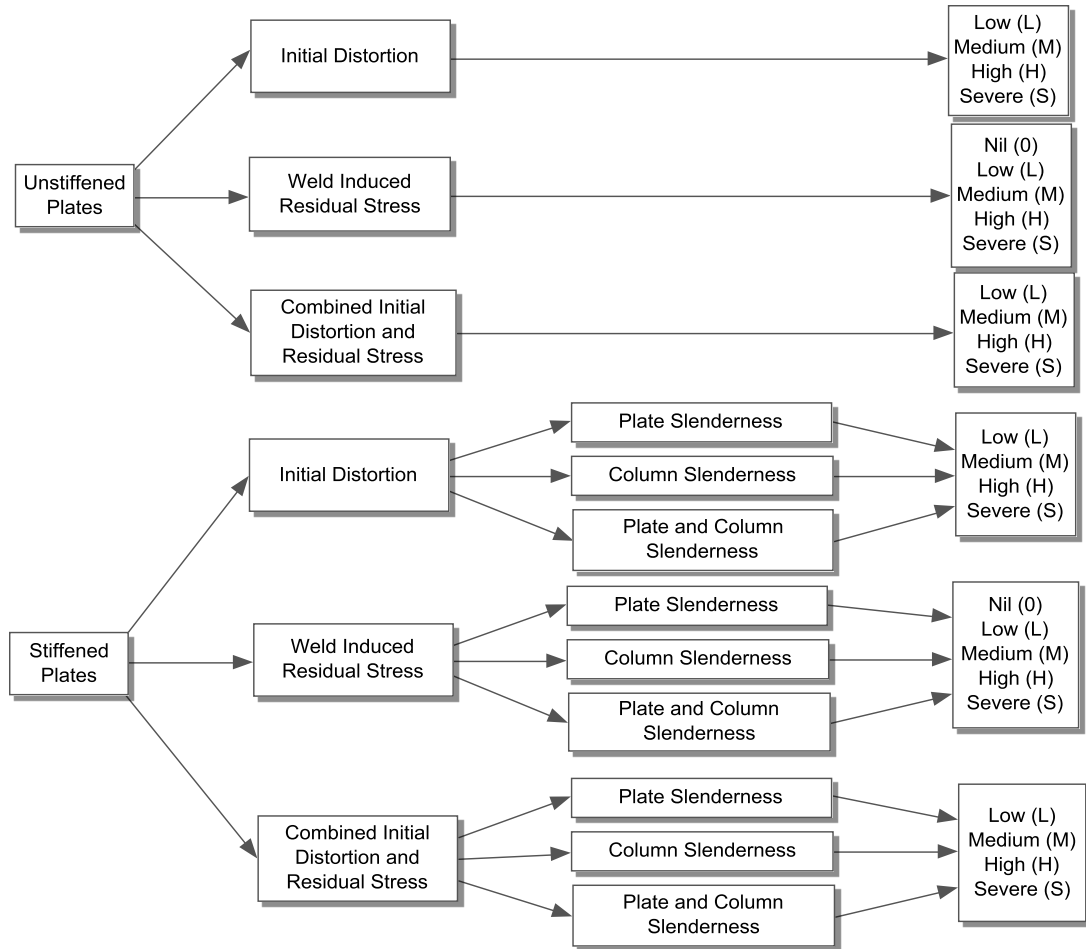
Figure 6-8 Scheme of analysis

It is impossible to analyse all the individual scantlings used in the ship or any offshore structures. The simplest way is to predict the performance of the structure based on the range of different slenderness parameters. In this study, it is planned to undertake analyses on some typical structural configuration with varying thickness (for range of plate slenderness) and OBP (for range of column slenderness) for performance pattern of plated structures under the influence of weld induced geometrical imperfections and residual stresses.

Table 6-3 Range of slenderness parameters for plates

		Plate Thickness t_p (mm)	OBP	β	λ
Unstiffened Plates	Varying β and λ	6		5.57	18.42
		8		4.18	13.82
		12		2.78	9.21
		16		2.09	6.91
		20		1.67	5.53
Stiffened Plates	Varying β (λ≈constmat)	6		5.57	0.46
		8		4.18	0.48
		12	200X12	2.78	0.53
		16		2.09	0.57
		20		1.67	0.61
	Varying λ		120X6	2.78	1.27
			160X8	2.78	0.79
		12	200X12	2.78	0.53
			370X16	2.78	0.23
			430X20	2.78	0.19
	Varying β and λ	6	120X6	5.57	1.01
		8	160X8	4.18	0.70
		12	200X12	2.78	0.53
		16	370X16	2.09	0.23
		20	430X20	1.67	0.20

The entire analysis is carried out with a plate size of 2400mm length and 800mm width or stiffener spacing (aspect ratio, a/b=3). The plate thicknesses used are 6mm, 8mm, 12mm, 16mm and 20mm to cover the range of plate slenderness β from 1.67 to 5.57. The OBP used are, OBP120, OBP160, OBP200, OBP370 and OBP430 to cover the column slenderness λ from 0.19 to 1.27 as illustrated in Table 6-3. The above scantling variations are expected to cover a comprehensive range of slenderness parameter which is commonly used in the ship building industry, particularly for the construction of Type-45 destroyer of BAE Systems. The details of FE analysis procedure is discussed in Chapter 4. All the numerical results for the unstiffened and stiffened plates under the imperfection effects are given in Table 6-4 to Table 6-7.

6.4 Design Curves for Unstiffened Plates

The behaviour of unstiffened plates is important in structures where there are limited stiffening is provided. The superstructures in ships are generally fabricated with large plates where the stiffer spacing is more with comparatively small stiffeners than the lower decks. In these locations, the strengthening effect of stiffeners will be lesser and the strength of the structure is predominantly governed by the strength of plates alone.
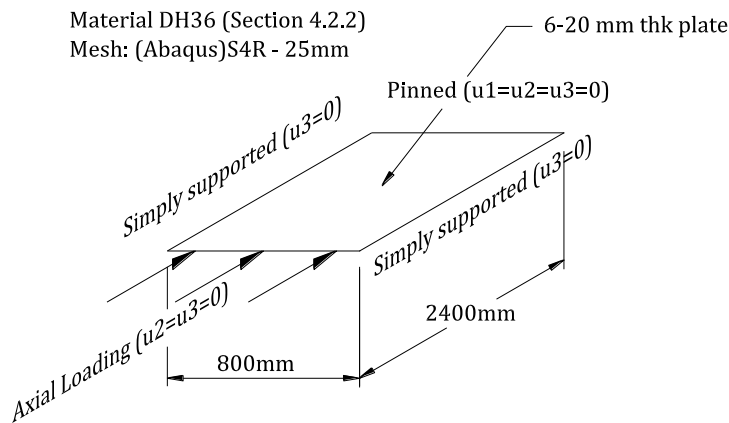
Figure 6-9 Geometrical dimensions, material, mesh, support and loading arrangements for the FE Analysis of unstiffened panels

Considering the parametric definition of distortions, the slender plates with large stiffener spacing will have more geometrical distortion. The welding operations produce residual stresses along the length of plates. For unstiffened plates, the longitudinal residual stress at the butt welding is taken into consideration. So the analysis of plate portions without considering the attached stiffeners is hence important in the design of superstructure.

The details of the FEA model for the fabrication imperfection sensitivity are illustrated in Figure 6-9. The numerical results are given in Table 6-4.

6.4.1 Effect of Plate Slenderness
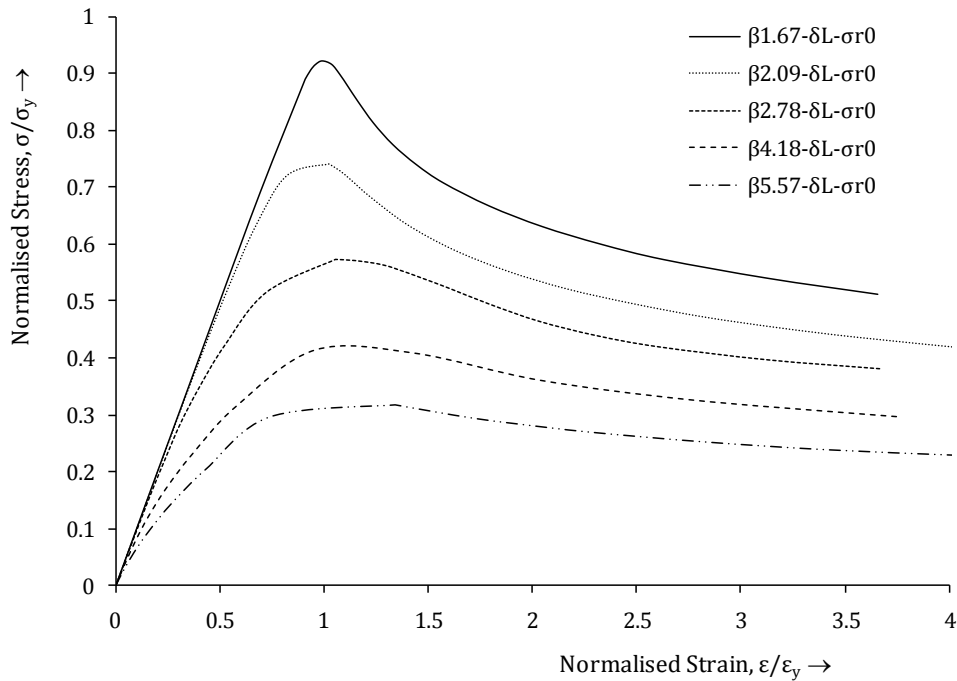
Figure 6-10 Effect of plate slenderness β on the strength of unstiffened panels

For an unstiffened panel, the plate configuration can be well represented by the plate slenderness parameter and is appears to be a direct measure of plate strength. Figure 6-10 shows the influence of slenderness parameter (β) in the buckling behaviour of unstiffened plates with same size and aspect ratio, a/b=3 (which is the most common aspect ratio used in the ship building) by varying the thicknesses from 6mm to 20mm as given in Table 6-3.

The pattern of behaviour with changing slenderness reveals interesting facts about the performance of unstiffened plates under the compressive loading. As it is expected, the thick plates show better axial capacity. The thin plates appear to withstand the collapse strength for an extended strain. In other words, thick plate found to lose the strength more quickly compared to thin plates when the structural ultimate strength is reached. So it is assumed that the post buckling stability is more for comparatively thin plates.

6.4.2 Effect of Initial Distortion
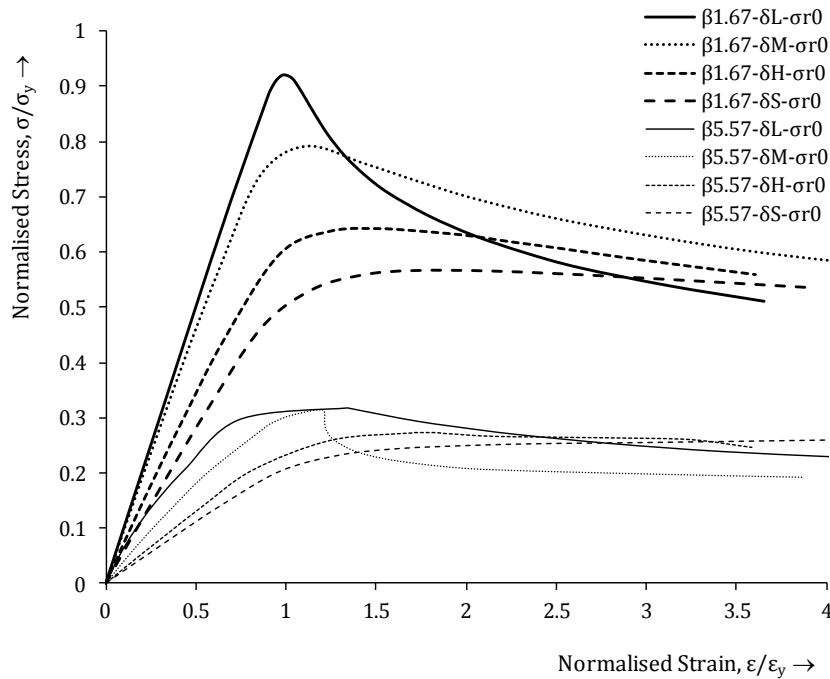
Figure 6-11 Effect of initial distortion for Thin and Thick Unstiffened Plates

The parametric plate distortions in plates are according to the values mentioned in Table 6-2. Figure 6-11 illustrate the buckling behaviour of unstiffened plates with the higher and lower values of plate slenderness under the influence of initial distortion. The plots show the fact that the influence of initial imperfection is more dominant in the lower range of plate slenderness. It is quite interesting to observe that thick plates are affected greatly with the distortion affects compared to thin plates. The distortion creates an effect similar to the strain hardening in thin plates.

Figure 6-12 illustrates the effect of varying distortion on the strength of unstiffened plates in the specified range of plate slenderness. The results are presented in two different formats, based on the slenderness for varying distortions and based on distortion for varying slenderness suitable for the design processes. For an average level of distortion, a strength loss of 5% to 15% can be expected for unstiffened plates of the specified slenderness range.
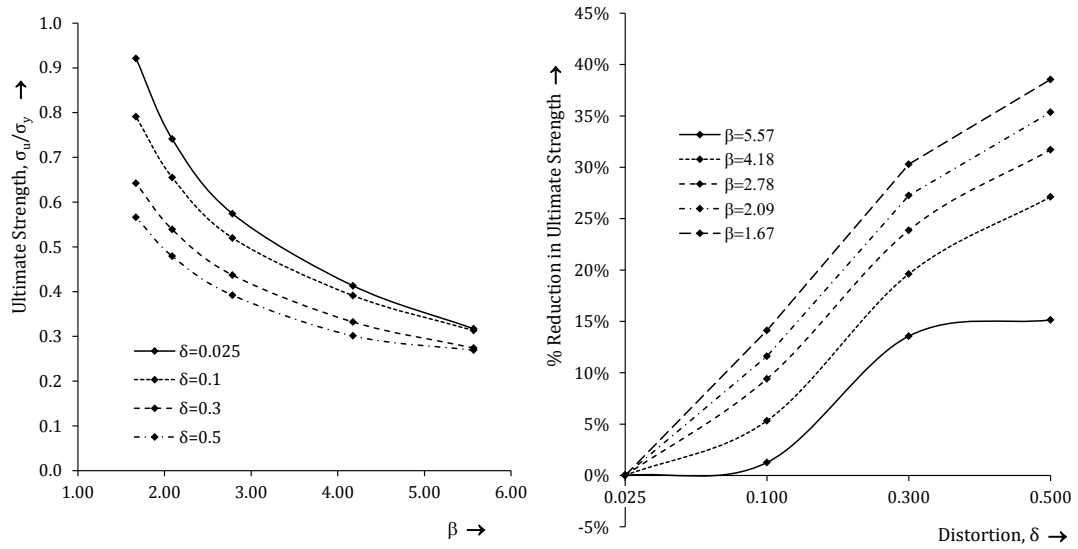
Figure 6-12 Effect of Initial Distortion for varying Slenderness of Unstiffened Plates

6.4.3 Effect of Weld Induced Residual Stresses
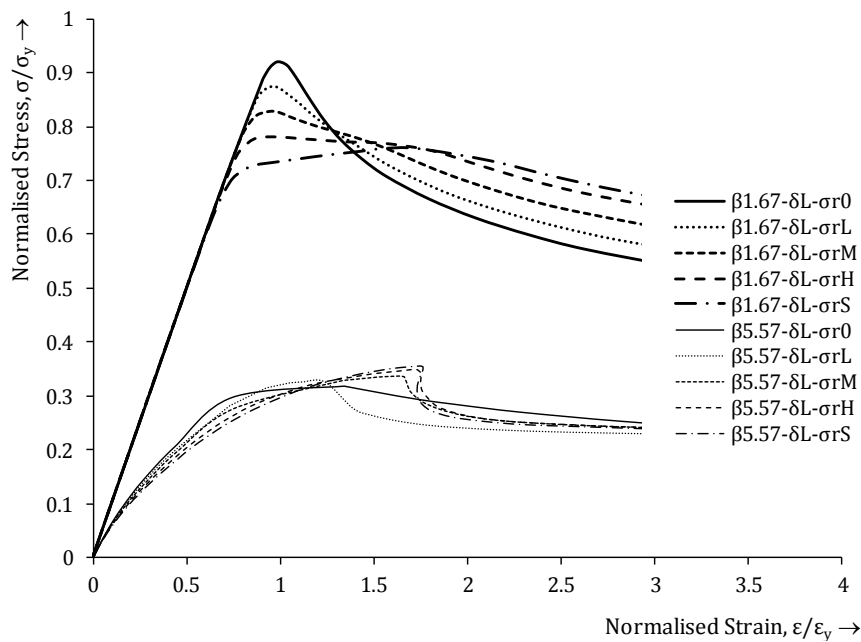
Figure 6-13 Effect of Weld induced Residual Stress for Thin and Thick Unstiffened Plates

The influence of weld induced residual stress on thin and thick plates are shown in the Figure 6-13. For thick plates, the buckling strength reduces and post buckling strength increases with increasing residual stress. For thin plates, the buckling strength increases with increasing residual stress at an increased strain level with slight reduction in post buckling strength. A sudden dip is

observed for thin plates with residual stress. This is because of the fact that at the point of ultimate stress, the trapped residual stress creates a favouring moment to accelerate the instability and sudden loss of capacity.
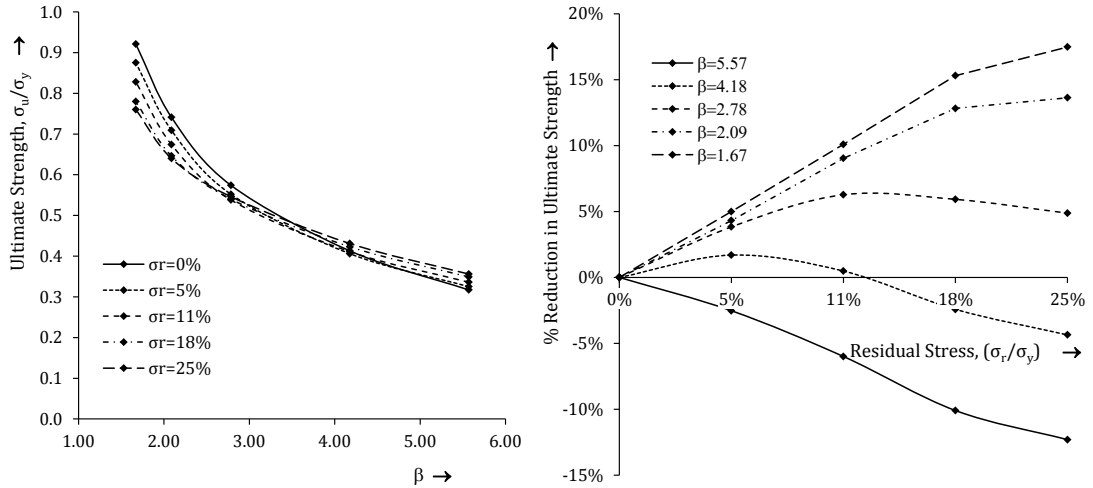
Figure 6-14 Effect of Weld Induced Residual Stress for varying Plate slenderness for Unstiffened Plates

The consequence of weld induced residual stress for the specific range is plotted two ways and illustrated in Figure 6-14. From the plot of strength versus slenderness with varying residual stress levels, the transformation from strength reduction at lower slenderness to strength increase at high slenderness demonstrate a specific range of slenderness (say, around 3.75) where the effect of residual stress tends to zero.

The plots for different slenderness show a pattern of variation of strength with varying residual stress. These plots can be effectively used for the design of plates for the selection of appropriate plate slenderness and estimate of strength loss. An average strength loss of 10% can be expected for thick plates with moderately heavy welding.

6.4.4 Combined Effect of Distortion and Residual Stresses

The combined effect of distortion and residual stresses for the thickest and thinner plates are shown in Figure 6-15. A mix of the above discussed trends is

observed for the combined case. The thin plates appear to show more strength with increased imperfection at an extended strain level.
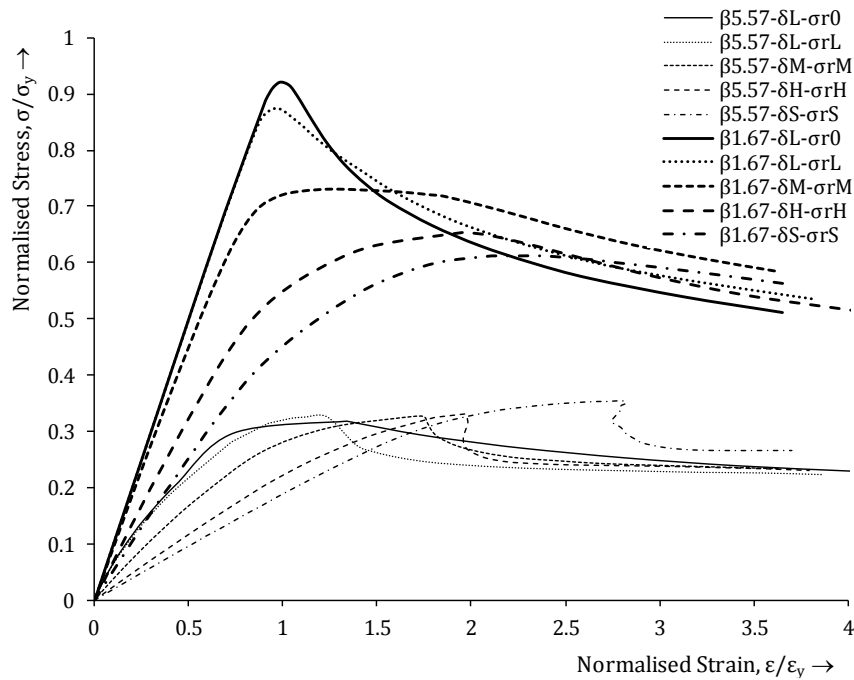
Figure 6-15 Combined Effect of Initial Distortion and Weld induced Residual Stress for Thin and Thick Unstiffened Plates
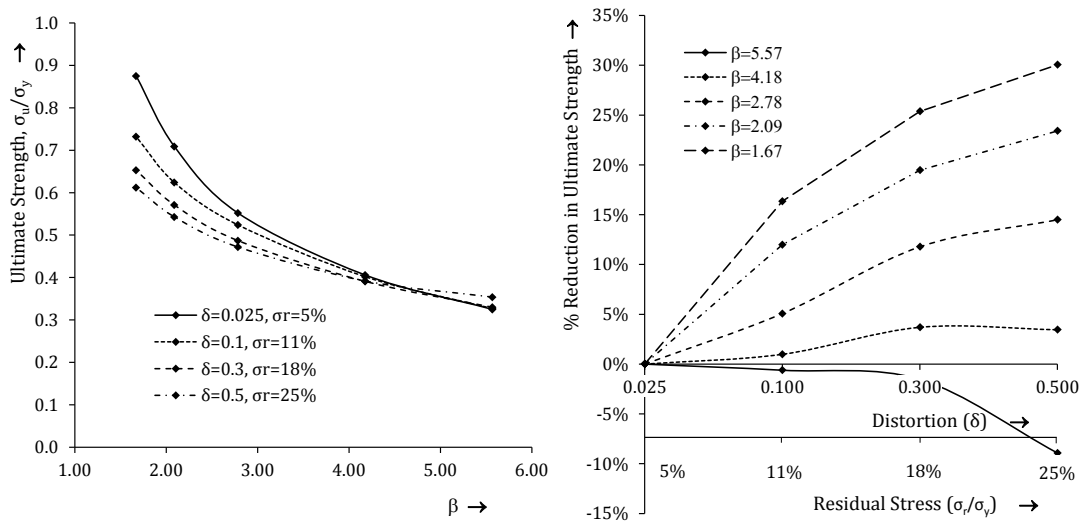
Figure 6-16 Combined Effect of Distortion and Residual Stress for varying Plate slenderness

Figure 6-16 illustrates the variation of strength of the unstiffened plates under the combined influence of distortion and residual stresses. The combined action of distortion and residual stress appear to increase the compressive ultimate

strain of the structure. The pattern of variation indicates the possibility of certain range of slenderness where the effect of combined action of distortion and residual stress is a minimum. So the above facts of extended strain and non affected range of slenderness can be used for the design of similar structures as an additional design criterion. 15% to 20% strength loss can be expected for a medium distortion and residual stress case of unstiffened plates.

6.5   Design Curves for Stiffened Plates

The distortions in stiffened plates are considered as a major factor for assessing its quality of fabrication and usefulness. The distortion apart from affecting its strength, affects the aesthetics of the structure as well. When the distortion cannot be allowed due to specific requirement of flatness where strength is not a criterion, the finishing and levelling is needed heavy investment.

The details of the FEA model for the fabrication imperfection sensitivity are illustrated in Figure 6-17. The numerical analyses results for the stiffened plates with varying distortion and residual stress conditions are tabulated in Table 6-5 to Table 6-7.
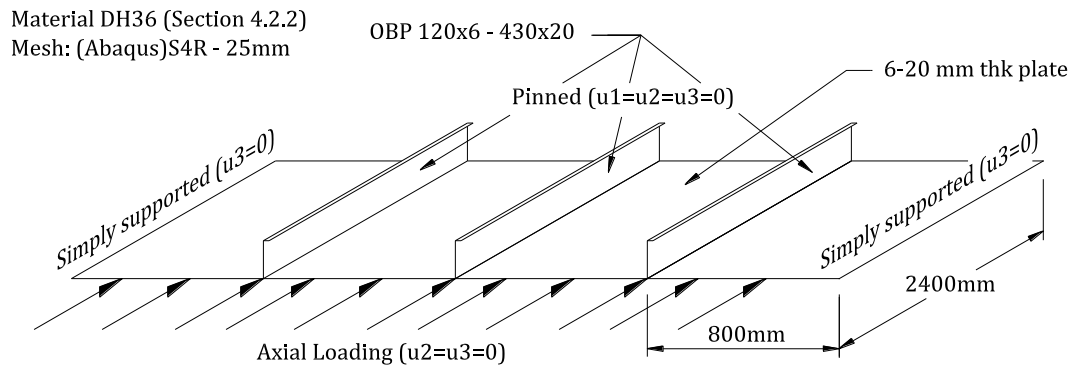
Figure 6-17 Geometrical dimensions, material, mesh, support and loading arrangements for the FE Analysis of stiffened panels

6.5.1 Effect of Initial Distortion

The distortions in stiffened plates are quite complex as there can be endless number of distortion profiles or mode shapes. In this study, the stiffened plates

are analysed for the individual contribution of increasing amplitudes of plate distortion, stiffener bowing and stiffener warping. Further analyses are performed with generalised distortion including three of these factors varying uniformly as L, M, H and S as illustrated in Table 6-2 .

6.5.1.1 Plate Slenderness
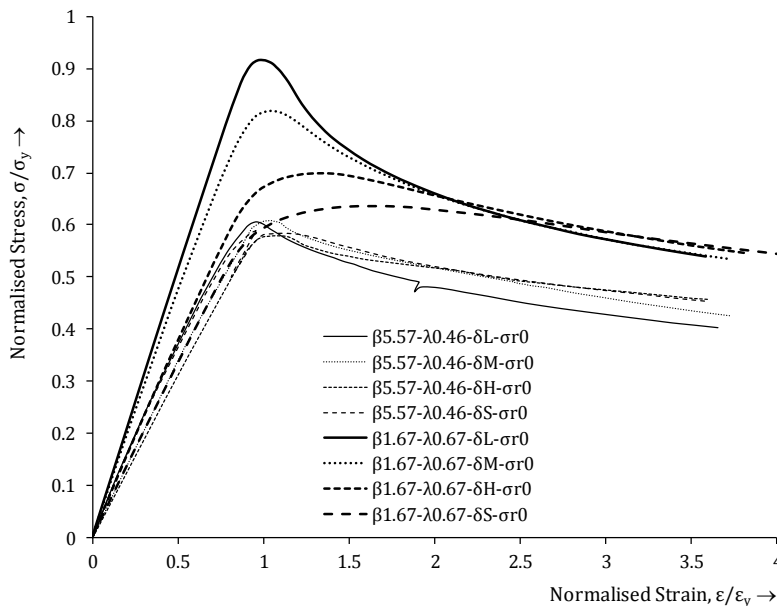
Figure 6-18 Effect of initial distortion on thick and thin stiffened plates (with nearly constant column slenderness, λ)

These analyses are presented based on the levels of imperfection and structural configurations proposed in Table 6-2 and Table 6-3. For stiffened plates as explained earlier, the strength variation is plotted based on its plate slenderness, column slenderness and combined increment of plate and column slenderness from the numerical experiments with the range of scantlings explained in Section 6.2. The analyses are carried out by keeping the stiffener constant (OBP200) with varying plate thickness to achieve the comparison of results with a fairly constant range of column slenderness.

Figure 6-18 shows that structures with thick plates found to lose the strength more rapidly than thin plates based on the plate slenderness. Figure 6-19 shows the effect of geometrical distortion on the strength of stiffened plates based on the plate slenderness (β). Unlike the unstiffened plates, the effect is found to be

very prominent when β<3 for stiffened plates. It is observed that an average distortion reduces the strength of stiffened plates up to about 10%.
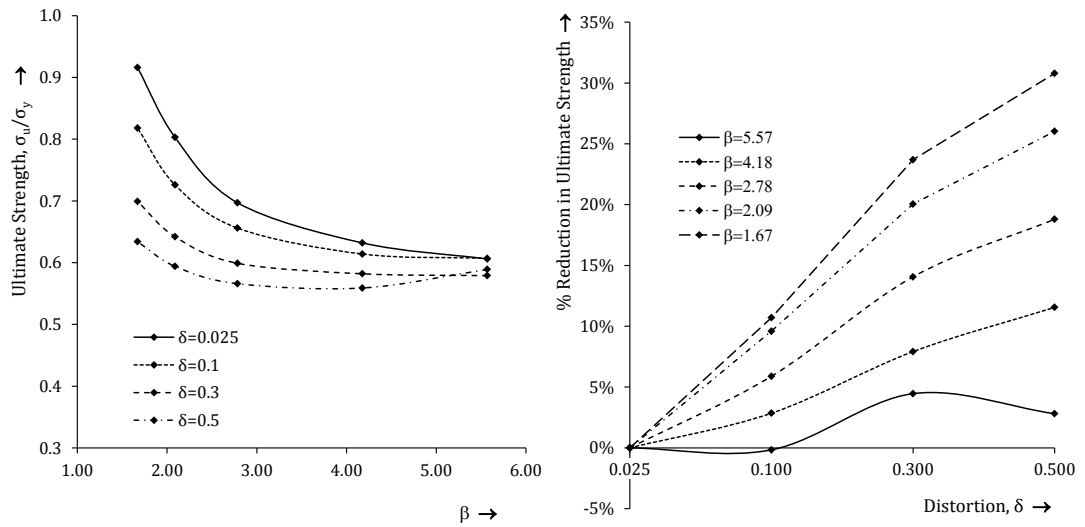
Figure 6-19 Effect of Initial Distortion for varying Plate slenderness of stiffened panels

6.5.1.2 Column Slenderness
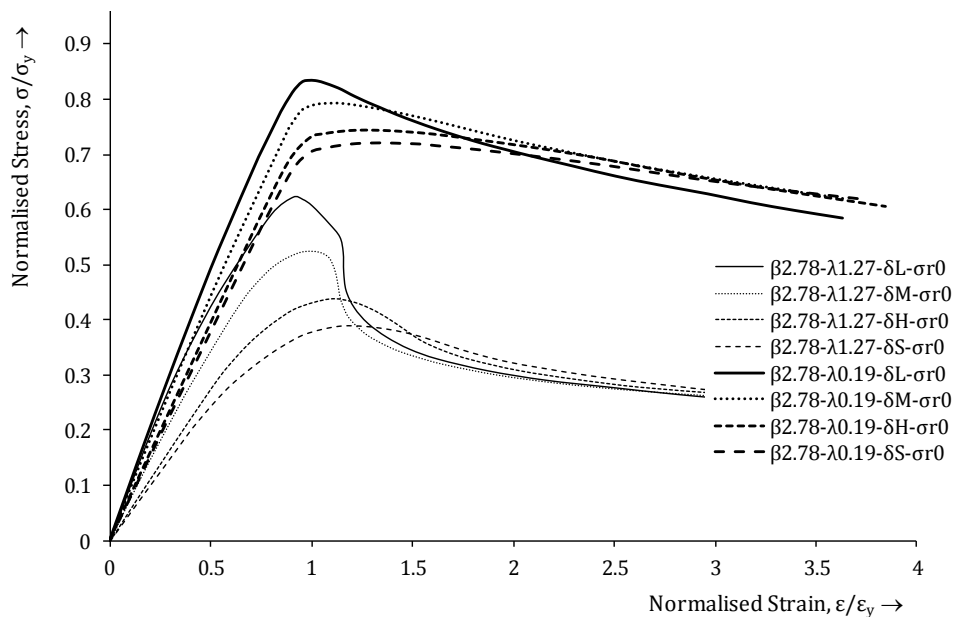
Figure 6-20 Effect of initial distortion on stocky and slender stiffened plates (with constant plate slenderness, β)

The column slenderness is the major parameter for the representation of stiffened panels in a beam column approach. So the performance of the stiffened panels based on the column slenderness is of great importance in the rule based

design approaches. During these set of analysis, the plate thickness kept constant (12mm) and the OBP were varied to achieve a varying range of column slenderness with constant plate slenderness. The results are given in Table 6-6.

Figure 6-20 shows the comparison of buckling performances for the upper and lower range of column slenderness. The effect of distortion appears to effect in the entire range of column slenderness. The slender structures are more vulnerable to the distortion in the column slenderness point of view. As the slenderness value increases, the buckling curves indicate the possibility of stiffener tripping failure resulting in a sudden collapse of structure.
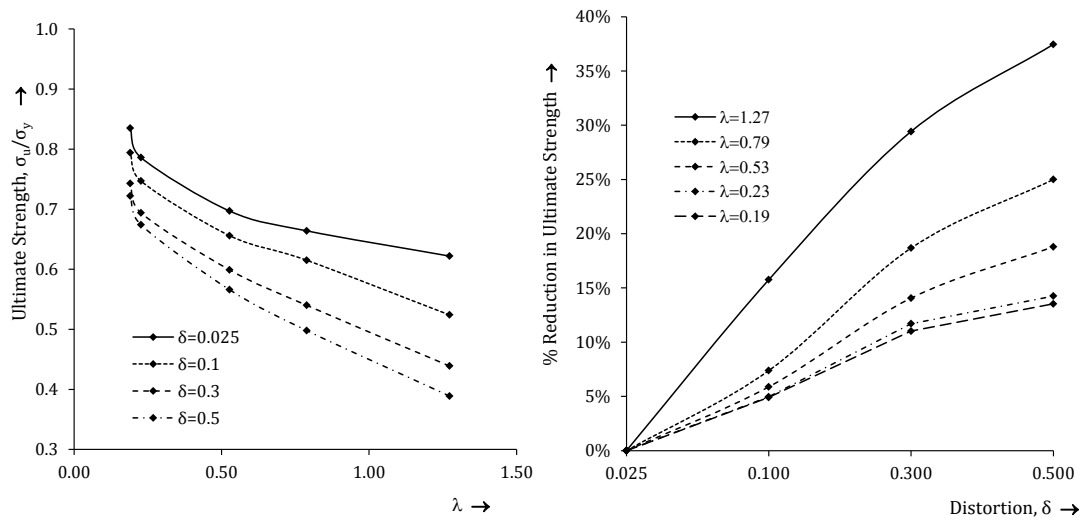
Figure 6-21 Effect of Initial Distortion for varying Column slenderness of stiffened panels

Figure 6-21 shows the comprehensive effect of parametric distortions on the strength of stiffened plated structures based on the column slenderness. The loss of strength for an average distortion is found to be in the range of 15%.

6.5.1.3 Plate and Column Slenderness
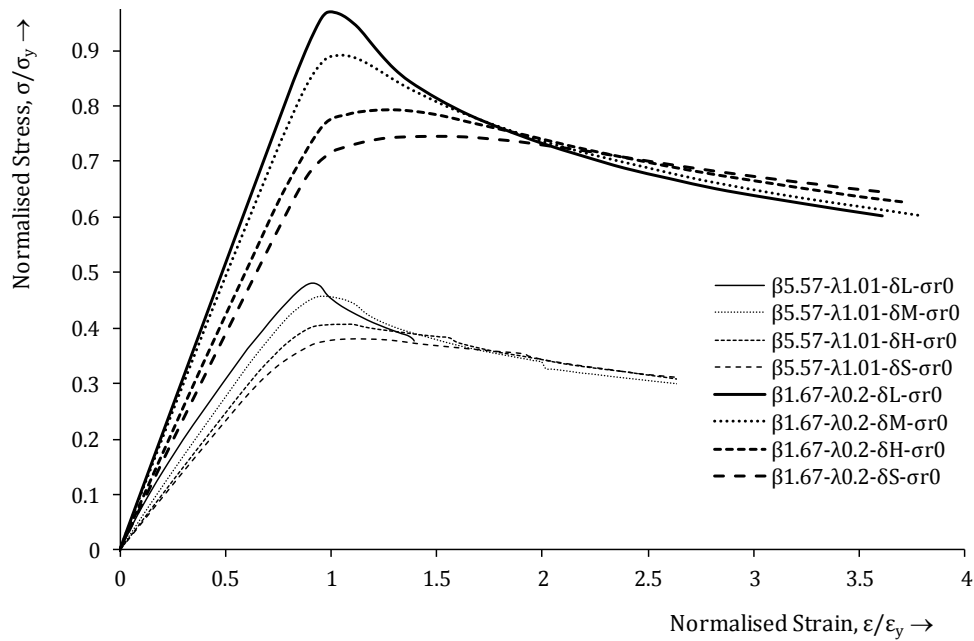
Figure 6-22 Effect of initial distortion on stocky-thick and slender-thin stiffened plates (with varying plate and column slenderness)

While selecting the scantlings for a ship structure for stronger areas or sections, the choice is more realistically done with the selection of matching thickness and stiffeners. So the effect of distortion when varying both the slenderness is also important and investigated within the range of scantlings used for the experiments.

Figure 6-22 shows the buckling behaviour of the two extreme ranges of scantlings used. Both the sets appear to create same reducing effects on strength with varying distortions. Figure 6-23 shows the trend of strength variation of stiffened panels with increasing distortion. An average level of distortion is expected to produce nearly 10% reduction in the strength of the stiffened plated structure.
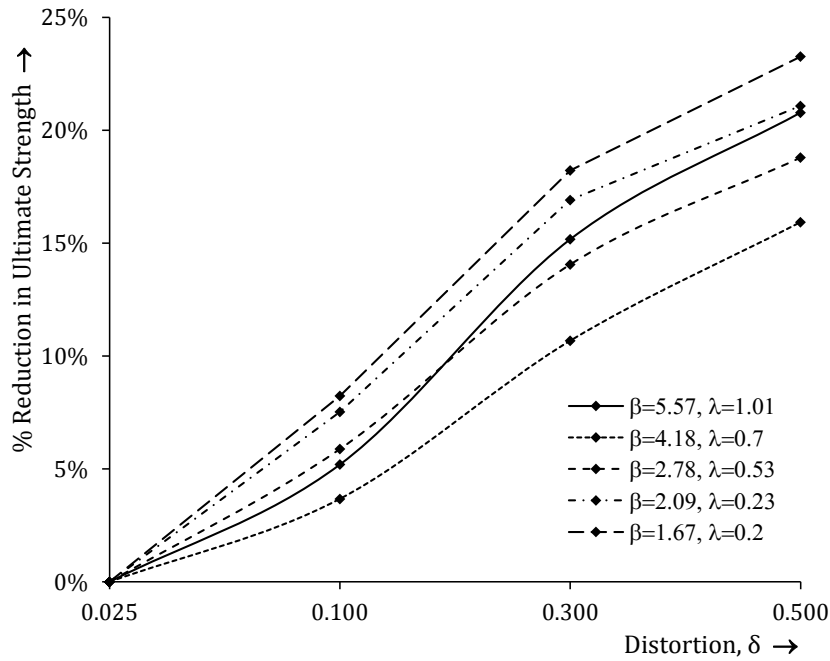
Figure 6-23 Effect of Initial Distortion on the strength of Stiffened Plates with varying Plate and Column slenderness

6.5.2 Effect of Weld Induced Residual Stress

The weld induced residual stress is present in the stiffened plates as self-equilibrating blocks of tension and compression as explained in the previous chapters. The effect of increasing residual stress is needed for design of stiffened plated structures for a sensible estimate of the buckling and post buckling strength of the structure.

6.5.2.1 Plate Slenderness

The influence of residual stress based on plate slenderness in the buckling behaviour of two extreme ranges is presented in Figure 6-24. As the amount of residual stress increases, the thick plates are found to lose strength considerably with an extended strain at collapse. Thin plates do not show much reduction in strength. The post buckling strength found to increases for the entire range of slenderness as shown in Figure 6-24.
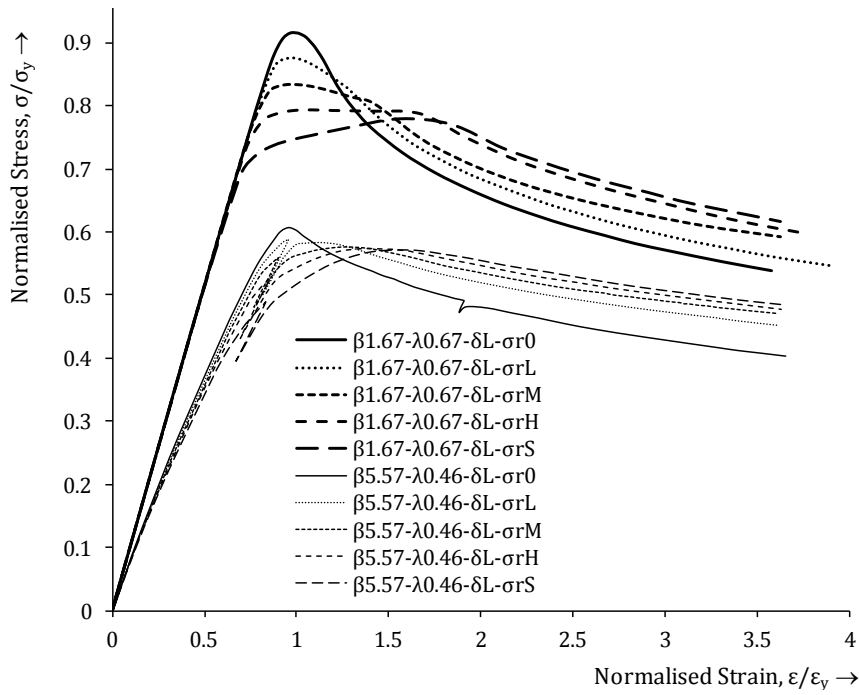
Figure 6-24 Effect of weld induced residual stress on thick and thin stiffened plates (with nearly constant column slenderness, λ)
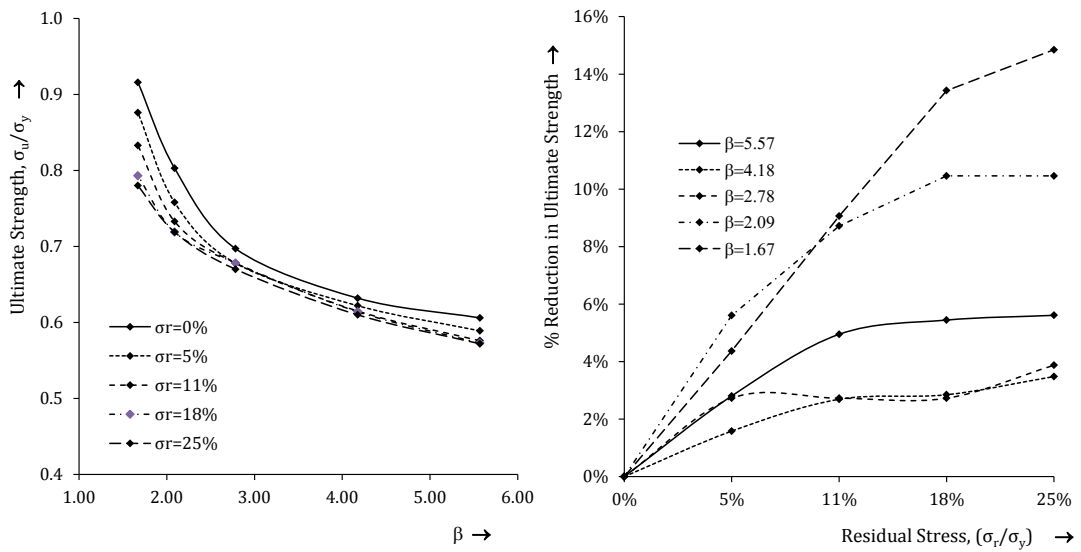
Figure 6-25 Effect of Weld Induced RS for varying Plate slenderness

Figure 6-25 shows the variation of strength with respect to plate slenderness for increasing levels of residual stresses. Residual stress produces non uniform patterns of performance for various levels of plate slenderness and it again appears to reduce the strength by about 10% for an average level of residual stress.

6.5.2.2 Column Slenderness
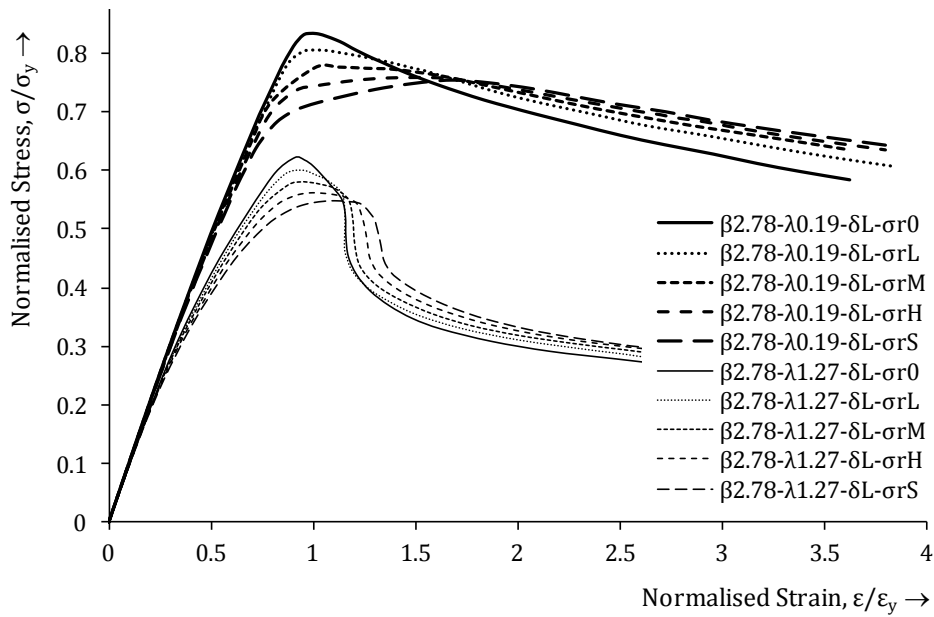
Figure 6-26 Effect of weld induced residual stress on stocky and slender stiffened plates (with constant plate slenderness, β)
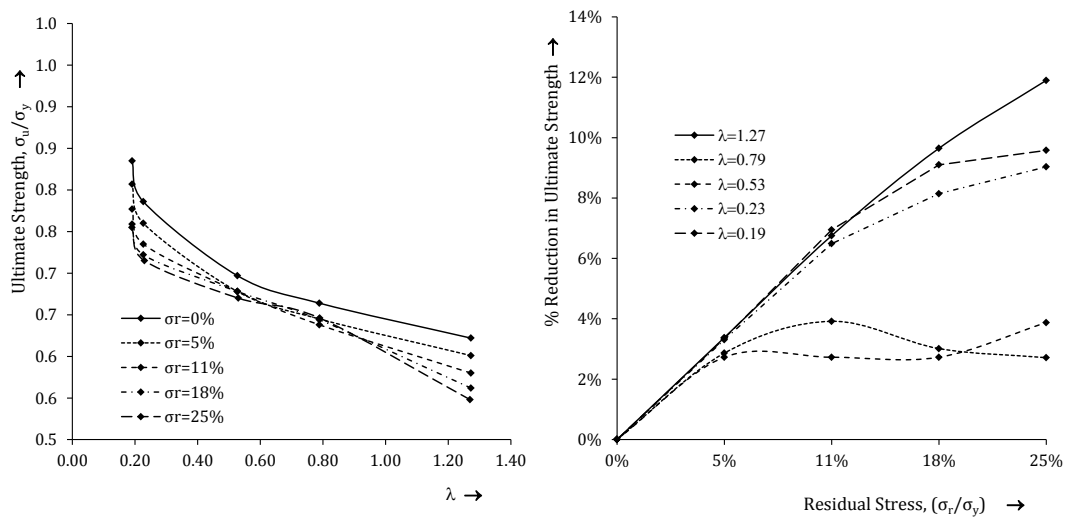
Figure 6-27 Effect of Weld Induced Residual Stress for varying Column slenderness

The buckling behaviour of upper and lower limit of column slenderness under the effect of residual stress is shown in Figure 6-26. The behaviour under the effect of residual stress varies with respect to the level of column slenderness. Figure 6-27 shows that the effect of residual stress is getting minimised at around column slenderness λ≈0.65. Above and beyond this value, the effect

spreads as observed from the plot. An average level of distortion produces 6-8% reduction in strength for the range of scantlings used for this study.

6.5.2.3 Plate and Column Slenderness
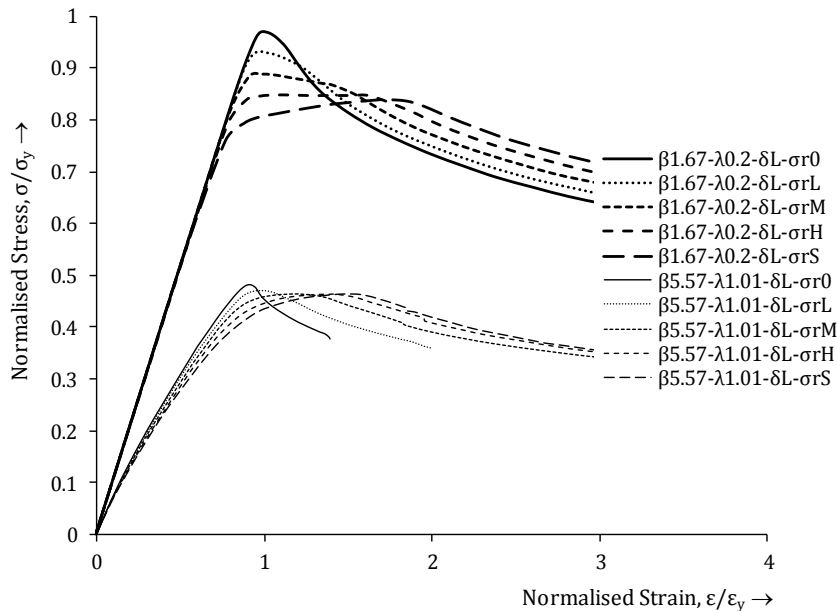
Figure 6-28 Effect of weld induced residual stress on stocky-thick and slender-thin stiffened plates (with varying plate and column slenderness)

The effect of residual stress under the combined variation of plate and column slenderness is illustrated in Figure 6-28. The increase in residual stress produces reduction in strength and increase in the post buckling strength. For thin plates, there is not much reduction of strength observed but the post buckling strength increases slightly. Figure 6-29 shows the effect of residual stress for varying the combined slenderness. From the comparison, it appears that the distortion reduces the strength considerably and the residual stress increases the strain range and post buckling strength.
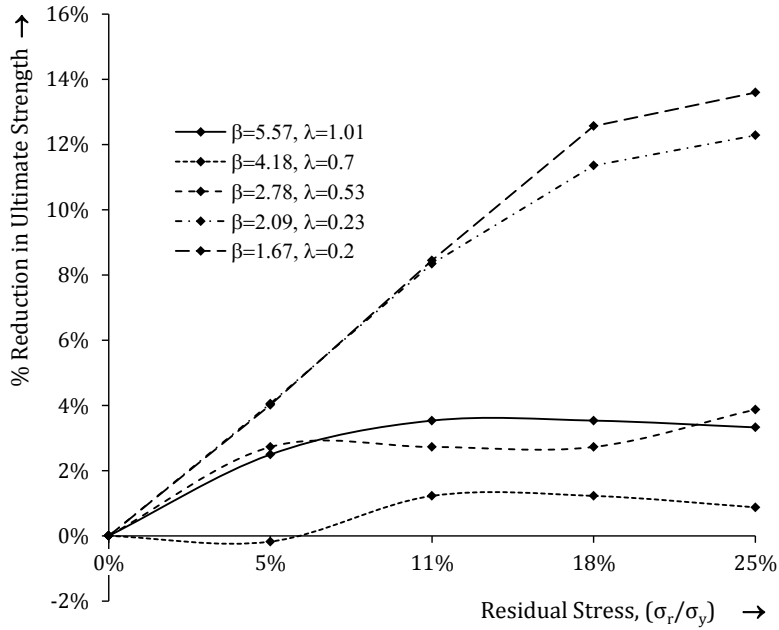
Figure 6-29 Effect of Weld Induced Residual Stress on the strength of Stiffened Plates with varying Plate and Column slenderness

6.5.3 Combined Effect of Distortion and Residual Stresses

So far the distortion and residual stresses are considered separately on the structures to account for the effects on the strength. In reality, the distortion and residual stresses are simultaneous phenomenon and the presence of either distortion or residual stress is an indirect measure of the other.

6.5.3.1 Plate Slenderness

Figure 6-30 shows the buckling performances of structures with the higher and lower range of slenderness parameters. Thick plates with heavy stiffeners are found to be more sensitive to the imperfection parameters than light or slender structures.

Figure 6-31 shows the combined influence of imperfection parameters based on the plate slenderness. The thick plates with β<3 is found to experience more strength loss. The overall strength reduction with medium distortion and residual stress is about 15%.
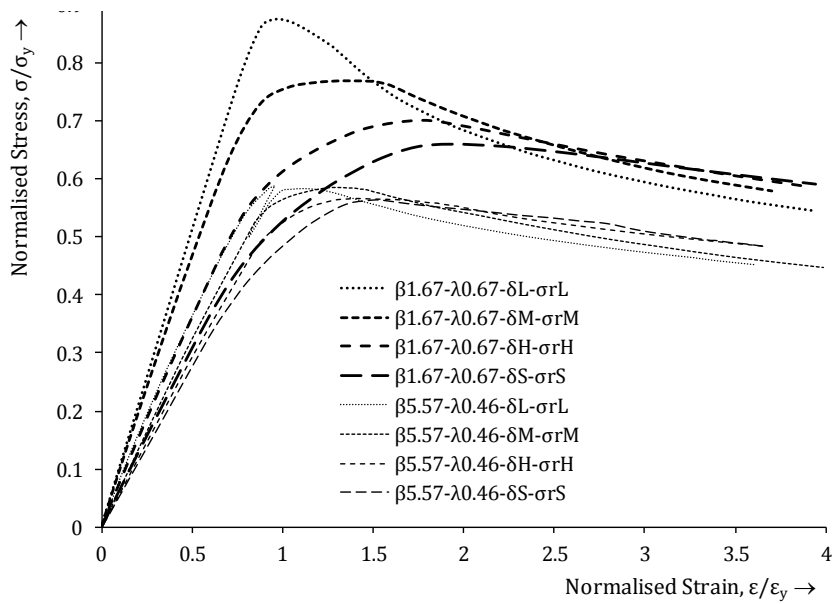
Figure 6-30 Effect of combined initial distortion and weld induced residual stress on thick and thin stiffened plates (with nearly constant column slenderness, λ)
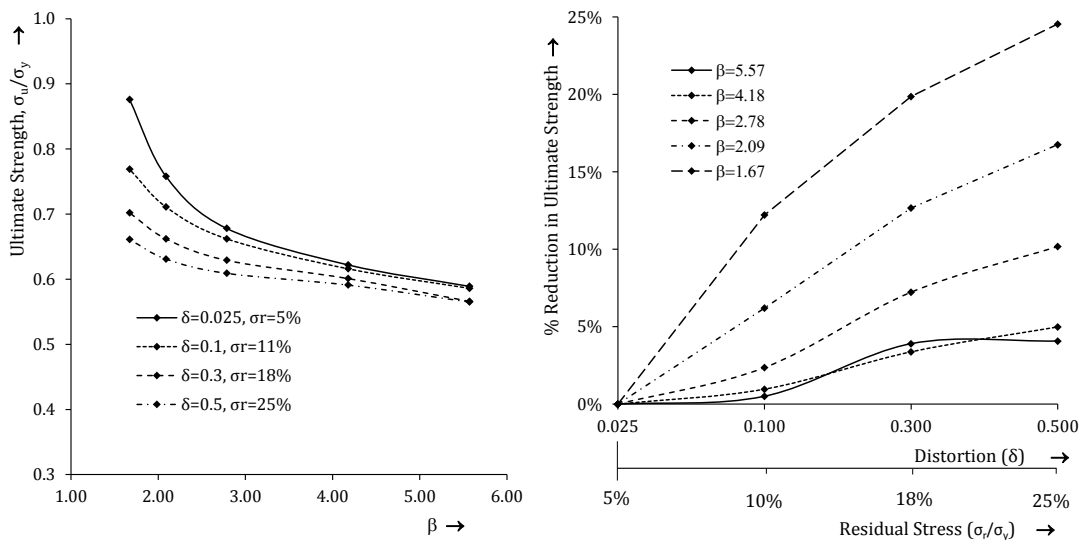
Figure 6-31 Effect of Combined Initial Distortion and Weld Induced Residual Stress for varying Plate slenderness

6.5.3.2 Column Slenderness

Figure 6-32 illustrates the effect of combined distortion and residual stress on the buckling behaviour based on the column slenderness. The effect appears to be an overlay of distortion and residual stresses described in the previous section. The lightest or slender structures are affected greatly compared to the thick structures in an ultimate strength point of view.
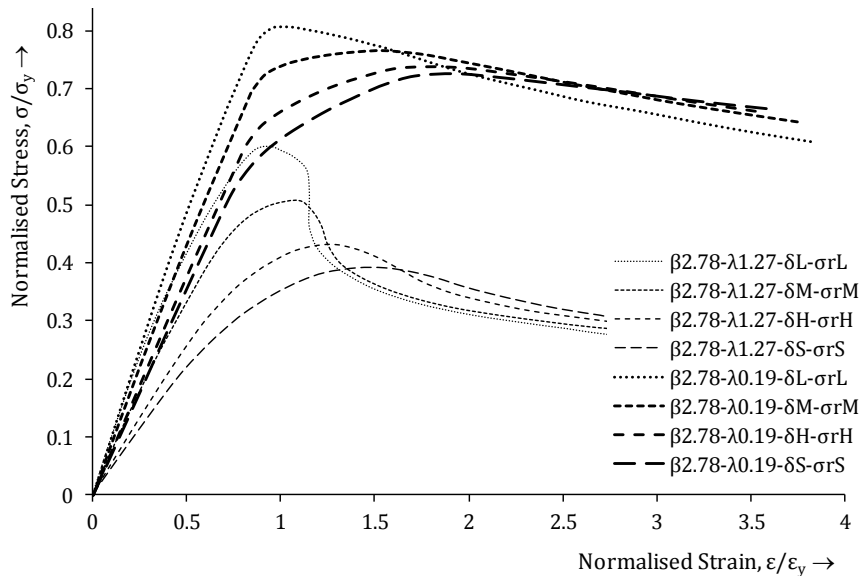
Figure 6-32 Effect of combined initial distortion and weld induced residual stress on stocky and slender stiffened plates (with constant plate slenderness, β)
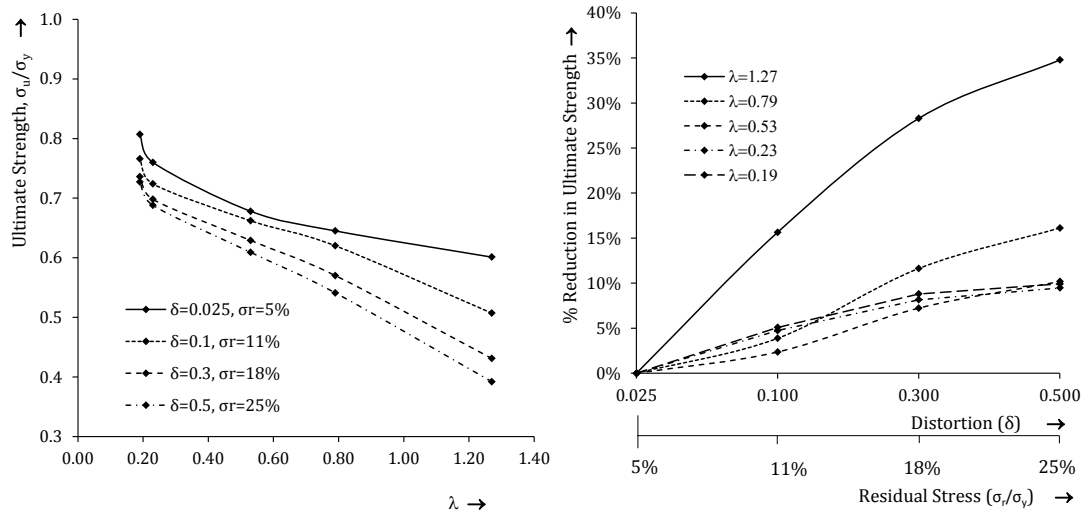
Figure 6-33 Effect of Combined Initial Distortion and Weld Induced Residual Stress for varying Column slenderness

Figure 6-33 shows the variation of strength for the full range of slenderness parameters. When column slenderness is being concerned, the plot indicates that the variation in strength is more as the column slenderness increases. The average distortion and residual stress experience a strength reduction of 15% from the near perfect structural configuration.

6.5.3.3 Plate and Column Slenderness
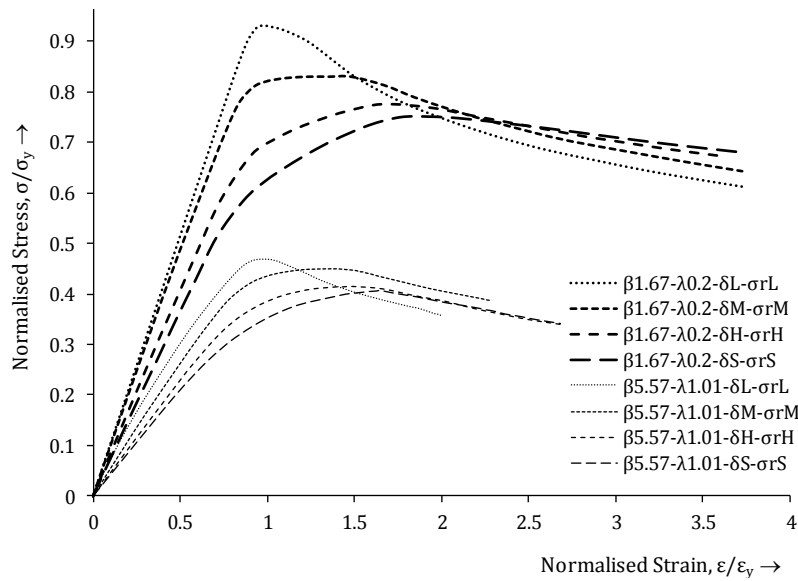
Figure 6-34 Effect of combined initial distortion and weld induced residual stress on stocky-thick and slender-thin stiffened plates (with varying plate and column slenderness)
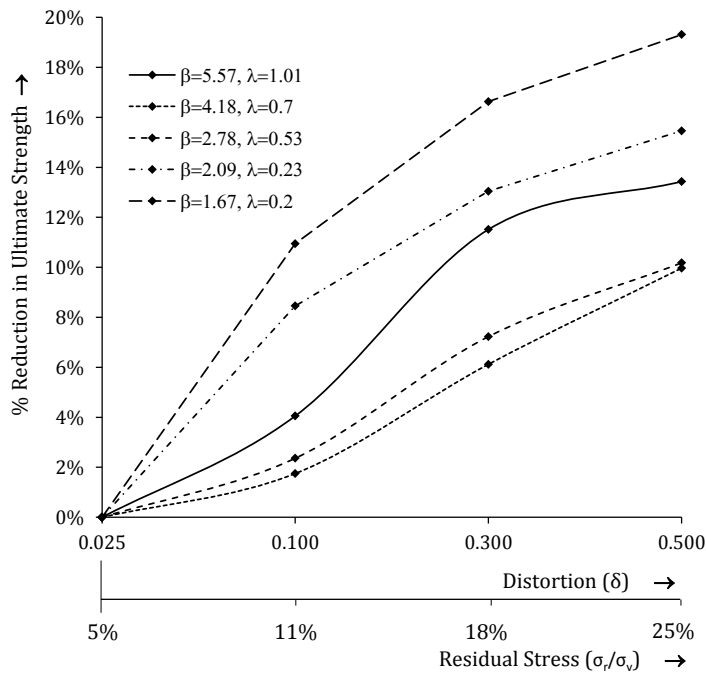
Figure 6-35 Effect of Combined Initial Distortion and Weld Induced Residual Stress on the strength of Stiffened Plates with varying Plate and Column slenderness

Figure 6-34 shows the structural behaviour of stiffened plates of two extreme scantlings in the range of our study. Here both the plate thickness and OBP sizes are changed to vary the plate and column slenderness. It can be observed that

the distortion and residual stresses affect the structural behaviour as the structure becomes stocky. Figure 6-35 shows the combined influence of distortion and residual stress when the plate and column slenderness of the stiffened plate increases together. An average imperfection experience nearly 12% reduction of strength.

The above illustrated design curves can be used for a wide range of scantlings normally employed in the ship building industry. The curves for unstiffened and stiffened plates are presented in two forms based on the slenderness. The response for any scantling which is not explicitly on any curve can be interpolated to get the corresponding strength. Similarly the distortion parameters can also be interpolated within the range to estimate the respective strength. When predicting the strength for stiffened panels, both the plate and column slenderness should be considered.

Table 6-4 FE Strength Analysis results for Unstiffened Plates–Varying plate thickness
(axb=2400mmx800mm, σ_y=355MPa, E=203.5GPa and υ=0.3)

Sl No.	Plate Thk. t_p (mm)	OBP	β	Distortion ($\delta = w/t_p\beta^2$)	Residual Stress (σ_r/σ_y)	Ultimate strength (σ_u/σ_y)
1	6	US	5.57	0.025	0%	0.317
2				0.025	5%	0.325
3				0.025	11%	0.336
4				0.025	18%	0.349
5				0.025	25%	0.356
6				0.100	0%	0.313
7				0.100	11%	0.327
8				0.300	0%	0.274
9				0.300	18%	0.330
10				0.500	0%	0.269
11				0.500	25%	0.354
12	8	US	4.18	0.025	0%	0.413
13				0.025	5%	0.406
14				0.025	11%	0.411
15				0.025	18%	0.423
16				0.025	25%	0.431
17				0.100	0%	0.391
18				0.100	11%	0.402
19				0.300	0%	0.332
20				0.300	18%	0.391
21				0.500	0%	0.301
22				0.500	25%	0.392
23	12	US	2.78	0.025	0%	0.574
24				0.025	5%	0.552
25				0.025	11%	0.538
26				0.025	18%	0.540
27				0.025	25%	0.546
28				0.100	0%	0.520
29				0.100	11%	0.524
30				0.300	0%	0.437
31				0.300	18%	0.487
32				0.500	0%	0.392
33				0.500	25%	0.472
34	16	US	2.09	0.025	0%	0.741
35				0.025	5%	0.709
36				0.025	11%	0.674
37				0.025	18%	0.646
38				0.025	25%	0.640
39				0.100	0%	0.655
40				0.100	11%	0.624
41				0.300	0%	0.539
42				0.300	18%	0.571
43				0.500	0%	0.479
44				0.500	25%	0.543
45	20	US	1.67	0.025	0%	0.921
46				0.025	5%	0.875
47				0.025	11%	0.828
48				0.025	18%	0.780
49				0.025	25%	0.760
50				0.100	0%	0.791
51				0.100	11%	0.732
52				0.300	0%	0.642
53				0.300	18%	0.653
54				0.500	0%	0.566
55				0.500	25%	0.612

US-Unstiffened panel, OBP- Offset bulb plate

Table 6-5 FE Strength Analysis results for Stiffened Plates-Varying Plate thickness
(axb=2400mmx800mm, σ_y=355MPa, E=203.5GPa and υ=0.3)

Sl No.	Plate Thk. t_p (mm)	OBP	β	λ	Distortion ($\delta= w/t_p\beta^2$)	Residual Stress (σ_r/σ_y)	Ultimate strength (σ_u/σ_y)
1	6	200X12	5.57	0.46	0.025	0%	0.606
2					0.025	5%	0.589
3					0.025	11%	0.576
4					0.025	18%	0.573
5					0.025	25%	0.572
6					0.100	0%	0.607
7					0.100	11%	0.586
8					0.300	0%	0.579
9					0.300	18%	0.566
10					0.500	0%	0.589
11					0.500	25%	0.565
12	8	200X12	4.18	0.48	0.025	0%	0.632
13					0.025	5%	0.622
14					0.025	11%	0.615
15					0.025	18%	0.614
16					0.025	25%	0.610
17					0.100	0%	0.614
18					0.100	11%	0.616
19					0.300	0%	0.582
20					0.300	18%	0.601
21					0.500	0%	0.559
22					0.500	25%	0.591
23	12	200X12	2.78	0.53	0.025	0%	0.697
24					0.025	5%	0.678
25					0.025	11%	0.678
26					0.025	18%	0.678
27					0.025	25%	0.670
28					0.100	0%	0.656
29					0.100	11%	0.662
30					0.300	0%	0.599
31					0.300	18%	0.629
32					0.500	0%	0.566
33					0.500	25%	0.609
34	16	200X12	2.09	0.57	0.025	0%	0.803
35					0.025	5%	0.758
36					0.025	11%	0.733
37					0.025	18%	0.719
38					0.025	25%	0.719
39					0.100	0%	0.726
40					0.100	11%	0.711
41					0.300	0%	0.642
42					0.300	18%	0.662
43					0.500	0%	0.594
44					0.500	25%	0.631
45	20	200X12	1.67	0.61	0.025	0%	0.916
46					0.025	5%	0.876
47					0.025	11%	0.833
48					0.025	18%	0.793
49					0.025	25%	0.780
50					0.100	0%	0.818
51					0.100	11%	0.769
52					0.300	0%	0.699
53					0.300	18%	0.702
54					0.500	0%	0.634
55					0.500	25%	0.661

Table 6-6 FE Strength Analysis results for Stiffened Plates-Varying OBP (axb=2400mmx800mm, σ_y=355MPa, E=203.5GPa and υ=0.3)

Sl No.	Plate Thk. t_p (mm)	OBP	β	λ	Distortion ($\delta= w/t_p\beta^2$)	Residual Stress (σ_r/σ_y)	Ultimate strength (σ_u/σ_y)
1	12	120X6	2.78	1.27	0.025	0%	0.622
2					0.025	5%	0.601
3					0.025	11%	0.580
4					0.025	18%	0.562
5					0.025	25%	0.548
6					0.100	0%	0.524
7					0.100	11%	0.507
8					0.300	0%	0.439
9					0.300	18%	0.431
10					0.500	0%	0.389
11					0.500	25%	0.392
12	12	160X8	2.78	0.79	0.025	0%	0.664
13					0.025	5%	0.645
14					0.025	11%	0.638
15					0.025	18%	0.644
16					0.025	25%	0.646
17					0.100	0%	0.615
18					0.100	11%	0.620
19					0.300	0%	0.540
20					0.300	18%	0.570
21					0.500	0%	0.498
22					0.500	25%	0.541
23	12	200X12	2.78	0.53	0.025	0%	0.697
24					0.025	5%	0.678
25					0.025	11%	0.678
26					0.025	18%	0.678
27					0.025	25%	0.670
28					0.100	0%	0.656
29					0.100	11%	0.662
30					0.300	0%	0.599
31					0.300	18%	0.629
32					0.500	0%	0.566
33					0.500	25%	0.609
34	12	370X16	2.78	0.23	0.025	0%	0.786
35					0.025	5%	0.760
36					0.025	11%	0.735
37					0.025	18%	0.722
38					0.025	25%	0.715
39					0.100	0%	0.747
40					0.100	11%	0.724
41					0.300	0%	0.694
42					0.300	18%	0.698
43					0.500	0%	0.674
44					0.500	25%	0.688
45	12	430X20	2.78	0.19	0.025	0%	0.835
46					0.025	5%	0.807
47					0.025	11%	0.777
48					0.025	18%	0.759
49					0.025	25%	0.755
50					0.100	0%	0.794
51					0.100	11%	0.766
52					0.300	0%	0.743
53					0.300	18%	0.736
54					0.500	0%	0.722
55					0.500	25%	0.727

Table 6-7 FE Strength Analysis results for Stiffened Plates-Varying Plate thk & OBP
(axb=2400mmx800mm, σ_y=355MPa, E=203.5GPa and υ=0.3)

Sl No.	Plate Thk. t_p (mm)	OBP	β	λ	Distortion ($\delta = w/t_p\beta^2$)	Residual Stress (σ_r/σ_y)	Ultimate strength (σ_u/σ_y)
1	6	120X6	5.57	1.01	0.025	0%	0.481
2					0.025	5%	0.469
3					0.025	11%	0.464
4					0.025	18%	0.464
5					0.025	25%	0.465
6					0.100	0%	0.456
7					0.100	11%	0.450
8					0.300	0%	0.408
9					0.300	18%	0.415
10					0.500	0%	0.381
11					0.500	25%	0.406
12	8	160X8	4.18	0.70	0.025	0%	0.571
13					0.025	5%	0.572
14					0.025	11%	0.564
15					0.025	18%	0.564
16					0.025	25%	0.566
17					0.100	0%	0.550
18					0.100	11%	0.562
19					0.300	0%	0.510
20					0.300	18%	0.537
21					0.500	0%	0.480
22					0.500	25%	0.515
23	12	200X12	2.78	0.53	0.025	0%	0.697
24					0.025	5%	0.678
25					0.025	11%	0.678
26					0.025	18%	0.678
27					0.025	25%	0.670
28					0.100	0%	0.656
29					0.100	11%	0.662
30					0.300	0%	0.599
31					0.300	18%	0.629
32					0.500	0%	0.566
33					0.500	25%	0.609
34	16	370X16	2.09	0.23	0.025	0%	0.863
35					0.025	5%	0.828
36					0.025	11%	0.791
37					0.025	18%	0.765
38					0.025	25%	0.757
39					0.100	0%	0.798
40					0.100	11%	0.758
41					0.300	0%	0.717
42					0.300	18%	0.720
43					0.500	0%	0.681
44					0.500	25%	0.700
45	20	430X20	1.67	0.20	0.025	0%	0.971
46					0.025	5%	0.932
47					0.025	11%	0.889
48					0.025	18%	0.849
49					0.025	25%	0.839
50					0.100	0%	0.891
51					0.100	11%	0.830
52					0.300	0%	0.794
53					0.300	18%	0.777
54					0.500	0%	0.745
55					0.500	25%	0.752

6.6 Summary

A wide range of plate and column slenderness parameters which are common in the ship building industry are subjected to rigorous FE analysis using a validated numerical model to understand the effect of distortions and residual stresses individually and in combination. The results are plotted in a design curve format so as to use for the design and strength estimation purposes. The most important observation from the study is that, the strength reduction with respect to imperfection parameters is not directly proportional to the parametric values of the imperfections as incorporated in most of the analytical approaches. The slender structures are not found to experience a proportional loss of structural strength with increasing distortion or residual stresses. This is because of the fact that the slender structures can allow and accommodate more elastic deformations before the onset of plasticity. The residual stresses found to reduce the strength of structure but as the slenderness increases, it increases the strength and post buckling strength to a little extent. In other words, if the distortion is taking the structural configuration far away from the buckling configuration, the strength of the structure remains unaffected or slightly increases.

The analysis results state the fact that thick plates with β<3 is found to experience more strength loss compared to thin plates with increasing distortion and residual stresses. It is observed that the geometrical distortion influences more on the strength compared to residual stresses and the residual stress produce strain hardening effects and increased post buckling strength in the buckling behaviour of plated structures.

The designers can incorporate the proposed design curves to quantify the effect of geometrical distortions and residual stresses on the strength of stiffened panels. The slenderness and imperfection values which are within the range can be linearly interpolated to match the exact structural parameters of interest.

Chapter 7.   Strength of Stiffened Cylinders

7.1 Introduction

Like the stiffened plates, another important structural component in the offshore marine engineering world is the stiffened cylinders. These are extensively used in buoyant semi-submersible and Tension leg type offshore platforms. The legs of these structures are designed as Stiffened cylinders because of its inherent capability to resist high axial loads and bending moments with lateral pressure loads.

The stiffened cylinders are classified as ring stiffened, stringer stiffened and ring-stringer stiffened cylinders which is also known as orthogonally stiffened cylinders. Ring stiffened cylinders are made of fabricated cylinder with ring frames welded externally or internally at wide spacing. Stringer stiffened cylinders will have equally spaced longitudinal stiffeners known as stringers welded internally or externally around the fabricated cylinder throughout the length. Orthogonally stiffened cylinders will have both of these stiffeners. The stiffeners can be of many types like flat bar, angle bar and T bar etc. The structure is fabricated by butt welding process from cold or hot-formed plates so that the structural continuity of the stiffeners and the cylinder is established. The welding introduces geometrical distortion and residual stresses in the structure in addition to the pre-fabrication and mechanical handling imperfections. The strength of the structure is mainly dependent on the basic geometrical and material structural design parameters. At certain ideal conditions, the strength prediction considering the basic structural parameters could be reasonably accurate. But this approach never can represent any real life situation. It involves a lot of known and unknown parameters which potentially governs the structural behaviour. Some of them are the effect of geometrical imperfections, residual stresses, type and direction of stiffeners (whether internal or external) etc. The contribution of these parameters on the

structural behaviour at different loading and support conditions will be surprisingly different.

Researchers from the last century (Timoshenko, P. and Gere, J. (1961), Windenburg D F, Trilling C. (1934), Von Mises R (1929) etc.) rigorously investigated the underlying mechanisms of this category of structures and predicted the structural behaviour under various loading conditions. Many of these closed form relations in terms of the basic geometrical and material design parameters predicts the behaviour reasonably accurate. The revolutionary developments in the computing realm within the last century increased the power of numerical analysis to a great extent that it can predict results much closer to the reality.

The modern design approaches consider structural reliability as one of the essential criteria to be satisfied for structural integrity. The design optimisation with reliability based approaches need a tool to predict the structural capacity very accurately and hence the strength analysis of structures with a higher degree of accuracy is quite important and crucial in the reliability based design processes. The reliability calculations need a tool for accurate evaluation of structural response with combinations of design variables from within the statistical spread of each parameter. This is to plot the failure surface and hence to evaluate the shortest distance to represent the reliability index or safety margin of the structure. Although the numerical analysis tools validated with reasonable model uncertainty factor are absolutely suitable for this purpose but the time and cost of computation become a major factor to prefer an analytical method. Considering the above facts, an analytical approach in terms of basic structural design parameters to predict the structural capacity is more suitable for the reliability analysis. Moreover, a component level reliability assessment for a huge structure with number of local structural parts at a preliminary design stage cannot afford much time and expense. The necessity of a good analytical strength model for initial design process is hence very important at this instance. There are various rule based design codes available for the

assessment of structural capacity of stiffened cylindrical structures under different loading conditions. DNV-RP-C202 and API BUL 2U are two of the major industry recommended codes in practice.

Author proposes a modified version of existing RCC formulation for the strength assessment of ring stiffened and ring-stringer stiffened cylinders. The bias for knockdown factor for both the ring and orthogonally stiffened cases are modified based on experimental results for similar structures conducted within last century. The codes and the proposed formulation are compared statistically with respect to mean and COV of a large population of screened test data.

7.2 Strength Models in Design Codes

There are many rule based design codes used for the strength evaluation of stiffened cylinders. The major practicing codes for the strength prediction of stiffened cylinders which are compared in this study are,

7.2.1 DNV-RP-C202

DET NORSKE VERITAS (DNV) is an independent organisation undertakes classification, certification, and other verification and consultancy services relating to quality of ships, offshore and onshore installations, and carries out extensive research within these areas. DNV has established number of technical documents in relation to offshore and onshore structures, systems, material, operations etc.

DNV-RP-C202 treats the buckling stability of shell structures and proposes the formulations based on the load and resistance factor design format (LRFD). The code formulas are on an assumption that the edges are effectively supported by ring frames, bulkheads or end closures. The buckling analyses with respect to different modes of buckling are considered as semi-empirical. It is because of the fact that there is not enough agreement between theoretical and experimental buckling loads. The code explains the discrepancy as a result of

geometric distortions and residual stresses and the nonlinear material behaviour beyond the scope of formulation.

7.2.2 API-Bul-2U

This design code is proposed by American Petroleum Institute as one among various technical documents for offshore and onshore structural analysis and design. The document provides stability criteria for the structural integrity assessment against buckling of large diameter stiffened or unstiffened circular cylindrical members when subjected to axial load, bending, shear and external pressure acting independently or in combination.

The document follows the concept of linear bifurcation (classical) analyses for the buckling strength calculation of cylinders and curved shells. The reduction in the buckling strength for shells are then addressed with capacity reduction factors which implicitly taking care of the initial imperfections, geometrical non linearity and effect of boundary conditions. The material nonlinearity is then accounted using a plasticity reduction factor it includes the effect of fabrication induced residual stresses.

7.2.3 RCC

The rule case format has been proposed by a committee (RCC) established by ABS (American Bauru of Shipping) and Conoco Inc. to develop design rules for tension leg platforms. One of the tasks of the committee was to formulate design guidance for the ultimate strength of stiffened cylindrical component structure subjected to various kinds of loadings. The ring and stringer cylinders under axial and bending forces provide a much lighter structure than one having ring frames alone.

The formulation is based on an approach similar to that developed for flat stiffened panels in which two modes of failure are considered for axial compression, one due to shell buckling and the other is the stiffener tripping. In

this formulation, the critical buckling stress is determined assuming single half-wave forms between rings. The critical stress is then given as the summation of the buckling stress for an unstiffened shell between rings and that for the stringer acting as a column between rings. A reduced effective width is used based on curved shell element buckling. The bias factors for the elastic knock-down factors were taken from test results of aerospace industry. The welding residual stress effect is taken into account by structural tangent modulus. Inelastic effect is considered through Ostenfield-Bleich formula. The external pressure formulation is based on an energy approach in which the material is assumed to be rigid perfectly plastic and the strain hardening effects are neglected. The plastic collapse approach considers the formulation of three plastic hinges in the stiffeners and three plastic hinges in both circumferential and longitudinal directions of the shell. The interaction equation is based on the Odland-Faulkner equation.

7.3   Elements of Strength Model for Stiffened Cylinders

The general philosophy followed by most of the codified rules for the ultimate strength of stiffened cylinders is nearly same. The strength evaluation of the structural element starts from the assessment of the elastic critical buckling strength of perfect cylinders.

Figure 7-1 Flow diagram of a typical strength model

The variation to this theoretical value is then accounted by applying appropriate shell knockdown factor so that the elastic critical buckling strength of the Imperfect cylinder (as built structure) is obtained. A reduction factor is then applied considering the slenderness of the structure and material strength to achieve the ultimate strength of the stiffened cylinder.

The shell knockdown factor represents the effect of geometrical imperfections on the buckling strength of the structure. The reduction factor includes the effect of residual stresses and structural slenderness.

7.3.1 Buckling of Cylinders

A perfect cylindrical shell under uniform axial compression in the small deflection range can buckle elastically in three modes depending on its length (*L*), cross-section radius (*R*) and thickness (*t*). It can predominantly buckle about its cross sections in two modes, concertina and chessboard buckling as shown in Figure 7-2(a) and (b) and can buckle as a column. The simplest mode is the third mode, the overall Euler buckling as a strut with a critical buckling stress,

$$\sigma_E = \frac{\pi^2 E R^2}{4L^2}$$ (7-1)
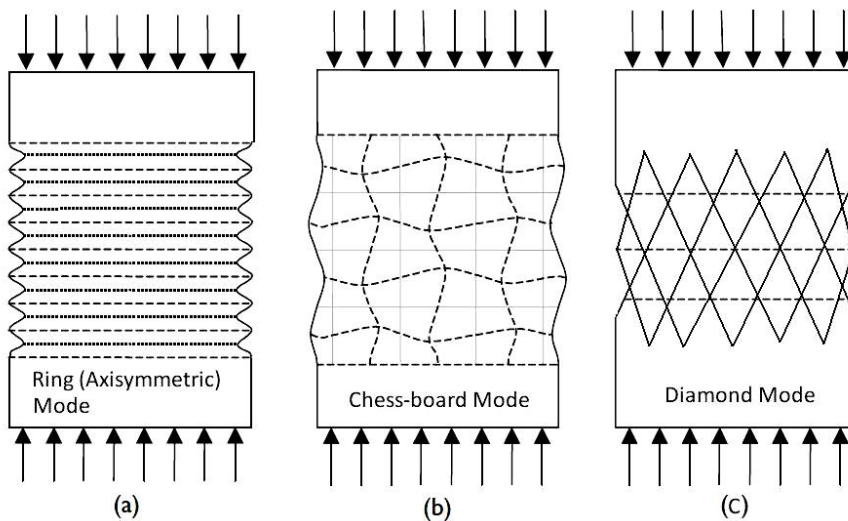
Figure 7-2 Cylindrical Shell Modes of Failure

The first two modes involve cross-sectional distortions are represented diagrammatically in Figure 7-2. The last two represent the transition from initial chessboard buckling to a post-buckled stage when the cylinder snaps through into a diamond form at a lower equilibrium load.

For short cylinders, the observed mode of buckling is assumed to be axisymmetric radial displacements varying sinusoidal along the length known as concertina buckling. This is shown in Figure 7-2(a) and can be defined using the relation,

$$w = w_m \sin\left(m\pi x / L\right) \tag{7-2}$$

Where *m* is the number of half wave along the length *L* and *w* is the radial displacement at *x* with maximum displacement w_m at the centre of each half wave.

A straightforward strain energy analysis which allows for both hoop radial stretching and lengthwise bending leads to the elastic buckling solution:

$$\sigma_{cr} \leq \frac{EL^2}{m^2\pi^2 R^2} + \frac{m^2\pi^2 Et^2}{L^2 12\left(1-v^2\right)} \tag{7-3}$$

It is seen that this symmetrical buckling is similar to buckling of a bar on an elastic foundation. Differentiating Equation (7-3) with respect to *m* leads to the minimum buckling stress as,

$$\min \sigma_{cr} = \frac{E\left(t/R\right)}{\sqrt{3(1-v^2)}} = 0.605E\left(\frac{t}{R}\right) \tag{7-4}$$

$$\left. \begin{array}{l} \text{when m}^4 = \dfrac{12(1-v^2)}{\pi^4} \dfrac{L^4}{R^2 t^2} = \dfrac{12Z^2}{\pi^4} \\[2mm] \text{and wave length L/m = } 1.73\sqrt{R/t} \end{array} \right\} \tag{7-5}$$

It is observed for the above equations that minimum buckling stress and wave length do not depend on cylinder length. It can also be shown that the minimum buckling strength is same for chess board mode buckling.

7.3.2 Orthogonally Stiffened Cylinders in Compression

Figure 7-3 depicts the geometry, notation and uniform loads assumed to act on an orthogonally stiffened cylinder of ring frames and axial stringers.   Also shown is the Tee stiffener cross-section notation.
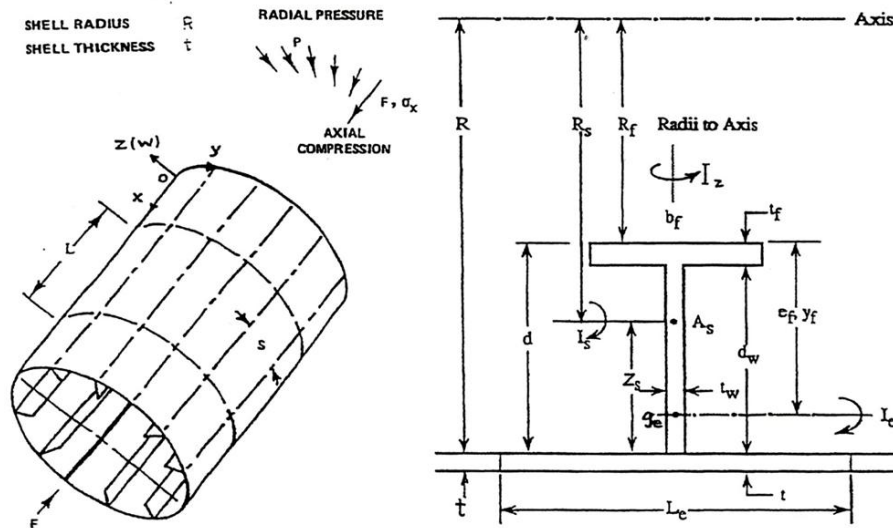
Figure 7-3 Stiffened Cylinder Geometry and Loads

Figure 7-4 shows the modes of failure which need to be considered. Basically the stiffened cylinder structure can buckle and eventually fail in two ways. Snap-through buckling occurs by a sudden reverse of the curvature locally at certain combination of axial loads and the successive bending moments and results in a total failure as there is no chance of moment redistribution. Other failure type is the classical type of bifurcation buckling. Various local and overall buckling modes of stiffened cylinders are shown in Figure 7-4. The mode which most dominates design and structural weight is variously referred to as 'bay instability' and 'panel buckling; but inter-frame collapse is less ambiguous and is used here.
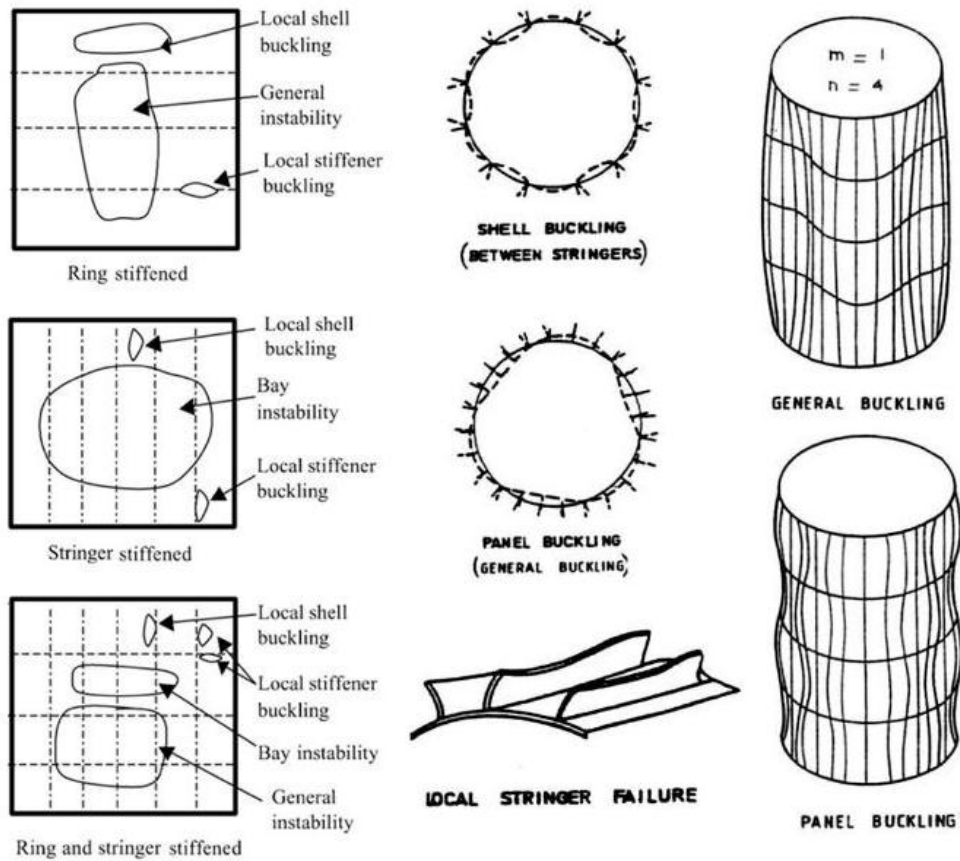
Figure 7-4 Stiffened Cylinder Modes of Failure

The approach taken is to liken the failure model to that of a flat stiffened panel wrapped up into a stiffened cylinder, as illustrated in Figure 7-5. The curved shell between stringers is the most important load carrying element. The analysis will follow that established for flat panels, but with stabilising effects of curvature included.   As with flat panels, an effective width approach is fundamental to achieving the best accuracy.
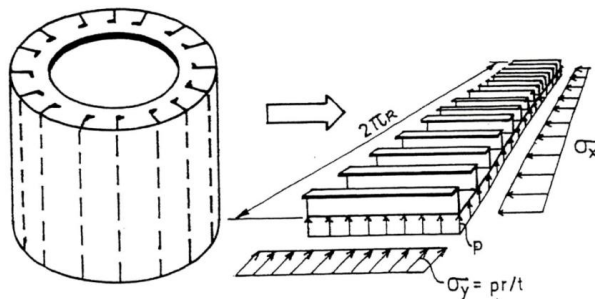
Figure 7-5 Stringer Stiffened Cylinder between Ring Frames

7.4   Knockdown Factor in RCC Code

The analysis revel that there is large variation exists between the experimental test results and the theoretical bucking strength prediction for both cylinder and curved shells. This deviation is predominantly a consequence of initial imperfections. The reduction from the theoretical buckling load is addressed with a term called knockdown factor denoted by ρ. So the elastic buckling strength of imperfect cylinder can be represented as,

$$\sigma_e = \rho\sigma_{cr} \tag{7-6}$$

where σ_{cr} is the lowest critical stress for cylinders and curved shells.

7.4.1.1 Ring Stiffened Cylinder

For unstiffened and ring stiffened cylinder, the knockdown factor is mainly dependent on the Batdorf length parameter. It further shows dependency on R/t so that over the range 100 < R/t < 2000, the value of ρ varies from just below 0.1 to just over 0.9, with the biggest scatter in the range R/t = 200 to 500. For most offshore structures the range of R/t for unstiffened tubes and ring framed large diameter cylinders is generally R/t = 200. It also observed that, for the larger L/R there is bigger knockdown (lower ρ). It is no doubt due to the higher probability of damaging deviations from the true circle occurring over the increased length. The small buckling wavelengths are assumed to be the major factor causing local shape imperfections to be much more serious than in flat compressed plates. Considering the above facts, RCC proposes the knockdown factor for unstiffened and ring stiffened cylinder as,

$$\rho = B\rho_n C \tag{7-7}$$

where ρ_n is the natural knockdown factor and C is a length dependent coefficient as given below.

$$C = \begin{cases} 1 & \text{for} \quad Z_l \geq 2.85 \\ \dfrac{1.425}{Z_l} + 0.175 & \text{for} \quad Z_l < 2.85 \end{cases} \tag{7-8}$$

Batdorf length-wise slenderness parameter, $Z_l = \dfrac{L^2}{Rt}\sqrt{1-v^2}$

$$\rho_n = \begin{cases} 0.75 - 0.142(Z_l - 1)^{0.4} + 0.003Z_l\left(1 - \dfrac{R}{300t}\right) & \text{for} \quad 1 \leq Z_l < 20 \\ 0.35 - 0.0003\dfrac{R}{t} & \text{for} \quad Z_l \geq 20 \end{cases} \tag{7-9}$$

The results show some scatter with the above factors and then introduced the parameter *B* which is the Bias for knock down factor to account the deviations.

$$B = \begin{cases} 1.2 & \text{for} \quad \lambda_n \geq 1 \\ 1 + 0.2\lambda_n & \text{for} \quad \lambda_n < 1 \end{cases} \tag{7-10}$$

where $\lambda_n = \sqrt{\dfrac{\sigma_y}{\rho_n C \sigma_{cr}}}$ \hfill (7-11)

7.4.1.2 Stringer Stiffened Cylinder

Similar to the case of unstiffened and ring stiffened cylinders, the stringer and orthogonally stiffened cylinders also shows the effect of imperfection with a reduction in the buckling strength. As shell slenderness, which is the Batdorf width parameter (Z_s) increases, the behaviour becomes more unstable and imperfection-sensitivity is greater. RCC proposes the knockdown factor for stringer and orthogonally stiffened cylinder as,

$$\rho = B\rho_n \tag{7-12}$$

where ρ_n is the natural knockdown factor as given below.

$$\rho_n = \begin{cases} 1 - 0.919 Z_s^{1.25} + 0.0024 Z_s \left(1 - \dfrac{R}{300t}\right) & \text{for} \quad Z_s \leq 11.4 \\ 0.27 + \dfrac{1.5}{Z_s} + \dfrac{27}{Z_s^2} + 0.008\sqrt{Z_s}\left(1 - \dfrac{R}{300t}\right) & \text{for} \quad 11.4 < Z_s \leq 70 \end{cases} \tag{7-13}$$

Batdorf length-wise slenderness parameter, $Z_s = \dfrac{s^2}{Rt}\sqrt{1-v^2}$

where, $s = \dfrac{2\pi R}{N}$, N- number of stringers

The scatter in the results is managed with a Bias for knock down factor B.

$$B = \begin{cases} 1.25 & \text{for} \quad \lambda_n > 1 \\ 1 + 0.25\lambda_n & \text{for} \quad \lambda_n \leq 1 \end{cases} \tag{7-14}$$

where $\lambda_n = \sqrt{\dfrac{\sigma_y}{\rho_n \sigma_{cr}}}$ \hfill (7-15)

7.5 Proposed Knockdown Factor for Elastic Buckling Strength

The RCC code has taken the bias for knockdown factor B straight from the aerospace industry. The loading, support, material, fabrication, environmental conditions etc. are quite different in the offshore industry. So a straight forward adaptation is not safe for the design purposes. The strength performance under different loading conditions is to be addressed differently for offshore design purposes. The author proposes modified bias for knockdown factors considering various loading conditions particularly applicable for the offshore industry. The coefficients are obtained using a least square fit to match the predictions close to the experimental values.

7.5.1 Proposed Knockdown Factor - Ring Stiffened Cylinder

The results for the ring stiffened panels are separated and the predicted results with the RCC formulation is compared with the experimental results. While fitting the curve with the predictions, the bias shows more sensitivity with the

type of loading. The least square fitting process has been performed for the sets of results with different loading conditions and the bias for knockdown factor for ring stiffened cylinder is expressed as,

$$B = \begin{cases} D_1 & \text{for } \lambda_n < 1 \\ 1 + (D_1 - 1)\lambda_n & \text{for } \lambda_n \geq 1 \end{cases} \tag{7-16}$$

$$D_1 = \begin{cases} 1.40 \text{ - for Axial loading} \\ 1.20 \text{ - for Radial loading} \\ 1.30 \text{ - for Combined loading} \end{cases} \tag{7-17}$$

The scatter of the results has brought down significantly with the above Bias factor which is illustrated latter in this chapter.

7.5.2 Proposed Knockdown Factor - Stringer Stiffened Cylinder

Similar to the previous analysis the bias for knockdown factor for stringer or orthogonally stiffened cylinder is expressed as,

$$B = \begin{cases} D_2 & \text{for } \lambda_n > 1 \\ 1 + (D_2 - 1)\lambda_n & \text{for } \lambda_n \leq 1 \end{cases} \tag{7-18}$$

$$D_2 = \begin{cases} 1.60 \text{ - for Axial loading} \\ 1.25 \text{ - for Radial loading} \\ 2.10 \text{ - for Combined loading} \end{cases} \tag{7-19}$$

Again, the scatter of the results has found to reduce significantly with the above Bias factor which is illustrated in a following section. The coefficients can be further modified subjected to the availability of suitable test results. A stepwise procedure of the modified RCC formulation for the capacity assessment of ring and ring-stringer stiffened cylinders for axial, radial and combined loading conditions is given in Appendix C.

7.6 Experimental Data

The experimental test results are collected from a wide literature survey over the last century. It is observed that majority of the experimental works on

stiffened cylinders are being undertaken during 1960's to 1980's and there is not much experimental works available recently as the researches are comfortable with the numerical results with the increased capabilities and accuracy. This work incorporates data from various experimental programs undertaken across the world for stiffened cylinders as illustrated in Table 7-1. The details of sources are given in the reference.

Table 7-1 Source of Test data

Ref. ID	Reference	Ring Stiffened			Stringer Stiffened		
		Axial	Radial	Combined	Axial	Radial	Combined
A	Dwight, J.B. (1982)	3	-	-	-	-	-
B	White, J.B. and Dwight, J.B. (1977)	7	-	-	-	-	-
C	White, J.B. and Dwight, J.B. (1978)	9	-	23	-	-	-
D	Sridharan, S. and Walker, A.C. (1980)	4	-	-	-	-	-
E	Walker, A.C. and Davies, P. (1977)	8	-	-	-	-	-
F	Agelidis, N.A., Harding, J.E. and Dowling, P.J. (1982)	26	-	-	-	-	-
G	Dowling, P.J. and Harding, J.E. (1982)	-	35	-	-	-	-
H	Weller, T., Singer, J. and Batterman, S.C. (1974)	-	14	-	-	-	-
I	Becker, H. and Gerard, G. (1962)	-	-	7	-	-	-
J	Das, P.K., Faulkner, D. and Guedes da Silva (1991)						
	ABS/Conoco	-	-	-	14	8	22
	CBI	-	-	-	1	1	4
	Imperial college	-	-	-	6	-	-
	Glasgow	-	-	-	3	-	-
	DNV	-	-	-	4	-	-
K	Seleim, S. S. and Roorda J. (1986)	-	10	-	-	-	-
L	Ralph, E.E. (1963)	-	14	-	-	-	-
M	Walker, A.C. and McCall, S. (1987, 1988)	-	1	3	-	2	-
N	Birch, R.S. and Norman Jones (1990)	-	-	-	11	-	-
O	Ross, C. T. F. and Johns, T. (1998)	-	3	-	-	-	-
P	Ross, C. T. F. and Sadler, J.R. (2000)	-	9	-	-	-	-
	Total	57	86	33	39	11	26

The data collected can be classified based on various factors as follows.

1. Geometrical properties: The major geometrical properties for a stiffened cylinder are length between ring frames (L), the mean radius (R), shell thickness (t), Ring stiffener dimensions (height and thickness of web and flange) and number of bays, Stringer stiffener dimensions (height and thickness of web and flange) and number of stringers or spacing.

2. Material properties: the mechanical properties of the material like, yield stress, Young's modulus and poisons ratio.

3. Method of production: cylinders can be produced by many methods depends on its size, material, intended use etc. Particularly for marine applications, the welding process is the major method of fabrication but riveted fastenings also is used very rarely.

4. Test conditions: These are majorly the boundary conditions and the direction of applied load. The experimental results considered here are for the axial load, radial load and combined loads.

Since the buckling strength of stiffened cylinders are very sensitive to initial imperfections as previously mentioned, it is really a matter to be considered while screening data. If the initial imperfection is too far from the influence region considered in the formulation, the results can show a large variation for the predicted results. Most of the available test results are not explicitly providing sufficient data in that respect. In the case of marine structures, the material is normally steel and the fabrication process is predominantly welding. This produces residual stresses in the structure which affects the strength of the structure quite significantly. So the data collected from various technical documents which are presented here are subjected to critical examination to avoid any unreliable data which falls outside the scope of the proposed formulation. Out of the collected data as given in Table 7-1, many data items found to be unreliable and involving other influence parameters which are outside the scope of this work. There are many data showing huge variation because of some unknown factors. After a careful examination, some data have eliminated and the number of data used for each case is presented in Table 7-2.

Table 7-2 Screened Data

	Ring Stiffened			Stringer Stiffened		
	Axial	Radial	Combined	Axial	Radial	Combined
Total data collected	57	86	33	39	11	26
Data used for the analysis	40	65	27	30	9	25

The data used for the comparative analysis and for the evaluation of modified parameters for the proposed formulation falls in the range of design parameters

given in Table 7-3. Hence the proposed formulation is applicable for the same range of parameters.

Table 7-3 Range of data based on various design parameters

	L/R	R/t	s/t	Z_l	Z_s
Min	0.06	14.99	0.00	1.56	0.00
Max	8.15	529.23	132.77	1550.92	46.49

7.7 Statistical Comparison of Strength Models

In the simplest way, a good analytical strength model should predict the strength of the structure accurately under the imposed loading and support conditions. As mentioned earlier, because of the assumptions and approximations considered in the analytical relations along with the unaccounted factors, there always remain a certain percentage of error in the structural strength prediction. So a strength model can be rated based on the deviation from the experimental results. The best way to quantify this uncertainty is with the modelling parameter. This modelling parameter is also known as the model uncertainty factor X_m.

Model uncertainty factor, $X_m = \dfrac{\text{Experimental Value}}{\text{Predicted Value}}$

The data collected are carefully arranged and tabulated with all the necessary inputs for the code based design. The data is then pushed through the analytical relations of DNV, API, RCC and the Recommended Models for stiffened cylinders. The strength predicted by each of the models is then compared with the experimental results to evaluate the model uncertainty factor X_m which is the ratio of experimental value to the theoretical prediction for each set of data. The mean and COV of the model uncertainty factor X_m is then evaluated for each case. The predicted and experimental strength (ϕ-Predicted and ϕ-Test) which are normalised with respect to yield stress are then plotted to show the closeness of experiment with prediction and the scatter in each case. For combined loading cases, the model uncertainty is plotted against L/R ratio as it is not straight forward to represent the strength for a combined loading case.

7.7.1 Ring stiffened Cylinders

The Ring stiffened cylinders are basically checked against the local shell buckling which is the dominant failure mode in this type of structures.

7.7.1.1 Under Axial Compression

Table 7-4 Experimental results of Ring Stiffened Cylinders under Axial Loading

| Sl. No. | Ref. ID | Shell Properties | | | Stiffener Properties | | | | | Material properties | | Collapse Load |
| | | | | | Dim. of ring stiffeners | | | | | | | |
		Length (L)	Radius (R)	Thickness (T)	NB	h_{wr}	t_{wr}	h_{fr}	t_{fr}	E (GPA)	σ_y (N/mm2)	N_{sd} (kN)
1	A	746.50	749.70	3.520	3	48.00	3.52			205.0	281.0	2940.0
2	A	746.50	750.00	3.520	3	48.00	3.52			205.0	281.0	2990.0
3	A	446.50	449.50	3.520	3	24.00	3.52			205.0	281.0	2490.0
4	B	120.70	122.30	0.810	3	6.50	0.81			214.0	314.0	145.0
5	B	120.70	122.30	0.810	3	6.50	0.81			214.0	314.0	147.0
6	B	120.70	122.30	0.810	3	6.50	0.81			214.0	223.0	124.0
7	B	120.70	122.30	0.810	5	13.00	0.81			200.0	286.0	127.0
8	B	120.70	122.30	0.810	5	13.00	0.81			200.0	286.0	134.0
9	B	39.70	203.30	0.810	3	6.50	0.81			209.0	296.0	191.0
10	B	201.70	203.30	0.810	3	13.00	0.81			209.0	296.0	188.0
11	C	70.00	601.60	3.100	9	-30.00	5.00			205.0	335.0	3190.0
12	C	70.00	501.60	3.050	9	-30.00	5.00			205.0	338.0	3100.0
13	C	100.00	601.60	3.100	7	-30.00	5.00			205.0	315.0	2740.0
14	C	145.00	601.60	3.100	5	-30.00	5.00			205.0	343.0	2650.0
15	C	145.00	601.60	3.150	5	-30.00	5.00			205.0	335.0	2700.0
16	C	210.00	601.60	3.100	7	-30.00	5.00			205.0	340.0	2690.0
17	C	210.00	601.60	3.100	7	-30.00	5.00			205.0	316.0	2640.0
18	C	295.00	601.60	3.200	5	-30.00	5.00			205.0	314.0	2770.0
19	C	295.00	601.60	3.150	5	-30.00	5.00			205.0	280.0	2350.0
20	D	562.60	3175.00	6.350	5	101.60	6.35	76.20	6.35	199.0	276.0	11700.0
21	D	278.10	3175.00	6.350	11	101.60	6.35	76.20	6.35	199.0	276.0	17500.0
22	E	108.80	998.40	3.200	10	23.00	3.20			201.0	531.0	5600.0
23	E	108.80	998.40	3.220	10	23.00	3.20			198.0	325.0	3460.0
24	E	222.80	998.40	3.150	16	45.00	3.20			203.0	346.0	3450.0
25	E	335.50	998.40	3.200	10	48.00	4.50			200.0	323.0	3290.0
26	F	24.40	190.90	0.383	7	-1.60	1.25			196.0	198.0	57.8
27	F	23.40	190.90	0.383	7	-2.40	1.87			196.0	198.0	55.6
28	F	23.80	190.90	0.381	11	-1.60	1.25			196.0	198.0	53.6
29	F	15.80	190.90	0.381	11	-2.40	1.87			196.0	198.0	61.5
30	F	15.20	190.90	0.388	10	-1.60	1.87			206.0	242.0	78.7
31	F	11.00	190.90	0.388	10	-1.60	1.25			196.0	198.0	52.0
32	F	73.40	191.20	0.746	10	-2.40	1.87			203.0	245.0	162.0
33	F	49.40	191.20	0.739	10	-3.20	2.49			203.0	245.0	164.0
34	F	35.50	191.20	0.739	11	-3.20	2.49			203.0	245.0	158.0
35	F	23.30	191.20	0.721	15	-3.20	2.49			203.0	245.0	166.0
36	F	23.30	191.30	0.789	9	-3.20	2.49			203.0	545.0	325.0
37	F	13.60	191.00	0.513	11	-1.60	1.25			200.0	456.0	175.0
38	F	13.00	191.00	0.513	11	-2.40	1.87			200.0	456.0	172.0
39	J	890.00	570.00	2.000	20	32.00	2.00			216.0	234.0	1060.0
40	J	760.00	570.00	6.000	8	95.00	6.00			216.0	300.0	6253.0

The 40 data items used for the statistical comparison of results under axial compression for ring stiffened cylinders are represented in Table 7-4. The source of each data can be identified from the corresponding Ref.ID which is described in Table 7-1.

Table 7-5 illustrate the statistical results of model uncertainty factor X_m for DNV, API, RCC and the Proposed strength model. The values indicate that the Proposed model has better statistical parameters compared to other strength models for the axial strength of ring stiffened cylinders. There is a 10% variation in the mean value and nearly 0.5% reduction in the spread of the results.

Table 7-5 Statistical comparison of X_m for Ring Stiffened Cylinder under Axial Loading

	DNV	API	RCC	Proposed Model
Mean	1.28	1.15	1.10	1.00
COV	17.94%	11.84%	11.04%	9.62%
Population	40			
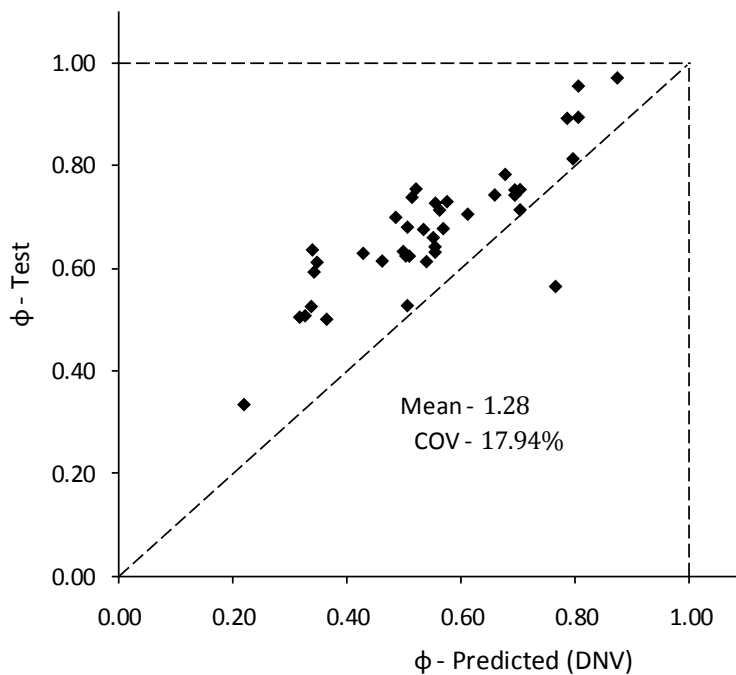
Figure 7-6 DNV prediction for Ring Stiffened Cylinders under Axial Compression

Figure 7-6 to Figure 7-9 show the comparison of predicted and experimental data for the different strength models. The strength prediction of the Proposed

model is more accurate compared to the other approaches in terms of its statistical measures. Figure 7-9 shows the spread of the results about its mean line having a low bias to the unity with less COV.
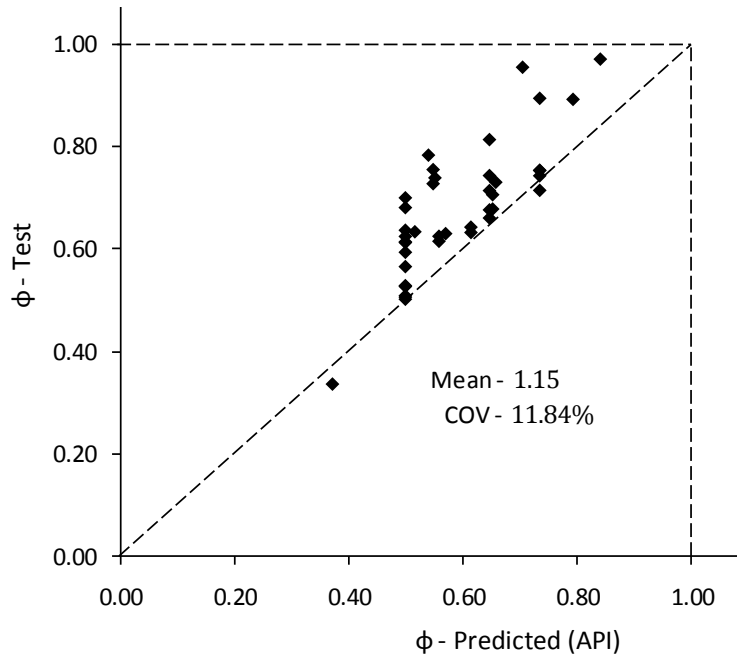
Figure 7-7 API prediction for Ring Stiffened Cylinders under Axial Compression
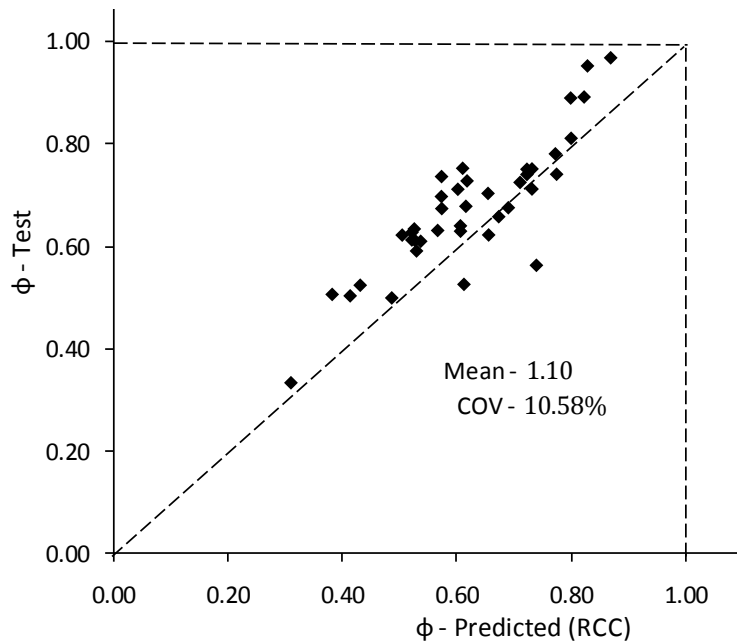
Figure 7-8 RCC prediction for Ring Stiffened Cylinders under Axial Compression
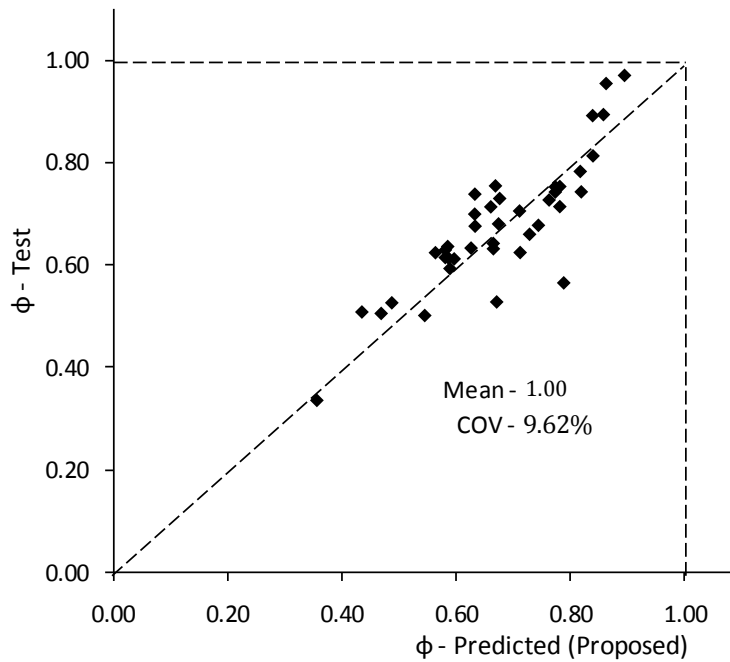
Figure 7-9 Proposed prediction for Ring Stiffened Cylinders under Axial Compression

7.7.1.2 Under Radial Pressure

Table 7-6 shows the screened data used for the analysis of ring stiffened cylinders under radial pressure load. There are 65 data items presented from various sources described in Table 7-1. There are six data (from Sl. No 49 to 64, Ref ID: K) for aluminium material also included for the analysis.

Table 7-6 Experimental results for Ring Stiffened Cylinder under Radial pressure

| | | Shell Properties | | | Stiffener Properties | | | | Material properties | | | Collapse Load |
| | | | | | Dim. of ring stiffeners | | | | | | | |
Sl. No.	Ref. ID	Length (L)	Radius (R)	Thickness (T)	NB	h_{wr}	t_{wr}	h_{fr}	t_{fr}	E (GPA)	σ_y (N/mm2)	ν	P_{sd} (N/mm^2)
1	G	128.56	699.80	5.842	14	42.90	4.46	28.60	6.35	203.0	347.0	0.3	2.7300
2	G	128.56	699.80	5.918	14	42.90	4.46	28.60	6.35	206.0	369.0	0.3	2.8300
3	G	128.56	700.00	5.969	14	42.90	4.46	28.60	6.35	204.0	329.0	0.3	2.9300
4	G	128.56	700.00	6.071	14	42.90	4.46	28.60	6.35	204.0	316.0	0.3	2.9700
5	G	128.56	700.00	6.121	14	42.90	4.46	28.60	6.35	206.0	320.0	0.3	3.0400
6	G	146.90	700.00	6.121	12	42.90	4.46	28.60	6.35	209.0	318.0	0.3	2.8300
7	G	146.90	699.80	5.715	12	42.90	4.46	28.60	6.35	205.0	329.0	0.3	2.6600
8	G	146.90	700.00	6.121	12	42.90	4.46	28.60	6.35	209.0	318.0	0.3	2.9700
9	G	146.90	699.80	5.893	12	42.90	4.46	28.60	6.35	206.0	350.0	0.3	2.9000
10	G	146.90	700.00	6.020	12	42.90	4.46	28.60	6.35	198.0	320.0	0.3	2.7600
11	G	158.23	700.00	6.020	11	42.90	4.46	28.60	6.35	204.0	332.0	0.3	2.5500
12	G	158.23	699.80	5.918	11	42.90	4.46	28.60	6.35	206.0	330.0	0.3	2.4500
13	G	158.23	700.00	6.071	11	42.90	4.46	28.60	6.35	202.0	327.0	0.3	2.6200
14	G	158.23	700.00	6.248	11	42.90	4.46	28.60	6.35	204.0	320.0	0.3	2.7300
15	G	158.23	700.00	6.096	11	42.90	4.46	28.60	6.35	204.0	320.0	0.3	2.5200

Table 7-6 Experimental results for Ring Stiffened Cylinder under Radial pressure (Continued)

Sl. No.	Ref. ID	Length (L)	Radius (R)	Thickness (T)	NB	h_{wr}	t_{wr}	h_{fr}	t_{fr}	E (GPA)	σ_y (N/mm2)	ν	P_{sd} (N/mm^2)
		Shell Properties				Dim. of ring stiffeners				Material properties			Collapse Load
16	G	187.00	700.00	6.020	9	42.90	4.46	28.60	6.35	202.0	330.0	0.3	2.3500
17	G	187.00	699.80	5.893	9	42.90	4.46	28.60	6.35	203.0	342.0	0.3	2.3100
18	G	187.00	700.00	5.969	9	42.90	4.46	28.60	6.35	201.0	310.0	0.3	2.3100
19	G	187.00	700.00	6.045	9	42.90	4.46	28.60	6.35	204.0	311.0	0.3	2.4100
20	G	187.00	699.80	5.918	9	42.90	4.46	28.60	6.35	206.0	309.0	0.3	2.2800
21	G	171.40	700.00	6.147	10	47.60	4.90	31.70	7.92	203.0	327.0	0.3	3.1100
22	G	171.40	700.00	6.274	10	47.60	4.90	31.70	7.92	202.0	352.0	0.3	3.0000
23	G	171.40	700.00	6.325	10	47.60	4.90	31.70	7.92	202.0	349.0	0.3	3.1700
24	G	171.40	700.00	6.223	10	47.60	4.90	31.70	7.92	203.0	341.0	0.3	2.9000
25	G	171.40	700.00	6.274	10	47.60	4.90	31.70	7.92	202.0	376.0	0.3	2.9700
26	G	171.40	700.50	7.188	10	42.90	4.46	28.60	6.35	205.0	340.0	0.3	3.5900
27	G	171.40	700.50	7.341	10	42.90	4.46	28.60	6.35	205.0	322.0	0.3	3.7300
28	G	171.40	700.50	7.341	10	42.90	4.46	28.60	6.35	206.0	330.0	0.3	3.5200
29	G	171.40	700.50	7.341	10	42.90	4.46	28.60	6.35	210.0	320.0	0.3	3.4500
30	G	128.50	700.00	6.270	12	50.80	6.35			205.0	301.0	0.3	3.8600
31	G	128.50	700.00	6.270	12	50.80	6.35			205.0	291.0	0.3	3.3100
32	G	128.50	700.10	6.430	12	25.40	12.70			205.0	301.0	0.3	3.8600
33	G	128.50	700.10	6.400	12	25.40	12.70			205.0	330.0	0.3	3.6600
34	G	128.50	700.00	6.270	12	38.10	4.46	14.30	14.30	205.0	319.0	0.3	3.3800
35	G	128.50	700.00	6.350	12	38.10	4.46	14.30	14.30	205.0	308.0	0.3	3.3500
36	H	800.00	199.50	12.573	5	-78.70	13.28			204.0	272.0	0.3	15.2000
37	H	797.10	196.20	13.081	5	-78.50	13.13			204.0	408.0	0.3	18.5000
38	H	1125.40	196.90	13.132	4	-77.20	13.03			194.0	242.0	0.3	14.6000
39	H	1530.30	197.00	13.132	2	-77.70	13.03			194.0	242.0	0.3	12.4000
40	H	1538.30	197.30	11.024	2	-78.20	11.13			196.0	260.0	0.3	9.3200
41	H	592.10	197.70	9.754	7	-76.50	9.91			202.0	289.0	0.3	12.8000
42	H	1614.60	198.80	9.601	2	-79.50	9.78			200.0	231.0	0.3	7.4500
43	H	1615.10	198.20	8.280	2	-80.00	8.18			201.0	287.0	0.3	6.0000
44	H	403.00	199.40	6.604	11	-65.80	6.96			194.0	278.0	0.3	7.8700
45	H	435.10	198.90	6.833	10	-69.60	6.88			206.0	371.0	0.3	8.3500
46	H	603.30	198.70	6.833	7	-71.10	7.04			206.0	371.0	0.3	8.2800
47	H	1447.70	199.80	6.452	3	-63.20	6.68			197.0	276.0	0.3	3.1100
48	H	609.70	603.20	9.627	3	101.60	9.52			190.0	259.0	0.3	2.9300
49	K	49.28	128.02	2.032	17	7.37	3.56			69.0	241.3	0.4	3.0310
50	K	63.50	128.02	2.032	13	8.38	4.06			69.0	241.3	0.4	2.8332
51	K	74.17	128.02	2.032	11	9.14	4.57			69.0	241.3	0.4	3.1896
52	K	88.90	128.02	2.032	9	9.91	5.08			69.0	241.3	0.4	2.9421
53	K	88.90	128.02	2.032	9	9.91	5.08			69.0	241.3	0.4	3.5185
54	K	63.50	128.02	2.032	13	8.38	4.06			69.0	241.3	0.4	3.1193
55	M	40.00	160.30	0.600	4	4.80	0.60			208.0	387.0	0.3	0.5500
56	O	18.97	51.48	1.267	3	6.00	6.10			200.0	244.0	0.3	11.1720
57	O	12.66	51.47	1.246	3	6.00	5.95			200.0	244.0	0.3	13.1720
58	P	7.00	76.79	0.216						200.0	463.6	0.3	1.2070
59	P	10.10	76.65	0.293						200.0	369.1	0.3	1.1790
60	P	15.75	76.65	0.295						200.0	384.9	0.3	0.8900
61	P	19.40	76.65	0.296						200.0	384.9	0.3	0.7240
62	P	22.25	76.65	0.299						200.0	369.1	0.3	0.6210
63	P	26.50	76.64	0.295						200.0	400.1	0.3	0.5790
64	P	29.00	76.64	0.294						200.0	400.1	0.3	0.5138
65	P	34.80	76.65	0.295						200.0	369.1	0.3	0.4280

Table 7-7 shows the statistical analysis results for DNV, API, RCC and the Proposed strength model. Figure 7-10 to Figure 7-13 show the comparison of predicted and experimental data for different approaches. The average and spread of the population shows better central tendency compared to the other approaches.

Table 7-7 Statistical comparison of X_m for Ring Stiffened Cylinder under Radial Loading

	DNV	API	RCC	Proposed Model
Mean	0.98	1.35	1.03	1.00
COV	19.43%	19.09%	21.19%	17.67%
Population	65			

The radial collapse pressure is often found to exceed the yield hoop pressure. i.e., the normalised strength value exceeds 1 in many cases. The API strength model predicts the strength for all cases below 1 and shows large error for number of cases. This indicates that the plastic collapse concept used in the DNV, RCC and Proposed strength models are based on realistic assumptions.
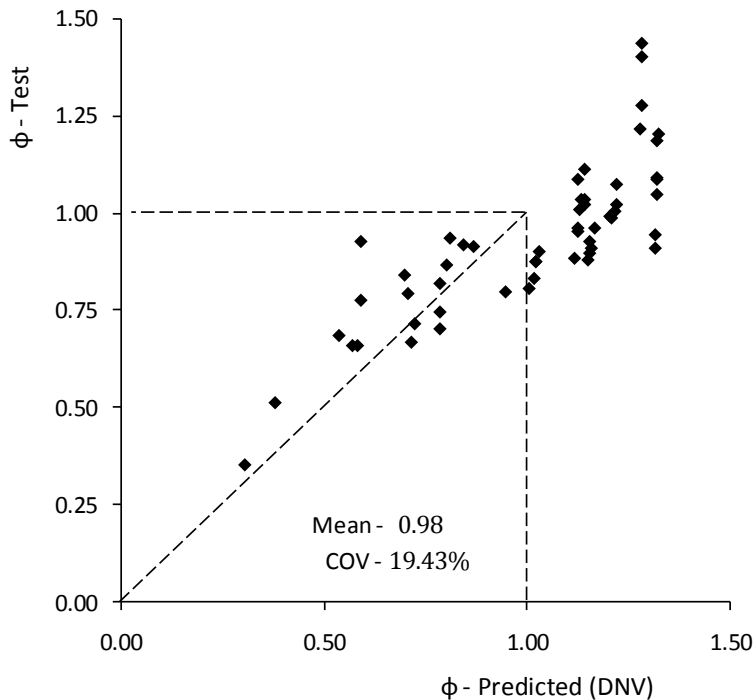
Figure 7-10 DNV prediction for Ring Stiffened Cylinders under Radial Pressure
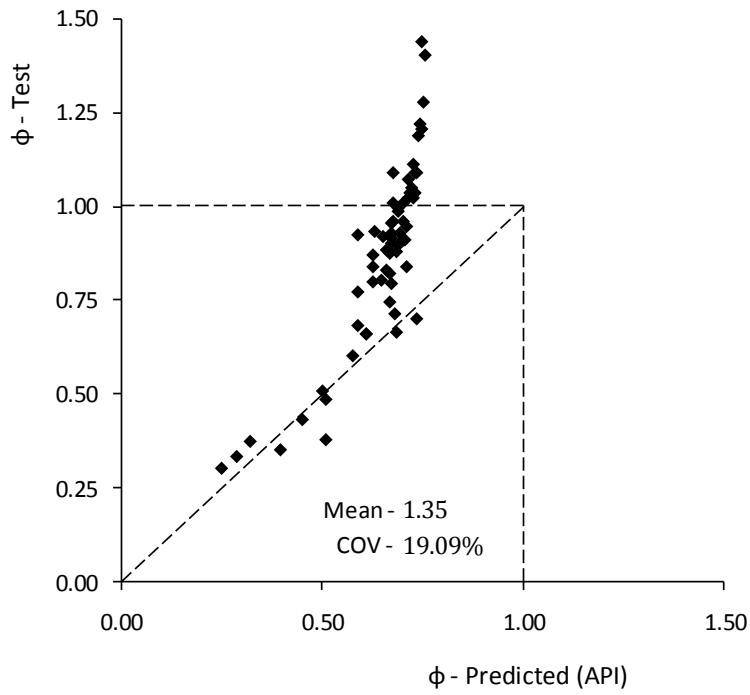
Figure 7-11 API prediction for Ring Stiffened Cylinders under Radial Pressure
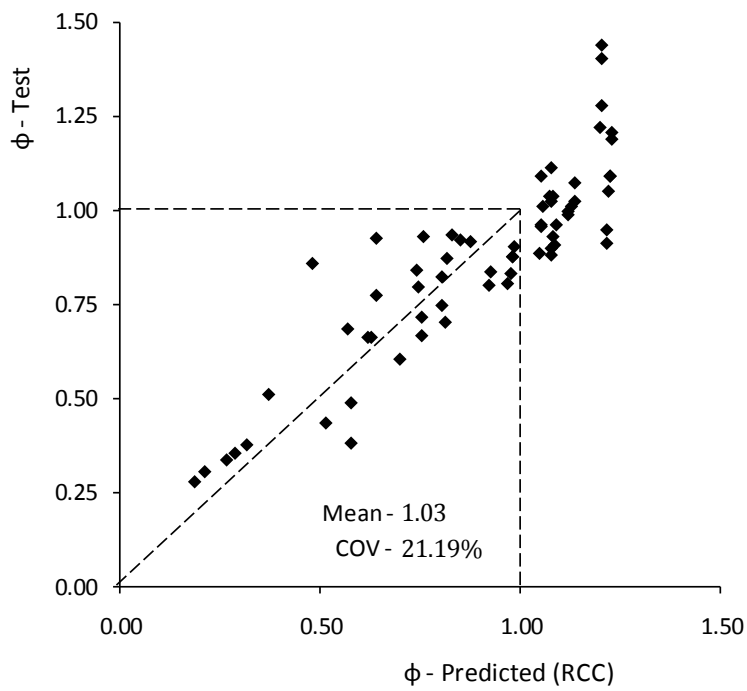
Figure 7-12 RCC prediction for Ring Stiffened Cylinders under Radial Pressure
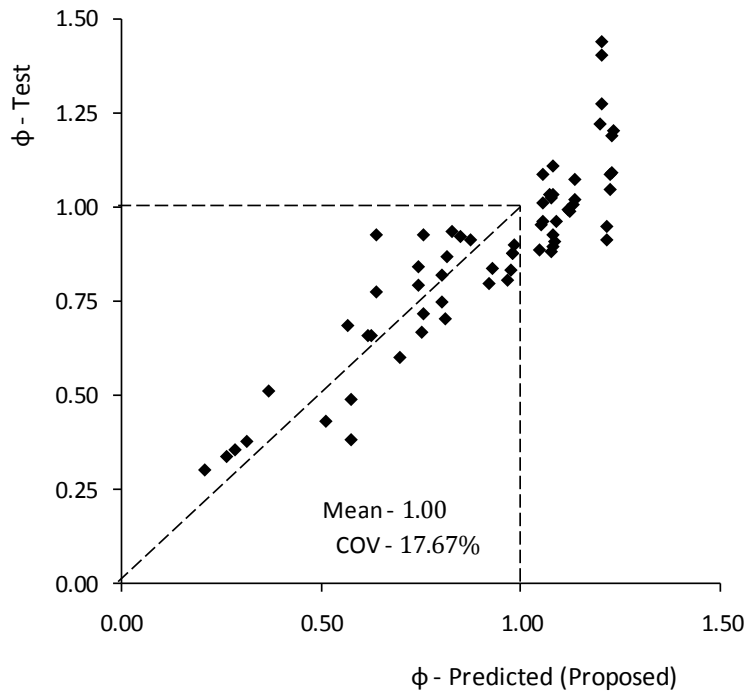
Figure 7-13 Proposed prediction for Ring Stiffened Cylinders under Radial Pressure

7.7.1.3 Under Combined Axial Compression and Radial Pressure

Table 7-8 shows the screened data used for the analysis of ring stiffened cylinders under combined axial load and radial pressure. There are 27 data items presented from various sources described in Table 7-1.

175

Table 7-8 Experimental results for Ring Stiffened Cylinder under Combined loading

Sl. No.	Ref. ID	Shell Properties			Stiffener Properties				Material properties		Collapse Load	
						Dim. of ring stiffeners						
		Length (L)	Radius (R)	Thickness (T)	NB	h_{wr}	t_{wr}	h_{fr}	t_{fr}	E (GPA)	σ_y (N/mm2)	N_{sd} (kN)	P_{sd} (N/mm^2)
1	D	2262.60	3175.00	6.350	1	95.20	6.35	76.20	6.35	199.0	276.0	1800.0	0.032
2	D	2262.60	3175.00	6.350	1	95.20	6.35	76.20	6.35	199.0	276.0	3400.0	0.028
3	D	2262.60	3175.00	6.350	1	95.20	6.35	76.20	6.35	199.0	276.0	5550.0	0.024
4	D	1125.60	3175.00	6.350	1	95.20	6.35	76.20	6.35	199.0	276.0	204.0	0.086
5	D	1125.60	3175.00	6.350	1	95.20	6.35	76.20	6.35	199.0	276.0	2120.0	0.08
6	D	1125.60	3175.00	6.350	1	95.20	6.35	76.20	6.35	199.0	276.0	4040.0	0.074
7	D	1125.60	3175.00	6.350	1	95.20	6.35	76.20	6.35	199.0	276.0	6310.0	0.065
8	D	556.30	3175.00	6.350	1	95.20	6.35	76.20	6.35	199.0	276.0	10400.0	0.141
9	D	840.70	3175.00	6.350	1	95.20	6.35	76.20	6.35	199.0	276.0	204.0	0.124
10	D	840.70	3175.00	6.350	1	95.20	6.35	76.20	6.35	199.0	276.0	2440.0	0.117
11	D	840.70	3175.00	6.350	1	95.20	6.35	76.20	6.35	199.0	276.0	4680.0	0.107
12	D	840.70	3175.00	6.350	1	95.20	6.35	76.20	6.35	199.0	276.0	7240.0	0.09
13	D	840.70	3175.00	6.350	1	95.20	6.35	76.20	6.35	199.0	276.0	9920.0	0.048
14	D	840.70	3175.00	6.350	1	95.20	6.35	25.40	6.35	199.0	276.0	204.0	0.124
15	D	840.70	3175.00	6.350	1	95.20	6.35	25.40	6.35	199.0	276.0	2440.0	0.11
16	D	840.70	3175.00	6.350	1	95.20	6.35	25.40	6.35	199.0	276.0	4680.0	0.103
17	D	840.70	3175.00	6.350	1	95.20	6.35	25.40	6.35	199.0	276.0	7240.0	0.083
18	D	840.70	3175.00	6.350	1	76.20	6.35			199.0	276.0	204.0	0.124
19	D	840.70	3175.00	6.350	1	76.20	6.35			199.0	276.0	2440.0	0.11
20	D	840.70	3175.00	6.350	1	76.20	6.35			199.0	276.0	4680.0	0.097
21	D	840.70	3175.00	6.350	1	76.20	6.35			199.0	276.0	9340.0	0.076
22	D	840.70	3175.00	6.350	1	76.20	6.35			199.0	276.0	9920.0	0.048
23	I	665.90	222.30	13.560	6	-61.00	13.56			207.0	381.0	80.1	17.9
24	I	1372.90	298.70	13.110	4	-74.40	12.95			209.0	359.0	0.0	10.4
25	M	40.00	160.30	0.600	4	4.80	0.60			208.0	387.0	29.6	0.5
26	M	24.00	160.10	0.600	3	3.00	0.60	6.00	0.84	208.0	387.0	58.4	1.0000
27	M	24.00	160.10	0.600	3	3.00	0.60	6.00	0.84	208.0	387.0	123.0	0.5000

Table 7-9 shows the statistical results of the ring stiffened cylinders under combined axial compression and Radial pressure for a population of 27 data for DNV, API, RCC and the Proposed strength model. The API model shows the lowest bias. The proposed strength model shows less scatter compared to all the other strength models.

Table 7-9 Statistical comparison of X_m for Ring Stiffened Cylinder under Combined Loading

	DNV	API	RCC	Proposed Model
Mean	1.46	1.07	1.14	1.17
COV	19.49%	21.71%	18.34%	16.41%
Population	27			

Figure 7-14 to Figure 7-17 show the comparison of predicted and experimental data for the different approaches.
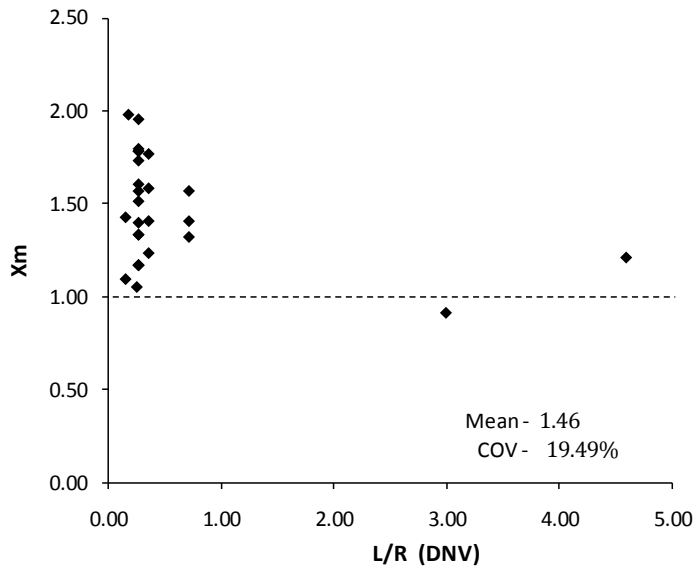
Figure 7-14 DNV prediction for Ring Stiffened Cylinders under Combined Loading
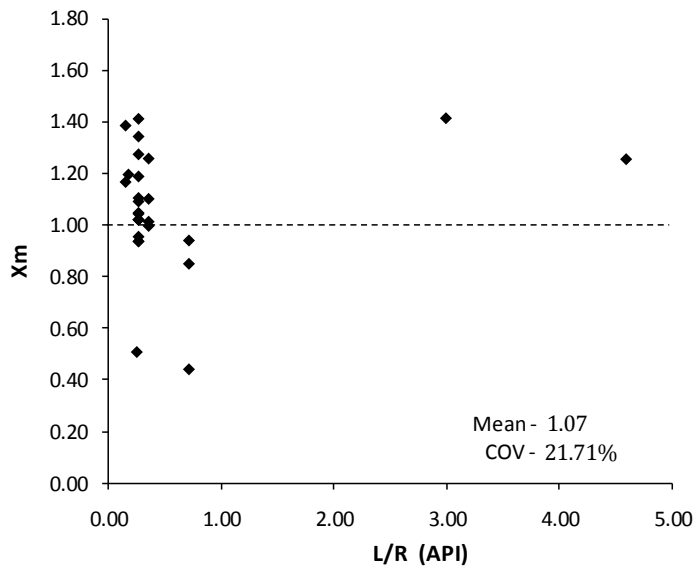
Figure 7-15 API prediction for Ring Stiffened Cylinders under Combined Loading
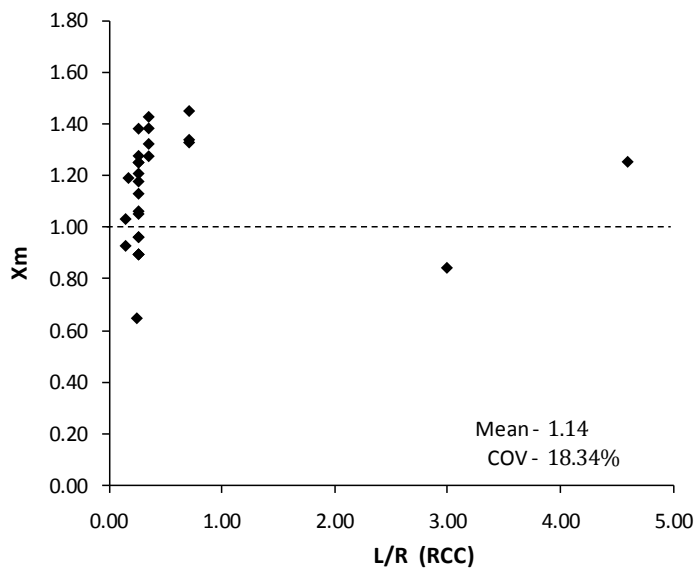
Figure 7-16 RCC prediction for Ring Stiffened Cylinders under Combined Loading
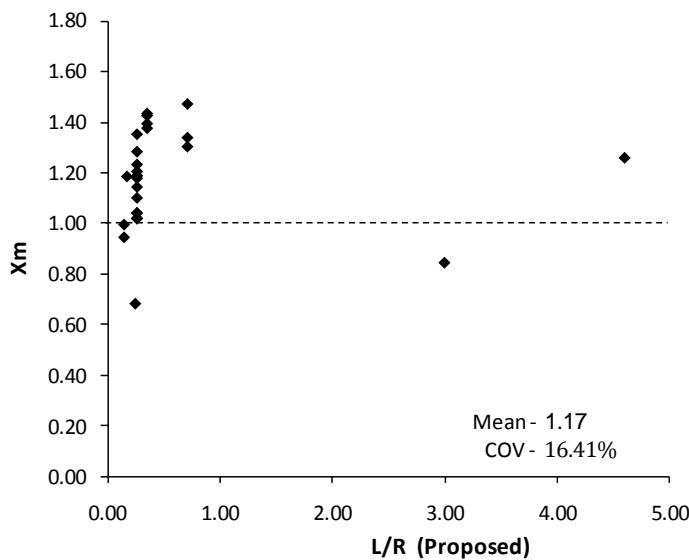
Figure 7-17 Proposed prediction for Ring Stiffened Cylinders under Combined Loading

7.7.2 Ring and Stringer (Orthogonally) Stiffened Cylinders

The stringer stiffened cylinders and orthogonally stiffened cylinders are considered in one category for the strength analysis. For strength analysis, these two types are considered as stiffened curved shells bounded by stringers alone or both stringers and rings.

7.7.2.1 Under Axial Compression

Table 7-10 shows the screened data used for the analysis of ring-stringer stiffened cylinders under axial load. There are 30 data items presented from various sources described in Table 7-1.

Table 7-10 Experimental results for Ring and Stringer Stiffened Cylinder under Axial compression

| | | Shell Properties | | | Stiffener Properties | | | | | | Material properties | | Collapse Load |
| | | | | | Dim. of ring | | Dim. of Stringers | | | | | | |
Sl. No.	Ref. ID	Length (L)	Radius (R)	Thickness (T)	NB	h_{wr}	t_{wr}	N_s	h_{ws}	t_{ws}	E (GPA)	σ_y (N/mm2)	N_{sd} (kN)
1	J	228.60	571.50	1.958				36	30.48	1.94	218.3	386.5	2344.8
2	J	228.60	569.20	2.047				36	30.48	2.07	209.0	409.0	3062.3
3	J	228.60	570.50	1.963				18	30.48	1.94	221.0	387.6	1950.3
4	J	571.50	570.80	1.877				36	30.48	1.88	198.1	412.8	2653.3
5	J	571.50	569.30	2.192				36	30.48	2.16	212.2	512.5	3436.2
6	J	571.50	571.00	1.900				36	30.48	1.86	215.3	442.0	2260.7
7	J	571.50	568.50	1.963				18	30.48	1.95	210.5	419.0	1945.1
8	J	381.00	949.20	1.994				24	30.48	1.95	201.5	408.4	2351.7
9	J	762.00	951.70	1.908				48	30.48	1.94	210.5	412.0	3592.2
10	J	762.00	953.30	1.956				48	30.48	1.96	196.0	418.0	3349.1
11	J	762.00	950.80	1.880				24	30.48	1.95	204.5	423.0	2298.6
12	J	289.50	361.20	1.946				40	30.48	1.95	199.7	342.9	2199.1
13	J	289.50	362.80	2.085				40	30.48	2.01	195.9	342.9	1943.3
14	J	65.00	160.00	0.840				40	6.72	0.84	201.0	348.0	357.0
15	J	65.00	160.00	0.840				20	6.72	0.84	201.0	348.0	321.0
16	J	65.00	160.00	0.840				40	13.44	0.84	201.0	348.0	430.0
17	J	65.00	160.00	0.840				40	6.72	0.84	201.0	348.0	277.0
18	J	180.00	160.00	0.840				40	13.44	0.84	201.0	348.0	270.0
19	J	400.05	571.50	1.900	3	38.10	1.90	36	22.86	1.90	216.0	371.1	2775.7
20	N	150.00	31.21	1.580				4	-23.00	1.58	211.0	263.0	126.0
21	N	150.00	31.21	1.580				4	24.00	1.58	211.0	263.0	110.0
22	N	150.00	31.21	1.580				4	-14.00	1.58	211.0	263.0	118.0
23	N	150.00	31.21	1.580				4	15.00	1.58	211.0	263.0	112.0
24	N	150.00	31.21	1.580				4	-7.00	1.58	211.0	263.0	114.0
25	N	150.00	31.21	1.580				4	7.00	1.58	211.0	263.0	96.0
26	N	150.00	31.21	1.580				8	-7.00	1.58	211.0	263.0	116.0
27	N	150.00	31.21	1.580				12	-7.00	1.58	211.0	263.0	124.0
28	N	150.00	31.21	1.580				4	-4.00	1.58	211.0	263.0	100.0
29	N	150.00	31.21	1.580				8	-4.00	1.58	211.0	263.0	110.0
30	N	150.00	31.21	1.580				12	-4.00	1.58	211.0	263.0	112.0

Table 7-11 shows the statistical results of the ring-stringer stiffened cylinders under Axial compression for a population of 30 for DNV, API, RCC and the Proposed strength model.

Table 7-11 Statistical comparison of X_m for Ring-Stringer Stiffened Cylinder under Axial Loading

	DNV	API	RCC	Proposed Model
Mean	1.02	1.07	1.05	1.01
COV	21.57%	14.67%	14.01%	14.17%
Population	30			

Figure 7-18 to Figure 7-21 show the comparison of predicted and experimental data for the different approaches. The Proposed model predicts the strength almost similar to that of the API and RCC model and which is better compared to API and DNV models.
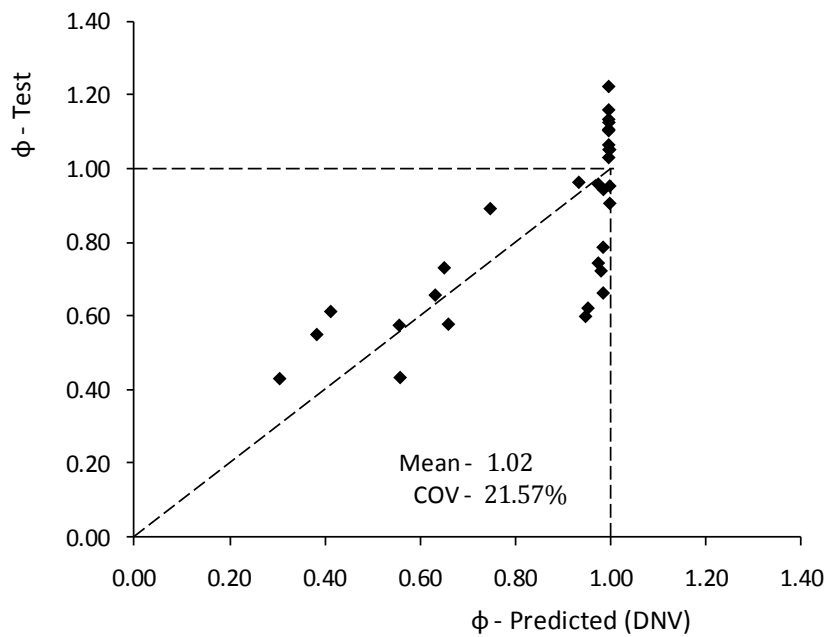
Figure 7-18 DNV prediction for Ring-Stringer Stiffened Cylinders under Axial Compression
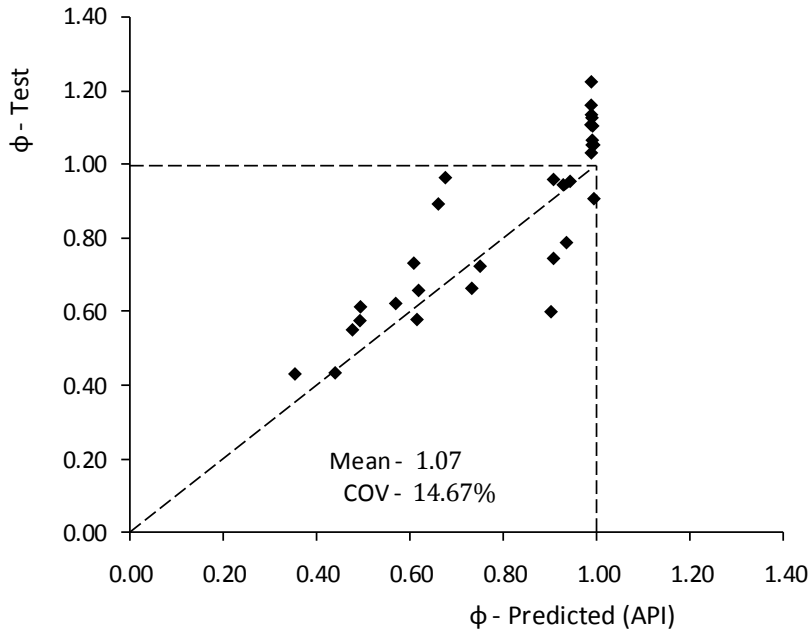
Figure 7-19 API prediction for Ring-Stringer Stiffened Cylinders under Axial Compression
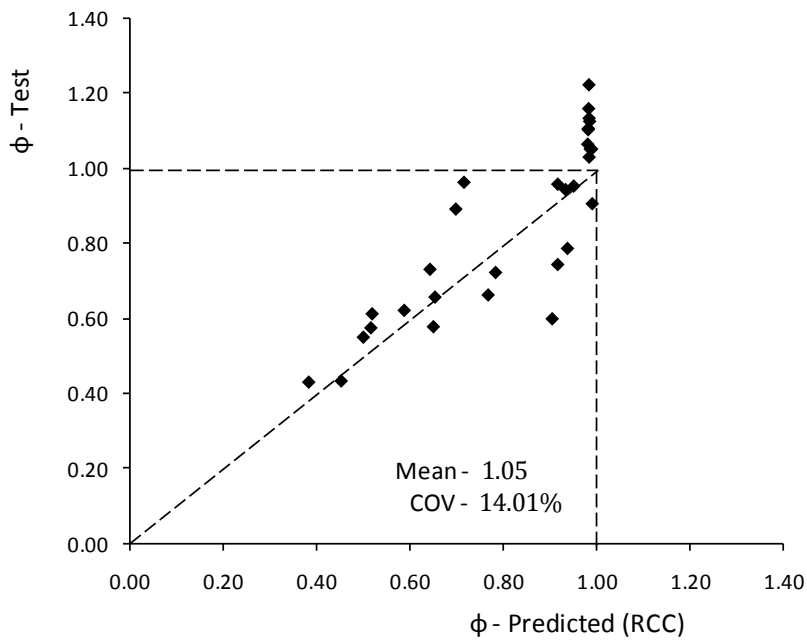
Figure 7-20 RCC prediction for Ring-Stringer Stiffened Cylinders under Axial Compression
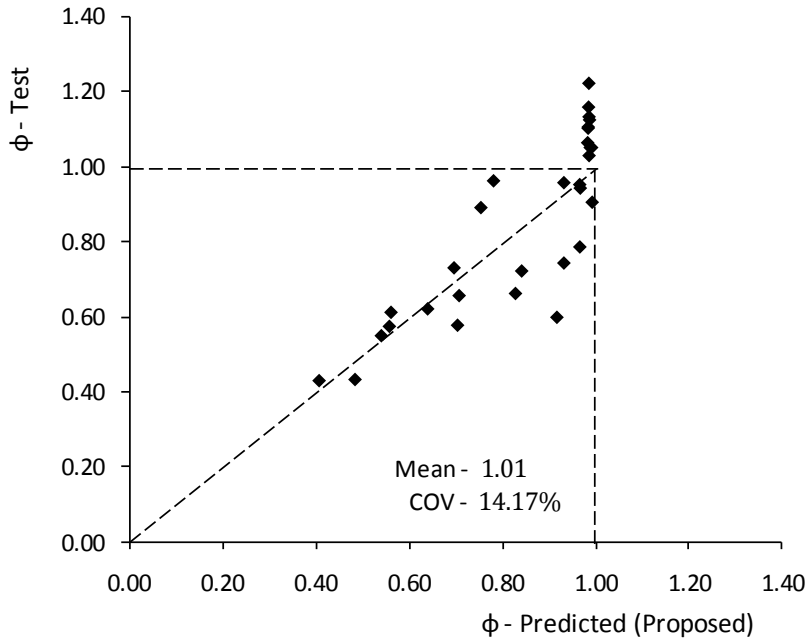
Figure 7-21 Proposed prediction for Ring-Stringer Stiffened Cylinders under Axial Compression

7.7.2.2 Under Radial Pressure

Table 7-12 shows the screened data used for the analysis of ring stiffened cylinders under radial pressure loading. There are 9 data items presented from various sources described in Table 7-1.

Table 7-12 Experimental results for Ring and Stringer Stiffened Cylinder under Radial pressure

| | | Shell Properties | | | Stiffener Properties | | | | | | Material properties | | Collapse Load |
| | | | | | Dim. of ring | | Dim. of Stringers | | | | | | |
Sl. No.	Ref. ID	Length (L)	Radius (R)	Thickness (T)	NB	h_{wr}	t_{wr}	N_s	h_{ws}	t_{ws}	E (GPA)	σ_y (N/mm2)	P_{sd} (N/mm^2)
1	J	228.60	571.40	1.956				36	30.48	1.91	215.7	393.2	0.79
2	J	228.60	569.20	1.948				18	30.48	1.94	203.1	385.9	0.76
3	J	571.50	570.20	1.920				36	30.48	1.92	209.2	396.7	0.35
4	J	381.00	949.70	1.961				48	30.48	1.97	200.5	408.4	0.34
5	J	381.00	953.60	1.974				24	30.48	1.95	198.2	409.0	0.31
6	J	762.00	949.80	1.938				48	30.48	1.91	210.2	403.4	0.17
7	J	762.00	950.90	1.895				24	30.48	1.91	202.4	421.9	0.15
8	J	289.60	360.70	1.928				40	30.48	1.93	192.2	325.7	1.04
9	M	96.00	160.30	0.600	2	6.40	0.80	40	4.80	0.60	208.0	387.0	0.36

Table 7-13 shows the statistical results of the ring-stringer stiffened cylinders under radial pressure for a population of 9 for DNV, API, RCC and the Proposed strength model. The recommended approach is same as that of RCC and it is quite similar to the API formulation. The Proposed model appears better

compared to DNV and API codes in terms of mean and spread of the model uncertainty factor.

Table 7-13 Statistical comparison of X_m for Ring-Stringer Stiffened Cylinder under Radial Pressure

	DNV	API	RCC	Proposed Model
Mean	1.33	1.12	1.06	1.06
COV	47.38%	21.54%	18.38%	18.38%
Population	9			

Figure 7-22 to Figure 7-24 show the comparison of predicted and experimental data for the different approaches. The RCC model is not shown as it is exactly similar to the proposed model.
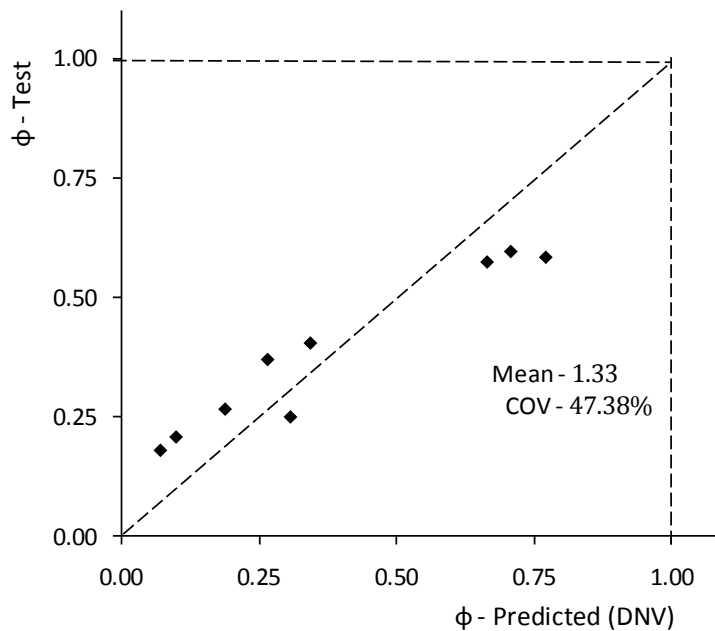
Figure 7-22 DNV prediction for Ring-Stringer Stiffened Cylinders under Radial Pressure
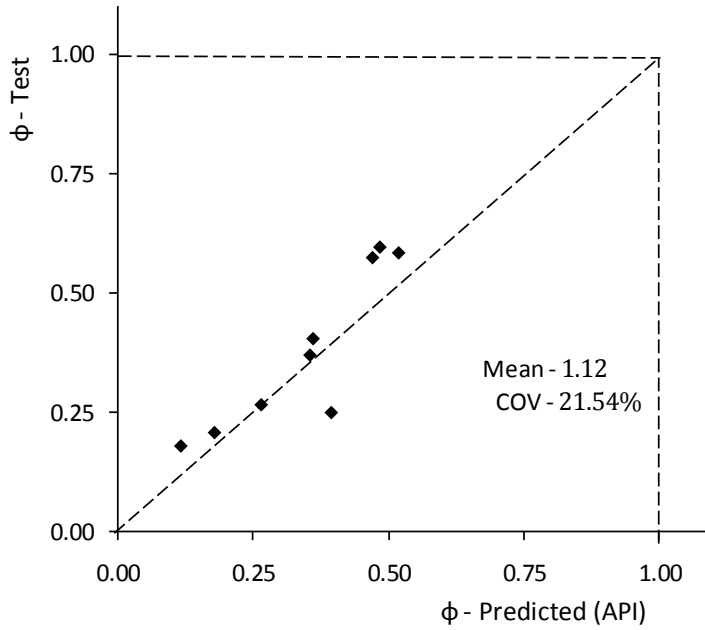
Figure 7-23 API prediction for Ring-Stringer Stiffened Cylinders under Radial Pressure
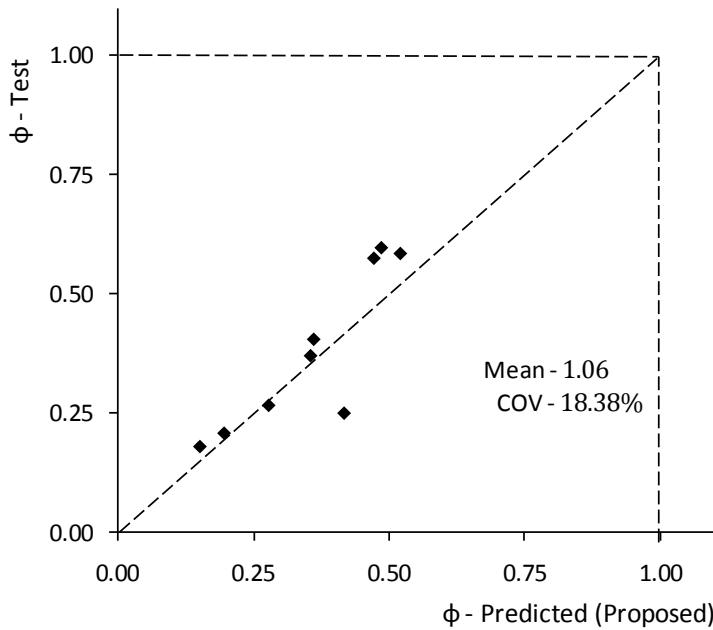
Figure 7-24 Proposed prediction for Ring-Stringer Stiffened Cylinders under Radial Pressure

7.7.2.3 Under Combined Axial Compression and Radial Pressure

Table 7-14 shows the screened data used for the analysis of ring stiffened cylinders under radial pressure loading. There are 25 data items presented from various sources described in Table 7-1.

Table 7-14 Experimental results for Ring and Stringer Stiffened Cylinder under Combined loading

| Sl. No. | Ref. ID | Shell Properties | | | Stiffener Properties | | | | | | Material properties | | Collapse Load | |
| | | | | | Dim. of ring | | | Dim. of Stringers | | | | | | |
		Length (L)	Radius (R)	Thickness (T)	NB	h_{wr}	t_{wr}	N_s	h_{ws}	t_{ws}	E (GPA)	σ_y (N/mm2)	N_{sd} (kN)	P_{sd} (N/mm^2)
1	J	228.60	571.10	1.966				36	30.48	1.96	217.7	395.7	755.8	0.736
2	J	228.60	571.80	1.961				18	30.48	1.94	209.5	390.5	647.5	0.629
3	J	571.50	570.80	1.854				36	30.48	1.86	210.5	425.0	349.9	0.335
4	J	571.50	570.10	1.976				18	30.48	1.97	217.2	425.3	303.2	0.290
5	J	381.00	953.20	1.971				48	30.48	1.98	207.7	398.4	935.6	0.324
6	J	381.00	951.70	1.963				24	30.48	1.80	200.1	404.6	815.4	0.282
7	J	762.00	954.90	1.961				48	30.48	1.96	209.4	406.2	421.7	0.139
8	J	762.00	954.20	1.803				48	30.48	1.82	203.2	406.3	446.7	0.148
9	J	762.00	953.20	1.895				24	30.48	1.91	205.5	422.6	381.4	0.125
10	J	289.60	361.00	1.943				40	30.48	1.94	193.0	341.5	513.6	1.032
11	J	228.60	569.40	1.958				36	30.48	1.92	216.2	396.9	1911.7	0.520
12	J	228.60	570.50	1.956				18	30.48	1.93	201.7	384.7	1272.5	0.345
13	J	571.50	571.50	1.908				36	30.48	1.87	208.3	391.8	1042.9	0.283
14	J	571.50	570.30	1.946				18	30.48	1.88	207.4	417.5	820.1	0.223
15	J	381.00	953.20	1.969				48	30.48	1.98	207.7	398.4	2546.1	0.248
16	J	381.00	952.10	1.958				24	30.48	1.96	202.5	415.7	1524.5	0.170
17	J	762.00	956.60	1.925				48	30.48	1.90	206.9	422.3	1376.2	0.134
18	J	762.00	950.50	1.829				48	30.48	1.81	199.1	417.9	1270.7	0.124
19	J	762.00	953.40	1.880				24	30.48	1.88	204.9	422.6	973.2	0.095
20	J	289.60	360.40	1.963				40	30.48	1.96	197.8	341.8	1405.2	0.787
21	J	571.50	569.60	1.971				18	30.48	1.92	200.5	432.7	242.6	0.285
22	J	400.05	571.50	1.900	3	45.72	1.90	36	30.48	1.90	216.0	375.4	2368.6	0.233
23	J	400.05	571.50	1.900	3	38.10	1.90	36	22.86	1.90	216.0	377.2	324.5	0.389
24	J	400.05	571.50	1.900	3	38.10	1.90	48	22.86	1.90	216.0	378.1	2949.5	0.248
25	J	533.40	952.50	1.900	3	45.72	1.90	48	30.48	1.90	216.0	384.5	2384.2	0.081

Table 7-15 shows the statistical results of the ring and stringer stiffened cylinders under combined axial compression and radial pressure for a population of 25 for DNV, API, RCC and the Proposed strength model.

Table 7-15 Comparison of X_m for Ring-Stringer Stiffened Cylinder under Combined Loading

	DNV	API	RCC	Proposed Model
Mean	1.84	1.33	1.34	1.18
COV	43.82%	22.19%	21.02%	19.87%
Population	25			

Figure 7-25 to Figure 7-28 shows the comparison of predicted and experimental data for the different approaches. The Proposed model is showing low bias and COV compared to DNV, API and RCC models.
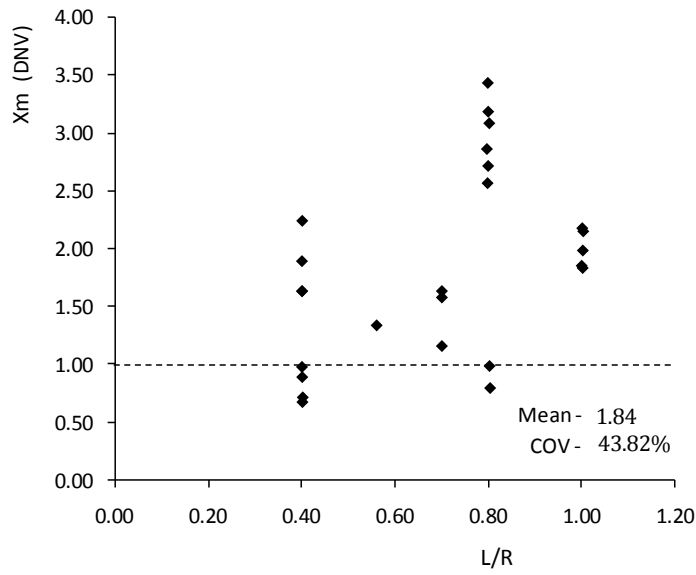
Figure 7-25 DNV prediction for Ring-Stringer Stiffened Cylinders under Combined Loading
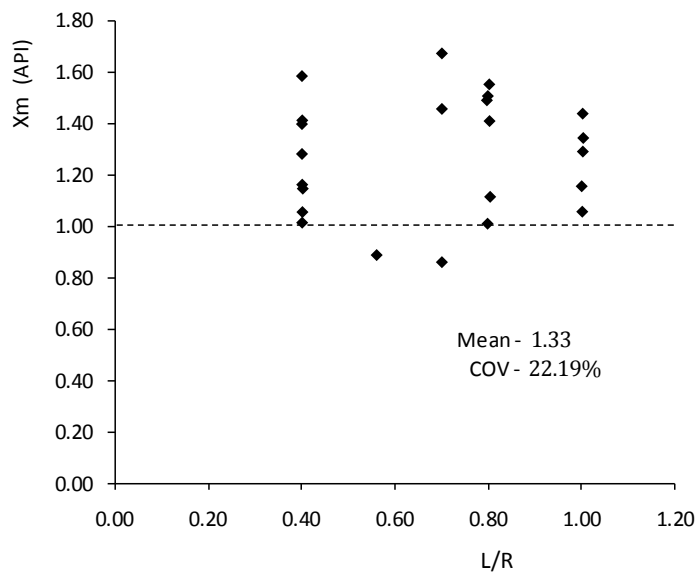
Figure 7-26 API prediction for Ring-Stringer Stiffened Cylinders under Combined Loading
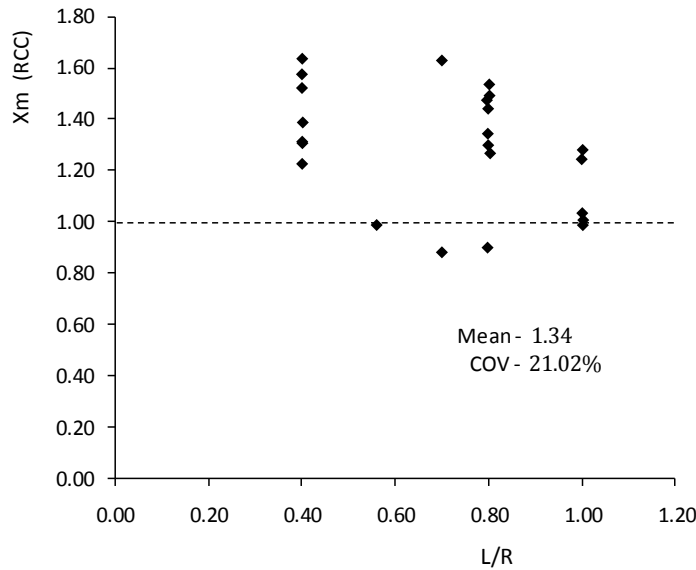
Figure 7-27 RCC prediction for Ring-Stringer Stiffened Cylinders under Combined Loading
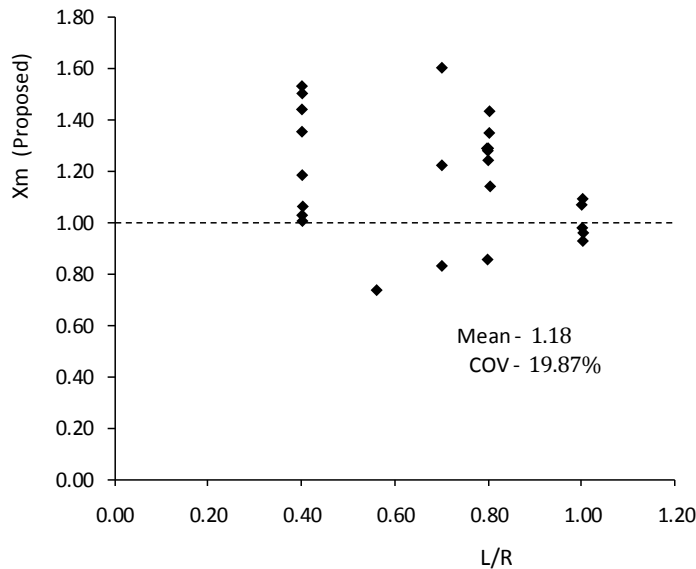
Figure 7-28 Proposed prediction for Ring-Stringer Stiffened Cylinders under Combined Loading

7.8 Summary

The proposed strength model is a modification of the existing RCC code with a new definition of bias for knockdown factor. The results of the analysis indicate the fact that the empirical constants selected must be dependent on the type of loading. In codes, for simplicity, some of the empirical constants are assumed as fixed for all the loading situations and structural configurations. This mainly happens when the range of experiments considered for the evaluation of such

constants does not show much variation in the values. This may induce error in prediction and can vary the results too far in certain random combinations of variables. The reduction of the uncertainty can be accomplished through the comparison and redefinition of empirical constants. With a large number of experimental data, we can do critical analysis and modify the values of such constants and some empirical relations to achieve better results. In this study, the number of combined loading cases is pretty low. More rational definitions of empirical parameters can be achieved with more number of test data and hence can bring the uncertainty very low to provide robust strength models.

The analyses with the experimental results illustrate the fact that the Proposed model which is a modified RCC Model, predicts the structural capacity more accurately in most cases compared to API and DNV codes. The statistical parameters of the analysis show that the Proposed model is more stable in predicting the strength of the stiffened cylinders compared to the DNV and API codes. The experimental data available for the radial pressure load cases for ring-stringer stiffened cylinders are very less and it is required to do further investigation to acquire more data. The design equations and the model uncertainty factors presented in this study are suitable for reliability analysis, sensitivity analysis and evaluating the partial safety factors for similar structures.

The study can be extended with the validated Finite Element Model for the imperfection sensitivity like distortion and weld induced residual stresses. The work is beyond the scope of this thesis and it can be investigated further. The validation of the model is done latter in Chapter 8 for the reliability analysis of stiffened cylinders using Response Surface Method.

Chapter 8. Reliability Analysis

8.1 Introduction

Structural design has traditionally been based on deterministic analysis. Past decades have seen design codes increasingly addressed the use of a limit-state design as a suggested alternative to traditional working stress design. The traditional deterministic method of ship structural design assumes that all the factors affecting the strength and the load applied to the structure are known and that the strength and load-effects are then a known function of these parameters. High implied margins of safety are introduced by ensuring that estimates of such parameters are conservative. The methods of structural analysis give lower bound solutions to collapse loads and the applied loads are multiplied by suitably large load factors. For these reasons and because empirical design rules are formulated to give safe estimates of strength, completed structures are on average appreciably stronger than their nominal as-designed ultimate capacity. In reality these relationships are only approximations and the Material properties, section dimensions etc. exhibit appreciable variability in a statistical sense and the loads assumed in the design often contain a high degree of uncertainty.

Uncertainty is inherent in most observable phenomena in the world; that is they cannot be predicted with certainty. In general multiple outcomes can be obtained from the repeated measurement of the same physical phenomena. Among these, some outcomes are most probable than the other and these outcomes does not follow any patterns. The occurrence of multiple outcomes without any patterns is described as uncertainty, randomness or stochastic. In general, all the parameters of interest in engineering analysis and design have some degree of uncertainty and thus need to be considered as random variables.

What is reliability? As far as the structural integrity is being concerned, most of the parameters related to load and resistance are random quantities. The

primary task of planning and structural design is to ensure satisfactory performance, i.e., to ensure that the capacity or resistance is greater than demand or load during the system's useful life. In view of the uncertainties in the problem, satisfactory performance cannot be absolutely assured. Instead, assurance can only be made in terms of the probability of success in satisfying some performance criterion. In engineering terminology, this probabilistic assurance of performance is referred to as reliability. Reliability is the compliment of the failure probability and is a rational measure of safety.

Need for reliability: The traditional approach of considering the uncertain parameters to be deterministic and accounted for the uncertainties through the use of empirical safety factors derived based on the past experience do not absolutely guarantee the adequate level of safety or satisfactory performance. These safety factors do not provide any information on the influence the different parameters of the system have on safety. The engineering design is basically a trade-off between maximising safety levels and minimising cost. The above mentioned deterministic safety factors do not provide adequate information to achieve optimal use of the available resources to maximise safety. On the other hand, probabilistic analysis brings rationality to the consideration of uncertainty in design by incorporating the experience and expertise in determining the uncertainties and hence provides the required information for optimum design. This capability of reliability analysis is accepted and appended in various codes like American Institute of Steel Construction (AISC) Load and Resistance Factor Design (LRDF) (1986, 1994) specifications, European and Canadian structural design specifications etc.

Measures of reliability: Reliability is the probability of successful performance associated with a particular performance criterion. The commonly used term for the measure of reliability is the 'probability of failure' and is the converse of reliability. An engineering system will have several components and performance criteria. The reliability or probability of failure should be considered for the individual components against all the performance criteria.

Apart from that, overall system reliability also comes into picture based on the series or parallel arrangement of these components.

A measure of reliability in the context of design specification is the safety factor, whose value provides a qualitative measure of safety. The nominally observed value of load (service load) is multiplied with the safety factor known as the load factor which is greater than 1 to obtain the design load. The nominal value of the resistance of the system is multiplied by safety factor known as the resistance factor which is less than 1 to obtain the allowable resistance.

For practical structures and performance criteria, the computation of probability of failure is difficult due to various reasons. A first-order estimate of the minimum distance from the mean point to the failure surface is used in the probabilistic design specifications as the reliability index or safety index denoted by β.

8.2 Structural Reliability Analysis

For a structure, the satisfactory performance under operation is characterised with a number of performance functions or limit states. The reliability analyses have to be carried out for all limit states in order to ensure satisfactory performance of the structural system. For marine structures, the major limit states in accordance with the different requirements are,

1. Ultimate Limit State (Strength, Moment)
2. Serviceability Limit State (Deflection, Vibration)
3. Fatigue Limit State (Stress levels, number of stress cycles)
4. Accident Limit State

8.2.1 Procedure of Structural Reliability Analysis

In general, the objective in structural design is to ensure that the strength of structure or the system is higher than the loads to which the system can be exposed. The problem is to account for the uncertainty associated with

quantification of the load or the strength of the structure. The uncertainty stems from physical uncertainties (natural loads and materials), statistical uncertainty (sparse data) and model uncertainty. The overall objective of structural reliability methods is to quantify these uncertainties to provide a better basis for decision-making regarding the dimensions of the structure or with respect to maintenance issues.

In general, for calculating structural reliability, the following procedure is suggested.

1. Establish target reliability, i.e. decision model
2. Identify all possible and significant failure modes of the structure or operation under consideration.
3. Formulate failure criteria and establish a relevant failure limit state function for each of mode of failure.
4. Choose and identify stochastic variables and parameters for each failure mode of the structure or operation under consideration.
5. Calculate the reliability or failure probability of the structure of each failure mode of the structure or operation under consideration.
6. Assess the structure reliability against the given target reliability.
7. Document to the structure design.

8.2.2 Methods of Reliability Analysis

The evaluation of the probability of failure which is the estimate of convolution integral can be performed in the following ways:

1. Direct integration (possible only in some special cases)
2. Simulation methods, such as using Monte Carlo simulation, and
3. Analytical approximation of the integral that are simpler to compute, these can be grouped into two types: first-order reliability methods (FORM) and second-order reliability methods (SORM).

8.2.3 Criteria for Selection of Methodology

A reliability method that gives acceptable estimates of the reliability for the structure or structural components shall be used. The choice of the reliability methods must be justified. When the limit state is a linear function, the FORM or SORM can be used to verify the results of the simulation and direct integral methods. Analytical FORM and SORM reliability estimate can generally be verified by simulation. When the number of basic random variables is under 5, the integral methods can be used to verify the results of analytical methods and simulation methods. In general, simulation methods can be used to verify the results of other methods. A local reliability estimate by FORM at a single design point can be verified by a SORM estimate. The best methods to calculate marine structure reliability can be summarised as follows:

1. For linear failure limit function or the failure probability less than 0.05, the analytical FORM and SORM reliability estimates are suggested.
2. Under 5 variables, the direct integration method is suggested.
3. The others except the above are calculated best by means of simulation methods (e.g. Monte Carlo Method)
4. For implicit limit state function, FORM, SORM or response surface method could be selected.

This thesis uses analytical approximation method for reliability analysis. The limit state of interest can be linear or nonlinear functions of the basic variables. FORM can be used to estimate of probability of failure (convolution integral) when the limit state function is a linear function of uncorrelated normal variables or when the nonlinear limit state function is represented by a first-order (linear) approximation with equivalent normal variables. SORM estimates the probability of failure by approximating the nonlinear limit state function, including a linear limit state function with correlated non-normal variables, by a second order representation.

8.2.4 Target Reliability

Target reliability is a standard that has to be met in design or in service in order to ensure that certain safety levels are achieved. A Reliability analysis can be used to verify that such target reliability is achieved for a structure or structural element. One of the difficulties in this context is that the uncertainties included in a structural reliability analysis will deviate from those encountered in real life. This is because:

1. The reliability analysis does not include gross errors which may occur in real life.
2. The reliability analysis, due to lack of knowledge, includes statistical uncertainty and model uncertainty in addition to physical uncertainty (often referred to as epistemic) which is present in real life.
3. The reliability analysis may include uncertainty in the probabilistic model due to distribution tail assumptions.

When carrying out structural reliability analysis, an appropriate safety level should be selected based on factors like consequence of failure, relevant design codes, accessibility to inspection and repair, etc. Target probability levels have to be met in design in order to ensure that certain safety levels are achieved.

A design is safe if, $\beta > \beta_0$

where,β is the safety index as estimated from analysis and β_0 is the target safety index

The selection of target reliabilities is difficult task since these values are not readily available and need to be generated or selected. Minimum value of Target reliabilities depend on the consequence and nature of failure, and to the extent possible should be validated against well-established cases that are known to have adequate safety. The regulatory bodies or classification societies and/or professions agree upon a reasonable value. This may be used for novel

structures where there is no prior history. Recommended target safety indices for hull girder (primary), stiffened panel (secondary) and un-stiffened plate (tertiary) modes of failure and the corresponding notional probabilities of failure are summarized in Ship Structure Committee Reports No-368 and 373 (Mansour *et al.,*1993 and 1994). These lifetime values are based on professional judgement in view of the extensive reliability analysis performed in these projects (SSC-368 & SSC-373) together with the values reviewed in the literature. Based on these reports the acceptable reliability indices and probability of failure values are presented in Table 8-1.

Table 8-1 Values of acceptable target reliability index (β) and probabilioty of failure (Pf) based on SSC-368 (1993) and SSC-373 (1994) (Mansour et al., 1993 and 1994).

Failure Mode	Commercial Ships	Naval Ships
Primary (initial yield)	$5.0\ (2.9 \cdot 10^{-7})$	$6.0\ (1 \cdot 10^{-9})$
Primary (ultimate)	$3.5\ (2.3 \cdot 10^{-4})$	$4.0\ (3.2 \cdot 10^{-5})$
Secondary	$2.5\ (6.2 \cdot 10^{-3})$	$3.0\ (1.4 \cdot 10^{-3})$
Tertiary	$2.0\ (2.3 \cdot 10^{-2})$	$2.5\ (6.2 \cdot 10^{-3})$

8.2.5 CALREL Program

The CALREL program is a commercial general purpose Reliability analysis code. The program has extensive facilities to customise the input parameters and the performance functions. The code uses, FORM, SORM and simulation methods to compute reliability index and the probability of failure. The code provides sensitivity factors and partial factors. The code can be used for the reliability analysis of any process or phenomenon subjected to the availability of an explicit performance function in terms of the basic influencing variables.

8.3 Response Surface Method (RSM)

The most important requirement for the reliability analysis procedure discussed so far is the performance function and its gradient in terms of the material and geometrical parameters of the structure. There are many situations where the suitability of mathematical models is questioned. The

major aspects in this perspective are the accuracy and applicability of the mathematical performance model and the very existence of a reliable closed form mathematical model.

Generally, the mathematical models are developed based on some assumptions and simplifications. In the case of buckling strength of plated structures, there are many assumptions incorporated in the formulation right from the effective width approach to the strain hardening and the empirical approach for the residual stresses etc. In Chapter 5, the comparison of results for the formula based approaches and numerical approach shows wide scatter for a parametric study based on distortion. Moreover, the formulation is based on a column collapse approach and the failure modes considered are the plate induced and stiffener tripping type. In reality, the overall grillage buckling can also interact with the local buckling modes at specific levels of distortion and structural configuration. This is generally ignored and the predictions can be far from reality in certain cases if the judgement is based on the local mode of buckling alone. Also, the formulation cannot really incorporate effects due to the material and geometrical nonlinearities. For example, there is no satisfactory analytical model available for the strength of plated structures which can effectively incorporate both the distortion and residual stresses under combined non-uniform (ramped) axial compression and lateral pressure with one end clamped, other end pin joined with sides are simply supported. The above conditions can be generated with the existing strength models only after imposing a lot of approximations and major adjustments. In the present situation, the availability of mathematical models is restricted to a limited number of structural problems and there are a lot of situations where the performance modelling is really difficult or may be impossible due to geometric, performance and material complexities and if the number of variables are too large. In many practical cases, the performance function many not be in a differential form with respect to the random variables of interest. So the solution of structural reliability using FORM or SORM is not possible if the failure domain or performance function is

not able to represent with an accurate mathematical model or if such a model does not exist. In such situations, simulation based method is the best alternative with suitable numerical methods like finite element analysis. This method is going to be computationally expensive as there are numerous simulations are to be carried out with different input values to get the probability of failure.

The above situation can be effectively tackled by using the Response Surface Method(RSM) first proposed by Box and Wilson (1951). The method was developed over the years for various industrial and engineering areas. Rackwitz (1982) proposed a method to utilize RSM for the structural reliability analysis. In this method, an approximate linear or nonlinear performance function is generated in terms of the design variables using deterministic numerical method (say, the finite element method) as a platform for the experiments. The finite element experiments are conducted at sufficient number of design points to approximate the response function. This function can be used for the FORM or SORM reliability calculations. It can also be used to facilitate sensitivity analysis without changing the code of commercial structural software.

8.3.1 GLAREL Program

GLAREL is an in-house developed program for the structural reliability analysis using response surface method. (Yu, *et al.*, 2002).

Figure 8-1 shows the method of reliability analysis using coupled response surface method and FE analysis. The initial experimental points are based on the mean values of the basic variables or influencing parameters. A linear response surface with the sampling points centred at $\mu_i \pm f_i\sigma_i$. The centre point μ_i is fitted by stepwise regression as the initial approximation. The factor f_i is used to define the sampling range, usually $f = 3$ is used in the first approximation to include the maximum range of variability for the basic variables in the failure region. As the calculated design point reaches nearer to

the actual design point, f can be gradually reduced to $f \approx 1$ according to

$$f^{(i)} = \sqrt{f^{(i-1)}} \; .$$
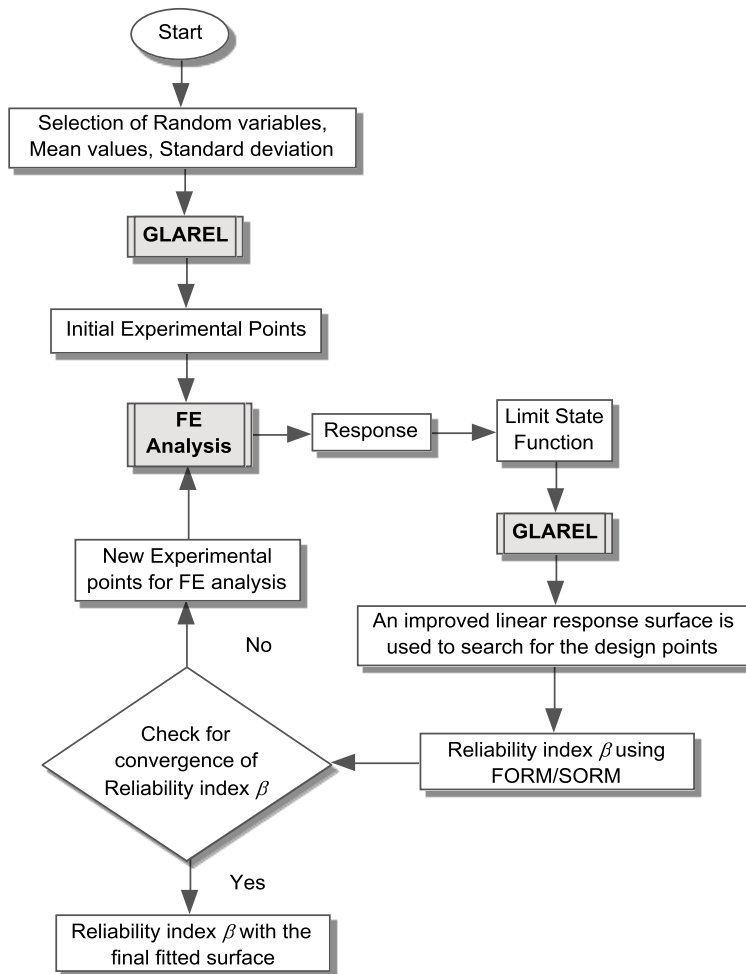
Figure 8-1 Flow chart Reliability analysis procedure with of coupled RSM and FE Analysis using GLAREL Computer code

FORM is used to calculate the reliability index $\beta^{(1)}$ and the corresponding $X^{*(1)}$ with the initial response function. The new experiment points are defined around the design point $X^{*(1)}$ as $X_i^* \pm f_i \sigma_i$. The new design point $X^{*(k)}$ and corresponding $\beta^{(k)}$ (k=1,2,3,..) are calculated. The exercise continues till $\left| X^{*(k)} - X^{*(k-1)} \right|$ or $\left| \beta^{(k)} - \beta^{(k-1)} \right|$ is less than the specified tolerances. When the criterion is met, the probability of failure is calculated as $p_f = \Phi\left(-\beta^{(k)}\right)$ and

terminates the program. The second order response surface function in terms of the basic variables is also given by the program.

8.4   Reliability Analysis of Stiffened Plates

The reliability analysis of stiffened plates can be carried out in many ways based on the design considerations and the particular response. There are numerous geometrical, material and loading parameters which affects the performance of stiffened plated structures. This study analyse the reliability of a typical stiffened plated structure scantling for the effects of imperfection parameters on the structural reliability and the sensitivity of each imperfection parameters under different load factors. The reliability analysis is carried out with the analytical FORM/SORM method using the commercial computer code CALREL with the strength formulation proposed by Falkner and the modified method by Pu and Das. Reliability evaluation is carried out with the Response Surface Method (RSM) using the GLAREL computer code with a Finite element model to fit the response surface for the structural performance.

8.4.1 Limit State Function (LSF)

The strength limit state function considered for the stiffened plated structure is,

$$g(X) = X_m R - S \tag{8-1}$$

where X_m is the model uncertainty factor, R is the strength response and S is the load acting on the structure.

The reliability of the structure is calculated at different proportion of the ultimate capacity of the structure evaluated at the mean point of the design variables. The reliability analysis of the stiffened plate is carried out with a structural scantling which is used for the imperfection sensitivity analysis explained in Chapter 6. The scantling of the typical stiffened plate is a:b:t:OBP:σ_y=2400:800:20:200:355. The parametric definition of distortion and residual stress are associated with the thickness and yield stress of the stiffened

plate respectively. The reliability analysis is carried out with these parameters as random variables. The properties of each variable are illustrated in Table 8-2. The standard deviation of the imperfection parameters is taken as 30% in order to cover the range from negligible amount to a severe level of imperfection. The load is applied as a fraction of the ultimate capacity of the structure. Two types of distribution are used for the load to test the influence of the distribution.

Table 8-2 Properties of random variables-Stiffened Plates

No.	Random Vaiable	Symbol	Distribution	Mean	COV
1	Yield stress, (N/mm^2)	σ_y (X_1)	Lognormal	355.00	10%
2	Thickness of the plate (mm)	t_p (X_2)	Normal	20.00	5%
3	Distortion (mm)	δ (X_3)	Lognormal	8.37	30%
4	Residual stress (σ_r/σ_y)	RS (X_4)	Lognormal	0.125	30%
5	Model Uncertainty factor	X_m (X_5)	Normal	1.00	6%
6	Axial Load, (N/mm^2)	S (X_6)	Lognormal, Weibull	k	20%

k=26%, 39%,52% and 65%

The strength R is taken as a function of the design variables,

$$R = f\left(\sigma_y, t, \delta, RS, X_m, S\right) = f(X_1, X_2, X_3, X_4, X_5, X_6) \tag{8-2}$$

The analytical formulations provide the response as $R = \sigma_u/\sigma_y$. The load S is taken as a percentage of the R evaluated at the mean point of design variables,

$$S = kf(X_{1m}, X_{2m}, X_{3m}, X_{4m}, X_{5m}, X_{6m}) = k\left(\frac{\sigma_u}{\sigma_y}\right)_{\text{at the mean point}} \tag{8-3}$$

where $k = P/P_u$, is the fraction of the ultimate load applied on the structure. Therefore, the limit state function is represented as,

$$g(X) = X_m R - S = X_m f(X_1, X_2, X_3, X_4, X_5, X_6) - k\left(\frac{\sigma_u}{\sigma_y}\right)_{\text{at the mean point}} \tag{8-4}$$

8.4.2 Reliability Analysis Results

The reliability analysis is carried out using Analytical Method and the RSM. Typical input files for the CLREL program is given in Appendix D. Table 8-3 illustrate the analysis results for the two approaches with three analytical

formulations. The type of distribution is very sensitive to the reliability index as expected. For a stiffened plate used in ship structures, the Weibull distribution should be assumed.

Table 8-3 Reliability index for Stiffened plate (OBP200-PLT20-α3-Y355) for RSM and Analytical approaches

		β							
Method		RSM+FEM(Proposed) (GLAREL)		Faulkner (CALREL)		Das&Pu (CALREL)		Proposed empirical (CALREL)	
P/P_u ↓	Distribution→	LN	WB	LN	WB	LN	WB	LN	WB
26%		5.77	3.96	6.18	3.97	5.92	3.89	5.83	3.86
39%		4.14	3.19	4.34	3.20	4.12	3.11	4.03	3.08
52%		2.93	2.54	3.04	2.54	2.83	2.44	2.75	2.39
65%		1.97	1.92	2.02	1.92	1.83	1.79	1.75	1.74

RSM-Response surface method, LN-Lognormal, WB-Weibull

Figure 8-2 shows the variation of reliability with respect to the applied load for different methods for two types of Load distributions. Figure 8-2(a) shows the results from the RSM using GLAREL and Finite Element Model. The result shows that as the load increases the reliability reduces and it appears to coincide at about 65% of the ultimate strength and the reliability in the order of 2.
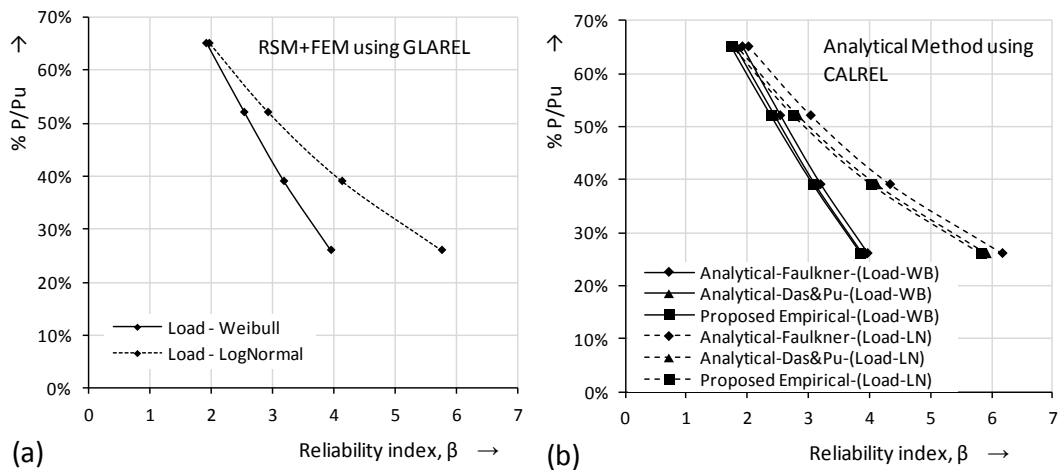
Figure 8-2 Variation of Reliability index with increasing Load for Stiffened Plate (OBP200-PLT20-α3-Y355), (a)Using RSM (b)Using Analytical formulations

The change in distribution type produces a substantial effect on the reliability estimate of the structure when the load is small and the structure is at higher range of safety. It reveal the fact that appropriate selection of the distribution type is such an important aspect of reliability analysis and an erroneous

selection lead to awful results far away from the reality. From the results, it is observed that the above mentioned issue is so significant when designing structures which require higher reliability index.

Figure 8-2(b) shows the results for the analytical approach. The Faulkner, Das&Pu and the proposed empirical methods are plotted. The Faulkner method is sensitive to the weld induced residual stress but not to the initial distortion of the structure. Das&Pu method takes both the effects into account and show reduced reliability index as an indication of the effect of distortion. The proposed empirical method predicts the results close to the Das&Pu method.
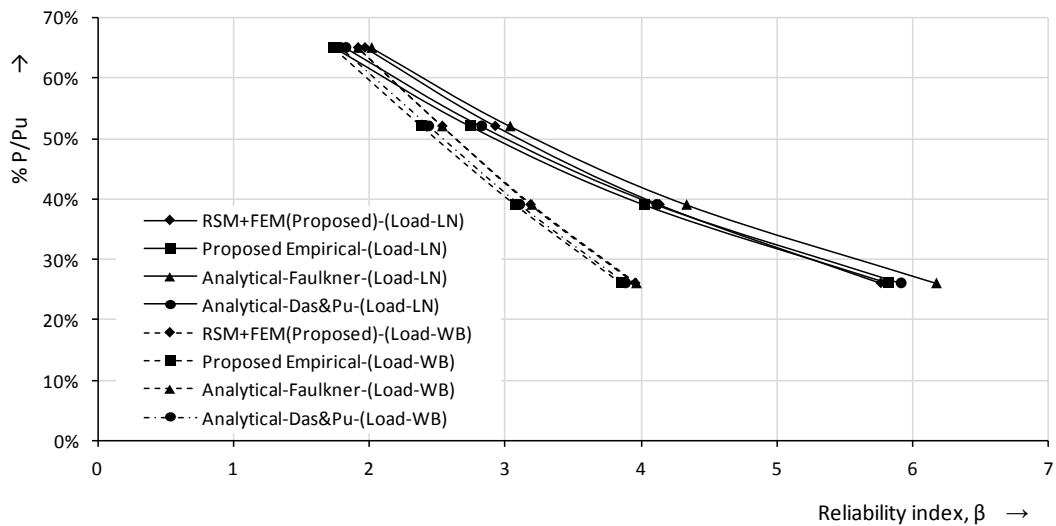
Figure 8-3 Comparison of RSM and Analytical Methods for a Stiffened Plate

Figure 8-3 shows the comparison of the reliability analysis by both the RSM and Analytical methods. The results show a reasonable degree of closeness which in a way validates the accuracy of RSM and the FE Models used for the reliability analysis of stiffened plates. So the reliability analysis with complicated loads and influencing parameters for non-standard or some specific response can be performed with RSM when robust analytical solution is unavailable for the particular structural performance.

Table 8-4 Sensitivity factors and partial safety factors of the reliability analysis of stiffened panel with Weibull distribution for the Load

P/Pu			26%	39%	52%	65%
	β		3.89	3.11	2.44	1.79
	pf		4.93E-05	9.33E-04	7.44E-03	3.64E-02
Analytical-Das&Pu Method-(CALREL)	Design Points (x*)	σ_y (X^*_1)	335.50	336.00	336.80	338.40
		t_p (X^*_2)	19.90	19.90	19.91	19.91
		δ (X^*_3)	8.31	8.30	8.28	8.26
		RS (X^*_4)	0.12	0.12	0.12	0.12
		X_m (X^*_5)	0.97	0.98	0.98	0.98
		S (X^*_6)	243.80	244.30	245.10	246.60
	sensitivity vector (δ_i)		0.14	0.17	0.21	0.25
			0.03	0.03	0.04	0.05
			-0.03	-0.04	-0.05	-0.06
			-0.01	-0.02	-0.02	-0.03
			0.11	0.13	0.16	0.20
			0.02	-0.13	-0.28	-0.47
	Partial Safety Factors $(\gamma_{xi}$ or $\Upsilon_{xi})$	Υ_{xi}	1.06	1.06	1.05	1.05
		Υ_{xi}	1.01	1.01	1.00	1.00
		γ_{xi}	0.99	0.99	0.99	0.99
		γ_{xi}	0.97	0.97	0.97	0.97
		γ_{xi}	0.97	0.98	0.98	0.98
		γ_{xi}	3.43	2.29	1.73	1.39
RSM - (GLAREL)	β		3.96	3.19	2.54	1.92
	pf		3.73E-05	7.05E-04	5.62E-03	2.75E-02
	Design Points (x*)	σ_y (X^*_1)	333.06	333.51	334.40	336.12
		t_p (X^*_2)	19.88	19.88	19.89	19.89
		δ (X^*_3)	8.48	8.47	8.44	8.39
		RS (X^*_4)	0.12	0.12	0.12	0.12
		X_m (X^*_5)	0.97	0.98	0.98	0.98
		S (X^*_6)	251.58	251.98	252.94	254.82
	Partial Safety Factors $(\gamma_{xi}$ or $\Upsilon_{xi})$	Υ_{xi}	1.07	1.06	1.06	1.06
		Υ_{xi}	1.01	1.01	1.01	1.01
		γ_{xi}	1.01	1.01	1.01	1.00
		γ_{xi}	0.98	0.98	0.98	0.98
		γ_{xi}	0.97	0.98	0.98	0.98
		γ_{xi}	3.54	2.37	1.78	1.44

Table 8-4 illustrate the design points, sensitivity factors and Partial safety factors of the analysis for the RSM and Das&Pu analytical method with Weibull distribution for the Load as given in Table 8-3.
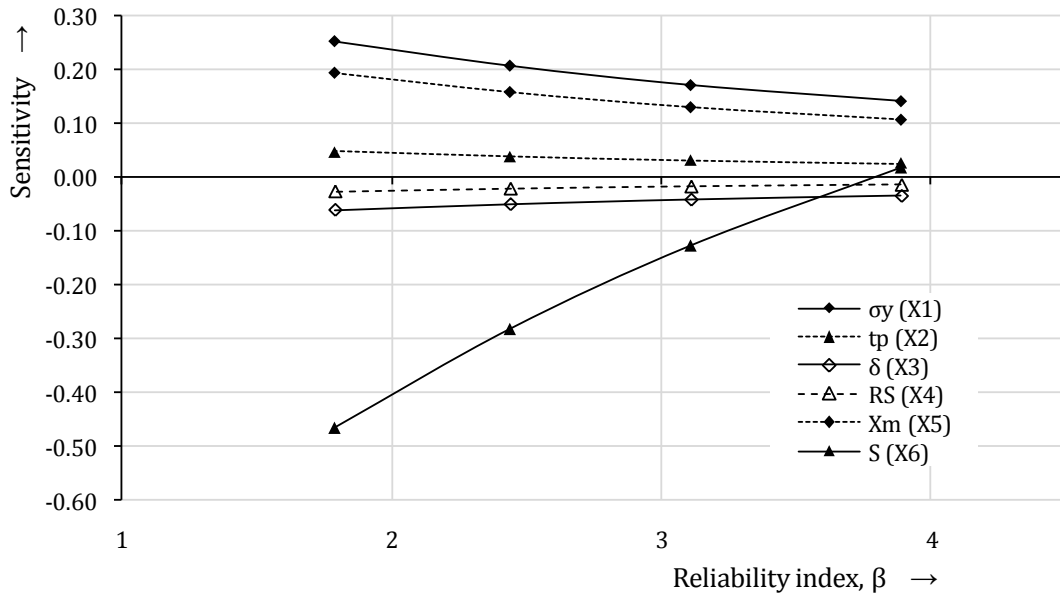
Figure 8-4 Sensitivity of the random variables at different levels of structural reliability from the analytical method (Das & Pu Method)

The sensitivity of the random variables for different levels of reliability is represented in Figure 8-4. As the load increases, the model uncertainty factor and yield stress of the material starts to become more sensitive. The distortion and residual stress remain nearly same at all levels of load and the sensitivity is equal to the thickness of the plate or even more. The distortion appears to be more sensitive to the reliability than the residual stress.

(a) Analytical Method (CALREL) Reliability index, β →   (b) RSM (GLAREL)   Reliability index, β →
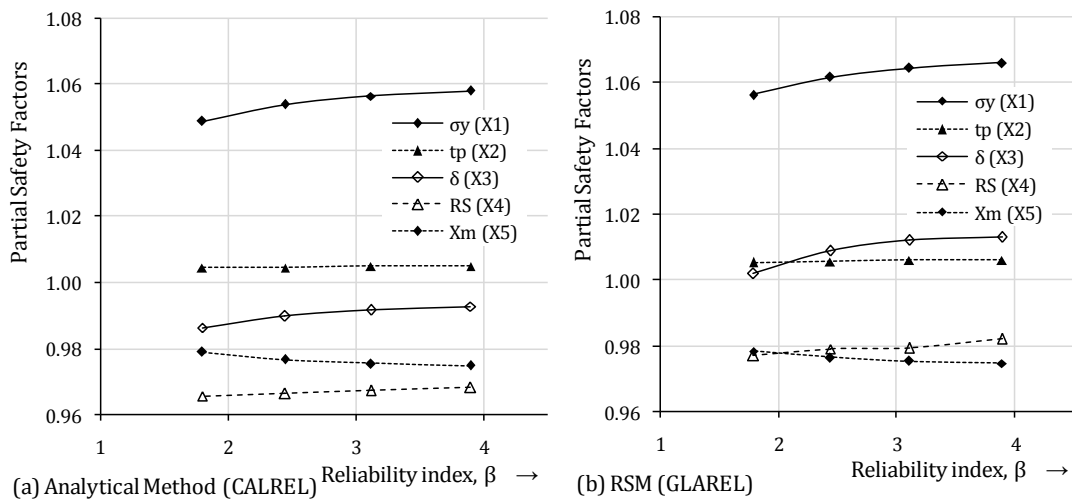
Figure 8-5 Partial safety factors of the random variables for Analytical and RSM approaches

Figure 8-5 shows the comparison of Partial safety factors (PSF) obtained from both the RSM and analytical approaches. The results shows good correlation and it proves the RSM useful for the assessment of the PSFs of the design variables which are not explicitly included in the analytical formulations. It is interesting to note that the trend of PSFs for the distortion and residual stresses are different for RSM and Analytical approaches. It is because of the reason that these factors are treated differently in both the approaches.

8.5 Reliability Analysis of Stiffened Cylinders

The reliability analysis of the stiffened cylinders is carried out with the proposed analytical model and RSM using a validated Finite element Model. A typical Ring stiffened cylinder and a Stringer stiffened cylinder is taken for the analysis trials with varying proportion of the ultimate load of the respective cylindrical structures. The details of the models are given in Table 8-5. The experimental and FEA collapse loads are perfectly matching for both the models. Both the models are subjected to two load cases, axial and combined axial and radial loading. For the combined loading case, the radial pressure is treated as a random variable with a mean and COV and the analysis is carried out to solve for the ultimate axial load under the action of the radial load.

Table 8-5 Structural details of the stiffened cylinders

Type	Shell Properties			Stiffener Properties						Material properties			Exp. Collapse Load (kN)	FE Collapse Load (kN)
				Dim. of ring		Dim. of Stringers								
	Length (L)	Radius (R)	Thk (t)	Bays	Web height (hwr)	Web thk. (twr)	No. of Stringer (Ns)	Web height (hws)	Web thk. (tws)	E (GPA)	σ_y (MPA)	ν		
Ring Stiffened Cylinder	120.70	122.3	0.81	5	13.00	0.81	0	0.00	0.00	200.0	286.0	0.30	134.00	134.31
Stringer Stiffened Cylinder	571.50	568.5	1.96	1	0.00	0.00	18	30.48	1.96	210.5	419.0	0.30	1945.1	1962.74

hfr,tfr & hfs,tfs - flange heights and thicknesses of ring and stringer stiffeners respectively and are zero for the above cases

8.5.1 Limit State Function

The strength limit state function considered for both the ring stiffened and stringer stiffened cylinders is same as that for the stiffened plate and is given as,

$$g(X) = X_m R - S = X_m f(X_1, X_2, X_3, X_4, X_5) - k \left(\frac{\sigma_u}{\sigma_y}\right)_{\text{at the mean point}} \tag{8-5}$$

The properties of each variable are illustrated in Table 8-6. The distributions for all the variables are assigned as Lognormal. Considering a marine structure with cylindrical legs, the axial load (the weight of the platform and facilities) is assumed to follow a lognormal distribution rather than extreme distributions. The analysis could also be extended with different distributions according to the prevailing sea conditions and other environmental conditions.

8.5.2 Reliability Analysis Results of Ring Stiffened Cylinders

The reliability analysis for the ring stiffened cylinder is carried out using the RSM with a validated FE Model and using the proposed analytical formulation given in Chapter 7 with the CALREL computer code. The sample input files for the CALREL code are given in Appendix D. The details of the model used for the analysis is given in Table 8-5.

Table 8-6 Properties of random variables - Ring stiffened cylinders

No.	Random Vaiable	Symbol	Distribution	Mean	COV
1	Yield stress, (N/mm^2)	σ_y (X_1)	Lognormal	286.00	10%
2	Thickness of the shell (mm)	t_p (X_2)	Lognormal	0.81	5%
3	Radial Pressure (N/mm^2)	P_r (X_3)	Lognormal	0.03	10%
4	Model Uncertainty factor	X_m (X_4)	Lognormal	1.00	10%
5	Axial Load, (N/mm^2)	S (X_5)	Lognormal	k	10%

k=40%, 53%,66% and 80%

For the ring stiffened cylinders, the load is varied from 40% to 80% of the axial ultimate capacity of the structure without radial loading at the mean points of the random variables. Table 8-7 shows the reliability indices for the axial and combined loading cases with varying proportion of loads.

Table 8-7 Reliability index for Ring stiffened cylinders under Axial and Combined loading

P/Pu	β			
	RSM(GLAREL)		Proposed Analytical(CALREL)	
	RSA	RSC	RSA	RSC
40%	5.68	4.26	6.05	4.83
53%	3.92	2.76	4.25	3.05
66%	2.54	1.52	2.85	1.66
80%	1.39	0.44	1.68	0.52

RSA-Ring stiffened cylinder with Axial Loading
RSC-Ring stiffened cylinder with Combined Loading

Figure 8-6 show that the axial and combined loading cases introduce a fairly constant offset in between the two curves. Both the methods illustrate the same trend of reliability variation.

(a)

(b)
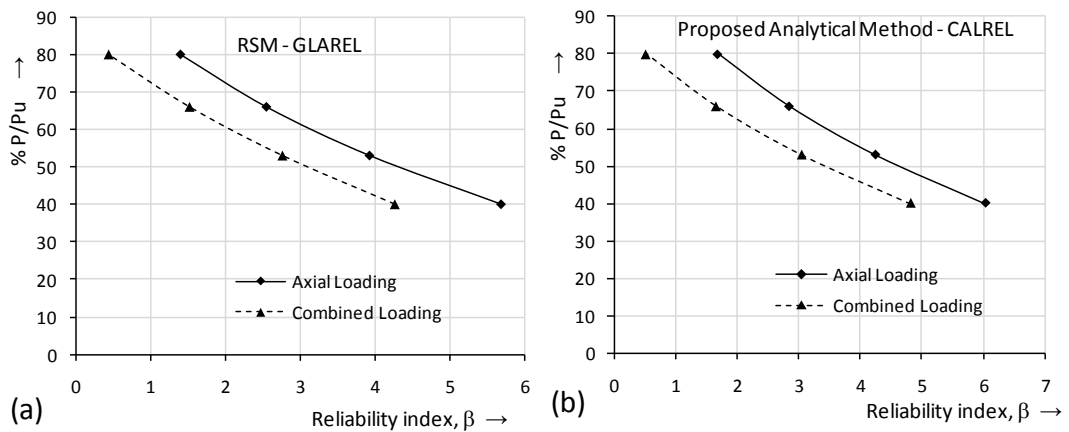
Figure 8-6 Variation of Reliability index with increasing Load for axial and combined loading cases of Ring stiffened cylinders (a)Using RSM (b)Using the Proposed analytical formulation

Figure 8-7 compares the results from both the methods and are in good correlation with each other. The RSM approach provides lower estimates of reliability compared to the analytical approach. The axial loading case shows better correlation compared to combined loading situation.

The variation in the results can be assumed to be because of the inherent stiffness of the mathematical model. But the reliability plots show same trend of variation and it is reasonable to rely on both the approaches according to the requirement and selection of variables.
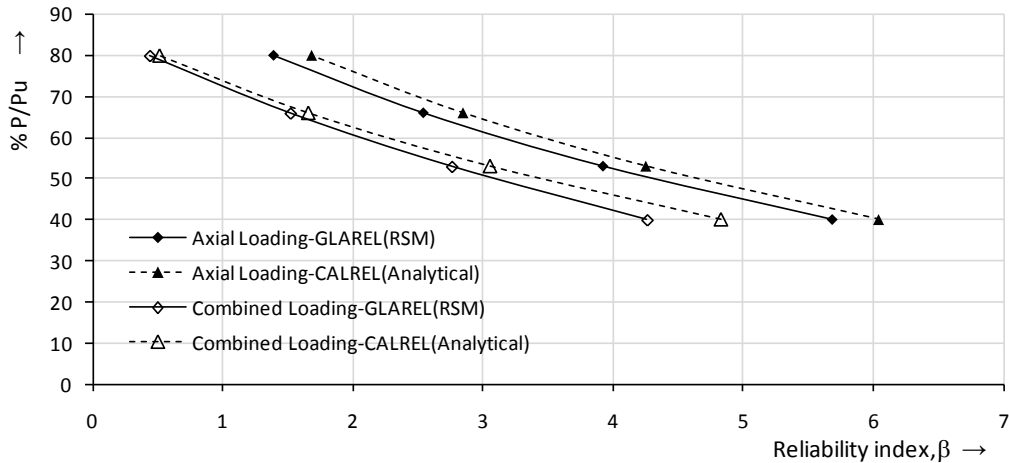
Figure 8-7 Comparison of RSM and Proposed Analytical Method for Stringer stiffened cylinders

8.5.3 Reliability Analysis Results of Stringer Stiffened Cylinders

The stringer stiffened cylinder is also subjected to axial and combined loading cases. The details of the model used for the analysis is given in Table 8-5. For the Stringer stiffened cylinders, the load is varied from 35% to 104% of the axial ultimate capacity of the structure without radial loading at the mean points of the random variables. Here the load is applied to a higher value in order to see the trend of reliability index near to zero.

Table 8-8 Properties of random variables-Stringer stiffened cylinder

No.	Random Vaiable	Symbol	Distribution	Mean	COV
1	Yield stress, (N/mm^2)	σ_y (X_1)	Lognormal	419.00	10%
2	Thickness of the shell (mm)	t_p (X_2)	Lognormal	1.96	5%
3	Radial Pressure (N/mm^2)	P_r (X_3)	Lognormal	0.072	10%
4	Model Uncertainty factor	X_m (X_4)	Lognormal	1.00	10%
5	Axial Load, (N/mm^2)	S (X_5)	Lognormal	k	10%

k=35%, 52%, 70%, 87% and 104%

Table 8-9 shows the reliability indices for the axial and combined loading cases at different proportions of the ultimate capacity of the structure. The values show that the trend and the estimates of reliability are in good correlation for the axial loading case. For the combined loading case, the analytical approach appears to be a little optimistic.

Table 8-9 Reliability index for Stringer stiffened cylinders

P/Pu	RSM-GLAREL		Proposed Analytical-CALREL	
	SSA	SSC	SSA	SSC
35%	6.13	4.32	6.69	5.78
52%	4.32	2.27	4.04	3.28
70%	2.44	0.71	2.15	1.48
87%	0.92	-0.64	0.69	0.07
104%	-0.25	-1.75	-0.51	-1.08

SSA-Srtinger stiffened cylinder with Axial Loading
SSC-Srtinger stiffened cylinder with Combined Loading

The variation in the results can be assumed to be because of the lack of consideration of all the failure modes in the analytical treatment and due to various assumptions and empirical constants used.
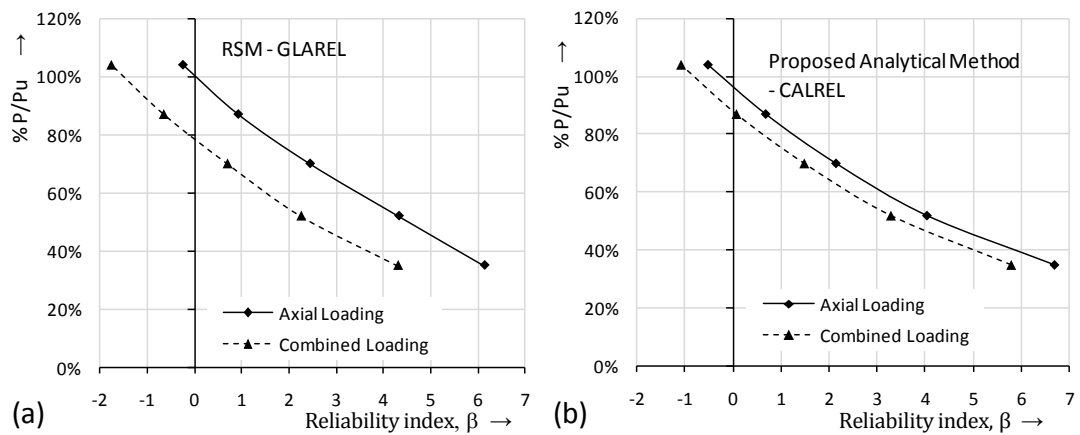
Figure 8-8 Variation of Reliability index with increasing Load for axial and combined loading cases of Stringer stiffened cylinders (a)Using RSM (b)Using the Proposed analytical formulation

Figure 8-8 shows the variation of the reliability index with varying load for both the axial and combined cases with RSM and the proposed analytical approaches. The comparison shown in Figure 8-9 illustrates the fact that the estimates are quite matching for the axial loading case.

The analysis explained in Chapter 7 indicate that the analytical strength models for the combined loading of both the Ring stiffened and stringer stiffened cylinders have higher model uncertainty factor and COV compared to axial loading cases. So the inherent variability in the strength prediction of analytical

model is reflecting in the reliability prediction also. In such cases, it is recommended to cross check the reliability estimate with a suitable empirical formula or procedures like RSM.
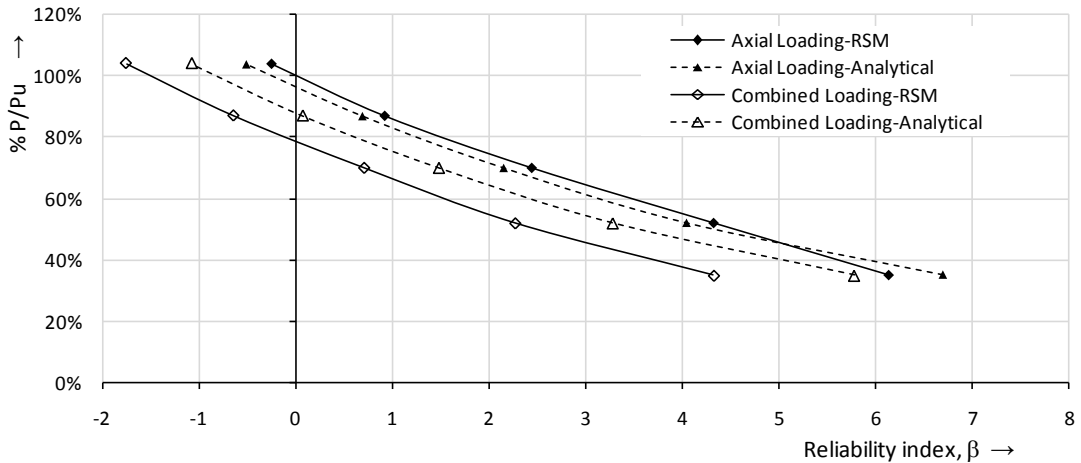
Figure 8-9 Comparison of RSM and Proposed Analytical Method for Stringer stiffened cylinders

8.6 Summary

The reliability analysis is a rational method for the assessment of structural integrity and safety compared to traditional factor of safety method. The reliability analysis considers the statistical nature of uncertainty in each design variable and provides guidance on the selection of the parameter values to achieve the desired level of safety. This method eventually provides the sensitivity of each parameter on the reliability of the structure which indirectly is the sensitivity on the response of the structure. The sensitivity measures help a designer to choose the correct variable to be adjusted for a better design with optimum service, strength and cost considerations. The decomposition of reliability index into suitable partial safety factors for design will ensure the structure with the target reliability appropriate for the structure with respect to the environmental and service conditions. This chapter provide an overview of the reliability procedure practiced in the offshore industry and briefly explaining the basic theories of reliability analysis. When a closed form performance function is not available or the design parameters of interest are not explicitly embedded in the mathematical model, the reliability assessment

becomes impossible. As an alternative, the Response surface method with a validated numerical analysis model is used to replace the strength model.

The reliability analysis of a typical stiffened plate is conducted for axial load under varying proportion of the ultimate capacity. The analysis is carried out using both the RSM and analytical approach. The results are compared and found to have close correlation. The sensitivity of the design and imperfection parameters are plotted for various load factors or reliability indices. The PSFs of the design variables also is proposed for a range of reliability indices. The reliability analysis results with the proposed empirical model show better closeness with the RSM approach with the validated FE Model. From the analysis, it is concluded that for the range of scantling slenderness discussed in the thesis, the proposed empirical strength model can be used for the reliability analysis with imperfection. The RSM must be used with the validated FE Model if the boundary conditions or the loading conditions vary.

Reliability analyses have done for Ring stiffened and Stringer stiffened cylinders with the proposed formulation explained in Chapter 7 and RSM method. The results are compared and found to have better correlation for the axial cases. There is a factor of variation in the combined loading case of the stringer stiffened cylinder when compared with the RSM. The variability in the reliability assessment is an indirect indication of the inconsistency of the strength model. The Analytical model is having comparatively higher model uncertainty factor and COV as explained in Chapter 7. This study revel the fact that the formulation is to be improved more so as to get more consistent reliability estimate of similar structures. The RSM approach with validated FE Model is particularly recommended for stiffened cylinders under combined loading.

Chapter 9. Discussions and Conclusions

9.1 Introduction

This thesis gives a framework for the strength and reliability analysis of plated structures and cylinders used for the offshore marine applications with improved strength models. The strength of these structures has been a topic of interest for centuries. With the evolution of the thin wall structures and steel material, the design of ship and other offshore structures has a significant role for the optimisation of strength, material, operating capacity etc. Many rule based design codes and classification societies came into existence claiming to be better alternatives and procedures. All the design codes and classification societies are revising own procedures every now and then as they get valuable information from the research or experiences. International Association of Classification Societies (IACS) provides reliable ground for the associated thirteen member classification societies and industry in implementing the Common Structural Rules (CSR) in a uniform and consistent manner to ensure the implementation of up to date technical developments.

In the present scenario of structural design, the numerical analysis tools have a significant role to predict the response and behaviour for a variety of technical problems which are specific to a particular situation and where rule based practices are unavailable. The efficiency and reliability of these methods are heavily improved over the years with comparatively straight forward interfaces to make the tools user friendly. Although the modern structural engineering capabilities with numerical techniques are believed to solve many structural engineering problems with extreme level of accuracy, it can never be labelled as perfect due to various approximations, modelling constraints and inherent randomness. There is still room to extend the predictive capacity of these analysis tools for perfect or nearly perfect results.

One of the major shortfalls in the rule based design codes and numerical methods of structural analysis is the incapability to account for the inherent randomness of the design parameters on the structural performance. According to the current design philosophy and increased technical knowledge, the reliability based design optimisation has been approved superior to the conventional load resistance factor design. The most important advantage of the reliability method is the ability to handle the inherent randomness of the design variables. The reliability assessment is significantly dependent on the performance of the strength model. Any improvement in the ability of predication of these strength models will fine tune the reliability estimate and which will intern optimise the structure for its safety, capacity and cost. The various aspects of this thesis can be summarised under the following categories,

1. Unstiffened and Stiffened Plates
2. Stiffened cylinders
3. Reliability analysis

9.2 Unstiffened and Stiffened Plates

The axial strength of the plated structures can be predicted with a reasonable degree of accuracy using many of the practicing codes or procedures. The fabrication induced imperfections and residual stresses are potential factors affecting the strength and overall behaviour of the structure. The design codes and other state of the art analytical formulations are handling these entities with suitable reduction factors. Since the effects of these imperfection parameters are entangled with other design parameters and considering randomness, a rational estimate of the effect of imperfection on the strength is practically quite difficult to achieve. Apart from that, the distortions and residual stresses are the two faces of the same problem or derived from the same cause. So when treating these two factors separately, it is always ignored the interaction between these two factors. The major analytical approaches for the strength analysis are based on the Euler column approach and Perry column

approach. The Faulkner method which is developed on the basis of Euler column approach incorporate the residual stress by using suitable effective width and reduced column slenderness to account for the imperfection effects. There are extensions of this method to incorporate the geometrical distortion. These approaches are not found to produce satisfactory results when compared with a validated numerical stiffened plate model. Similarly, the formulation based on Perry column approach incorporate the distortion in a straight forward manner but the trend of results varies when applied to stiffened plates. Apart from that, when applying these methods to stiffened plates, it is impossible to include all distortion forms and failure modes effectively. In reality, as the range of distortion parameters varies, the frame work of these formulations cannot confine such a complicated structural configuration to a typical column element. The author proposed a simple empirical formula for the prediction of the strength of stiffed panels incorporating the effects of plate and stiffener geometrical distortions, residual stresses and their interaction effects.

The hypothesis of the effect of imperfection are verified using a set of 10 experimental analysis conducted at the testing facility of CORUS (Presently, TATA Steel), Rotherham. The results confirmed the assumption of the strength reducing nature of imperfections. The increased distortion and residual stresses are found to reduce the structural strength. The stress relieving process found to enhance the strength also confirming the fact that, heat treatment relieve residual stresses effectively and enhances the structural capability. Considering the above facts, a set of rigorous nonlinear finite element analyses are carried out to develop a set of design curves for to account the effects of varying distortion, residual stresses and interaction of these factors on structural strength of unstiffened and stiffened plates. When comparing the test results with the FEA results, the model uncertainty factor appears almost unity with very low spread of 5.5%.

An accurate parametric FE model for the prediction of strength for the incorporation of geometrical distortion and residual stresses is also developed

and verified with the experimental test results. The comparison of the results for a typical structural scantling used for Type 45 destroyer war ship of BAE systems indicate that the empirical model shows better correlation with the FE predictions compared to the analytical models at extreme ranges of distortions. One of the interesting observations is that even though the analytical formulations could not accommodate all the modelling complexities within the mathematical frame, it can produce reasonable judgement. An ideal analytical formulation for stiffened plates is lying between Euler and Perry approaches. Conceptually, an ideal formulation in order to incorporate both the distortion and residual stresses can be realised if we can integrate Faulkner's reduced slenderness concept to Perry's formulation. But the construction of Perry's formula is such that the reduction in slenderness will increase the strength.

A wide range of plate and column slenderness parameters which are common in the ship building industry are subjected to a rigorous numerical analysis to understand the effect of distortions and residual stresses individually and in combination. The results are plotted in a design curve format so as to use for the design and strength estimation purposes. The most important observation from the study is that, the strength reduction with respect to imperfection parameters is not directly proportional to the parametric values of the imperfections as is incorporated in most of the analytical methods. The slender structures do not appear to experience a proportional loss of structural strength with increasing distortion or residual stresses. This is because of the fact that the slender structures can allow and accommodate more elastic deformations before the onset of plasticity. The residual stresses were found to reduce the strength of structure but as the slenderness increases, it increases the strength and post buckling strength to a small extent. In other words, if the distortion is taking the structural configuration far away from the buckling configuration, the strength of the structure remains unaffected or slightly increases. The analysis results state the fact that thick plates with $\beta<3$ is found to experience more strength loss compared to thin plates with increasing distortion and residual

stresses. It is observed that the geometrical distortion influences more on the strength compared to residual stresses and the residual stress produce strain hardening effects and increased post buckling strength in the buckling behaviour of plated structures.

On the basis of works undertaken and the discussions above, the main contributions of this thesis in this area are,

1. A critical review on the strength of plated structures and focusing on the Faulkner's approach and Perry-Robertson approach considering the imperfection sensitivity

2. A new empirical formula to predict the strength of stiffened plates incorporating fabrication imperfections

3. Experimental tests on the strength of stiffened panels to validate the effects of imperfections and comparison with numerical results

4. A parametric finite element model to predict the strength of unstiffened and stiffened plates with the realistic imperfections

5. Parametric definition of various geometric imperfections in stiffened plates

6. A relation to incorporate triangular variation of residual stresses in stiffener web or any part of the structure where only one side is welded

7. A set of design curves establishing the imperfection sensitivity of the stiffened panels for a wide range of imperfection and structural parameters

9.3 Stiffened Cylinders

If we look at the history of major offshore platform/rig collapses, the loss of Sea Gem self-elevating barge in 1965, Odeco Ocean Prince Semi-Sub in 1968, Transocean-III in 1974, Ranger-I in 1979, Parker 14-J Jack-up Barge in 2003 were predominantly initiated due to the failure of their legs. So the design of platform legs is as important as it is directly linked to the overall safety of

platforms/rigs for the normal operating conditions, extreme sea conditions and at the event of an accident. The design optimisation based on a target level of safety always leaving certain amount of risk. The alternative of building a structure with massive level of safety and redundancy is not pragmatic due to handling and cost considerations. So a healthy trade off between the safety and cost leads to an acceptable design solution. Looking on to the design of stiffened cylinders, the strength assessment accuracy and consistency will enhance the trade off process more effectively and is beneficial for both design safety and economical considerations.

All of the major practicing codes are developed based on the fundamental shell buckling theory. The general approach is to combine the elastic and inelastic capacity to judge the collapse strength. The calculation steps followed by each design codes to realise the above philosophy are different. There will be different intermediate parameters and empirical constants which are introduced to fit the results close to the actual experimental observations. These parameters, other influencing factors and numerical values are based on the experience and understanding of the respective individual or committee developing the methodology. Even though the CSR enforce the classification societies and industry to safeguard different approaches and predictions with reliable fundamental principles, each design codes keep their identity and always claim their competency with their own contributions.

The proposed model which a modified version of RCC model is developed based on the analysis of a huge number of test data collected form an extensive research of literature available. The results from the analysis indicated that the bias for the knockdown factor is a very sensitive parameter and is influenced by the type of loading. This is not considered in the existing formulation and the numerical values were not chosen sensibly. The above parameter also found sensitive to the type of stiffening methods used. On the basis of the above findings, separate set of bias for knockdown factors are proposed for both the ring and stringer stiffened cylinders from a careful numerical analysis. The

comparison of the proposed model with existing methods DNV, API and RCC shows a better correlation with the experimental data and giving satisfactory results for majority of the loading situations.

On the basis of works undertaken in the area of strength of stiffened cylinders and the discussions above, the main contributions of this thesis in this area are,

1. A critical review on the strength of stiffened cylinders
2. A new strength model for the strength of ring stiffened and stringer stiffened cylinders by modifying an existing strength model
3. A parametric Finite element model for the prediction of strength of stiffened cylinders under axial, radial or combined loading
4. Creating a data bank for the experimental results which are undertaken in the last century
5. A detailed comparison of the New strength model with the DNV, API and RCC design codes to validate the predictions

9.4 Reliability Analysis

The importance of a reliability based design optimisation is widely accepted by the offshore and aerospace industry as structural optimisation has more significance in these fields compared to other areas. The safety requirement and weight requirements are critical for structures in these areas due to increased risk of operations and extreme levels of uncertainty in the load and environmental parameters. The reliability analysis is broken down into component level to check whether the reliability requirement of the overall structures is met at every level of structural design. The decomposition of the reliability index into appropriate partial safety factors of each design parameters to cover the inherent randomness and its proper application in the design ensures that the intended safety requirements are achieved.

The reliability calculations for the stiffened panels are carried out using three analytical formulas explained in Chapter 3. The results are very close to each

other. Although the proposed empirical formulation and other formulations consider the imperfection parameters, it all simplifies the influences to fit into the limited frame of column collapse. The influence of imperfection parameters is quite evident in the reliability results. The Faulkner method shows slightly higher reliability index compared to other methods as other methods consider the geometric distortion also.

RSM is adopted to do the reliability analysis with the FE model and the results are found to exist in close correlation with those obtained from the analytical approaches and so close the estimate from empirical approach. If we look closely on to the derived partial factors, we can find the variation of partial factors are not that uniform in both the approaches. This is particularly because of the fact that treatment of variables in both the approaches is different. One of the important observations is that, the RSM approach with a validated Finite element model can produce reasonable estimate of structural reliability for stiffened plated structures. So the method is proved appropriate for structural problems where there is suitable analytical approaches are not available. In the case of stiffened plates where the analytical treatment of imperfection parameters is not satisfactory, the RSM is found suitable. So for extreme or specific type of imperfection parameters which is not possible to define explicitly in the analytical frame can be modelled using FEM and the RSM can be used to compute the reliability and subsequent partial factors. The reliability analysis of stiffened cylinders is also carried out using the proposed analytical formula and RSM to validate the results. For stringer stiffened combined loading case, it shows slightly more variation when comparing with RSM approach. The variation is believed to be due to the inherent randomness in the strength model. The trend of reliability variation with respect to the applied load is exactly matching with the RSM approach.

On the basis of works undertaken and the discussions above, the main contributions of this thesis in this area are,

1. A critical review on the methods and practices on the reliability analysis of marine structures
2. Application of response surface methodology for the reliability analysis of stiffed plates and cylinders
3. Partial factors for the imperfection parameters for the stiffened plates
4. Comparison of analytical and RMS results

9.5 Recommendations for Future Work

The development of an analytical method comprising Faulkner method of reduced slenderness for residual stress and Perry column approach for the distortion can exhibit better imperfection sensitivity. Even though the equivalent column approach for the stiffened panels can give better estimate, the application of simplified distortion modes in a real stiffened plate structure with multiple bays does not reflect the reality and the effects may not be predictable. This is the main reason for the structures not losing the strength proportionally with increasing imperfection. A study in this direction may open up the balancing nature of distortions in different sections of the same structure. This can be added to the analytical formulation to make more rational estimates of structural strength under the influence of imperfection parameters. The influence of residual stress as observed from the FE analysis is bit strange as it is found to increase the yield strain and post buckling strength at highest levels. This is a topic for further investigation as the analytical formulations throw little light in this direction.

The data base of load shortening curves created with increasing levels of individual and combined distortion parameters for various levels of structural slenderness can be used to develop a tool to predict the load shortening curves of structures with any combination of structural and imperfection parameters. The complete data has to be categorised and linearly/quadratically interpolated for in between points.

There are many parameters in the formulation of stiffened cylinders which provide plenty of room for further improvement. More number of test results can be collected for the combined loading cases to make a rational judgement of influencing coefficients and to understand the significance of each parameter. A more rigorous analysis with more data for the combined loading cases can produce better formula exhibiting better correlation. A set of numerical analysis can be performed with varying distortion and residual stresses to propose design curves for ring and stringer stiffened cylinders.

In this thesis the reliability is compared for different load proportions. Apart from that, the variation of design parameters and imperfection parameters also can be investigated in detail. In an industrial point of view, a rigorous reliability analysis may be carried out with different ranges of structural parameters with imperfection effects included to judge the influencing pattern and ranges of importance.

References

ABAQUS Version 6.6-1, Documentation collection.

ABS (March 2005) Commentary on the guide for buckling and ultimate strength assessment for offshore structures.

ABS, (February 1984), Model Code for Structural Design of Tension Leg Platforms, Conoco/ABS TLP Rule Case Committee (RCC)

Achintya Halder and Sankaran Mahadevan (2000), Reliability Assessment Using Stochastic Finite Element Analysis, John Wiley & Sons Ltd.

Agelidis, N.A., Harding, J.E. and Dowling, P.J. (1982), Buckling tests on stringer stiffened cylinder models subject to load combinations, Det Norske Veritas, Report 282-0298

Allen, H. G. and Bulson, P. S. (1980), Background to Buckling, McGraw-Hill Book Company Inc., New York-Toronto-London.

Ang, H. S. and Tang, W. H. (1984), Probability concepts in engineering planning and design, John Wiley & Sons, Inc., New York, Vol. II.

API (September 2000), API BULLETIN 2V. Design of Flat Plate Structures, Second edition.

API Bulletin 2U. (May 1997), Bulletin on Stability Design of Cylindrical Shells, 1st ed., (ANSI/API/Bull 2U-1992).

Baker, E. H. et al. (1972), Structural Analysis of Shells, McGraw-Hill Book Company Inc., New York-Toronto-London.

Bambach, M.R. and Rasmussen, K.J.R. (2002), Experimental Techniques For Testing Unstiffened Plates in Compression and Bending, Society for Experimental Mechanics, Vol. 44, No. 1, p 91-96

Becker, A.A. (2001), Understanding Non-linear Finite Element Analysis through Illustrative Benchmarks, Published by NAFEMS, Scotland, UK.

Becker, H. and Gerard, G. (1962), Elastic stability of orthotropic shells, Journal of aerospace sciences, 29, 505-512

Bilal M. Ayyub and Richard H.McCuen, (2000), Probability, Statistics and Reliability for Engineers and Scientists', Chapman & Hall/CRC press.

Birch, R.S. and Norman Jones (1990), Dynamic and Static Axial Crushing of Axially Stiffened Cylindrical Shells, Thin-Walled Structures, 9, 29-60

Biswas Pankaj, Mandal, N. R. and Sha, O.P. (2007), Three Dimensional Finite Element Prediction of Transient Thermal History and Residual Deformation due to Line Heating, Journal of Engineering for the Maritime Environment, Part M, Vol.221, pp17-30.

Bleich, F. (1952), Buckling Strength of Metal Structures, McGraw-Hill. N.Y.

Bleich, H.: Stress Distribution in the Flanges of Curved T and I Beams, David Taylor Model Basin, Translation 228.

Blodgett, O.W.: The Design of Welded Structures, James F. Lincoln Arc Welding Foundation, Ohio, USA.

Box, G. E. P. and Wilson, K.B. (1951), On the Experimental Attainment of Optimum Conditions (with discussion), Journal of the Royal Statistical Society Series B 13(1), 1–45

British Standard Institution, (1976), Specification for Unfired Fusion Welded Pressure Vessels, BS 5500, B.S.I., Section 3

Bruhn, E.F.: Analysis and Design of Flight Vehicle Structures, Tri-State Offset Company, Ohio, USA.

Bucher, C. G. (1988), Adaptive sampling – an iterative fast Monte Carlo procedure, Journal of structural safety, Vol. 5, 119-126

Bucher, C. G. and Bourgound, U. (1990), A fast and efficient response surface approach for structural reliability problems, Journal of structural safety, Vol. 7, 57-66

Bucher, C., Macke, M. and Most, T. (2006), Application of approximate response functions in structural reliability analysis, Third International ASRANet Colloquium, Glasgow, UK.

Bulson, P.S. (1970.), The Stability of Flat Plates, Chatto and Windus, London

Carlsen, C.A. (1977) Simplified Collapse Analysis of Stiffened Plates, DnV Norwegian Maritime Res. 4/1977.

Chang Doo Jang, Yong Tae Kim, Young Chun Jo, Hyun Su Ryu (2007), Welding Distortion Analysis of Hull Blocks Using Equivalent Load Method Based on Inherent Strain, 10th International Symposium on Practical Design of Ships and Other Floating Structures Houston, Texas, United States of America.

Cho, S. R., Choi, B. W. and Frieze, P. A. (1998), Ultimate strength formulation for ship's grillages under combined loadings, PRADS 98, Elsevier Sciences

Cho, S. R., Choi, B. W. and Song, I. C. (1998), Post ultimate behaviour of stiffened panels subjected to axial compression, Thin walled structures, 2nd International conference on thin walled structures, 433-440

Cladwell, J.B. (1965), Ultimate Longitudinal Strength, Trans. RINA, Vol. 107, 411-430

Clarsen, C. A. and Czujko, J. (1978), Specification of post welding distortion tolerances for stiffened plates in compression, Journal of structural engineer, Vol. 56A(5), 133-141

Cornell, C. A. (1967), Bounds on the reliability of structural systems, Journal of the structural division, ASCE (ST1), 93, 171-200

Cox, H.L. (1945), The Buckling of a Flat Rectangular Plate under Axial Compression and its Behaviour after Buckling, A.R.C., R&M No. 2041.

Crisfield, M.A. (1991), Non-Linear Finite Element Analysis of Solids and Structures: Essentials, Wiley, 4th edition

Crisfield, M.A. (1981), A fast incremental/iterative solution procedure that handles snap-through. Computer and Structures, Vol. 13, 55-62.

Crisfield, M.A. (1983), An arc-length method including line searches and accelerations. International Journal for Numerical Methods in Engineering, Vol. 19, 1269-1289

Cui, W. and Mansour, A. E. (1998), Effect of welding distortions and residual stresses on the ultimate strength of long rectangular plates under uni-axial compression, Journal of marine structures, Vol. 11(6), 251-269

Cui, W. and Mansour, A. E. (1999), Generalisation of a simplified method for predicting ultimate compressive strength of the panels, International ship building progress, 46:447, 291-303

Cui, W., Wang, Y. and Mansour, A. E. (1999), Stress concentration factor in plates with transverse butt weld misalignment, Journal of constructional steel research, Vol. 52, 159-170

Cui, W., Wang, Y. and Pedersen, P. T. (2002), Strength of ship plates under combined loading, Journal of marine strucutres, Vol. 15, 75-97

Cullington, D.W. and Beales, C. (1977), Residual Stresses and Distortions Measured During Construction of the Milford Haven Bridge, Jnl of Strain Analysis, vol. 12, no. 2, pp 123-129.

Das P.K., Thavalingam A. & Bai Y., (2003), Buckling and ultimate strength criteria of stiffened shells under combined loading for reliability analysis, Thin-Walled Structures 41, 69–88

Das, P., Moan, T., Gu X.K., Friis-Hansen, Hovem, L., Parmentier, G., Rizzuto, E., Shigemi, T., Spencer, J., (2006), Reliability Based Structural Design and Code Development', 16th International Ship and Offshore Structures Congress, Vol.2, Southampton, UK.

Das, P.K. (1987), The Reliability Analysis of Stiffened Cylinders Using Deterministic and Stochastic Approaches, Trans. Royal Institution of Naval Architects, vol. 129, 11 pp.

Das, P.K. and Faulkner, D. (1984), Safety Factor Evaluation for Cylindrical Components of Offshore Structures, loc cit 13

Das, P.K. and Zheng, Y. (2000), Cumulative formation of response surface and its use in reliability analysis, Probabilistic Engineering Mechanics, Elsevier Science Ltd., vol. 15, 309-315

Das, P.K., Faulkner, D. & Zimmer R.A., (June 1992), 'Selection of Robust Strength Models for Efficient Design of Ring and Stringer Stiffened Cylinders Under Combined Loads', Proc. of OMAE-92, Calgary, 12 pp.

Das, P.K., Faulkner, D. and Guedes da Silva (1991), Limit state formulations and Modelling for Reliability-based analysis of orthogonally stiffened cylindrical shell structural components, Department of Naval Architecture and Ocean Engineering, University of Glasgow, Report NAOE-91-26, Glasgow

Das, P.K., Faulkner, D. and Zimmer, R.A. (June 1992), Efficient Reliability Based Design of Ring and Stringer Stiffened Cylinders under Combined Loads, Proc 6th Intl Conf, BOSS, London.

Das, P.K., Frieze, P.A. and Faulkner, D. (1984), Structural Reliability Modelling of Stiffened Components of Floating Structures, Structural Safety, Vol. 2 (1), 3-16.

Das, P.K., Thavalingam, A., Hauch, S. & Bai, Y., (June 2001), 'A New Look at the Model Uncertainty of Stiffened Cylinders for Reliability Analysis', Proceedings of the 20th Intl Conference on Offshore Mechanics and Arctic Engineering (OMAE 2001), Rio de Janeiro, Brazil.

Das, P.K., Zanic, V. & Faulkner, D. (1993), 'Reliability Based Design Procedure of Stiffened Cylinders Using Multiple Criteria Optimisation Techniques', Offshore Technology Conference (OTC) '93, 17 pp.

Derek Graham, (2007), Predicting the collapse of externally pressurised ring-stiffened cylinders using finite element analysis, Marine Structures 20, 202–217

Det Norske Veritas (1977), Rules for the Design, Construction and Inspection of Offshore Structures, Appendix C, Steel Structures.

Det Norske Veritas (1978), Ship's Load and Strength Manual

Det Norske Veritas, (July 1992), Structural Reliability of Marine Structures, Classification Notes 30.6, Norway

Det Norske Veritas. (October 2002), Recommended Practice RP-C201. Buckling Strength of Plated Structures.

Det Norske Veritas. (October 2002), Recommended Practice RP-C202. Buckling Strength of Shells,

Ditlevsen, O., and Madsen, H.O. (1996), Structural Reliability Methods, John Wiley & Sons Ltd.

Dow, R.S., Smith, C.S. (1984), Effects of localized imperfections on compressive strength of long rectangular plates, Journal of Constructional Steel Research, 4, 51-76.

Dowling, P.J. and Harding, J.E. (1982), Experimental behaviour of ring and stringer stiffened shells, Buckling of shells in offshore structures, Ed. J.E. Harding, et al., London: Granada, 73-107

Dunbar, T. E., Pegg, N., Taheri, F. and Jiang, L. (2004), A computational investigation of the effects of localised corrosion on plates and stiffened panels, Marine structures, Vol. 17, 34-402

Dwight, J. B. and Moxham, K. E. (1969), Welded steel plates in compression, Structural engineer, Vol. 47, No. 2

Dwight, J.B. (1982), Imperfection levels in large stiffened tubulars, Buckling of shells in offshore structures, Ed. J.E. Harding, et al., London: Granada, 393-412

Dwight, J.B. and Ratcliffe, A.T. (1969), The Strength of Thin Plates in Compression, Symposium on Thin Walled Steel Structures, University College Swansea, 11-14 Sept., 1967. Published by Crosby Lockwood, Ed. by Rockley, K.C. and Hill, H.V.

Engineering Sciences Data Unit, Structures Sub-series, Data Sheets, vols. 1-10.

Fang, C. and Das, P. K. (2004), Hull girder ultimate strength of damaged ships, Proceedings of PRADS'2004

Fang, C. and Das, P. K. (2005), Survivability and reliability of damaged ships after collision and grounding, Ocean engineering, Vol. 32, No.3-4, 293-307

Faulkner D, Guedes Soares C. & Warwick DM., (1988), Modelling requirements for structural design and assessment. Integrity of Offshore Structures-3, IOS-87, Elsevier Applied Science.

Faulkner, D. (1987), Toward A Better understanding of Compression Induced Stiffener Tripping, International Conference of Steel and Aluminium Structures, vol 3, Cardiff, Elsevier Applied Science Publishers.

Faulkner, D. (1975a), A Review of Effective Plating for use in the Analysis of Stiffened Plating in Bending and Compression, Jnl of Ship Research, vol. 19, no. 1, pp 1-17.

Faulkner, D. (1975b), Compression Strength of Welded Grillages, Chapter 21 of Ship Structural Design Concepts, ed. Evans, J.H., Cornell Maritime Press.

Faulkner, D. (1975c), Strength of Welded Grillages under Combined Loads, Chapter 22 of Ship Structural Design Concepts, ed. Evans, J.H., Cornell Maritime Press.

Faulkner, D. (1977a), Effects of Residual Stresses on the Ductile Strength of Plane Welded Grillages and of Ring Stiffened Cylinders, Jnl of Strain Analysis, vol. 12, no. 2, pp 130-139.

Faulkner, D. (1977b), Compression tests on welded eccentrically stiffened plate panels, Steel Plated Structures, P.J. Dowlinf et al., (Eds), Crosby Lockwood Staples, London, pp 581-617.

Faulkner, D. (1979), Design Against Collapse for Marine Structures, Symp. on Advances in Marine Tech., Norwegian Institute of Technology.

Faulkner, D. (1988), Tension Leg Platforms – From Hutton to Jolliet, or Deeper Water Without Deep Pockets, Report to the Department's Sponsors, NAOE-88-26, University of Glasgow.

Faulkner, D. (1990-91), What is Wrong with Offshore Design Codes?, IESIS, Glasgow, February 1991 (published with Discussion in IESIS Transactions, vol 134.

Faulkner, D. (May 1993), Efficient Design of Orthogonally Stiffened Cylinders, Tensioned Buoyant Platforms Seminar, London, UCL and BPP Technical Services.

Faulkner, D. and Sadden, J. A. (1979), Towards a unified approach to ship structural safety, Trans. RINA, Vol. 121, 1-28

Faulkner, D., Adamchak, J.C., Snyder, G.J. and Vetter, M.F. (1973), Synthesis of Welded Grillages to Withstand Compression and Normal Loads, Computers and Structures, vol. 3, pp 221-246, Pergamon Press.

Faulkner, D., Chen, Y.N. and de Oliveira, J. G. (1983), Limit State Design Criteria for Stiffened Cylinders of Offshore Structures, ASME 4th Congress of Pressure Vessels and Piping Technology, Portland, Oregon, Paper 83-PVP-8.

Fisher-Cassie, Structural Analysis - Statically Indeterminate Structures, Longmans, Green and Co.

Freudenthal, A. M., (1956), Safety and the probability of structural failure, Trans. ASCE, 121

Frieze P.A., Das P.K. & Faulkner D., (1983), Partial safety factors for stringer stiffened cylinders under extreme compressive loads, PRADS 83, The 2nd International Symposium on Practical Design in Ship Building, Tokyo and Seoul, 475–482.

Fujikubo, M., Yao, T. and Varghese, B. (1997), Buckling and ultimate strength of plates subjected to combined loads, Proceedings of the 7th offshore and polare engineering conference, Vol. 4, 380-387

Gerard, G. (1962), Introduction to Structural Stability Theory, McGraw-Hill Book Company Inc., New York-Toronto-London.

Gordo, J. M., and Guedes Soares, C. (1997), Interaction equations for the collapse of tankers and containerships under combined bending moments, Journal of ship research, Vol. 41(3), 230-240

Grondin, G. Y., Chen, Q., Elwi, A.E. and Cheng, J.J.R. (1998), Buckling of stiffened steel plates—validation of a numerical model, Journal of Constructional Steel Research, Vol. 45(2), 125-148

Grondin, G. Y., Chen, Q., Elwi, A.E. Cheng, J.J.R. (1999), Buckling of stiffened steel plates—a parametric study, Journal of Constructional Steel Research 50, 151–175

Guedes Soares, C. (1988), Design equation for the compressive strength of unstiffened plate elements with initial imperfections, Journal of construction steel research, Vol 9, No 4, pp-287-310

Guedes Soares, C. (1992) Combination of Primary load effects in ship structures, Prob. Engg. Mech., Vol. 7, 103-111

Guedes Soares, C. (1992) Design equation for ship plate elements under uni-axial compression, Journal of Constructional steel research, Vol. 22, 99-114

Guedes Soares, C. and Gordo, J. M. (1996) Collapse strength of rectangular plates under transverse compression, Journal of Constructional steel research, Vol. 36(3), 215-234

Guedes Soares, C. and Gordo, J. M. (1996) Compressive strength of rectangular plates under biaxial load and lateral pressure, Journal of Thin walled structures, Vol. 24, 231-259

Guedes Soares, C. and Teixeira A. P. (2000), Structural reliability of two bulk carrier desigs, Journal of Marine structures, Vol. 13, 107-128

Guedes Soares, C., and Moan, T. (1988), Statistical Analysis of still water load effects in ship structures, Transaction of Society of Naval Architects and Marine Engineers, Vol. 96 (4), 129-156.

Guedes Soares, C., Hussein, A. W., (2009), Reliability and residual strength of double hull tankers designed according to the new IACS common structural rules, Ocean engineering Vol 36, p1446-1459.

Haglund, T. (1997), Shear buckling resistance of steel and aluminium plate girders, Thin Walled Structures, Vol. 29, 13-30

Hearne, E.J. Mechanics of Materials, Pergamon International Library.

Hinton, E. (1992), NAFEMS – Introduction to Nonlinear Finite Element Analysis, NAFEMS, Glasgow

Holyland. A. and Marvin R., (1994), System Reliability Theory Models and Statistical Methods, John Wiley & Sons Ltd.

Horne, M.R., and Narayanan, R. (1976), Ultimate capacity of stiffened plates used in girders, Proceedings of Institutions of civil engineers, Vol. 61, Part. 2, pp 253-280.

Horne, M.R., Montague, P. and Narayanan, R. (1977), Influence on strength of compression panels of stiffener section, spacing and welded connection, Proceedings of Institutions of civil engineers, Vol. 61, Part. 2, pp 1-20.

Hu, S.Z. (1993), A Finite Element Assessment of the Buckling Strength Equations of Stiffened Plates, The society of naval architects and marine engineers and the ship structure committee, A Paper presented at the Ship Structures Symposium '93, Sheraton National Hotel, Arlington, Virginia, November 16-17,

Hu, S.Z., and Jiang, L. (1998), A Finite Element simulation of the test procedure of stiffened panels, Marine Structures 11, 75-99.

Hu, S.Z., Chen, Q., Pegg, N., and Zimmerman, T.J.E. (1997), Ultimate Collapse Tests of Stiffened-Plate Ship Structural Units, Marine Structures 10, 587-610

Hughes, O. and Ma, M. (1996), Lateral distortional buckling of mono-symmetric I-beams under distributed vertical loads, thin walled structures, Vol. 26(2), 123-145

Hughes, O. F. and Ma, M. (1996), Elastic tripping of asymmetrical stiffeners, Computer and structures, Vol. 60(3), 369-389

Hughes, O. F. and Ma, M. (1996), Inelastic analysis of panel collapse by stiffener buckling, Computer and structures, Vol. 61(1), 107-117

Hughes, O. F. and Ma, M. (1996), Lateral distortional buckling of mono symmetric beams under point loads, Journal of engineering mechanics, Vol. 120(10), 1022-1029

Hughes, O. F., Ghosh, B. and Chen, Y. (2004), Improved predication of simultaneous local and overall buckling of stiffened plates, Journal of thin walled structures, Vol. 42, 827-856

Hughes, O.F. (1988), Ship Structural Design: a rationally based, computer-aided optimization approach, The Society of Naval Architect and Marine Engineers, New Jersey.

Hurst, G. L. and Campbell, R.B. (1997), Evaluation of finite element modelling practices for stiffened structures, BOSS, 3, 19-33

Hutchinson, J. W. and Koiter, W. T. (1970), Post-buckling Theory', Applied Mechanics Review, vol 23, pp 1353-1366

Hutchinson, J.W. and Amazigo, J.C. (1967), Imperfection sensitivity of eccentrically stiffened cylindrical shells, American Institute of Aeronautics and Astronautics, Vol. 5, 392-401

Imtiaz A. Sheikh, Gilbert Y. Grondin and Alaa E. Elwi, (2001), Stiffener Tripping in Stiffened Steel Plates", Structural engineering report 236, Department of Civil & Environmental Engineering, University of Alberta.

ISSC 2003, Proceedings of the 15th International Ship and Offshore Structures Congress Volume 3, San Diego, USA

ISSC 2009, Proceedings of the 17th International Ship and Offshore Structures Congress Volume 1, Seoul, Korea

Jensen, J. J., Amdahl, J., Caridis, P., Chen, T. Y., Cho, S. R., Damonte, R., Kozliakov, V. V., Reissmann, C., Rutherford, S. E., Yao, T. and Estefen, S. F. (1994), Report of ISSC technical committee III.I – Ductile collapse, 12th International ship and offshore structures congress, Canada, Elsevier Science Ltd., 299-387

Jensen, J. J., Banke, L. and Dogliani, M. (1994), Long term predictions of wave induced loads using a quadratic ship theory, Proceedings of international conference on ship and marine research (NAV' 94), Rome, Vol. 1, 1-14

Jensen, J. J., Pedersen, P. T. and Petersen, J. B. (1992), Stresses in container ships, Jahrbuch der sciffbautechnischen gesellscahft, Vol. 86, 143-150

Jeom Kee Paik and Anil Kumar Thayamballi (2003), Ultimate Limit State Design of Steel-Plated Structures, John Wiley & Sons, Ltd, the Atrium, Southern Gate, Chichester, West Sussex PO19 8SQ, England.

Johnston, B.G. (1976), Guide to Stability Design Criteria for Metal Structures, 3rd Edition, Wiley.

Kamtekar, A.G., White, J.D. and Dwight, J.B. (1977), Shrinkage Stresses in a Thin Plate with a Central Weld, Jnl of Strain Analysis, vol. 12, no. 2, pp 140-147.

Kendrick, S. (March 1955), Analysis of results of static pressure tests of Chatham submarine models, Naval Construction Research Est. (now ARE), Dunfermline, Ref No R218

Kendrick, S. (1984), How Safe Are Design Codes?, Marine and Offshore Safety, Edited by Frieze, P. A. et al, Elsevier.

Khan, I. A. and Das, P. K. (2008), Reliability analysis of intact and damaged ships considering combined vertical and horizontal bending moments, Ships and Offshore Structures, Vol. 3(4), 371–384

Khosrow Ghavami and Mohammad Reza Khedmati (2006), Numerical and experimental investigations on the compression behaviour of stiffened plates, Journal of Constructional Steel Research, Vol 62, p 1087–1100

Kim, S. H. and Na, S. W. (1997), Response surface method using vector projected sampling points, Structural safety, Vol. 19(1), 3-19

Kirchhoff, G. (1850). Uber das gleichgwich und die bewegung einer elastischen scheibe, J. Angew. Math., 40, 51-88.

Koichi Masubuchi (1980), Analysis of Welded Structures: Residual Stresses, Distortion, and Their Consequences, International Series on Materials Science and Technology, Oxford, New York, Pergamon Press

Koiter, W. T., (1956), Buckling and Post-Buckling of a Cylindrical Panel Under Axial Compression, trans Natl Aero Res Inst Amsterdam, vol 20, no 71.

Koji Masaoka and Alaa Mansour (2008), Compressive Strength of Stiffened Plates With Imperfections: Simple Design Equations, Journal of Ship Research, Vol. 52, No. 3, pp. 227–337

Krasovskya,V.L.& Kostyrko,V.V. (2007), Experimental studying of buckling of stringer cylindrical shells under axial compression, Thin-Walled Structures 45, 877–882

Liu PL, Lin HZ & Der Kiureghian A. (1989), CALREL (CAL-Reliability): A general purpose structural reliability analysis program. Report UCB/SEMM 89/18, University of California, Berkeley.

Ma, M. and Hughes, O. (1996), Lateral distortional buckling of mono-symmetric I-beams under distributed vertical loads, thin walled structures, Vol. 26(2), 123-145

Madsen, H. O., Krenk, S. and Lind, N. C. (1986), Methods for structural safety, Prentice Hall.

Maerli, A., Das, P.K. and Smith, S. (2000), A Rationalisation of Failure Surface Equation for the Reliability Analysis of FPSO Structures, Intl Shipbuilding Progress, vol. 47 (450), 215-225.

Mahapatra, M. M., Datta, G. L., Pradhan, B. and Mandal, N. R., (2006), 3-D Finite Element Analysis to Predict the Effects of SAW Process Parameters on Temperature Distribution and Angular Distortions in Single Pass Butt Joints with Top and Bottom Reinforcements, International Journal of Pressure Vessels and Piping, Vol.83, No.10, pp721-729

Mahendran, M. (1997), Local plastic mechanisms in the thin steel plates under in plane compression, Thin walled structures, Vol. 27, 245-261

Mansour AE & Thayamballi A. (1993), Probability-based ship design procedures Draft report SR-1337, ship structure committee, Washington DC, USA.

Mansour AE & Thayamballi A. (1994), Loads and load combinations, ship structure committee Report No. SSC-373.

Mansour, A. E. (1971), Post buckling behaviour of stiffened plates with small initial curvature under combined loads, International ship building progress, 217-240

Mansour, A. E. (1972), Probabilistic design concepts in ship structural safety and reliability, Trans. SNAME, Vol. 80, 64-97

Mansour, A. E. (1990), An introduction to structural reliability theory, Ship structure committee report, SSC-351

Mansour, A. E. and Faulkner, D. (1973), On applying the statistical approach to extreme sea loads and ship hull strength, Trans. RINA, Vol. 115, 277-314

Mansour, A. E. and Wirsching, P. H. (1995), Sensitivity Factors and their Application to Marine Structures, Journal of Marine structures, Vol. 8, 229-255

McPherson, N.A. and Crow, A. (2006), Plate Requirements for Current Naval Vessel Builds, Conference on Achieving Profile & Flatness in Flat Products, Birmingham, UK.

Melchers. R.E. (1999), Structural Reliability Analysis and Prediction, John Wiley & Sons Ltd.

Miller C.D., (1982), Summary of buckling tests on fabricated steel cylindrical shells in the U.S.A.. In: Harding, Dowling and Agelidis, Editors, Buckling of Shells in Offshore Structures, pp. 429–472.

Miller CD., (1977), Buckling of axially compressed cylinders. J Struct Div Trans ASCE, vol 103, no, ST3, 1977:695–721.

Mindlin, R. D. (1951), Influence of rotatory inertia and shear on flexural motion of isotropic elastic plates, Journal of Applied Mechanics, ASME, 18, 31-38.

Morandi, A.C., Das, P.K. and Faulkner, D. (1995), Ring Frame Design in Orthogonally Stiffened Cylindrical Structures, paper OTC 7801, Offshore Technology Conference, Houston.

Morandi, A.C., Das, P.K. and Faulkner, D. (1996), Finite Element Analysis and Reliability Based Design of Externally Pressurised Ring Stiffened Cylinders, Transactions of The Royal Institution of Naval Architects (RINA), Part B, vol. 138.

Morandi, A.C., Faulkner, D. & Das, P.K., (1996), Frame Tripping in Ring Stiffened Externally Pressurised Cylinders, Journal of Marine Structures, vol. 9, no. 6, pp 585-608, 24 pp

Muckle, W. Strength of Ship's Structures, Edward Arnold Publishers Ltd., London.

Murugan, N., Narayanan, R. (2008), Finite element simulation of residual stresses and their measurement by contour method, Elsevier Ltd., Journal of Materials and Design

Niles and Newall: Airplane Structures, John Wiley and Sons Inc.

Nordenstrom, N. (1971), Methods for predicting long term distributions of wave loads and probability of failure of ships, DNV, Research and development report 71-2-S

Odland J., (1981), An experimental investigation of the buckling strength of ring-stiffened cylindrical shells under axial compression. Norwegian Maritime Research, No.4, p 22–39.

Odland, J. (1978), Buckling Resistance of Unstiffened and Stiffened Circular Cylindrical Shell Structures, Norwegian Maritime Research, vol 6, no 3

Odland, J. and Faulkner, D. (1981), Buckling of Curved Steel Structures – design formulations, Integrity of Offshore Structures, Edited by Faulkner, D. et al., Applied Science publishers.

Ozguc, O., Das, P. K., Barltrop, N. D. P. (2007), The new simple design equations for the ultimate compressive strength of imperfect stiffened plates, Ocean Engineering, Vol 34, Issue 7, p 970-986

References

Paik, J. K. (1997), A benchmark study of the ultimate strength formulations of the stiffened plates, Final report to ABS by Pusan national university, Department of naval architecture and ocean engineering, Korea

Paik, J. K. and Pedersen, T. (1996), A simplified method for predicting ultimate compressive strength of ship panels, International ship building progress, Vol. 43(434), 139-157

Paik, J. K., Thayampilli, A. K. and Kim, B. J. (2001), Advanced ultimate strength formulations for ship plating under combined biaxial compression/tension, edge shear and lateral pressure loads, Marine technology, Vol. 38(1), 9-25

Paik, J. K., Thayampilli, A. K. and Yang, S. H. (1998), Residual strength assessment of ships after collision and grounding, Marine technology, Vol. 35(1), 38-54

Paik, J. K., Thayampilli, A. K., and Lee, J. M. (2004), Effect of initial deflection shape on the ultimate strength behaviour of welded steel plates under biaxial compressive loads, Journal of ship research, Vol. 48(1), 45-60

Paik, J. K., Thayampilli, A. K., Terndrup Pedersen, P. and Park, Y. I. (2001), Ultimate strength of ship hulls under torsion, Ocean engineering, Vol. 28, 1097-1133

Panagiotis Michaleris and Andrew DeBiccari, (1996), Prediction of Welding Distortion, Edison Welding Institute, Columbus, Ohi, Paper presented at the AWS annual convention, April 1996, Chicago.

Pankaj Biswas and Mandal, N.R. (2008), Welding Distortion Simulation of Large Stiffened Plate Panels", Journal of Ship Production, Vol.24, No.1

Paul A. Frieze, (1994), The Experimental Response of Flat-Bar Stiffeners in Cylinders under External Pressure, Marine Structures, 7, 213-230

Peery, D.J, Aircraft Structures, McGraw-Hill Book Company Inc.

Pretheesh Paul C, Purnendu K. Das, Anthony Crow, Stuart Hunt (2010), Effect of residual stress on the buckling strength of stiffened plates, 5th International Asranet Conference, 14-16 June 2010, Edinburgh, Scotland.

Pretheesh Paul C, Purnendu K. Das, Anthony Crow, Stuart Hunt, (2009), The Effect of Distortion on the Buckling Strength of Stiffened Panels, Ship and Offshore Structures, Published; ISSN: 1754-212X (electronic) 1744-5302 (paper))

Pretheesh Paul C, Purnendu K. Das, Anthony Crow, Stuart Hunt, (2009), The Effect of Distortion on the Buckling Strength and post buckling behaviour of Stiffened Panels, Proceedings of the International conference on Floating structures for deep water operations , 21-23 September 2009, Glasgow, United Kingdom

Pretheesh Paul C., Subin K. K., Das, P.K. (2010), Reliability Analysis of Stiffened Shell structures for Offshore Applications', 5th International Asranet Conference, 14-16 June 2010, Edinburgh, Scotland.

Pu, Y., Das, P.K. and Faulkner, D. (1997), A Strategy for Reliability-Based Optimisation, Journal of Engineering Structures, vol. 19 (3), 276-282.

Pu, Y., Das, P.K. and Faulkner, D. (1997), Ultimate Compression Strength and Probabilistic Analysis of Stiffened Plates', Journal of Offshore Mechanics and Arctic Engineering (OMAE), vol. 119, 6 pp.

Purnendu K. Das, Subin K. K., Pretheesh Paul C. (2011), A revisit on Design and Analysis of Stiffened Shell structures for Offshore Applications, MARSTRUCT 2011, 28-30 March 2011, Hamburgh Germany.

Qi, E., Cui, W., Peng, X. and Xu, X. (1999), Reliability assessment of ship residual strength after collision and grounding, Journal of ship mechanics, Vol. 3(5), 40-46

Rackwitz, R. (1982), Response surfaces in structural reliability, Berichte zur Zuver-lÄassigkeitstheorie der Bauwerke 67, TU MÄunchen.

Rajashekhar, M. R. and Ellingwood, B. R. (1993), A new look at the response surface approach for the reliability analysis, Structural safety, Elsevier Science Publishers B. V., Vol. 12, 205-220

Ralph, E. Ekstrom, (1963), Buckling of cylindrical shells under combined torsion and hydrostatic pressure, Journal of Experimental Mechanics, 3, 192-197

Reddy, J. N. (1999), Theory and Analysis of Elastic Plates, 1st Ed., Taylor & Francis.

Riks, E., (1979), An incremental approach to the solution of snapping and buckling problems. International Journal of Solids and Structures, Vol. 15, 529-551.

Roark, R.J. and Young, W.C., Formulas for Stress and Strain, Fourth/Fifth Edition, McGraw-Hill book Company Inc.

Ross, C. T. F. and Johns, T. (1998), Plastic Axisymmetric Collapse of Thin-Walled Circular Cylinders and Cones Under Uniform External Pressure, Thin-Walled Structures, 30, 35–54

Ross, C. T. F. and Sadler, J.R. (2000), Inelastic shell instability of thin-walled circular cylinders under external hydrostatic pressure, Ocean Engineering, 27, 765–774

Rozbicki, M., Das, P.K. and Crow, A. (2001), The Preliminary Finite Element Modelling of a Full Ship, Journal of Intl Ship Building Progress, vol 48,no.3.

Sechler, E.E.: Elasticity in Engineering, John Wiley & Sons Inc.

Seely and Smith, Advanced Mechanics of Materials, Wiley and Sons Inc.

Seleim, S. S. and Roorda J. (1986), Buckling Behaviour of Ring-Stiffened Cylinders; Experimental Study, Thin-Walled Structures, 4, 203-222

Shanley, F.R. (1949), Analysis of General Instability of Stiffened Shells in Pure Bending, Journal of aerospace sciences, p 590

Shanley, F.R. (1967), Optimum Design of Eccentrically Loaded Columns, AM Soc. of Civil Engineers, Struct. Div. St 4.

Sheikh, I. A., Elwi, A. E. and Gordin, G. Y. (2003), Stiffened steel plates under combined compression and bending, Journal of constructional steel research, Vol. 59, 911-930

Singer, J., Arbocz, J., Weller, T. (1997), Buckling Experiments, Experimental Methods in Buckling of Thin-Walled Structures, Volume 1, Basic Concepts, Columns, Beams and Plates, John Wiley & Sons Inc.

Singer, J., Arbocz, J., Weller, T. (2002), Buckling Experiments, Experimental Methods in Buckling of Thin-Walled Structures, Volume 2, Shells, Built-up Structures, Composites and Additional Topics, John Wiley & Sons Inc.

Skjong, R, Bitner-Gregersen, E, Cramer, E, Croker, A, Hagen,Ø, Korneliussen, G, Lacasee, S, Lotsberg, I, Nadim, F and Ronold, Ko. (1995), Guidelines for Offshore Structural Reliability Analysis-General. Det Norske Veritas Report No 95-2018.

Smith, C.S. (1968), Elastic Buckling and Beam-Column Behaviour of Ship Grillages, Trans. RINA, vol. 110.

Smith, C.S. (1977), Influence of local compressive failure on ultimate longitudinal strength of a ship's hull, Proceedings of the international Symposium PRADS 77, Tokyo, 73-79

Smith, C.S. and Kirkwood, W. (1976), Influence of Initial Deformations and Residual Stresses on Inelastic Flexural Buckling of Stiffened Plates and Shells, Paper No. 35, Steel Plated Structures Conf., London, 6-9 July 1976, published by Crosby Lockwood.

Smith, C.S., Davidson, P.C., Chapman, J.C. and Dowling P.J. (1988), Strength and stiffness of ships' plating under in-plane compression and tension, Royal Institute of Naval Architects, Vol. 130, pp. 277–296.

Somerville, W.L., Swan, J.W. and Clarke, J.D. (1977), Measurement of Residual Stresses and Distortions in Stiffened Panels, Jnl of Strain Analysis, vol. 12, no. 2, pp 107-116.

Sridharan, S. and Walker, A.C. (1980), Experimental investigation of buckling behaviour of stiffened cylindrical shells, Dept of Energy U.K., Report OT-R7835, London.

Steen, E. (1995), Buckling of stiffened plates under combined loads-ABAQUS analysis, DNV report no. 95-0445

Steen, E. and Balling Engelsen, A. (1997), ABAQUS analysis – Plate buckling/GL code, DNV report no. 97-05606

Steen, E., Byklum, E., Vilming, K. and Ostvolds, K. (2004), Computerised buckling models for ultimate strength assessment of stiffened ship hull panels, 9th Symposium on practical design of ships and floating structures, Luebeck, Germany

Structural Stability Research Council Guide to Stability Design Criteria for Metal Structures, (1976), Edited by Bruce G Johnston, 3rd edn, John Wiley

Suneel Kumar, M., Alagusundaramoorthy, P. and Sundaravadivelu, R. (2009), Ultimate strength of stiffened plates with a square opening under axial and out-of-plane loads, Engineering Structures, Vol 31, p 2568-2579

Svein Kristiansen, (2005), Maritime Transportation, Safety Management and risk analysis, Elsevier.

Tatham, R.: Aeronautical Engineering, English Universities Press.

Teixeira, A.P., Guedes Soares, C. and Wang, G. (2005), Reliability based approach to determine the design loads for remaining life of ships, ABS Technical Paper.

Thimoshenko, P. & Gere, J. (1961), Theory of Elastic Stability, McGraw-Hill Book Company Inc., New York-Toronto-London.

Thoft-Christensen. P. and Murotsu Y. (1986), Application of Structural System Reliability Theory, Springer-Verlag, New York.

Thompson, J.D. (1977), Control of Distortion due to Welding and the Additional Cost Involved, Jnl of Strain Analysis, vol. 12, no. 2, pp 148-152.

Timoshenko and Goodier: Theory of Elasticity, McGraw-Hill.

Timoshenko, S.P. and Woinowsky-Krieger, S. (1959), Theory of Plates and Shells, 2nd Edition, McGraw-Hill.

Tsai, C. L., Park, S. C. and Cheng, W. T. (1999), Welding Distortion of a Thin-Plate Panel Structure, Welding Journal, Welding Research Supplement, pp. 156–165.

Tulk, J.D. and Walker, A.C. (1976), Model Studies of the Elastic Buckling of a Stiffened Plate, Journal of Strain Analysis, Vol 11, No 3, p137-143

Ueda, Y. and Yao, T. (1985), The influence of complex initial deflection modes on the behaviour and ultimate strength of rectangular plate in compression, Journal of constructional steel research, Vol. 5, 265-302

Viorel Deaconu, (2007), Finite Element Modelling of Residual Stress - A Powerful Tool in the Aid of Structural Integrity Assessment of Welded Structures", 5th Int. Conference Structural Integrity of Welded Structures (ISCS2007), Timisora, Romania, 20-21 Nov 2007.

Voce S. J., (1969), Buckling under external hydrostatic pressure of orthotropic cylindrical shells with evenly spaced equal strength circular ring frames, Ocean Engineering. Vol. 1, pp. 521-534. Pergamon Press.

Von Mises R., (1929), Stodola Festschrift. Zurich, p 418.

Walker, A.C. and Davies, P. (1977), the collapse of stiffened cylinders, international conference on steel plated structures, Paper 33, Ed. P.J.Dowling, et al., London: Crosby Lockwood Staples.

Walker, A.C. and McCall, S. (1987), Strength of damage ring and orthogonally stiffened shells—part I-:Plain ring stiffened shells, Thin Walled Structures, 5, 425-453

Walker, A.C. and McCall, S. (1988), Strength of damaged ring and orthogonally stiffened shells—Part II: T-ring and orthogonally stiffened shells, Thin Walled Structures, 6, 19-50

Walker, A.C.: The Design and Analysis of Cold-Formed Sections, Intertext Books.

Wang, W. and Moan, T. (1997), Ultimate strength analysis of stiffened plates in ships subjected to biaxial and lateral loading, International journal of offshore and polar engineering, Vol. 7(1), 22-29

Warwick, D.M. and Faulkner, D. (April 1989), Economic Structures From Improved Design Code Strength Modelling, Proc 4th Intl Colloquium on Stability of Metal Structures, Code Differences Around the World, SSRC, New York.

Welding Distortion Analysis of Hull Blocks Using Equivalent Load Method Based on Inherent Strain, (2008), Ship Structure Committee, SSC-453.

Weller, T., Singer, J. and Batterman, S.C. (1974), Influence of eccentricity of loading on buckling of stringer stiffened cylindrical shells, Thin shell structures: Theory, experiment and design, Ed. Y.C. Fung and E.E. Sechler, New Jersey: Prentice Hall, 305-324

Wempner, G.A. (1971), Discrete approximation related to nonlinear theories of solids. International Journal of Solids and Structures, Vol. 7, 1581-1599

White, J.B. and Dwight, J.B. (1977), Residual stresses and geometrical imperfections in stiffened tubulars, Cambridge University, Dept of Engg, Report CUED/C-Struct/TR.64.

White, J.B. and Dwight, J.B. (1978), Residual stresses in large stiffened tubulars, Cambridge University, Dept of Engg, Report CUED/C-Struct/TR.67.

Wittrick, W.H. (1952), Buckling of a Simply Supported Triangular Plate in Combined Compression and Shear, Report SM 197, Aeronautical Research Laboratories, Australia.

Yamaki, N. (1959), Postbuckling Behaviour of Rectangular Plates with Small Initial Curvature Loaded in Edge Compression, Jnl Applied Mechanics, pp 407-414.

Yao, T., Fujikubo, M., Yanagihara, D. and Irisawa, M. (1998), Consideration of FEM modelling for buckling/plastic collapse analysis of stiffened plates, Trans. West-Japan society of naval architects, Vol. 95, 121-128

Yu, L., Das, P. K. and Zheng, Y. (2001), Stepwise response surface method and its application in reliability analysis of ship hull structure, Proceedings of OMAE 2001, 20th International conference on offshore mechanics and arctic engineering, Rio de Janeiro, Brazil

Zheng, Y. and Das, P. K. (2000), Improved response method and its application to stiffened plate reliability analysis, Engineering structures, Elsevier science Ltd., Vol. 22, 544-551

Zheng, Y. and Das, P.K. (2000), Reliability Analysis of Stiffened Plates by Improved Response Method, Journal of Engineering Structures, vol. 22, no. 5, pp 544-551.

Zhi Shu and Moan, T. (2010), Reliability Analysis of Ultimate Strength of a Capesize Bulk Carrier in Hogging and Alternate Hold Loading Condition, ASME 2010 29th International Conference on Ocean, Offshore and Arctic Engineering (OMAE2010), June 6–11, 2010 , Shanghai, China

Zienkiewicz, O.C. and Taylor, R.L. (1991), The Finite Element Method; Solid and Fluid Mechanics, Dynamics and Non-linearity, volume 2. McGraw-Hill, London, 4th edition

Appendix A – Material Properties

Exova (UK) Ltd
Lochend Industrial Estate
Newbridge
Midlothian

EH28 8PL

T: 0131 333 4360
F: 0131 333 5135
E: edinburgh@exova.com
W: www.exova.com

Exova

Test Certificate

BAE SYS.SUR.FLEET SOLUTIONS
1048 GOVAN ROAD
LINTHOUSE
GLASGOW
G51 4XP

Attn: Norrie McPherson

REF No   E 102199   : Issue   1
Page   1 of 1
Ord No   BLANKET
Date Tested 20/04/11
Date Reported 20/04/11

Item   -   FLAT BAR SECTION : IDENTIFIED TC BAR
                 4mm THK. : DH36 MATERIAL

Specification -   Client's Requirements

Tensile Test - EN ISO 6892-1: 2009

	Dimensions [mm]	Area [mm^2]	GL [mm]	YS [N/mm^2]	UTS [N/mm^2]	%E1	%RA	Comments
001:Parent	20.09x 4.42	88.80	50.00	405	574	28.5	N/A	Nil

Certificate Comments

This is an electronic copy. See original certificate for terms and conditions.
----------------------------- End of Text -----------------------------

Tested by   EDINBURGH LAB.

For and on behalf of
Exova (UK) Ltd

UKAS
TESTING
0172

Exova (UK) Ltd
Lochend Industrial Estate
Newbridge
Midlothian

EH28 8PL

T: 0131 333 4360
F: 0131 333 5135
E: edinburgh@exova.com
W: www.exova.com

Exova

Test Certificate

BAE SYS.SUR.FLEET SOLUTIONS
1048 GOVAN ROAD
LINTHOUSE
GLASGOW
G51 4XP

REF No	E 102198	: Issue 1
Page	1 of 1	
Ord No	BLANKET	
Date Tested	20/04/11	
Date Reported	20/04/11	

Attn: Norrie McPherson

Item   -   PLATE SECTION : IDENTIFIED TC PLATE
           4mm THK. PLATE : DH36 MATERIAL

Specification   -   Client's Requirements

Tensile Test - EN ISO 6892-1: 2009

	Dimensions [mm]	Area [mm^2]	GL [mm]	YS [N/mm^2]	UTS [N/mm^2]	%E1	%RA	Comments
001:Parent	19.88x 5.04	100.20	50.00	339	459	31.5	N/A	Nil

Certificate Comments

This is an electronic copy. See original certificate for terms and
conditions.
----------------------------- End of Text -----------------------------

Tested by   EDINBURGH LAB.

For and on behalf of
Exova (UK) Ltd

UKAS

0172

II

Exova (UK) Ltd
Lochend Industrial Estate
Newbridge
Midlothian

EH28 8PL

T: 0131 333 4360
F: 0131 333 5135
E: edinburgh@exova.com
W: www.exova.com

exova

Test Certificate

BAE SYS.SUR.FLEET SOLUTIONS
1048 GOVAN ROAD
LINTHOUSE
GLASGOW
G51 4XP

REF No	E 100746	: Issue 1
Page	1 of 2	
Ord No	BLANKET	
Date Tested	07/02/11	
Date Reported	08/02/11	

Attn: Norrie McPherson

Item   -   PLATE SECTION : IDENTIFIED No.1
                 4mm THK. PLATE : DH36 MATERIAL

Specification   -   Client's Requirements

Tensile Test - EN ISO 6892-1: 2009

	Dimensions [mm]	Area [mm²]	GL [mm]	0.20NPS [N/mm²]	UTS [N/mm²]	%E1	%RA	Comments
001:Parent	4.21x 24.57	103.44	50.80	367	478	N/A	N/A	Nil

Charpy Test - EN 10 045-1: 1990

	Position	Dimensions [mm]	Denomination	Test Temp [°C]	Energy Absorbed [Joules]	Average [Joules]	Comments
002:Parent	N/A	10x2.5x2V	N/A	-20.0	22, 24, 24	23	Nil

Micro Examination - Customer Requirement

	Position	Details	Comments
003:Microstructural Exam	T-T	N/A	See Below

Item 03:   The un-etched structure was examined, consists of an even dispersion
             of spheroidal non-metallic inclusions of varying size and grey colour.
             The microstructure, revealed after etching with 2% Nital, consists of
             a fine grained Ferrite and Pearlite structure.

Certificate Comments

This is an electronic copy. See original certificate for terms and
conditions.
----------------------------- End of Text -----------------------------

Tested by   EDINBURGH LAB.

For and on behalf of
Exova (UK) Ltd

UKAS
0172

Test Certificate

BAE SYS.SUR.FLEET SOLUTIONS
1048 GOVAN ROAD
LINTHOUSE
GLASGOW
G51 4XP

Attn: Norrie McPherson

REF No   E 100747   : Issue   1
Page   1 of 2
Ord No   BLANKET
Date Tested   07/02/11
Date Reported   08/02/11

Item   -   PLATE SECTION : IDENTIFIED No.2
               4mm THK. PLATE : DH36 MATERIAL

Specification   -   Client's Requirements

Tensile Test - EN ISO 6892-1: 2009

	Dimensions [mm]	Area [mm²]	GL [mm]	YS [N/mm²]	UTS [N/mm²]	%E1	%RA	Comments
001:Parent	5.28x 24.59	129.84	50.80	400	504	33.5	N/A	Nil

Charpy Test - EN 10 045-1: 1990

	Position	Dimensions [mm]	Denomination	Test Temp [°C]	Energy Absorbed [Joules]	Average [Joules]	Comments
002:Parent	N/A	10x2.5x2V	N/A	-20.0	25, 21, 24	23	Nil

Micro Examination - Customer Requirement

	Position	Details	Comments
003:Microstructural Exam	T-T	N/A	See Below

Item 03: The un-etched structure was examined, consists of an even dispersion
          of spheroidal non-metallic inclusions of varying size and grey colour.
          The microstructure, revealed after etching with 2% Nital, consists of
          a fine grained Ferrite and Pearlite structure.

Certificate Comments

This is an electronic copy. See original certificate for terms and
conditions.
----------------------------- End of Text -----------------------------

Tested by   EDINBURGH LAB.

For and on behalf of
Exova (UK) Ltd

UKAS
0172

Exova

BAE SYS.SUR.FLEET SOLUTIONS
1048 GOVAN ROAD
PLATE SECTION : IDENTIFIED No.2
4mm THK. PLATE : DH36 MATERIAL

REF No   E 100747   : Issue   1
Page   2 of 2

Photographs - Customer Requirement

	Location	Position	Magnification	
004:Micro Section	N/A	T-T	x400	

E100747

0.02 mm
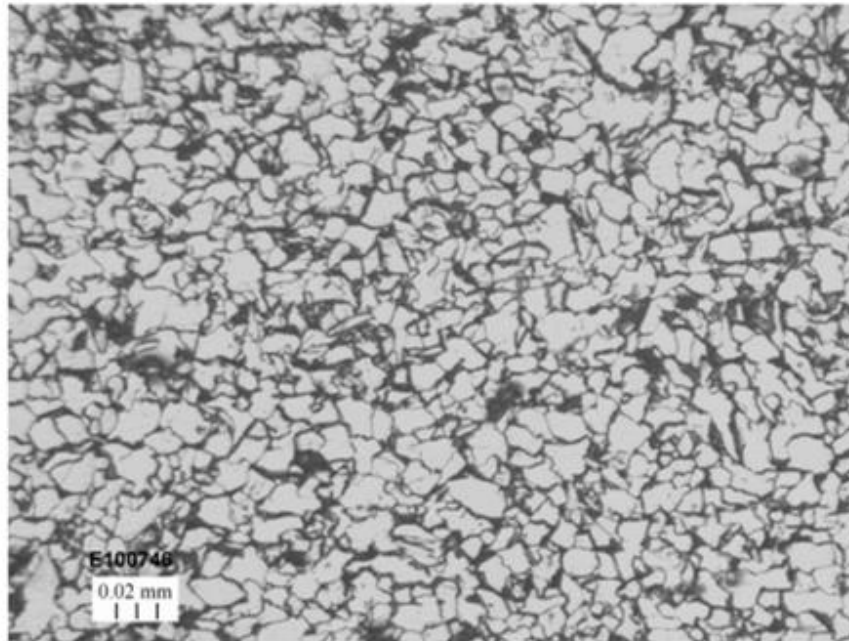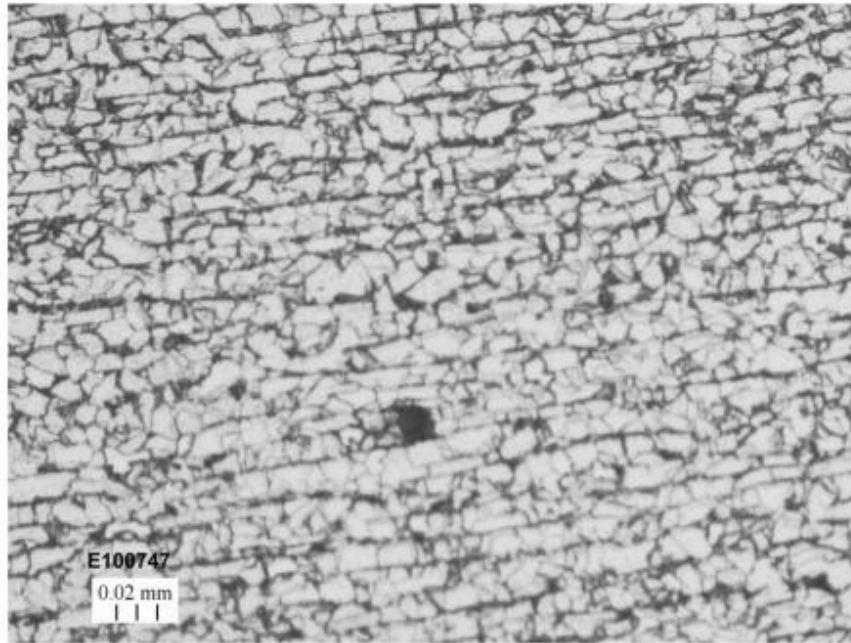
This document may not be reproduced other than in full, except with the prior written approval of the issuing laboratory.
These results pertain only to the item(s) tested as sampled by the client unless otherwise indicated.

UKAS
TESTING
0172

Appendix B – Experimental Test Results

B.1 Load-Extension Curves from Experiments and FE Analysis
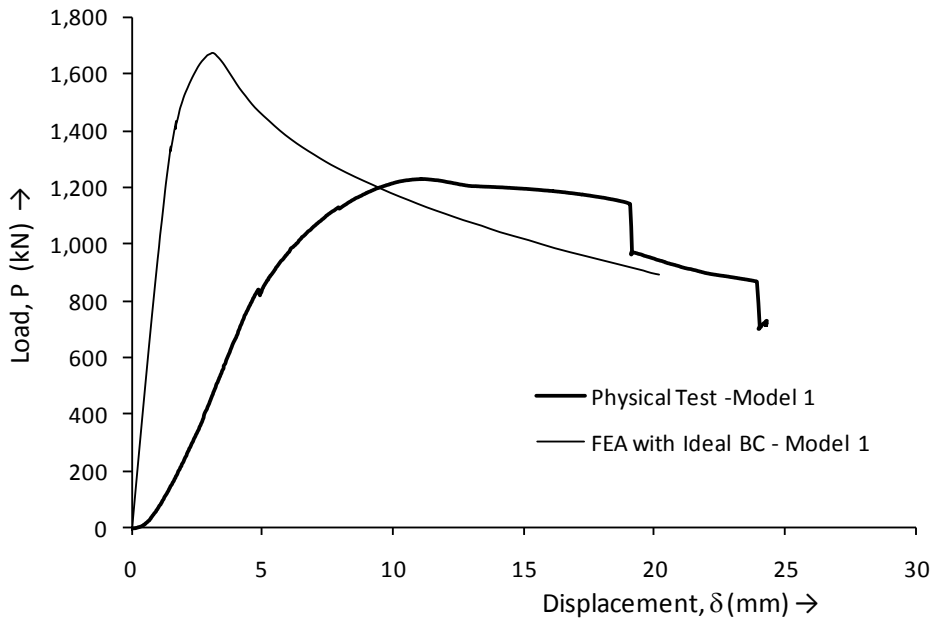
Figure B-1. Load-Displacement Plot of Ideal FE and Test of Model 1
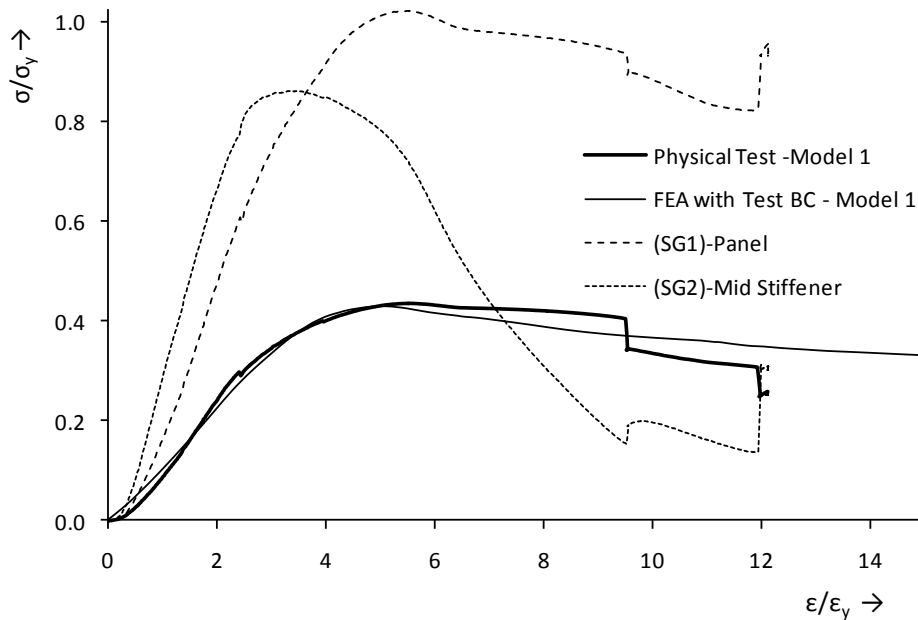
Figure B-2. Non-dimensional Strength Plot of FE (Test BC) and Test Results of Model 1
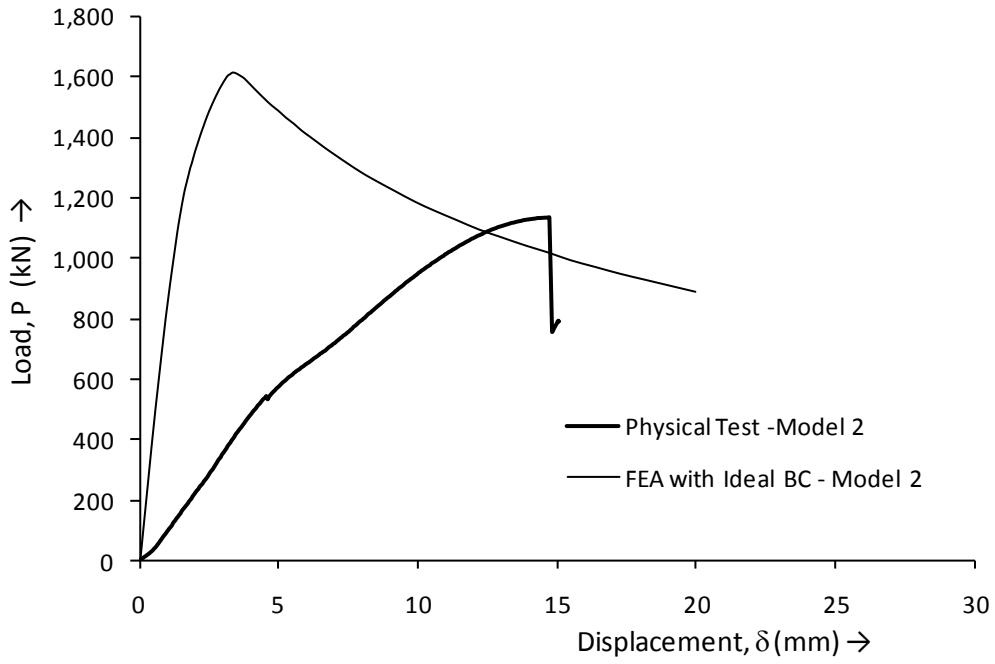
Figure B-3. Load-Displacement Plot of Ideal FE and Test of Model 2
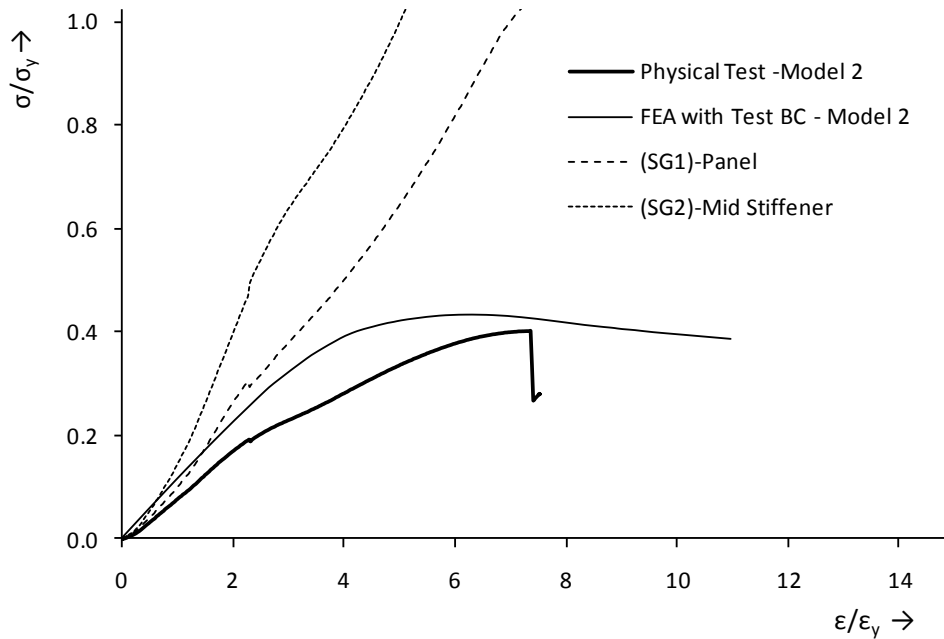
Figure B-4. Non-dimensional Strength Plot of FE (Test BC) and Test Results of Model 2
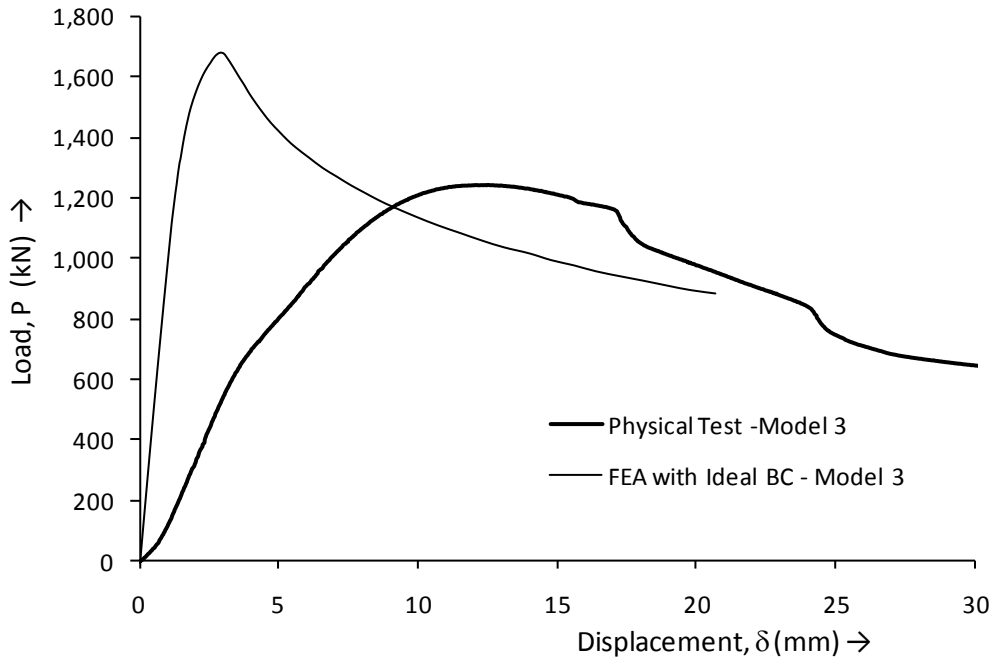
Figure B-5. Load-Displacement Plot of Ideal FE and Test of Model 3
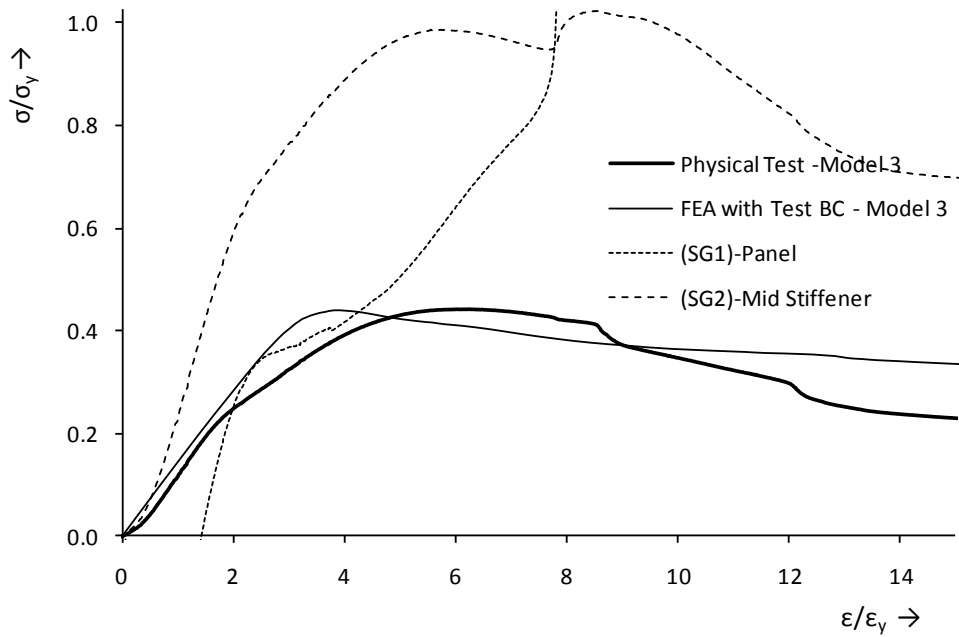
Figure B-6. Non-dimensional Strength Plot of FE (Test BC) and Test Results of Model 3
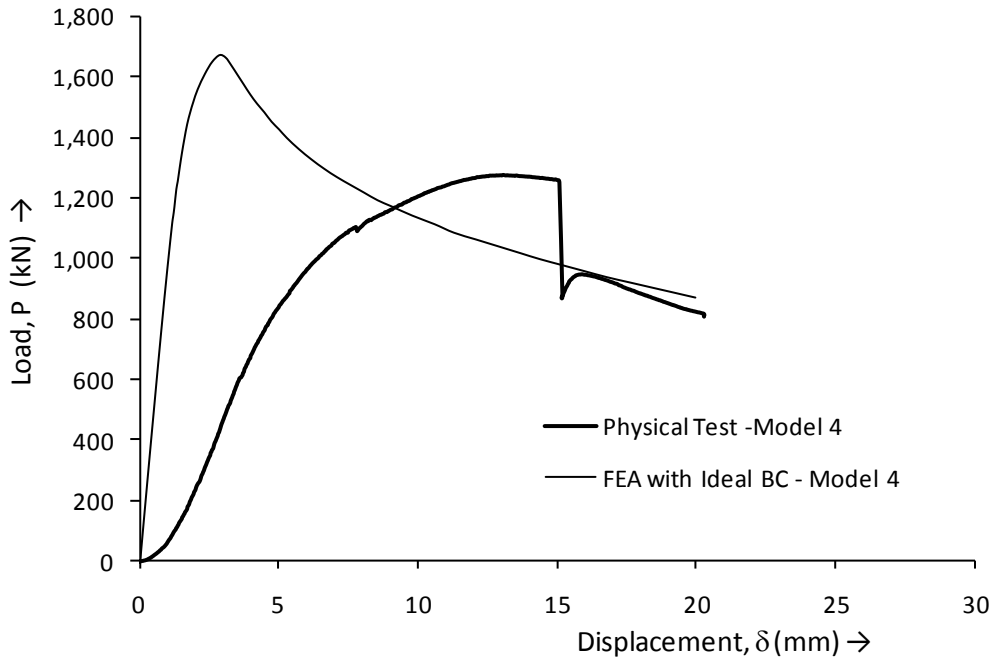
Figure B-7. Load-Displacement Plot of Ideal FE and Test of Model 4
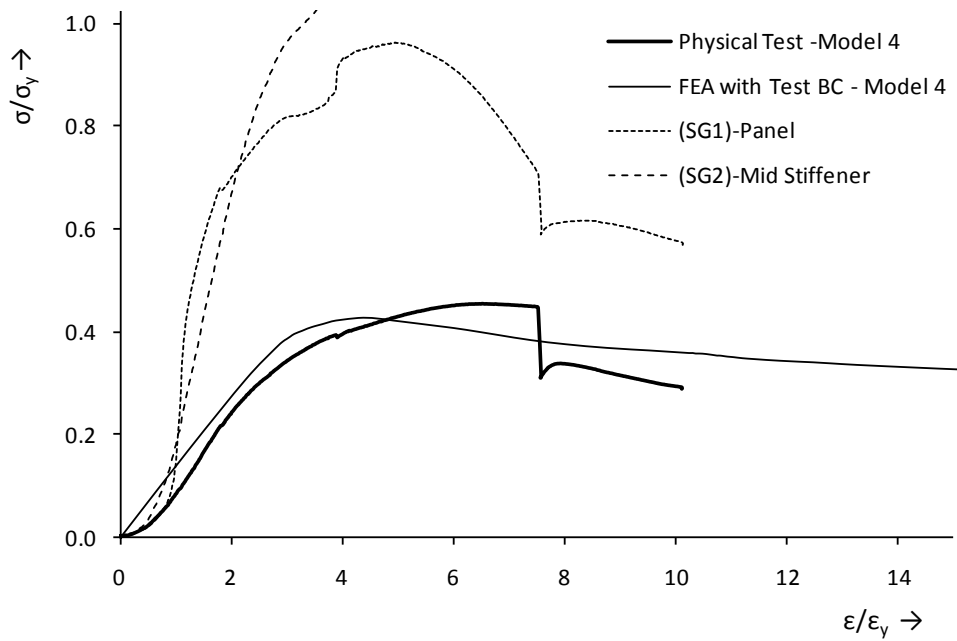
Figure B-8. Non-dimensional Strength Plot of FE (Test BC) and Test Results of Model 4
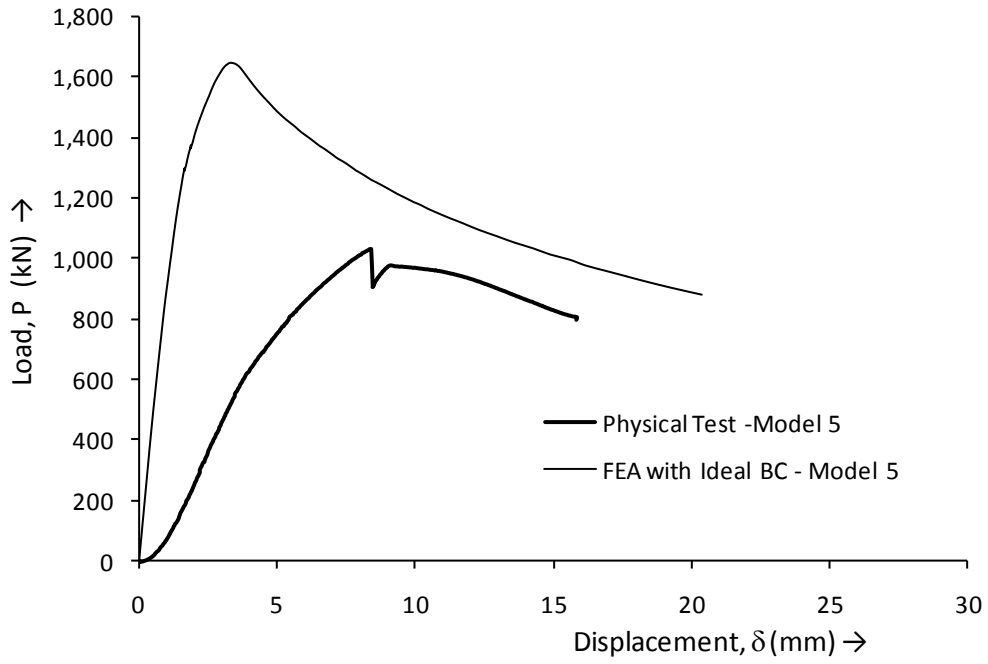
Figure B-9. Load-Displacement Plot of Ideal FE and Test of Model 5
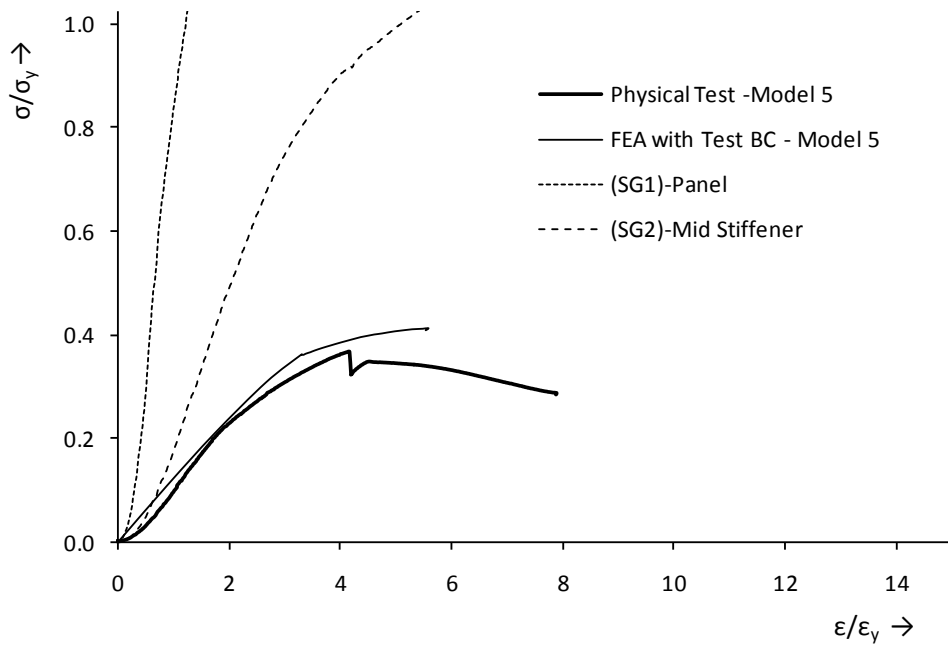
Figure B-10. Non-dimensional Strength Plot of FE (Test BC) and Test Results of Model 5
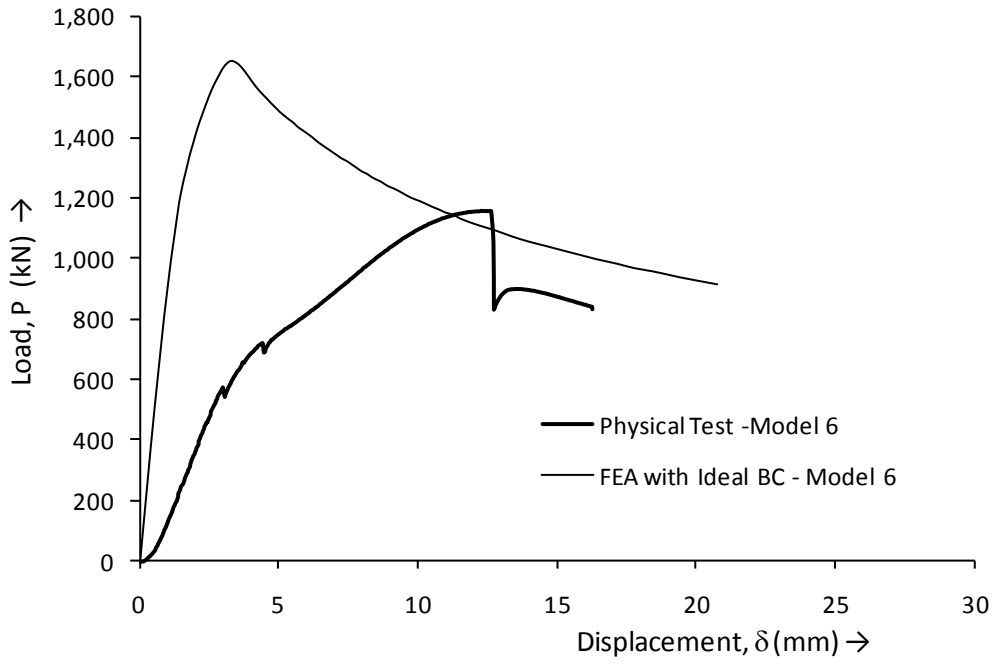
Figure B-11. Load-Displacement Plot of Ideal FE and Test of Model 6
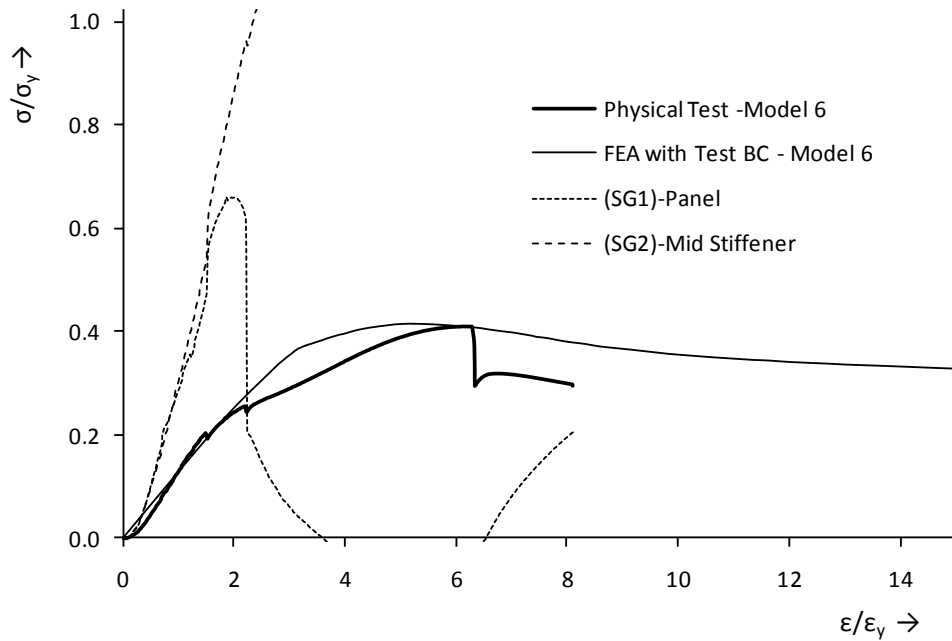
Figure B-12. Non-dimensional Strength Plot of FE (Test BC) and Test Results of Model 6
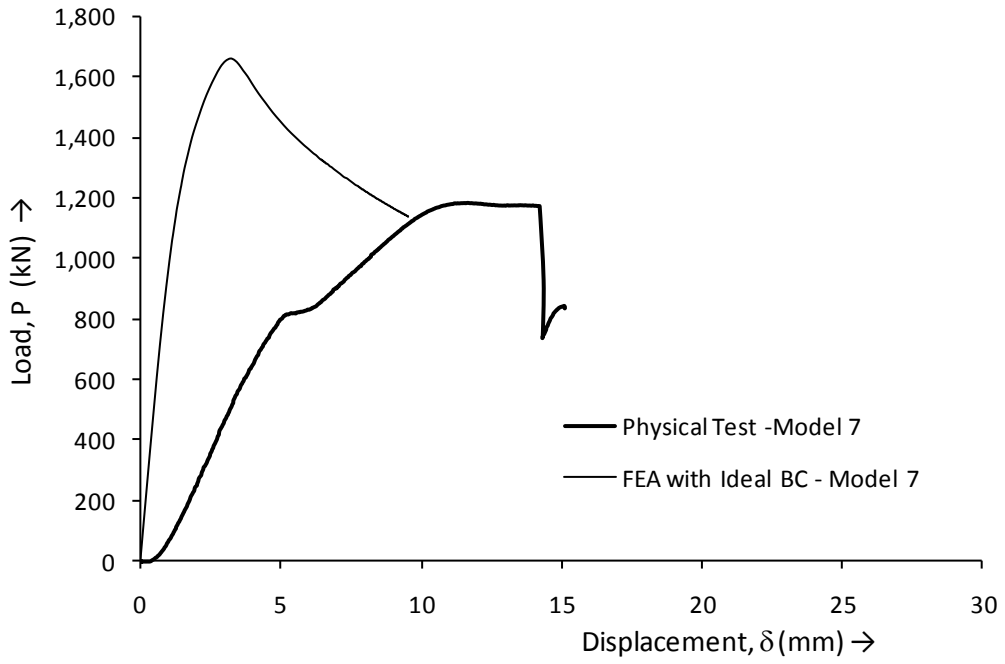
Figure B-13. Load-Displacement Plot of Ideal FE and Test of Model 7
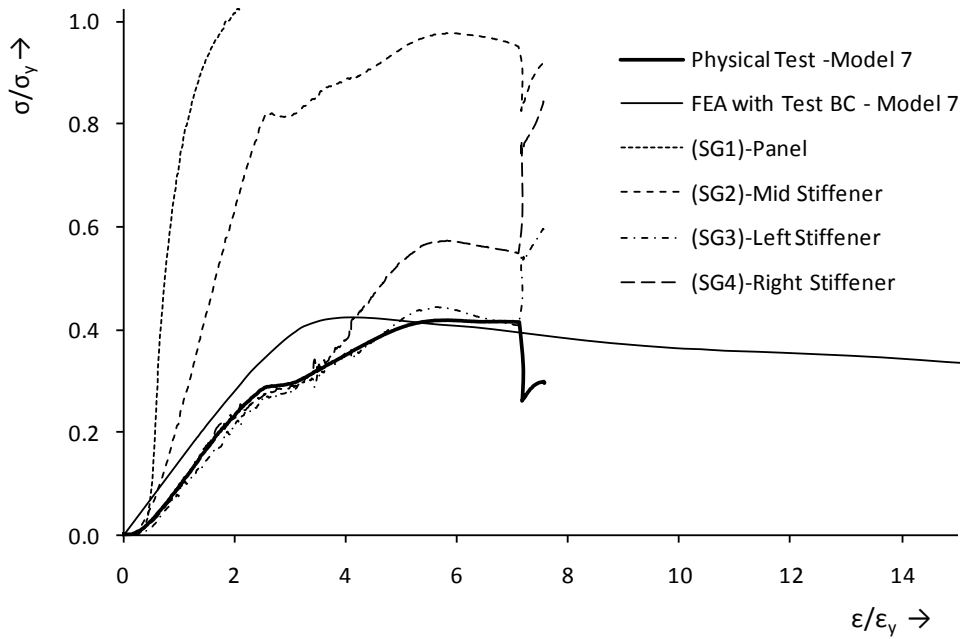
Figure B-14. Non-dimensional Strength Plot of FE (Test BC) and Test Results of Model 7
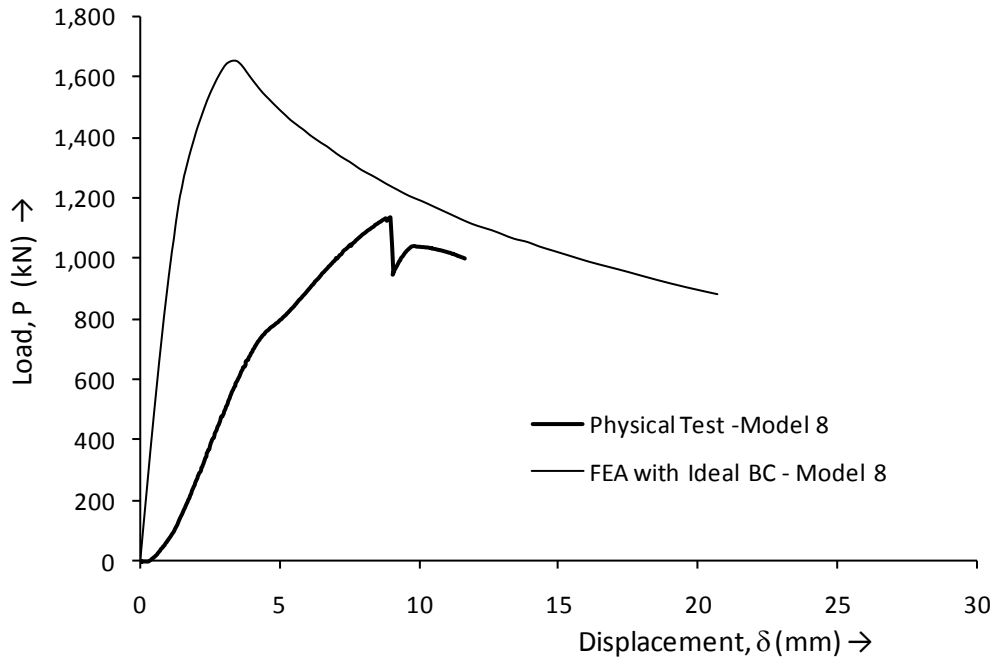
Figure B-15. Load-Displacement Plot of Ideal FE and Test of Model 8
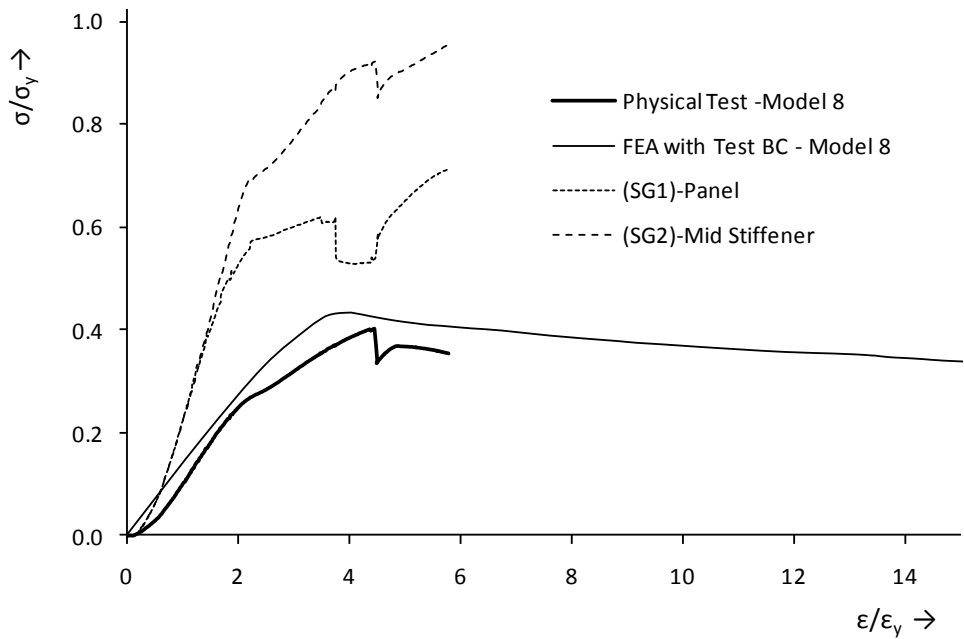
Figure B-16. Non-dimensional Strength Plot of FE (Test BC) and Test Results of Model 8
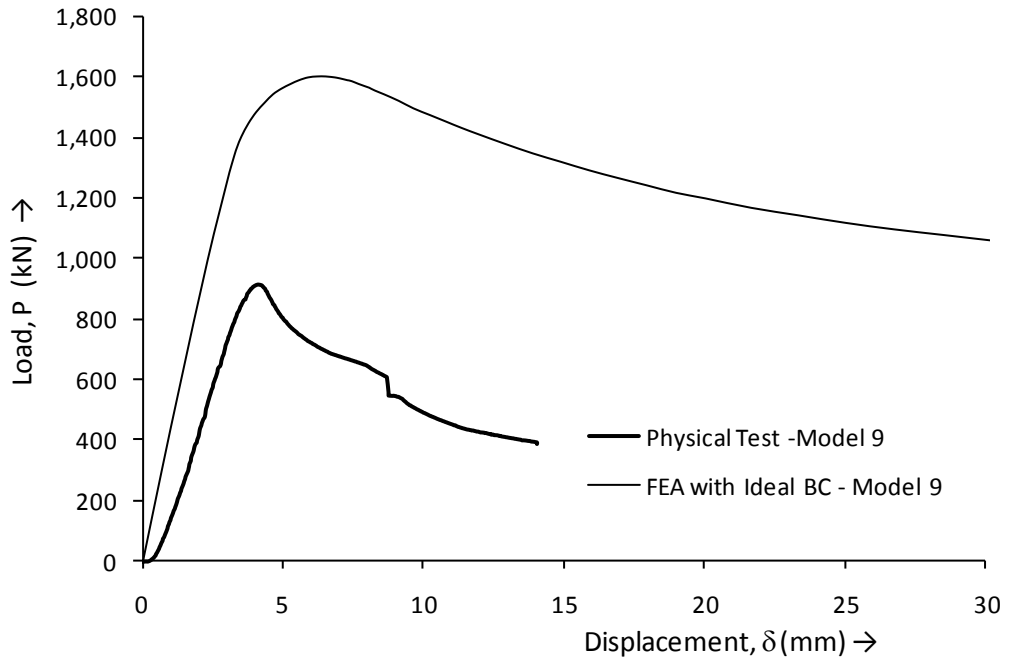
Figure B-17. Load-Displacement Plot of Ideal FE and Test of Model 9
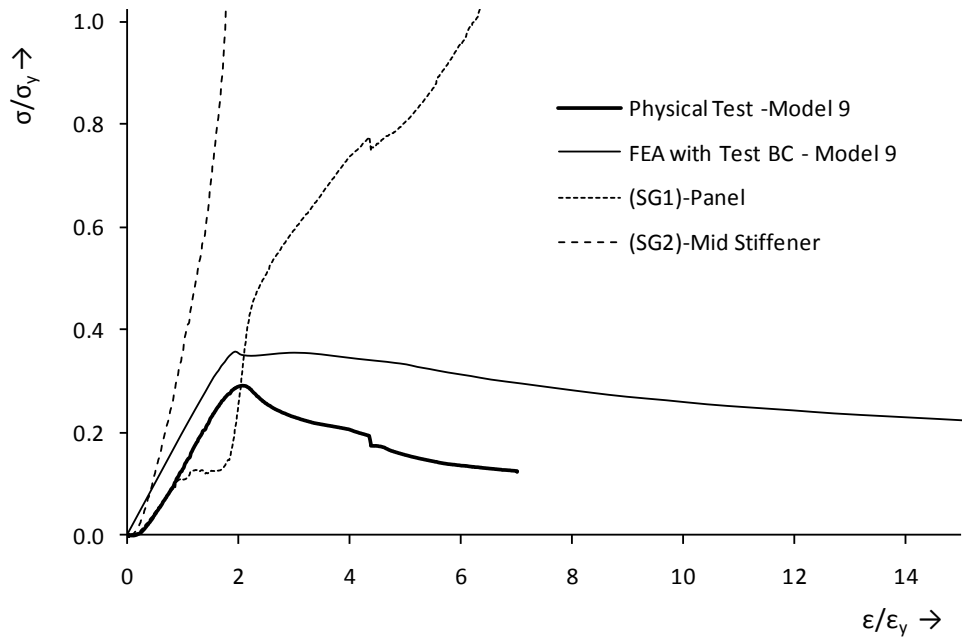
Figure B-18. Non-dimensional Strength Plot of FE (Test BC) and Test Results of Model 9
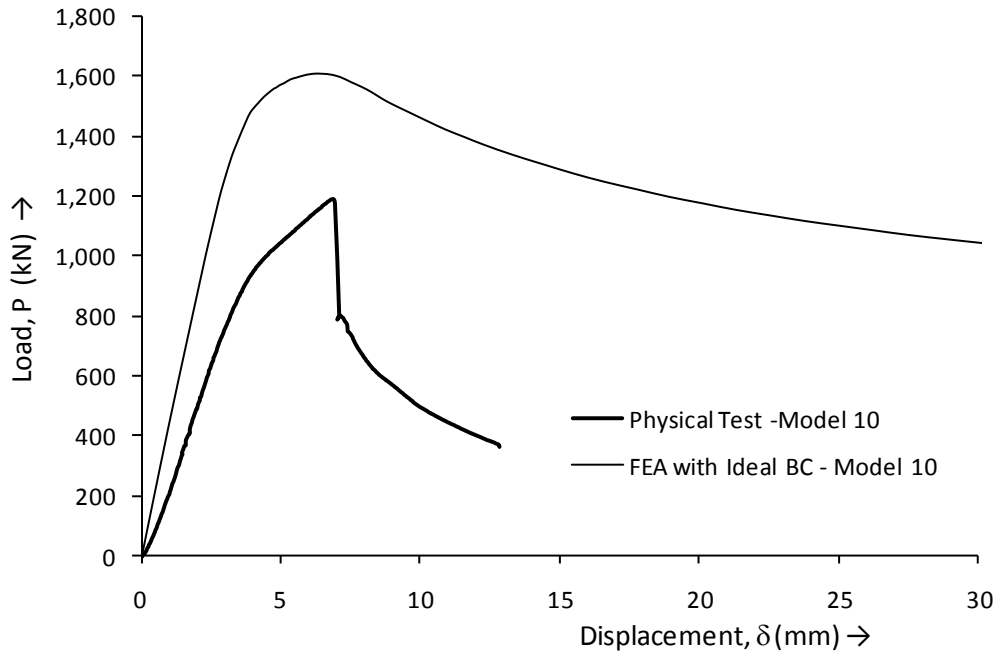
Figure B-19. Load-Displacement Plot of Ideal FE and Test of Model 10
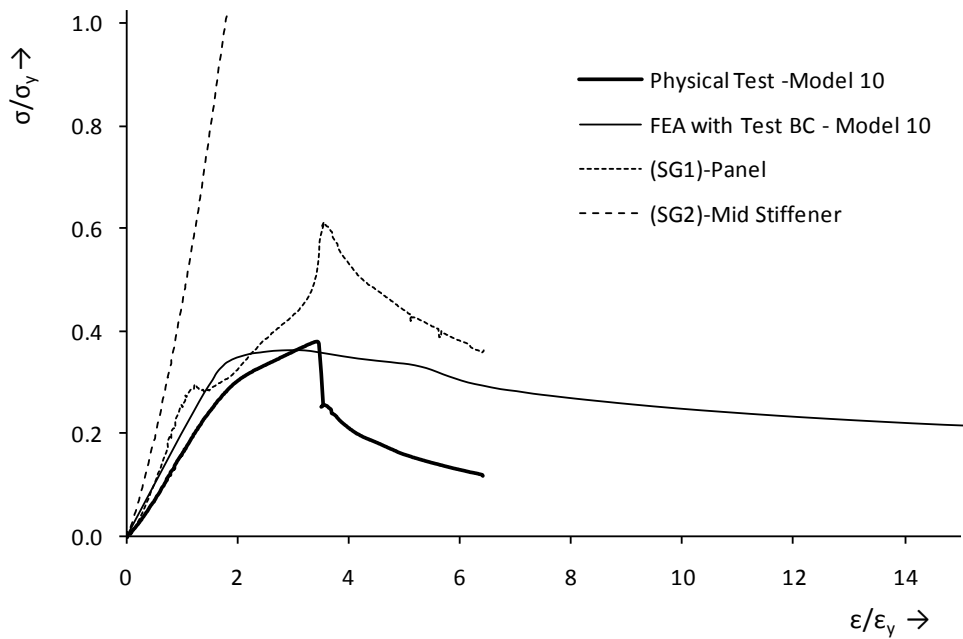
Figure B-20. Non-dimensional Strength Plot of FE (Test BC) and Test Results of Model 10

B.2 Panel Failure Pictures

Figure B-21. Panel 1

Figure B-22. Panel 2

Figure B-23. Panel 3

Figure B-24. Panel 4

Figure B-25. Panel 5

Figure B-26. Panel 6

Figure B-27. Panel 7
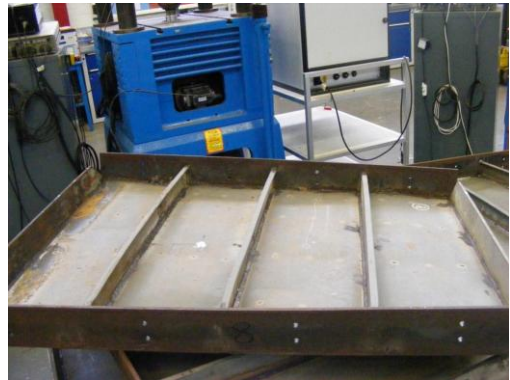
Figure B-28. Panel 8

Figure B-29. Panel 9

Figure B-30. Panel 10

Appendix C – Proposed Stiffened Cylinder Strength Formulation

C.1 Proposed Strength Model for Ring Stiffened Shells

C.1.1 Under Axial Compression

(i) The limit state approach estimate the elastic buckling strength of a ring stiffened cylinder subjected to axial compression as,

$$\sigma_e = B\rho_n C\sigma_{cr}$$

where classical elastic axial buckling stress of cylinders (Timoshenko & Gere, 1961),

$$\sigma_{cr} = \frac{1}{\sqrt{3(1-v^2)}}\frac{Et}{R} = 0.605\frac{Et}{R}$$

Knockdown factor,

$$\rho_n = \begin{cases} 0.75 - 0.142(Z_l - 1)^{0.4} + 0.003Z_l\left(1 - \dfrac{R}{300t}\right) & \text{for } 1 \le Z_l < 20 \\[2mm] 0.35 - 0.0002\dfrac{R}{t} & \text{for } Z_l \ge 20 \end{cases}$$

Batdorf length-wise slenderness parameter, $Z_l = \dfrac{L^2}{Rt}\sqrt{1-v^2}$

C is a Length dependent coefficient,

$$C = \begin{cases} 1 & \text{for } Z_l \ge 2.85 \\[2mm] \dfrac{1.425}{Z_l} + 0.175 & \text{for } Z_l < 2.85 \end{cases}$$

Bias for Knockdown factor,

$$B = \begin{cases} D_1 & \text{for } \lambda_n \ge 1 \\ 1 + (D_1 - 1)\lambda_n & \text{for } \lambda_n < 1 \end{cases}$$

where $\lambda_n = \sqrt{\dfrac{\sigma_y}{\rho_n C\sigma_{cr}}}$

and $D_1 = \begin{cases} 1.40 \text{ - for } \text{Axial loading} \\ 1.20 \text{ - for } \text{Radial loading} \\ 1.30 \text{ - for } \text{Combined loading} \end{cases}$

(ii) A quadratic interaction of $\lambda\sigma_y$ and σ_e can be used to predict the inelastic collapse stress.

$\sigma_c = \phi\sigma_y$

where Reduction factor for inelastic collapse, $\phi = \dfrac{1}{\sqrt{(1 + \lambda_e^4)}}$

and effective slenderness, $\lambda_e = \sqrt{\dfrac{\sigma_y}{\sigma_e}}$

Now the Model uncertainty factor for the axial load,

$X_m = \dfrac{\sigma}{\sigma_c}$

C.1.2 Under Hydrostatic Pressure

For hydrostatic pressure, the Proposed formulation is identical with the approach in BS5500 suggested by Faulkner D., Chen Y.N. and De Oliveira J.G, (1983). The inelastic hydrostatic collapse pressure is estimated as,

$p_{hc} = \begin{cases} 0.5\,p_{hm} & \text{for } p_y \geq p_{hm} \\ p_y\left(1 - 0.5\dfrac{p_y}{p_{hm}}\right) & \text{for } p_y < p_{hm} \end{cases}$

Von Mises, (1929) propose the solution for elastic hydrostatic buckling pressure of an unsupported cylinder is as follows.

$$p_{hm} = \dfrac{\dfrac{Et}{R}}{n^2 - 1 + \dfrac{1}{2}\left(\dfrac{\pi R}{L}\right)^2} \left\{ \dfrac{1}{\left[n^2\left(\dfrac{L}{\pi R}\right)^2 + 1\right]^2} + \dfrac{t^2}{12R^2\left(1 - \upsilon^2\right)}\left[n^2 - 1 + \left(\dfrac{\pi R}{L}\right)^2\right]^2 \right\}$$

Windenburg and Trilling, (1934) proposed a simplified expression as follows.

$$p_{hm} = \frac{\dfrac{1}{\sqrt{(1-\upsilon^2)(1+\upsilon)}} E\left(\dfrac{t}{R}\right)^2}{\dfrac{L}{\sqrt{Rt}} - 0.636} = \frac{0.919E\left(\dfrac{t}{R}\right)^2}{\dfrac{L}{\sqrt{Rt}} - 0.636}$$

The above expression does not provide satisfactory results for too small or too large values of $L/\sqrt{Rt}$. The above expression assumes pinned boundary condition at the supported cylinder end. Even though more advanced analytical expressions are available, the above expression is widely used because of the simplicity and the parameter P_{hm} has low influence in the prediction of inelastic collapse pressure.

Wilson (1966), proposed relatively simple linear equation for the circumferential yield stress of the cylindrical shell.

$$p_y = \frac{\sigma_y \left(\dfrac{t}{R}\right)}{1 - \gamma G}$$

where,

$$G = \frac{2\left[\sinh\left(\dfrac{\alpha L}{2}\right)\cos\left(\dfrac{\alpha L}{2}\right) + \cosh\left(\dfrac{\alpha L}{2}\right)\sin\left(\dfrac{\alpha L}{2}\right)\right]}{\sinh(\alpha L) + \sin(\alpha L)}$$

$$\gamma = \frac{J\left(1 - \dfrac{\upsilon}{2}\right)}{J + t_{rh}t + \dfrac{2Nt}{\alpha}}$$

$$J = A_r \left(\frac{R}{R_{cr}}\right)^2, \quad \alpha = \frac{1.285}{\sqrt{Rt}} \quad \text{and} \quad N = \frac{\cosh(\alpha L) - \cos(\alpha L)}{\sinh(\alpha L) + \sin(\alpha L)}$$

G and N are transcendental functions of αL, ie, which cannot be expressed in terms of algebraic operations or satisfy a polynomial equation.

The Model uncertainty factor for the hydrostatic pressure load,

$$X_m = \frac{p}{p_{hc}}$$

C.1.3 Under Radial Pressure

Assuming a linear interaction between axial load and radial pressure load, the proposed model predicts the elastic radial collapse pressure as follows.

$$p_{rm} = \frac{p_{hm}}{1 - 0.5 p_{hm} \dfrac{\left(\dfrac{R}{t}\right)}{\sigma_e}}$$

Now the inelastic collapse pressure under radial pressure load is computed similar to the hydrostatic case as below.

$$p_{rc} = \begin{cases} 0.5 p_{rm} & \text{for } p_y \geq p_{rm} \\ p_y \left(1 - 0.5 \dfrac{p_y}{p_{rm}}\right) & \text{for } p_y < p_{rm} \end{cases}$$

The Model uncertainty factor for the radial pressure load,

$$X_m = \frac{p}{p_{rc}}$$

C.1.4 Under Combined Axial Compression and Radial Pressure

Most of the design codes handle the combined loading based on an interaction approach. The general interaction expression is in the following form.

$$\left(\frac{\sigma}{\sigma_c}\right)^m + \left(\frac{p}{p_{rc}}\right)^n = 1$$

The above expression demonstrates the limiting criteria for the structure stability under combined loading. Hence, there exist a number of loading combinations which can cause the collapse of the structure. Eventually, the above expression provides the model uncertainty factor for combined loads at which a structural collapse occurs.

The best results with the available data is noticed with *m=1* and *n=2.*

Therefore,

$$X_m = \left(\frac{\sigma}{\sigma_c}\right) + \left(\frac{p}{p_{rc}}\right)^2$$

C.2 Strength Modelling of Stringer/Orthogonally Stiffened Shells

C.2.1 Under Axial Compression

Das, Faulkner and Zimmer, (1992) proposed the design strength of the ring and stringer stiffened cylinders under axial, radial and combined loading. It is basically RCC formulation with a revised value for the bias of knockdown factor. The steps to calculate the axial strength are as follows.

(i) The elastic buckling stress for perfect shell under curved panel formulation,

$$\sigma_{cr} = \begin{cases} 0.904E\left(\dfrac{t}{s}\right)^2\left(4+\dfrac{3Z_s^2}{\pi^4}\right) & \text{for } Z_s \leq 11.4 \\[2ex] 0.605E\left(\dfrac{t}{R}\right) & \text{for } Z_s > 11.4 \end{cases}$$

$$Z_s = \frac{s^2}{Rt}\sqrt{1-v^2}, \quad s = \frac{2\pi R}{N}$$

(ii) The lower bound knockdown factor,

$$\rho_n = \begin{cases} 1-0.019Z_s^{1.25}+0.0024Z_s\left(1-\dfrac{R}{300t}\right) & \text{for } Z_s \leq 11.4 \\[2ex] 0.27+\dfrac{1.5}{Z_s}+\dfrac{27}{Z_s^2}+0.008\sqrt{Z_s}\left(1-\dfrac{R}{300t}\right) & \text{for } 11.4 < Z_s \leq 70 \end{cases}$$

(iii) Bias for knockdown factor,

$$B = \begin{cases} D_2 & \text{for } \lambda_n > 1 \\ 1+(D_2-1)\lambda_n & \text{for } \lambda_n \leq 1 \end{cases}$$

where $\lambda_n = \sqrt{\dfrac{\sigma_y}{\rho_n \sigma_{cr}}}$

and $D_2 = \begin{cases} 1.60 \text{ - for Axial loading} \\ 1.25 \text{ - for Radial loading} \\ 2.10 \text{ - for Combined loading} \end{cases}$

(iv) Elastic buckling stress for imperfect shell,

$$\sigma_{es} = B\rho_n \sigma_{cr}$$

(v) Shell reduced slenderness parameter,

$$\lambda_r = \sqrt{\frac{\sigma_y}{\sigma_{es}}}$$

(v) The weld induced residual stress is incorporated using the width of the tension block η. For continuous structural fillet welds, $\eta = 4.5$. For light fillets or for significant shake down situation, $\eta = 3$. For stress relieved structures, $\eta = 0$.

$$K_r = \begin{cases} 1 - \dfrac{2\eta}{\left(\dfrac{s}{t}\right) - 2\eta} \dfrac{\lambda_r^4}{\left(1 + 0.25\lambda_r^4\right)^2} \dfrac{\lambda_r^2}{\left(1.05\lambda_r - 0.28\right)} & \text{for } \lambda_r > 0.53 \\[4mm] 1 & \text{for } \lambda_r \leq 0.53 \end{cases}$$

(vi) Effective width (minimum)

Shell effective width,

$$\frac{s_{em}}{s} = \begin{cases} \left(\dfrac{1.05}{\lambda_r} - \dfrac{0.28}{\lambda_r^2}\right) K_r & \text{for } \lambda_r \geq 0.53 \\[3mm] 1 & \text{for } \lambda_r < 0.53 \end{cases}$$

Shell reduced effective width,

$$\frac{s'_{em}}{s} = \begin{cases} \left(\dfrac{0.53}{\lambda_r}\right) K_r & \text{for } \lambda_r > 0.53 \\[3mm] 1 & \text{for } \lambda_r \leq 0.53 \end{cases}$$

(vii) MI of stringer and the reduced effective width of the shell

$$I'_e = I_s + \frac{A_s (d_{cs} + 0.5t)^2}{1 + \dfrac{A_s}{s'_{em}t}} + \frac{s'_{em}t^3}{12}$$

(viii) Elastic stress for stringer stiffened cylinder is the sum of column elastic stress considering the effective shell width and product of critical stress for smeared un-stiffened shell and shell knock down factor. The shell knockdown factor is assumed to be 0.75

$$\sigma_e = \left(\frac{\pi^2 E I'_e}{L^2 \left(A_s + s_{em}t\right)}\right) + \rho_s \left(\frac{0.605 E \left(\dfrac{t}{R}\right)}{\left(1 + \dfrac{A_s}{st}\right)}\right)$$

(ix) Imperfect elastic buckling parameter

$$\psi = \frac{\sigma_e}{\sigma_y}$$

(x) Ostenfeld-Bleich tangent modulus approach to find inelastic stress.

$$\sigma_c = \begin{cases} \left(1 - \dfrac{p_s(1-p_s)}{\psi}\right)\sigma_y & \text{for } \psi \geq p_s \\ \psi\sigma_y & \text{for } \psi < p_s \end{cases}$$

$$p_s = \frac{\sigma_{ps}}{\sigma_y}$$

The structural proportional limit p_s is 0.75 for stress relieved structures and 0.5 for all other cases.

(xi) Revised shell reduced slenderness parameter and revised effective shell width

$$\lambda_{re} = \sqrt{\frac{\sigma_c}{\sigma_{es}}} = \lambda_r \sqrt{\frac{\sigma_{es}}{\sigma_y}}$$

$$\frac{s_e}{s} = \begin{cases} \left(\dfrac{1.05}{\lambda_{re}} - \dfrac{0.28}{\lambda_{re}^2}\right)K_r & \text{for } \lambda_{re} \geq 0.53 \\ 1 & \text{for } \lambda_{re} < 0.53 \end{cases}$$

(xii) Average ultimate collapse stress

$$\sigma_u = \sigma_c\left(\frac{A_s + s_e t}{A_s + st}\right)$$

The Model uncertainty factor for the axial load,

$$X_m = \frac{\sigma}{\sigma_u}$$

C.2.2 Under Radial Pressure

The steps to calculate the axial strength are as follows.

(i) Local buckling pressure of un-stiffened shell

$$p_{eL} = \begin{cases} \left(\dfrac{1.27}{H^{1.18}+0.5}\right)E\left(\dfrac{t}{R}\right)^2 & \text{for } M_x > 1.5 \text{ and } H < 2.5 \\[2ex] \dfrac{0.92}{H}E\left(\dfrac{t}{R}\right)^2 & \text{for } 2.5 < H < 0.208\left(\dfrac{R}{t}\right) \\[2ex] 0.836C_p^{-1.061}E\left(\dfrac{t}{R}\right)^3 & \text{for } 0.208 < C_p < 2.85 \\[2ex] 0.275E\left(\dfrac{t}{R}\right)^3 & \text{for } C_p > 2.85 \end{cases}$$

Where

$$M_x = \frac{L}{\sqrt{Rt}}, \quad C_p = \frac{Ht}{R}$$

$H = M_x - 1.17 + 1.068k_1$ (k1=0 for radial pressure and 0.5 for hydrostatic pressure)

(ii) Plastic collapse pressure of stiffener shell combination

$$p_{cs} = \frac{16}{sL^2}A_s\,|d_{cs}|\,\sigma_y$$

(iii) Bay instability pressure

$$p_{cB} = \left(p_{eL} + p_{cs}\right)K_p$$

Where

Effective pressure correction factor,

$$K_p = \begin{cases} 0.25 + \dfrac{0.85}{500}g & \text{for } g \le 500 \\[2ex] 0.98 + \dfrac{0.12}{500}g & \text{for } 500 < g < 2500 \end{cases}$$

$$g = \frac{M_x M_\theta L t A_s}{I_s}, \quad M_\theta = \frac{s}{\sqrt{Rt}}$$

(iv) Bay instability stress

$$\sigma_{\theta cB} = p_{cB}\frac{(R+0.5t)}{t}K_{\theta L}$$

Where

$$K_{\theta L} = \begin{cases} 1 & \text{for } M_x \ge 3.42 \\ 1 - \xi\varepsilon & \text{for } M_x < 3.42 \end{cases}$$

$$\xi = \begin{cases} 1 & \text{for} \quad M_x \le 1.26 \\ 1.58 - 0.46 M_x & \text{for} \quad 1.26 < M_x < 3.42 \\ 0 & \text{for} \quad M_x \ge 3.42 \end{cases}$$

$$\varepsilon = \frac{\left(1 - 0.3 k_2\right)}{\left(1 + \dfrac{L_e t}{J}\right)}$$

$$k_2 = \frac{N_\phi}{N_\theta}, \quad N_\phi = \frac{N}{2\pi R}, \quad N_\theta = p(R + 0.5t), \quad J = A_r \left(\frac{R}{R_{cr}}\right)^2, \quad L_e = 1.56\sqrt{Rt} + t_{wr} \le L$$

The Model uncertainty factor for the radial pressure load,

$$X_m = \frac{p}{p_{\theta cB}}$$

C.2.3 Under Combined Axial Compression and Radial Pressure

The proposed interaction equation for the combined axial and radial loads is similar to the API Bul 2U with a different definition for the factor C$_c$.

$$\left(\frac{R_x}{\phi_x}\right)^2 + C_c R_x R_\theta + \left(\frac{R_\theta}{\phi_\theta}\right)^2 = 1$$

In which,
$$C_c = \frac{2\sqrt{\left(1 - \phi_x^2\right)\left(1 - \phi_\theta^2\right)}}{\phi_x \phi_\theta} - 1$$

where
$$R_x = \frac{\sigma}{\sigma_y}, \quad R_\theta = \frac{p(R + 0.5t)}{t\sigma_y}, \quad \phi_x = \frac{\sigma_u}{\sigma_y} \quad \text{and} \quad \phi_\theta = \frac{\sigma_{\theta cB}}{\sigma_y}$$

Since the above expression for combined loading characterises the limiting structural stability criteria, it represents the model uncertainty factor of the structure for the combined loading condition.

The model uncertainty factor for combined loading is,

$$X_m = \left(\frac{R_x}{\phi_x}\right)^2 + C_c R_x R_\theta + \left(\frac{R_\theta}{\phi_\theta}\right)^2$$

Appendix D – Inputs for CALREL Program

D.1 CALREL Input files - Stiffened plates

D.1.1 Variable input file

```
CALRel nrx=7 ntp=6
DATA
TITL nline title
1
Stiffened Plate-ultimate strength
FLAG icl,igr
1 0
OPTI iop,ni1,ni2,tol,op1,op2,op3
1,20,4,0.001
STAT igt(i),nge,ngm nv,ids,ex,sg,p3,p4,x0
1 7
x1                 1,2,355.0,35.5
x2                 2,1,20.,1.
x3                 3,2,8.37,2.51
X4                  4,2,4.00,1.20
X5                  5,2,0.125,0.04
x6                 6,1,1.0,0.06
x7                 7,13,71.0,14.2
PARA tp
2400.0,800.0,2960.0,11600000.0,117.0,203500.0
END
FORM ini=0
SENS isc=1 isv=0
SORM iso=3 itg=2
EXIT
```

D.1.2 Performance function subroutine (Proposed Empirical Method)

```
    subroutine ugfun(g,x,tp,ig)
    implicit real*8 (a-h,o-z)
    dimension x(7),tp(7)
    real*8 Ys,bp,rs,As,b,t,E,a,k1,k2
    real*8 Ie,Is,Zs,re,l,p,q,dp,ds,Xm,S,R
    Ys=x(1)
    t=x(2)
```

```
        rs=x(3)
        dp=x(4)
        ds=x(5)
        Xm=x(6)
        S=x(7)
        a=tp(1)
        bp=tp(2)
        As=tp(3)
        Is=tp(4)
        Zs=tp(5)
        E=tp(6)
c       ---Ultimate strength of stiffened plate - Empirical Method---

5       b=(bp/t)*(sqrt(Ys/E))
10      Ie=Is + ((As*(Zs+(t/2))**2)/(1+(As/(bp*t))))
15      re=(sqrt(Ie/(As+(bp*t))))
20      l=(a/(3.1416*re))*(sqrt(Ys/E))
25      p=dp/t
        q=ds/a
30      k1=1.29+0.44*l**2+0.09*b**2+0.09*(l*b)**2+0.36*l**4
        k2=0.14*p**2-0.05*q**2+1.33*rs**2+0.12*p*q*rs**2
        R=1/sqrt(k1+k2)

        go to(110,120) ig
 110    g = Xm*R*Ys-S
        return
 120    return
        end
```

D.2 CALREL Input files - Stiffened Cylinders

D.2.1 Variable input file

```
CALRel nrx=5 ntp=15
DATA
TITL nline title
1
Ring/Stringer Stiffened Cylinders-ultimate strength
FLAG icl,igr
1 0
OPTI iop,ni1,ni2,tol,op1,op2,op3
1,20,4,0.001
STAT igt(i),nge,ngm nv,ids,ex,sg,p3,p4,x0
1 5
```

```
x1                1, 2, 419. 0, 41. 9
x2                2, 2, 1. 96, 0. 1
x3                3, 2, 0. 072, 0. 007
x4                4, 2, 1. 0, 0. 1
X5                 5, 2, 83. 8, 8. 38
PARA tp
1, 2, 18, 571. 5, 568. 5, 0. 0, 0. 0, 0. 0, 0. 0, 30. 48, 1. 96, 0. 0, 0. 0, 210500, 0. 3
END
FORM ini=0
SENS isc=1 isv=0
SORM iso=3 itg=2
EXIT
```

D.2.2 Performance function subroutine for Ring Stiffened Cylinders

```
       subroutine ugfun(g, x, tp, ig)
       implicit real*8 (a-h, o-z)
       dimension x(20), tp(10)
        real*8 L, R, t, hwr, twr, hfr, tfr, hws, tws, hfs, tfs, E, Sy, nu, Nsd, Psd
        real*8 Scr, Zl, Rn, C, Ln, D, B, Se, Le, Phm, Ar, yr, Rcr, J, Al, H, F, G, Ga
        real*8 Py, Prm, Phc, Prc, Pc, Scc
        Sy=x(1)
        t=x(2)
        Psd=x(3)
        Xm=x(4)
         Nsd=x(5)
        Lty=tp(1)
        Pty=tp(2)
        Ns=tp(3)
         L=tp(4)
        R=tp(5)
        hwr=tp(6)
        twr=tp(7)
        hfr=tp(8)
        tfr=tp(9)
        hws=tp(10)
        tws=tp(11)
        hfs=tp(12)
        tfs=tp(13)
        E=tp(14)
        nu=tp(15)
c       Lty=1:Axial, Lty=2:Combined
c       Pty=1:Hydrostatic Pressure, Pty=2:Radial Pressure
c       ------Axial Loading of Ring stiffened cylinders--------
```

```
5       Scr=0.605*E*t/R
10      Zl=(L**2/(R*t))*sqrt(1-nu**2)
15      if(Zl.LT.20) then
        Rn=0.75-(0.142*(Zl-1)**(0.5))+0.003*Zl*(1-R/(300*t))
        else
        Rn=0.35-0.0002*R/t
        endif
20      if(Zl.LT.2.85) then
        C=0.175+1.425/Zl
        else
        C=1
        endif
25      Ln=sqrt(Sy/(Rn*C*Scr))
30      if(Lty.EQ.1) then
        D=1.4
        elseif(Lty.EQ.2) then
        D=1.3
        endif
35      if(Ln.LT.1) then
        B=1+(D-1)*Ln
        else
        B=D
        endif
40      Se=B*Rn*C*Scr
45      Le=sqrt(Sy/Se)
50      Sc=Sy/sqrt(1+Le**4)
c       ---Radial and combined Loading of Ring stiffened cylinders----
55      Phm=0.919*E*(t/R)**2/(L/sqrt(R*t)-0.636)
60      Ar=abs(hwr)*twr+hfr*tfr
65      yr=(twr*hwr**2/2+hfr*tfr*(abs(hwr)+tfr/2))/ Ar
70      if(hwr.LT.0) then
        Rcr=R-t/2-yr
        else
        Rcr=R+t/2+yr
        endif
75      J=Ar*(R/Rcr)**2
80      Al=1.285/sqrt(R*t)
85      H=(cosh(Al*L)-cos(Al*L))/(sinh(Al*L)+sin(Al*L))
90      F=Al*L/2
95      G=2*(sinh(F)*cos(F)+cosh(F)*sin(F))/(sinh(2*F)+sin(2*F))
100     Ga=J*(1-nu/2)/(J+twr*t+2*H*t/Al)
105     Py=(Sy*t/R)/(1-Ga*G)
110     Prm=Phm/(1-0.5*Phm*R/(t*Se))
115     if(Py.GE.Phm) then
        Phc=0.5*Phm
```

```
          else
          Phc=Py*(1-0.5*Py/Phm)
          endif
120       if(Py.GE.Prm) then
          Prc=0.5*Prm
          else
          Prc=Py*(1-0.5*Py/Prm)
          endif
125       if(Pty.Eq.1) then
          Pc=Phc
          elseif(Pty.Eq.2) then
          Pc=Prc
          endif
130       Scc=Sc*(1-Psd/Pc)**2
135       if(Lty.Eq.1) then
          R=Sc
          elseif(Lty.Eq.2) then
          R=Scc
          endif

          go to(200,210) ig
200       g=Xm*R-Nsd
          return
210       return
          end
```

D.2.3 Performance function subroutine for Stringer Stiffened Cylinders

```
          subroutine ugfun(g,x,tp,ig)
          implicit real*8 (a-h,o-z)
          dimension x(17),tp(3)
          real*8 L,R,t,hwr,twr,hfr,tfr,hws,tws,hfs,tfs,E,Sy,nu,Nsd
          real*8 Psd,Xm,s,Zs,Scr,Rn,Ln,D,B,Se,Lr,Kr,eta,sem,sdem,As
          real*8 ys,Zcs,Ia,Ib,Is,Ide,Sel,Rs,Se1,Se2,ps,Sc,Le,sef,Su
          real*8 Mx,Mt,k,H,Cp,Pel,Pcs,Kg,Kp,Pcb,Lef,Ar,yr,Rcr,J,Nf
          real*8 Nt,k1,ebs,psi,Ktl,Stcb,Cc,Rt,fx,ft,m,n,Suc
          Sy=x(1)
          t=x(2)
          Psd=x(3)
          Xm=x(4)
          Nsd=x(5)
          Lty=tp(1)
          Pty=tp(2)
```

```
          Ns=tp(3)
           L=tp(4)
          R=tp(5)
          hwr=tp(6)
          twr=tp(7)
          hfr=tp(8)
          tfr=tp(9)
          hws=tp(10)
          tws=tp(11)
          hfs=tp(12)
          tfs=tp(13)
          E=tp(14)
          nu=tp(15)
          eta=3
          Kf=0.75
          ps=0.5
c         Lty=1:Axial, Lty=2:Combined
c         Pty=1:Hydrostatic Pressure, Pty=2:Radial Pressure
c         Ns=number of stringers
c         eta=Residual stress parameter; 0-stressreleaved,
c          3-aftre shakedown, 4.5-fillet welded
c          Kf=Shell knock down factor assumed to be 0.75
c          ps=Load proportionality factor, assumed to be 0.5
c         ----Axial Loading of Stringer stiffened cylinders------
5         s=2*3.1416*R/Ns
10        Zs=(s**2/(R*t))*sqrt(1-nu**2)
15        if(Zs.GT.11.4) then
          Scr=0.605*E*t/R
          else
          Scr=0.904*E*((t/S)**2)*(4+(3*Zs**2)/3.1416**4)
          endif
20        if(Zs.LE.11.4) then
          Rn=1-0.019*Zs**1.25+0.0024*Zs*(1-R/(300*t))
          else
          Rn=0.27+(1.5/Zs)+(27/Zs**2)+0.008*sqrt(Zs)*(1-R/(300*t))
          endif
25        Ln=sqrt(Sy/(Rn*Scr))
30        if(Lty.EQ.1) then
          D=1.6
          elseif(Lty.EQ.2) then
          D=2.1
          endif
35        if(Ln.LE.1) then
          B=1+(D-1)*Ln
          else
```

```
         B=D
         endif
40       Se=B*Rn*Scr
45       Lr=sqrt(Sy/Se)
50       If(Lr.GT.0.53)then
         Kr=1-2*eta*Lr**6/((s/t-2*eta)*(1+0.25*Lr**4)**2*(1.05*Lr-0.28))
         else
         Kr=1
         endif
55       If(Lr.GE.0.53)then
         sem=s*Kr*(1.05/Lr-0.28/Lr**2)
         else
         sem=s
         endif
60       If(Lr.GT.0.53)then
         sdem=s*Kr*(0.53/Lr)
         else
         sdem=s
         endif
65       As=abs(hws)*tws+hfs*tfs
70       ys=(tws*hws**2/2+hfs*tfs*(abs(hws)+tfs/2))/ As
75       If(hws.LT.0)then
         Zcs=-t/2-ys
         else
         Zcs=t/2+ys
         endif
80       Ia=tws*abs(hws)**3/12+hfs*tfs**3/12
         Ib=tws*abs(hws)*(abs(hws)/2-ys)**2+hfs*tfs*(abs(hws)+tfs/2-ys)**2
         Is=Ia+Ib
85       Ide=Is+As*(Zcs+0.5*t)**2/(1+As/(sdem*t))+sem*t**3/12
90       Se1=3.1416**2*E*Ide/(L**2*(As+sem*t))
         Se2=Kf*0.605*E*t/(R*(1+As/(s*t)))
         Se1=Se1+Se2
95       Si=Se1/Sy
         If(Si.GE.ps)then
         Sc=(1-ps*(1-ps)/Si)*Sy
         else
         Sc=Si*Sy
         endif
100      Le=sqrt(Sc/Se)
105      If(Le.GT.0.53)then
         sef=s*Kr*(1.05/Le-0.28/Le**2)
         else
         sef=s
         endif
```

```
110     Su=Sc*(As+sef*t)/(As+s*t)
c       ------Combined Loading of Stringer stiffened cylinders-----
115     Mx=L/sqrt(R*t)
120     Mt=s/sqrt(R*t)
125     If(Pty.EQ.1)then
        k=0.5
        elseif(Pty.EQ.2)then
        k=0
        endif
130     H=Mx-1.17+1.068*k
135     Cp=H*t/R
140     If(Mx.GT.1.5.and.H.LT.2.5)then
        Pel=(1.27/(H**1.18+0.5))*E*(t/R)**2
        elseif(H.GE.2.5.and.H.LT.0.208*(R/t))then
        Pel=(0.92/H)*E*(t/R)**2
        elseif(Cp.GT.0.208.and.Cp.LT.2.85)then
        Pel=0.836*Cp**(-1.061)*E*(t/R)**3
        elseif(Cp.GE.2.85)then
        Pel=0.275*E*(t/R)**3
        endif
145     Pcs=16*As*abs(Zcs)*Sy/(s*L**2)
150     Kg=Mx*Mt*L*t*As/Is
155     If(Kg.LE.500)then
        Kp=0.25+0.85*Kg/500
        else
        Kp=0.98+0.12*Kg/500
        endif
160     Pcb=(Pel+Pcs)*Kp
165     If(1.56*sqrt(R*t)+twr.LT.L)then
        Lef=1.56*sqrt(R*t)+twr
        else
        Lef=L
        endif
        Ar=(abs(hwr)*twr+hfr*tfr)
170     If(Ar.EQ.0)then
        yr=0
        else
        yr=(twr*hwr**2/2+hfr*tfr*(abs(hwr)+tfr/2))/Ar
        endif
175     if(hwr.LT.0) then
        Rcr=R-t/2-yr
        elseif(hwr.GT.0) then
        Rcr=R+t/2+yr
        else
        Rcr=R
```

```
        endif
180     J=(abs(hwr)*twr+hfr*tfr)*(R/Rcr)**2
185     Nf=Nsd*t
190     Nt=Psd*(R+0.5*t)
195     if(Nt.EQ.0) then
        k1=0
        else
        k1=Nf/Nt
        endif
200     if(J.EQ.0) then
        ebs=0
        else
        ebs=(1-0.3*k1)/(1+Lef*t/J)
        endif
205     if(Mx.LE.1.26) then
        psi=1
        elseif(Mx.LT.3.42) then
        psi=1.58-0.46*Mx
         else
         psi=0
        endif
210     if(Mx.LT.3.42) then
        Ktl=1-ebs*psi
        else
         Ktl=1
        endif
215     Stcb=Pcb*(R+0.5*t)*Ktl/t
220     Rt=Psd*(R+0.5*t)/(Sy*t)
225     fx=Su/Sy
230     ft=Stcb/Sy
235     Cc=2*(sqrt((1-fx**2)*(1-ft**2))/(fx*ft))-1
240     m=fx**2*Cc*Rt
245     n=(Rt*fx/ft)**2-fx**2
250     Suc=Sy*(-m+sqrt(m**2-4*n))/2
255     if(Lty.Eq.1) then
        R=Su
        elseif(Lty.Eq.2) then
        R=Suc
        endif
        go to(500,510) ig
500     g=Xm*R-Nsd
        return
510     return
        end
```